7-1-2016

Automated Device to Measure Slurry Properties in Drilled Shafts

Miles Patrick Mullins
University of South Florida, mpmullin@mail.usf.edu

Automated Device to Measure Slurry Properties in Drilled Shafts

by

Miles P. Mullins

A thesis submitted in partial fulfillment
of the requirements for the degree of
Master of Science in Civil Engineering
Department of Civil and Environmental Engineering
College of Engineering
University of South Florida

Co-Major Professor: Rajan Sen, Ph.D.
Co-Major Professor: Abla Zayed, Ph.D.
Michael J. Stokes, Ph.D.

Date of Approval:
June 22, 2016

Keywords: Downhole Device, Drilling Mud, Drill Fluid,
Excavation Stabilization, Wet Construction

TABLE OF CONTENTS

LIST OF TABLES

LIST OF FIGURES

ABSTRACT

Slurry is the fluid within a drilled excavation that is introduced when an excavation is deeper than the water table or where additional stability is needed for loose sandy dry soils. Although construction practices vary greatly throughout the country and the world, slurry levels should be maintained above the existing ground water level by a suitable margin. The most widely used slurry type is mineral slurry formed by mixing dry clay powder with water; either bentonite or attapulgite powder may be used (attapulgite being used in saline water conditions). Regardless of whether the slurry material is mineral, polymer or natural, the construction practice must address the slurry properties to ensure the stability of the excavation is never compromised.

Proper performance of slurries used to stabilize drilled shaft excavations is maintained by assuring the density, viscosity, pH, and sand content stay within specified limits. These limits have been set either by past experience, research findings and/or by manufacturer recommended values. However, field slurry testing is time consuming as all measurements are manually performed. With the overwhelming advances in digital down-hole devices, it is not unreasonable to assume that slurry property tests are equally applicable to this trend. This formed the basis of this project.

The most commonly used test to indicate slurry viscosity is the Marsh Funnel Test which is essentially a timed flow for a fixed volume of slurry to exit a falling head funnel. Using a library of unique pressure versus flow rate responses for a wide range of slurry viscosities, an automated downhole device was designed and tested that incorporated this information to estimate viscosity in the excavation without the need to remove slurry in order to test. Direct measurement of slurry density was also incorporated into the device and the sand content was computed from density and the viscosity where the suspended solids that make up the density stems from both the slurry products and the soil cuttings.

CHAPTER 1: INTRODUCTION

1.1 Background

Slurry is the fluid within a drilled excavation that is introduced when an excavation is deeper than the water table or where additional stability is needed for loose sandy dry soils. Construction practices vary greatly throughout the country and the world, but slurry levels should be maintained above the existing ground water level by a suitable margin. It should be further noted that at no point is it acceptable to dig below the water table and allow the ground water to fill the excavation as a means to introduce slurry as this loosens the surrounding soil and promotes side wall collapse. While slurries can be categorized as mineral, polymer or natural, the most widely used slurry type is mineral slurry formed by mixing dry clay powder with water. Depending on the environmental conditions, either bentonite or attapulgite powder may be used (attapulgite being used in saline water conditions).

Although both mineral and polymer slurry have been shown to be effective in stabilizing an excavation, the mechanisms by which they provide this stability are quite different. Mineral slurries depend on a minimum density to ensure a significant clay mineral concentration has been achieved and to provide a sufficient lateral pressure on the excavation walls. Stability is further enhanced by the impervious barrier (filter cake) that quickly forms confining the slurry within the excavation. Without adequate clay mineral concentration, the filter cake will not form. Therein, the slurry density provides a measure of slurry suitability prior to being placed in the excavation.

The effectiveness of mineral slurries to form a filter cake/layer and sufficient lateral pressure allows the required fluid head to be the least of all slurry types.

Newer clay slurry products are now available that are enhanced with polymer additives that can perform equally well, but at lower clay/polymer powder concentrations. These products (known as high yield) are compared on the basis of similar viscosities and not density. Therein, high yield products produce on the order of 200 barrels (1bbl = 42gals) of slurry for every 2000lbs of powder whereas pure bentonite powders produce only 90 bbls of slurry for every 2000lbs of powder (both having similar viscosity). This equates to 0.23lbs/gal and 0.53lbs/gal for high yield and pure bentonite products, respectively. As both pure and high yield products are likely to be used on any given project, viscosity becomes a more important property and density is less telling of the true slurry performance potential. However, as the density is lower when using high yield products, a higher differential head between slurry level and ground water is needed to provide the same net effective lateral pressure against the side wall.

Slurry properties may require adjustments as different soils are encountered to provide a minimum performance level. As a result, slurry testing is often required to track proper slurry performance. Numerous tests and types of equipment have been developed for use in the field. Florida Standard Specifications for Road and Bridge Construction, Section 455 (FDOT, 2016) requires density, viscosity, and pH values to be established every 2 hours for the first 8 hours and then every 4 hours thereafter on 30 foot intervals starting at the bottom of excavation. The high frequency early on is to provide quick feedback as to the soil conditions and its effect on the slurry health. For example, if organic soils are encountered, the lower pH will cause the bentonite to

flocculate and thereby lose viscosity. Likewise, salinity in the soil or ground water can have the same effect. Early detection of these conditions prevents side wall sloughing due to performance deterioration of slurry. The slurry density, Marsh funnel viscosity, pH and sand content are the most common field tests. Sand content is most important just prior to concreting.

Proper performance of mineral slurries used to stabilize drilled shaft excavations is maintained by assuring the density, viscosity, pH, and sand content stay within state specified limits. These limits have been set either by past experience, research findings and/or by manufacturer recommended values. However, field slurry testing is time consuming as all measurements are manually performed. With the overwhelming advances in digital down-hole devices, it is not unreasonable to assume that slurry property tests are equally applicable to this trend.

Each of the slurry tests and equipment outlined above has contributory components that may aid in the development of an automated down-hole slurry testing device. By automating slurry testing, there exists the potential to improve the quality of the field data and the speed at which the information is collected. This thesis focuses on developing such a device.

1.2 Organization of Thesis

This thesis entailed five tasks in the process of developing an automated down-hole slurry testing device which will be discussed in the following Chapters. These include: Chapter 2, literature review; Chapter 3, development of automated equipment for each of the target slurry

properties; Chapter 4, laboratory trials using slurries with a wide range of properties; Chapter 5, field testing on site, and Chapter 6, summary and conclusions.

CHAPTER 2: LITERATURE REVIEW

2.1 State Slurry Specifications

Drill slurry is slightly heavier than water and is viscous enough to suspend small soil cuttings. When maintained correctly, the slurry level (at least 4ft above ground water for mineral slurry) provides lateral pressure in excess of the active earth pressure while also eliminating ground water intrusion. This coupled with the filter-cake that quickly forms on the excavation walls - as the net higher pressure slurry moves slowly into the surround soil – slurry provides stability to the excavation even with the motion of the drilling tool up and down the excavation walls. The quickest indicator of slurry health is measured by the pH which indicates whether or not an excavation has encountered organics (low pH) or other materials that compromise the integrity of the clay to water bond; but viscosity, density and sand content are the most important parameters in the successful construction/excavation of a drilled shaft. Viscosity is perhaps the most important of all in stabilizing the excavation provided the slurry level is properly maintained. To this end, state and federal agencies have established acceptable ranges for slurry property limits.

The rationale for mineral slurry property limits can be summarized as follows:

- Viscosity provides an indication of proper slurry product concentration. Where concentration may vary among products to achieve a target viscosity, the viscosity performance should not vary outside acceptable limits during different phases of construction. If too viscous, it may be difficult to de-sand before concreting or it

may even cling to reinforcing steel during concreting. If too thin, it cannot form a filter cake, stabilize the side walls nor suspend solids.

- Density also indicates the presence of suspended solids which may be the slurry product itself or cuttings. The importance of its magnitude: it should be high enough to promote side wall pressure, but not so high that it is difficult to displace during concreting. Therefore, lower density slurry could be offset by a higher differential fluid level to maintain adequate side wall pressure. High slurry density is not problematic during excavation.
- Sand content is only important at the time of concreting where suspended cuttings may deposit on the concrete surface, become encapsulated in the concrete, or simply mix with and degrade the concrete quality. As different concentrations of slurry product can suspend more or less sand (high viscosity with high gel strength holds more sand and vice versa), it is conceivable that a sliding scale of acceptable sand content could be developed. However, recall that 4% sand content (the present upper limit) is equivalent to nearly 8ft of loosely placed sand accumulation in a 100ft excavation. In short, less sand drastically reduces the occurrence of inclusions in the concrete.
- pH is useful to assess water quality prior to slurry mixing and as a first indicator of slurry breaking down during drilling. Most product manufacturers recommend a water pH of 8-9 prior to mixing. The bentonite will drive the pH up slightly. More bentonite product is needed to overcome low pH mixing water; simple cost effective additives like soda ash reduce the amount of bentonite needed. Organic soils can have pH values in the 5-6 range which will immediately make the slurry pH drop and the bentonite to flocculate. This reduces gel strength and the cutting suspension capabilities. Unfortunately, saltwater can have the same undesirable effects, but the pH of salt water ranges from 7.5 to 8.4 which may be less noticeable via pH testing.

In known regions of saltwater, attapulgite is used (initially mixed with freshwater). The downside, attapulgite requires twice as much product to achieve the same viscosity in freshwater and even more in saltwater.

Conceptually, the above considerations can be presented graphically using data adapted from a previous study (Figure 2.1). This shows three basic conditions: (1) always acceptable slurry which includes before introduction, during excavation, and while concreting, (2) acceptable only during excavation which implies too heavy or too viscous for concreting, and (3) never acceptable when considering slurry stabilization (may be acceptable for full length

temporary casing stabilization). Implied, however, is that sand content does not affect viscosity. Also, it should be emphasized that the data shown represents a given product and a higher or lower mix ratio may result from other products. The slurry property ranges, required values of density, viscosity, pH, and sand content are provided in the FDOT 455-Standard Specifications for Road and Bridge Construction (2016) and are shown in Table 2.1 (FDOT, 2016).

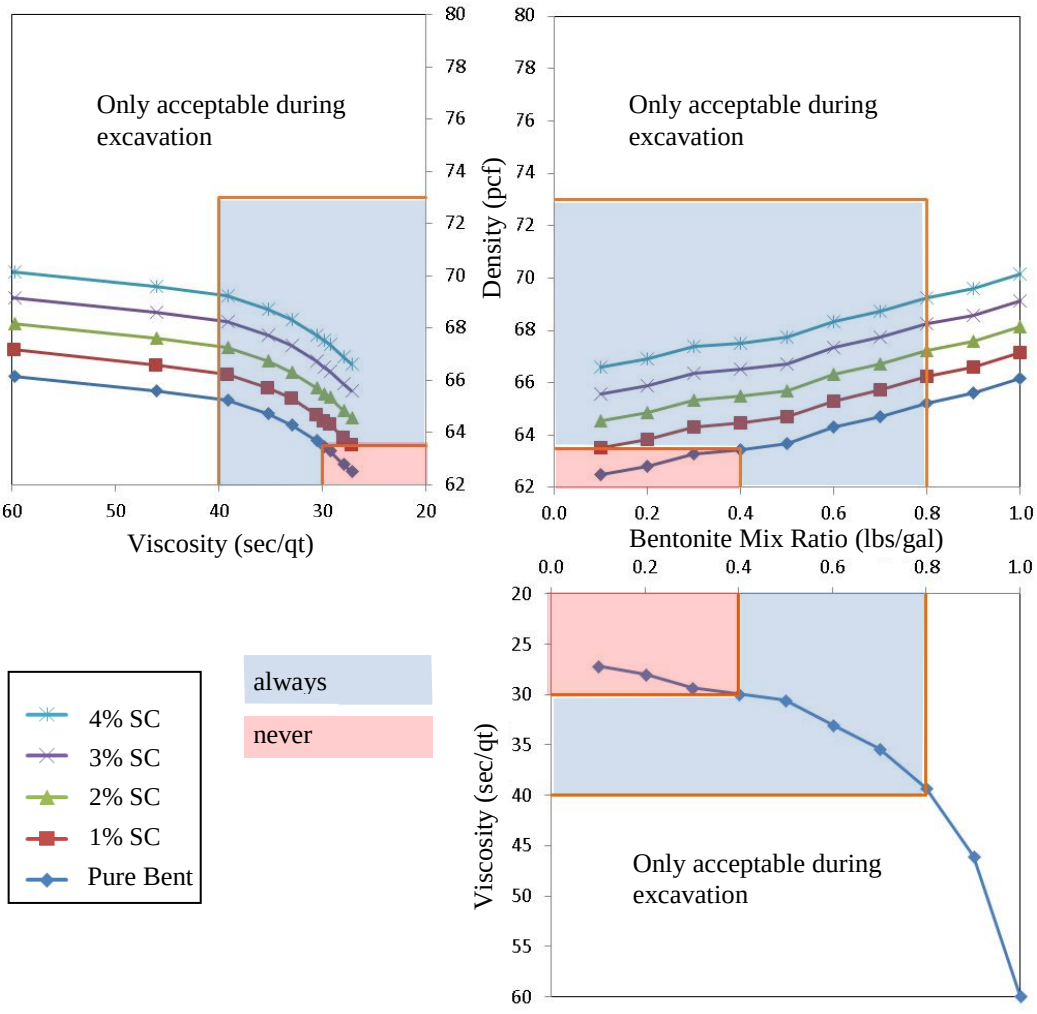

Figure 2.1. Example of acceptable slurry conditions during shaft construction.

Table 2.1. Drill slurry properties

Slurry Property	Range of Results (lb/ft^3)	Test Method
Density	64 – 73 pcf (fresh water) 66 – 75 pcf (salt water)	Mud density balance: FM 8-RP13B-1
Viscosity	30-40 seconds	Marsh Cone Method: FM 8-RP13B-2
pH	8-11	Electric pH meter or pH indicator paper strips: FM 8-RP13B-4
Sand Content	4% or less	FM 8-RP13B-3

Intrinsic to the preparation of properly performing slurry is the time dependency of each of these properties. Even when mixed carefully without clumping, the now wetted mineral absorbs the water slowly over a period of several hours. This means that properties change with time and must be monitored somewhat continuously. State specifications require a minimum of 4 sets of density, viscosity and pH tests in the first 8 hours of use. When results become consistent, pH testing is not required while density and viscosity tests are to be performed every 4 hours thereafter.

> "Perform a minimum of four sets of tests to determine density, viscosity, and pH value during the first 8 hours mineral slurry is in use. When the results show consistent behavior, discontinue the tests for pH value, and only carry out tests to determine density and viscosity during each four hours mineral slurry is in use." (FDOT, 2016)

As seen in Figure 2.2, to test slurry properties throughout a borehole currently requires a worker to drop a sampler to the full depth of the borehole and then retrieve the slurry sample to ground level for testing to occur. To determine if the slurry is within specifications requires a

separate test for each property identified in Table 2.1. This can be seen in both Figures 2.2 and 2.3. Following completion of the tests on the first (bottom) sample, the testing process is repeated with samples being obtained from the borehole in 30 foot elevation increments until the top of excavation is reached.

Figure 2.2. Sample collection and mud balance test.

Figure 2.3. Viscosity, pH and sand content testing

2.2 Density

The density of the drilling fluid is perhaps the simplest of tests/concepts as it is defined as the weight per unit volume. For a given viscosity, high yield products are lighter than pure bentonite products as the weight of material added per gallon is roughly half. The presence of large amounts of suspended solids, collected while drilling, will also increase the density of the slurry but should not be misinterpreted as bentonite product content. As noted above, densities that are too high are of particular concern in drilled shaft applications, where the slurry must be displaced during concreting. If too dense, the slurry is not as easily displaced, and mixing of the concrete and slurry may occur, reducing the quality of the concrete. However, the density level at which the slurry is too dense to be displaced by 135-140pcf fluid concrete has not been documented in the literature.

2.2.1 Existing Methods to Measure Slurry Density

To measure the density of the drilling fluid while in use, "any instrument that will permit accurate measurement within $^{1}/_{10}$ lb or ½ pcf" may be used (Wyo-Ben, 2011). A balance type scale, referred to as a "mud balance" is typically used, and is available from most major drilling fluid manufacturers. A mud balance is shown Figure 2.4.

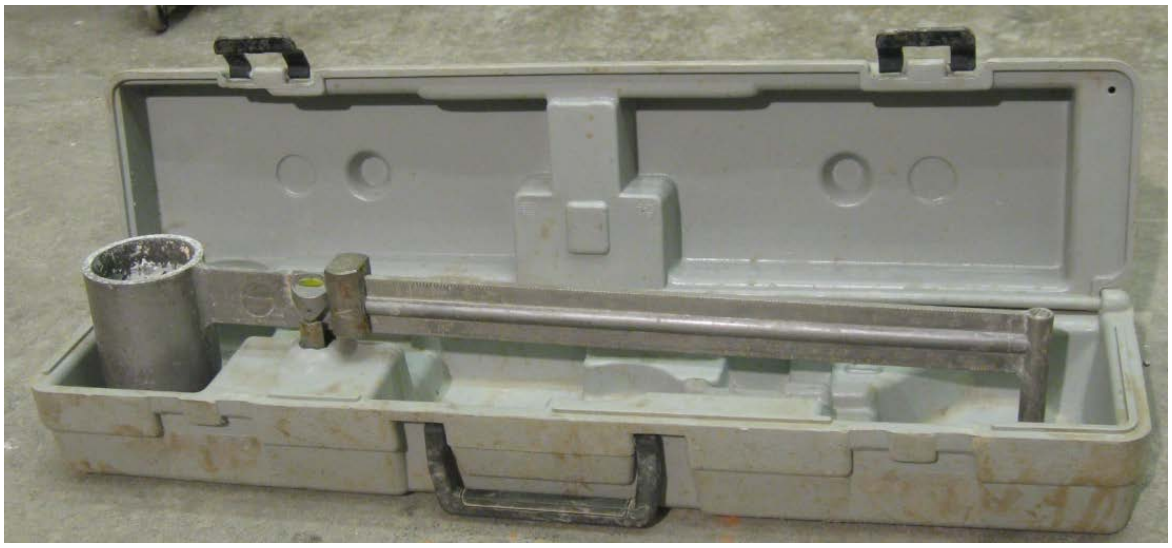

Figure 2.4. Mud balance with case

The proper procedure must be followed to determine the density of drilling fluids with a mud balance. The proper procedures are as follows:

(1) Fill the cup with the mud to be weighed.
(2) Place the lid on the cup and seat it firmly but slowly with a twisting motion. Be sure some mud runs out of the hole in the cap.
(3) With the hole in the cap covered with a finger, wash or wipe all mud from the outside of the cup and arm.
(4) Set the knife on the fulcrum and move the sliding weight along the graduated arm until the cup and arm are balanced.
(5) Read the density of the mud at the left-hand edge of the sliding weight.
(6) Report the result to the nearest scale division in $^{lb}/_{gal}$, $^{lb}/_{cu.\ ft}$, S.G., or $^{psi}/_{1000\ ft}$ of depth.
(7) Wash the mud from the cup immediately after each use. It is absolutely essential that all parts of the mud balance be kept clean if accurate results are to be obtained.
(8) Refer to [Mud Weight Conversion Table (Table 2.2)] for conversion to the desired units if not available on the balance.

Table 2.2. Mud weight conversion table (Wyo-Ben, 2011)

Mud Weight Conversion Table			
Lb per Gal	Lb per Cu Ft	Specific Gravity	Gradient, psi per 1000 Ft of Depth
6.5	48.6	0.78	338
7	52.4	0.84	364
7.5	56.1	0.9	390
8	59.8	0.96	416
8.3	62.4	1	433
8.5	63.6	1.02	442
9	67.3	1.08	468
9.5	71.1	1.14	494
10	74.8	1.2	519
10.5	78.5	1.26	545
11	82.3	1.32	571
11.5	86	1.38	597
12	89.8	1.44	623
12.5	93.5	1.5	649
13	97.2	1.56	675
13.5	101	1.62	701
14	104.7	1.68	727
14.5	108.5	1.74	753
15	112.2	1.8	779
15.5	115.9	1.86	805
16	119.7	1.92	831
16.5	123.4	1.98	857
17	127.2	2.04	883
17.5	130.9	2.1	909
18	134.6	2.16	935
18.5	138.4	2.22	961
19	142.1	2.28	987
19.5	145.9	2.34	1013
20	149.6	2.4	1039
20.5	153.3	2.46	1065
21	157.1	2.52	1091
21.5	160.8	2.58	1117
22	164.6	2.64	1143
22.5	168.3	2.7	1169
23	172.1	2.76	1195
23.5	175.8	2.82	1221
24	179.5	2.88	1247

For previous studies involving slurry density, a volumetric flask and scale (Figure 2.5) were used in lieu of the mud balance due to the low precision of the balance.

Standard Mud Balance Replaced with a Volumetric Flask and Scale

Figure 2.5. Mud balance kit, volumetric flask and scale

2.2.2 Concepts for Automating Density Measurement

There are several approaches to automating data collection for density. Archimedes principle (Figure 2.6) states that the buoyant force of a submerged object is a function of the density of the fluid and the volume displaced (Equation 1).

$$F_{buoyancy} = \rho_{fluid} * V_{displaced} \quad (1)$$

The buoyancy of a float of known volume submerged in slurry can provide a measure of the density of the slurry.

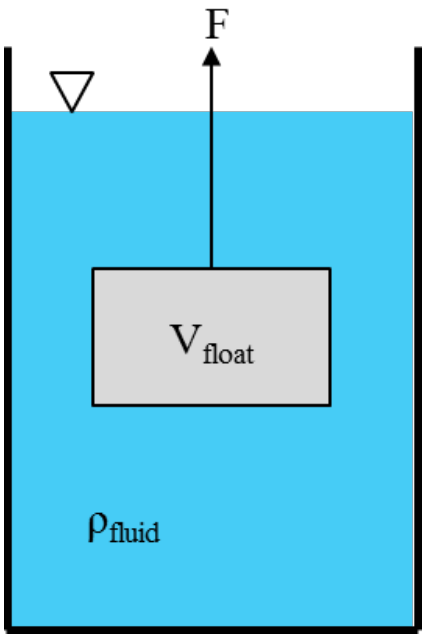

Figure 2.6. Archimedes principle

Weighing a known volume of a sample can also be used to determine the density (Equation 2).

$$Density = {}^{mass}/_{volume} \tag{2}$$

Alternately, hydrostatic pressure differentials may be used to quantify density (Figure 2.7). Defining the unit weight (γ), depth (h) and equation 3, it is possible to calculate density by comparing pressure data from two points in a slurry column, given the vertical distance between the points is known.

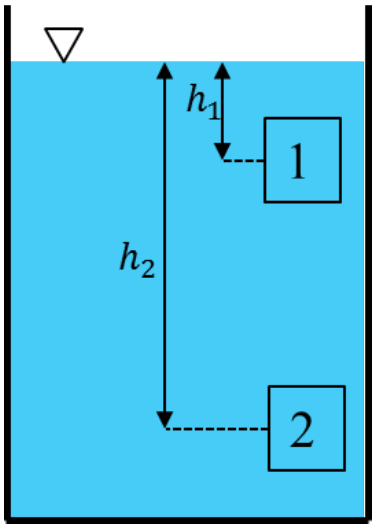

Figure 2.7. Hydrostatic pressure diagram

$$\gamma_{measured} = \frac{P_2 - P_1}{\Delta h} \tag{3}$$

2.2.3 Sensor Applications for Density Measurements

In order to measure buoyant forces or weigh a slurry sample, a load cell or strain gages may be used. Absolute or differential pressure transducers may be used for pressure measurements that in turn would give slurry density.

2.2.4 Sensor Availability for Density Measurements

Concepts such as that shown in Figure 2.6 can easily be implemented using off-the-shelf sensors like the load cells or strain gages shown in Figure 2.8a. S-type load cells are particularly robust and yet highly sensitive for small loads like that envisioned for this application. Another option can include tailor-made devices using strain gages (Figure 2.8b) which provide an unlimited amount of possibilities. However, a delta pressure approach to measure density would be best served with highly sensitive pressure transducers like Figure 2.8c.

(a) (b) (c)

Figure 2.8. Available instrumentation for density determination using an automated slurry profiling device. (a) load cell (Omega, 2015a), (b) metal foil bonded strain gages (Omega, 2015b, and (c) pressure transducer (Omega, 2015c)

2.3 Viscosity

The viscosity of a fluid is its tendency to resist flow under shear stress. It is defined as the ratio of shear stress to strain rate. For many fluids, viscosity varies with temperature but is otherwise a constant property. These are termed Newtonian fluids. However there is another category of fluids where viscosity varies depending on the rate at which the shear strain is induced. The latter are referred to as non-Newtonian fluids. Non-Newtonian fluids can be further classified by the direction in which the viscosity changes with shear rate. Fluids that exhibit an increase in viscosity at higher shear rates are classified as shear-thickening fluids and those that exhibit a decrease in viscosity at higher shear rates are classified as shear-thinning. Bentonite drilling slurry is a shear-thinning, non-Newtonian fluid. When drilling slurry is at rest, its behavior is more gel-like. However when it is exposed to high shear rates, such as when being pumped, it behaves as if it has been liquefied. Behavior of a non-Newtonian fluid is characterized by its viscoelastic properties, the study of which is rheology.

2.3.1 Existing Methods to Measure Slurry Viscosity

The Marsh funnel measurement of slurry viscosity is a standardized field test established by the American Petroleum Institute, API 13B-1.6.2. This test is not intended to provide a direct measurement of any particular fluid property, but rather to give an empirically defined indication of adequate viscosity and gel strength so as to provide sufficient borehole or excavation stability. The Marsh funnel test method simply measures the time required for one quart of material to drain from a standardized funnel bottom container under falling head conditions. In short, thicker liquids (more viscous) drain more slowly and vice versa. The test is performed on fluids that have been passed through a No. 12 sieve whereby particles smaller than 1.6 mm (1/16 in) in diameter can be present. The maximum capacity of the funnel for testing purposes is 1500 ml, and the accompanying measuring cup can handle a little more than one quart. Whereas the test records the time for 1 quart of slurry to pass through the funnel orifice, it should be noted that the funnel still contains fluid at the completion of the test. A Marsh funnel and measuring cup are shown in Figure 2.9.

Figure 2.9. Marsh funnel and cup.

To properly measure the Marsh viscosity of a drilling fluid, the following procedures must be followed:

(1) Hold funnel in upright position with index finger over outlet.
(2) Pour the test sample through the screen in top of the funnel until the mud level just reaches the underside of the screen.
(3) Remove finger from outlet and measure the number of seconds required for a quart of fluid to run out (Wyo-Ben, 2011).

Additionally, prior to the test, the funnel opening should be checked for any obstructions. Any obstruction in the funnel will directly affect the viscosity reading. The Marsh funnel and screen should also be washed and dried after each use.

Factors that affect the measured time are usually attributed to the gel strength / meniscus action of the fluid but may also be altered by suspended solids that typically do not contribute to gel strength. As a result, Marsh funnel viscosity tests are a good method of assessing the gel strength of new slurries wherein drill cuttings have not been introduced and become suspended in the slurry. Marsh funnel tests performed after drilling operations have commenced may not be able to differentiate between true gel strength and the apparent viscosity. Verifying this limitation is one aspect of this thesis. However, two types of devices are capable of making this distinction: viscometers and rheometers.

Viscometers and rheometers both measure the true viscosity of fluids (Marsh funnel is only an indication of viscosity). Viscometers are generally simpler and less costly. For this reason they are better suited to portable applications. Rheometers tend to have a larger range of testing parameters including variable temperature and pressure. For a non-Newtonian fluid such

as slurry, a rheometer is likely a better choice because of the ability to manipulate and monitor more variables such as shear rate (IESMAT, 2015). But as slurry applications have a rather limited range of temperatures and pressures, a viscometer is a reasonable and cost effective choice.

The most important reasoning for choosing a Marsh funnel over more precise viscometers is the simplicity in the field and that close correlations have been shown (Figure 2.10). The concern when it comes to automation is the possible influences of other suspended solids on the Marsh funnel results.

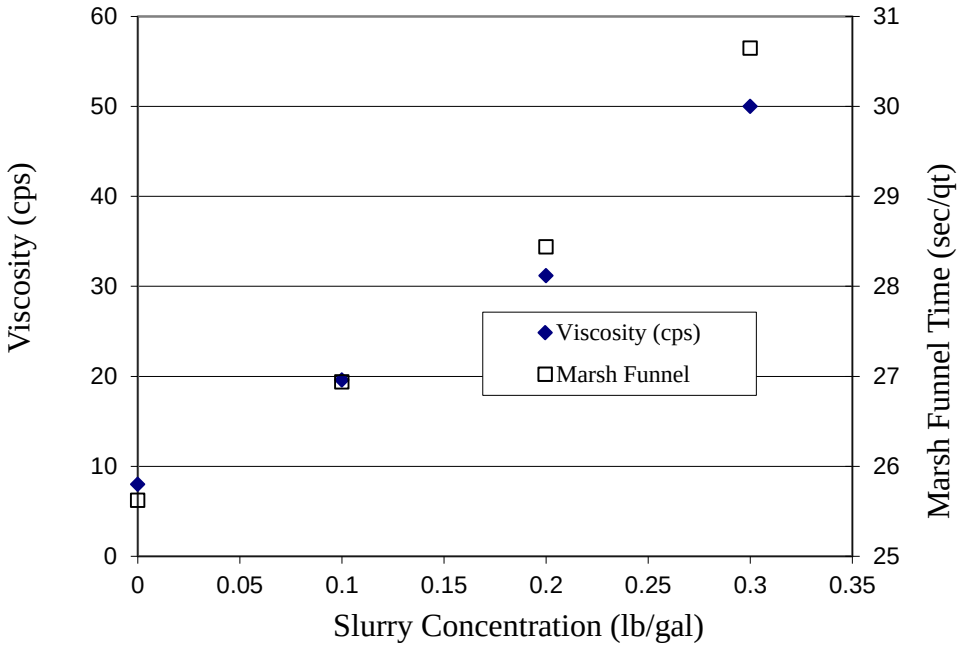

Figure 2.10. Similar responses from viscosity measured by viscometer and Marsh funnel (Mullins and Winters, 2010).

2.3.2 Concepts for Automating Viscosity Measurements

By taking a sample of slurry with a Marsh funnel test reading of 30 seconds and pumping it through an orifice while monitoring flow and pressure, a unique flow (Q) vs pressure (P) curve for a marsh funnel tested 30 second slurry may be developed. Building a collection of curves for a wide range of slurry viscosities may give the ability to define a slurry quickly and reliably by observing Q vs P data in real-time and matching the points to a specific viscosity curve. Figure 2.11 is an example of a Q vs P graph for a bentonite slurry created for another project. It is reasonable to assume that pressure will rise with the amount of bentonite product added for a given flow rate. A positive correlation between slurry concentration and pressure developed will be sought.

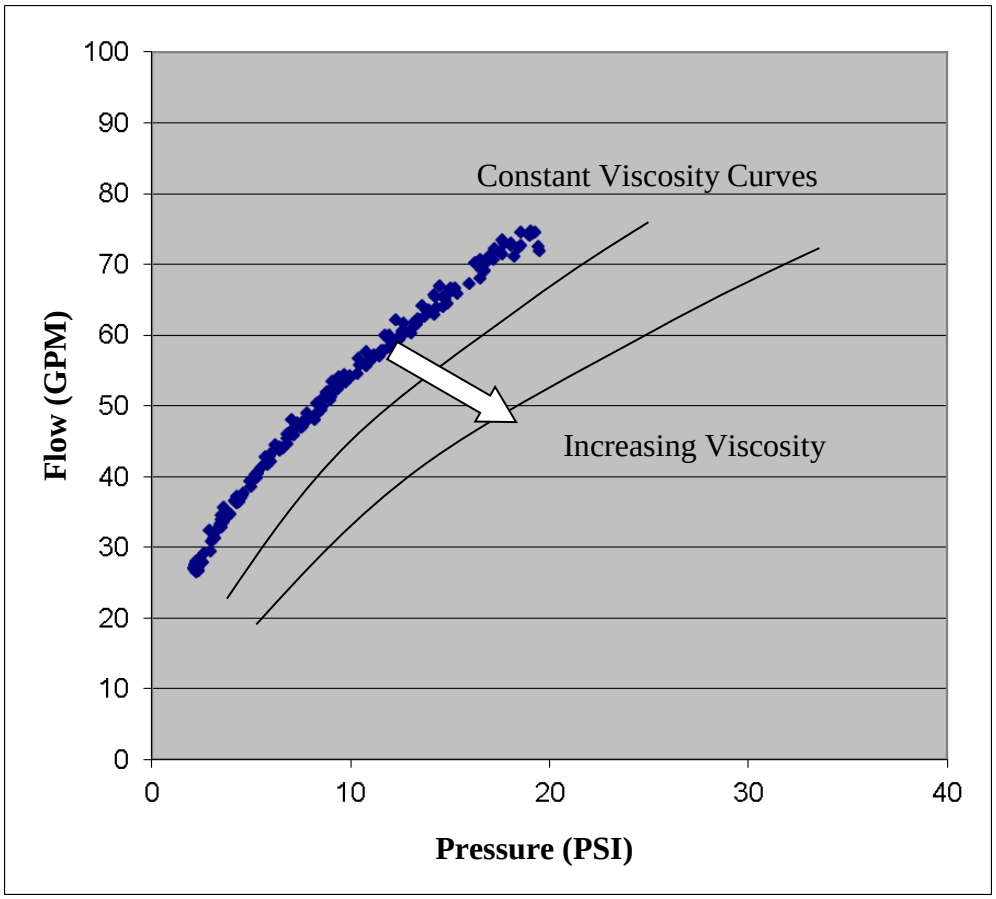

Figure 2.11. Bentonite slurry test adapted from previous study (Mullins and Winters, 2010)

2.3.3 Sensor Applications for Viscosity Measurements

Sensor applicability for viscosity determination will require measurements of both pressure and flow rate at a minimum. Selection of sensor types will be most dependent on measurement reliability. Factors like viscosity or amount of suspended solids affect different types of sensors in different ways. The 4 basic types of flow sensors being investigated for this thesis are differential pressure, electromagnetic, ultrasonic and mass.

Differential pressure flow meters work by reading a pressure loss across some type of flow restriction. From Bernoulli's equation illustrated in Figure 2.12, the pressure loss increases with the increase of velocity which is related to flow rate by the cross sectional area of the passage.

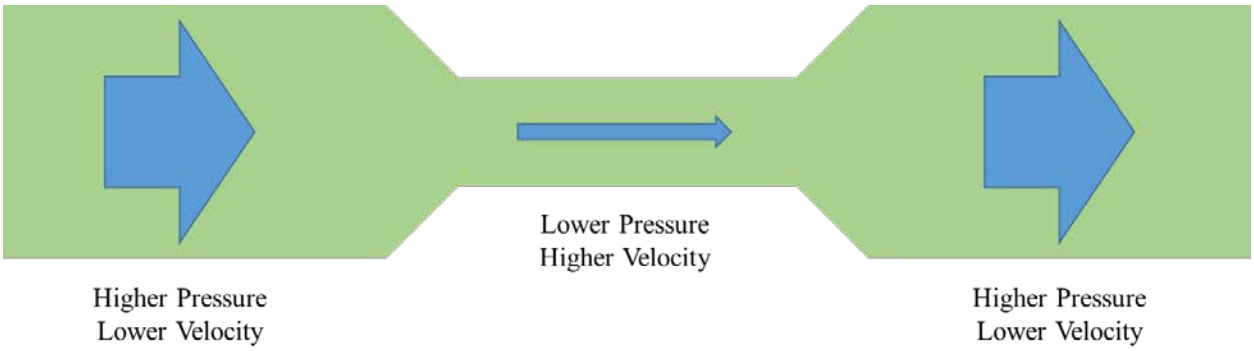

Figure 2.12. Bernoulli principle illustrated

Electromagnetic flow meters or "magmeters", operate utilizing Faraday's law of electromagnetic conduction. A magnetic field is introduced through the cross section of the pipe. A "…flow of a conductive liquid through the magnetic field will cause a voltage signal to be sensed by electrodes located on the flow tube walls. When the fluid moves faster, more voltage is

generated" (Universal Flow Monitors, 2015). Figure 2.13 displays an exploded concept view of a magmeter.

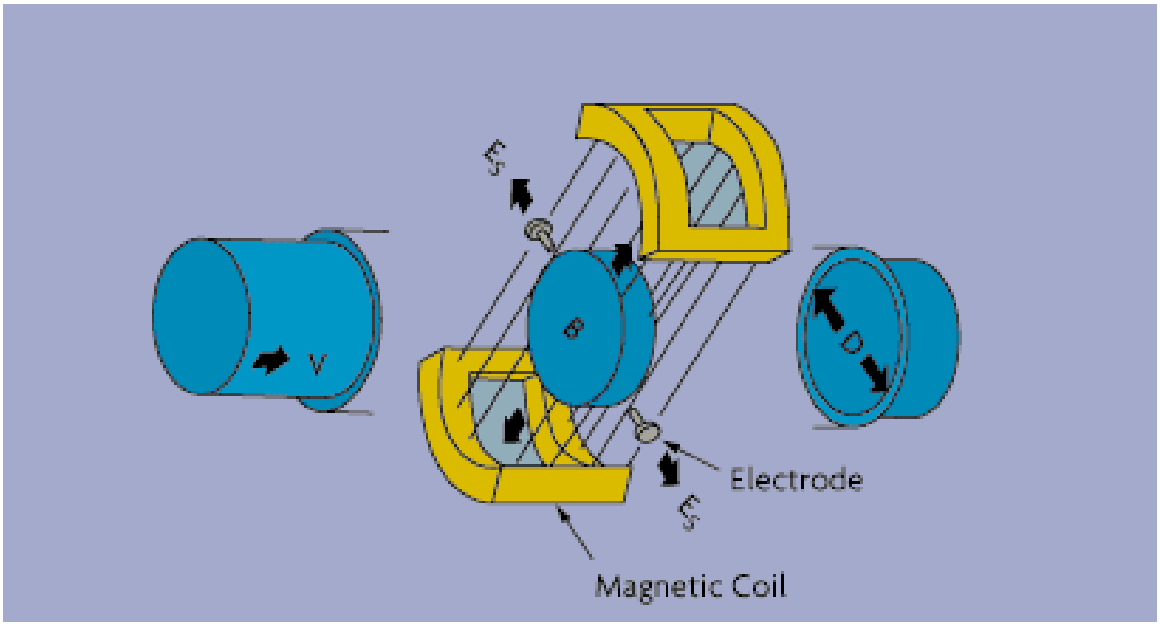

Figure 2.13. Components of electromagnetic flow meter or magmeter (Omega, 2015d)

Ultrasonic flow meters can be divided into two categories. Some use the Doppler shift to quantify flow. Others use the flight time difference of an ultrasonic signal being sent between two transducers, once with the signal against flow and once in the direction of flow (Omega, 2015e). This type of sensor is called a time-of-transit sensor. For the purpose of measuring flow of slurry from a jobsite, the Doppler shift sensor is more fitting, as the time-of-transit approach requires cleaner fluid (Omega, 2015f). The Doppler shift ultrasonic flow meter uses two transducers, one that emits an ultrasonic pulse, and another that receives the reflected pulse. The difference of the transmission frequency and the reflected frequency is a function of the velocity of the particle that reflected the sound wave. Figure 2.14 displays the Doppler sensor setup.

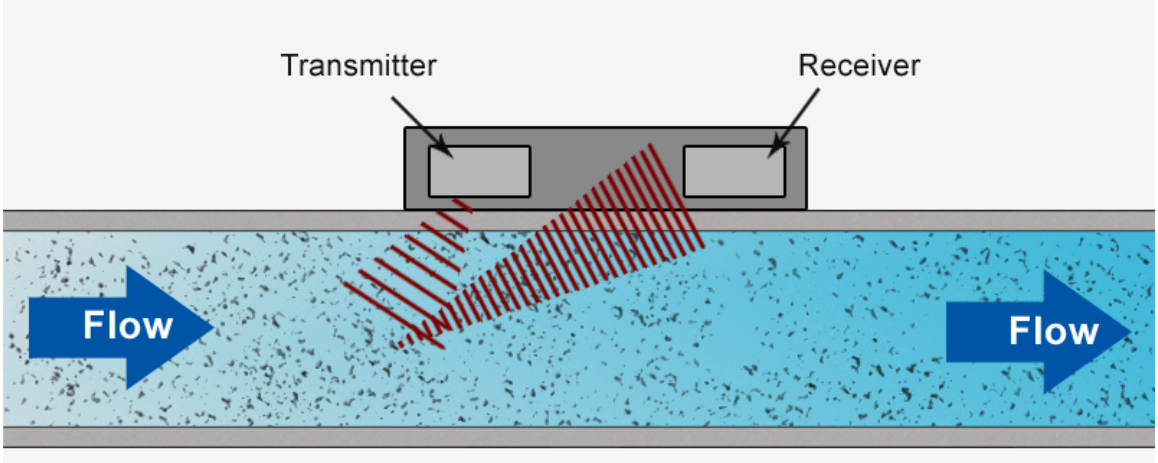

Figure 2.14. Doppler flow meter (Alicat, 2015)

Coriolis flow meters work by inducing movement in the form of vibrations into tubes through which fluid is flowing. The deflecting force (twist) on the pipe measured as a result of the Coriolis effect from the fluid flow is a function of mass flow rate (Omega, 2015g).

2.3.4 Sensor Availability for Viscosity Measurements

Concepts shown in Figures 2.12-2.14 are easily found implemented in readily available sensors. Figures 2.15 and 2.16 are examples of some currently produced sensors.

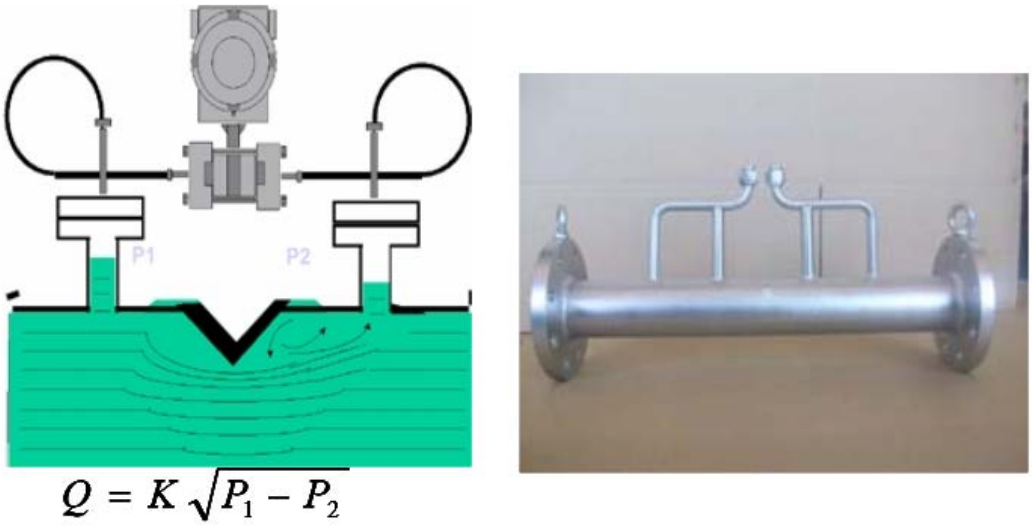

Figure 2.15. Differential pressure flow meter (Smart Measurement, 2015)

(a) (b)

Figure 2.16. Flow metering devices. (a) Electromagnetic flow meter (Omega, 2015i), (b) Ultrasonic Doppler flow meter (Omega, 2015j) © OMEGA ENGINEERING, INC. ALL RIGHTS RESERVED. REPRODUCED WITH THE PERMISSION OF OMEGA ENGINEERING, INC., STAMFORD, CT USA 06907, www.omega.com

Each flow sensor has unique limitations and reactions to different variables. These limitations must be identified and may be utilized for the benefit of the thesis. For instance, if a flow sensor used for the thesis is found to be sensitive to sand content, comparing data with another sensor known to be unaffected may give insight into the measure of sand content. This will only be possible if the skewed readings from the sand sensitive sensor are repeatable.

2.4 Sand Content

As previously mentioned, the sand content of a drilling fluid directly affects the density of the material which is really only a problem when concreting a shaft. However, sand content of a drilling fluid plays other confounding roles as well with regards to altering viscosity. Therefore, it is conceivable that sand content could artificially inflate viscosity and density to

within acceptable levels when there is very little mineral slurry product present. Some work has been done in this area, but making a definite determination of these effects is a primary step in automating slurry property measurements.

As the minimum viscosity limit (e.g. 30 sec/qt) largely controls the minimum slurry mix ratio (lbs dry powder per gallon of water), it therefore also controls the gel strength and sand suspension capability. As a result, only lower sand contents can be suspended in lower viscosity slurry. Therefore, soils that use (or can tolerate) lower viscosity slurry may not be able to hold the 4% maximum permissible sand content. Conversely, excavations in free flowing soils, that require higher viscosity slurry, could conceivably suspend even higher sand contents (hence, the concept of sliding scale based on sliding suspension capabilities). Higher sand contents are typically also controlled by upper density limits; although as mentioned above, the density level at which the slurry is too dense to be displaced by 135-140pcf fluid concrete has not been documented in the literature.

2.4.1 Existing Methods to Measure Slurry Sand Content

A sand content test kit consists of a vial with measured volume markings, a #200 sieve, and a funnel. When filled to the "Mud to Here" line, 25 ml of drilling fluid is in the vial. The percent volume markings are based on this volume of fluid, with 1% of the volume corresponding to 0.25 ml. A sand content test kit is shown in Figure 2.17.

Figure 2.17. Sand content testing kit.

To properly measure the sand content of a particular drilling fluid, the following procedures must be followed:

(1) Fill the sand content tube to the indicated mark with mud ["Mud to here" line]. Add water to the next mark ["Water to here" line]. Close the mouth of the tube and shake vigorously.

(2) Pour the mixture onto the clean, wet screen. Discard the liquid passing through the screen. Add more water to the tube, shake, and again pour onto the screen. Repeat until the wash water passes through clear. Wash the sand retained on the screen to free it of any remaining mud.

(3) Fit the funnel upside down over the top of the screen. Slowly invert the assembly and insert the tip of the funnel into the mouth of the tube. Wash the sand into the tube by spraying a fine spray of water through the screen (Tapping on the side of the screen with a spatula handle may facilitate this process). Allow the sand to settle, from the graduations on the tube, read the volume percent of the sand.

(4) Report the sand content of the mud in volume percent. Report the source of the mud sample. Coarse solids other than sand will be retained on the screen (e.g., lost circulation material, coarse barite, coarse lignite, etc.) and the presence of such solids should be noted.
(Wyo-Ben, 2011).

2.4.2 Concepts for Automating Sand Content Measurements

The simplest automated computation of sand content would come from correlations between pressure, flow rate and density. If viscosity is relatively insensitive to sand content, then the density provides the answer to the suspended solids content. Referring to Figure 2.11 above, the pressure that develops from a given flow rate identifies the viscosity. The difference in density between that normally associated with clean slurry would then be caused by suspended sand content. This would then require an inputted value of the baseline density of the slurry when introduced or a correlation from a library of slurry products. For example, Pure Gold bentonite slurry has a density of 64pcf for a 40 sec/qt slurry; high yield slurry would have a density closer to 63pcf for the same viscosity.

As mentioned in section 2.3.4, discrepancies in flow meter readings caused by the introduction of sand into slurry may also provide a means of measuring sand content. The 2nd portion of the thesis will be primarily motivated by testing flow rates of pure slurry with different types of flow meters. Then, by systematically adding sand to the slurry mix and observing flow readings, trends in the data may be identified in some meters that are correlated with the addition of sand.

2.4.3 Sensor Applications for Sand Content Measurements

The sensors listed in sections 2.3.3 and 2.3.4 will also be used to potentially measure sand content. The differential pressure flow meter will most likely be the least affected by sand content. If so, it will be used as the true flow rate, which may then be compared to sand affected flow meter data.

2.4.4 Sensor Availability for Sand Content Measurements

For the flow sensors mentioned above, see section 2.3.4. An alternative way to determine sand content is by using a device made by Hoffman & Hoffman. The SandSense SWD-3 is a particle counting device made to only count particles in the grain size range of sands (Hoffman, 2015). This device is large and weighs 36lbs.

2.5 pH

In an aqueous solution, there is an equilibrium of hydrogen ions (H+), and hydroxide ions (OH-). A pH number is the negative logarithm of the hydrogen ion concentration in a solution. On the pH scale, the full range is 0 to 14 and 7 is neutral. The further a pH number is below 7, the more acidic the sample is and similarly, above 7 denotes an alkaline reading.

Any addition of (acidic) hydrogen ions will decrease the (basic) concentration of hydroxide ions in a solution, thus making the solution decrease in pH. Soils with a strong presence of organic matter are acidic and if drilling in such soils occurs, the slurry pH can drop out of the target range. State specifications set the acceptable pH range from 8 to 11 (Table 2.1).

The quickest and simplest test used to monitor drilling fluid is a pH test. Manufacturers of drilling fluids and additives typically recommend a working pH range for their products of 8 to 10, depending on the product and the manufacturer. pH tests are first used to measure the quality of the mix water prior to introduction of drilling products. Potable water sources are usually near 6.5 to 7.5 which is typically considered to be too low to fully utilize some drilling fluids. If a potable water source is not available, water sources on site may be used, but might

exhibit even lower pH values. A rough rule of thumb for treating mix water is to use 4lbs of soda ash per 1000gals to bring neutral pH water to the correct manufacturer recommended levels (8 to 10). After initial mixing, pH is a relatively less important parameter; viscosity is the most important to borehole stability; density and sand content only important during concreting. If density, viscosity and sand content are satisfied at the time of concreting, pH has little bearing. But as noted earlier, the pH of the drilling fluid in use should be monitored while excavating since soil conditions can affect the pH of the drilling fluid.

2.5.1 Existing Methods to Measure Slurry pH

To monitor pH, two methods are available: pH strips (litmus paper) or a pH meter. Litmus is a weak acid and organic dye that is an acid-base indicator (Rutgers, 2015). This means that paper coated with litmus changes color when exposed to different pH conditions. When hydroxide ions of a basic solution are introduced, red litmus paper turns blue. When allowed to react with an acidic solution, blue litmus paper turns red. Litmus paper contains several reactive plates which change color when dipped into the drilling fluid. The colors are then matched up to a color key provided by the test strip manufacturer.

pH meters provide even greater ease of use; after placing the pH probe in the drill fluid, the pH is output to a digital screen on the device. Unfortunately, pH meters are prone to errors associated with probe contamination and require frequent calibration with control (known pH) fluids. Both pH strips and a pH meter are shown in Figure 2.18.

Figure 2.18. pH meter and strips

2.5.2 Concepts for Automating pH Measurements

As pH is a chemical reactivity measurement, concepts for automation have been thoroughly vetted by commercial equipment vendors. While pH is the least important and is rather only an indicator of why a slurry may be performing poorly, less focus will be placed on this parameter within this thesis.

2.5.3 Sensor Applications for pH Measurements

Off-the-shelf sensors will be sought that can be used in a pressurized state or within the pressure, flow, and density measuring devices. Industrial sensors are again the most likely choice as abrasion from particles in fluid flow could deteriorate the probe / sensor.

2.5.4 Sensor Availability for pH Measurements

A pH sensor currently on the market is shown in Figure 2.19. It is made to be used in-line using a threaded body design and pressurized application compatibility.

Figure 2.19. Available instrumentation for pH determination. PHE-5580-20 (Omega, 2015k)

With a wide range of off-the-shelf devices, the thesis goal of developing an automated slurry testing device was made possible. However, refining the selection of these devices formed the basis for the next two chapters.

CHAPTER 3: COMPONENT DEVELOPMENT AND TESTING

3.1 Overview

The overall goal of this thesis was to design and build an all-in-one slurry monitoring system capable of automatically measuring the viscosity, density, and sand content. As outlined in Chapter 2, the monitoring system was anticipated to use off-the-shelf instrumentation, but the Marsh funnel test, the standardized field test established for the measurement of slurry viscosity, does not lend itself to off-the-shelf product selection. It was therefore necessary to develop another method of determining viscosity. The proposed method would take advantage of the concept that a slurry with a given viscosity will produce a unique flow (Q) versus pressure (P) curve such as the one shown in Figure 2.11. Further verification of the flow-pressure relationship is presented, including the design of a practical means to generate and collect continuous flow and pressure data in real-time.

This chapter is divided into three sections: Section 3.1 presents the flow-pressure relationship as a function of slurry viscosity. This required developing a family of curves for a wide range of slurry viscosities and necessitated the design and construction of a laboratory experiment capable of accurately measuring the flow of a specific viscosity of slurry associated with a particular pressure. Section 3.2 shows what, if any, impact high levels of sand content has on the flow-pressure response of slurry. This was determined by repeating the first objective's experiments with slurries having similar viscosities but with high sand contents and comparing

the flow-pressure curves of the two. It should be noted that higher viscosity / higher clay content slurry can suspend higher sand contents and vice versa. Section 3.3 presents the design and construction of the viscosity monitoring component of the all-in one monitoring system. The objective included designing a slurry pumping system with instrumentation for monitoring both flow rate, pressure and density which included determining the optimum orifice diameter and length as it relates to the flow-pressure curves.

3.1.1 Proof of Concept for Automating Viscosity Measurements

By taking a sample of slurry with a known Marsh funnel test reading (e.g. 30sec/qt) and pumping it through an orifice while monitoring flow and pressure, a unique Q vs P curve for that Marsh funnel tested slurry may be developed. Building a collection of curves for a wide range of slurry viscosities can give the ability to define a slurry quickly and reliably by observing Q vs P data in real-time and matching the points to a specific viscosity curve.

Figure 3.1 is an example of a Q vs P graph for a bentonite slurry. It is reasonable to assume that pressure will rise with the amount of bentonite product added for a given flow rate. To this end, a simplified laboratory experiment was designed to verify the unique relationship between pressure and flow for a wide range of viscosities. In addition, to quantify the possible impacts of high sand contents on slurry viscosities, a second series of tests was performed using the same experimental design but on a slurry mixture which had additional sands added to increase its sand content.

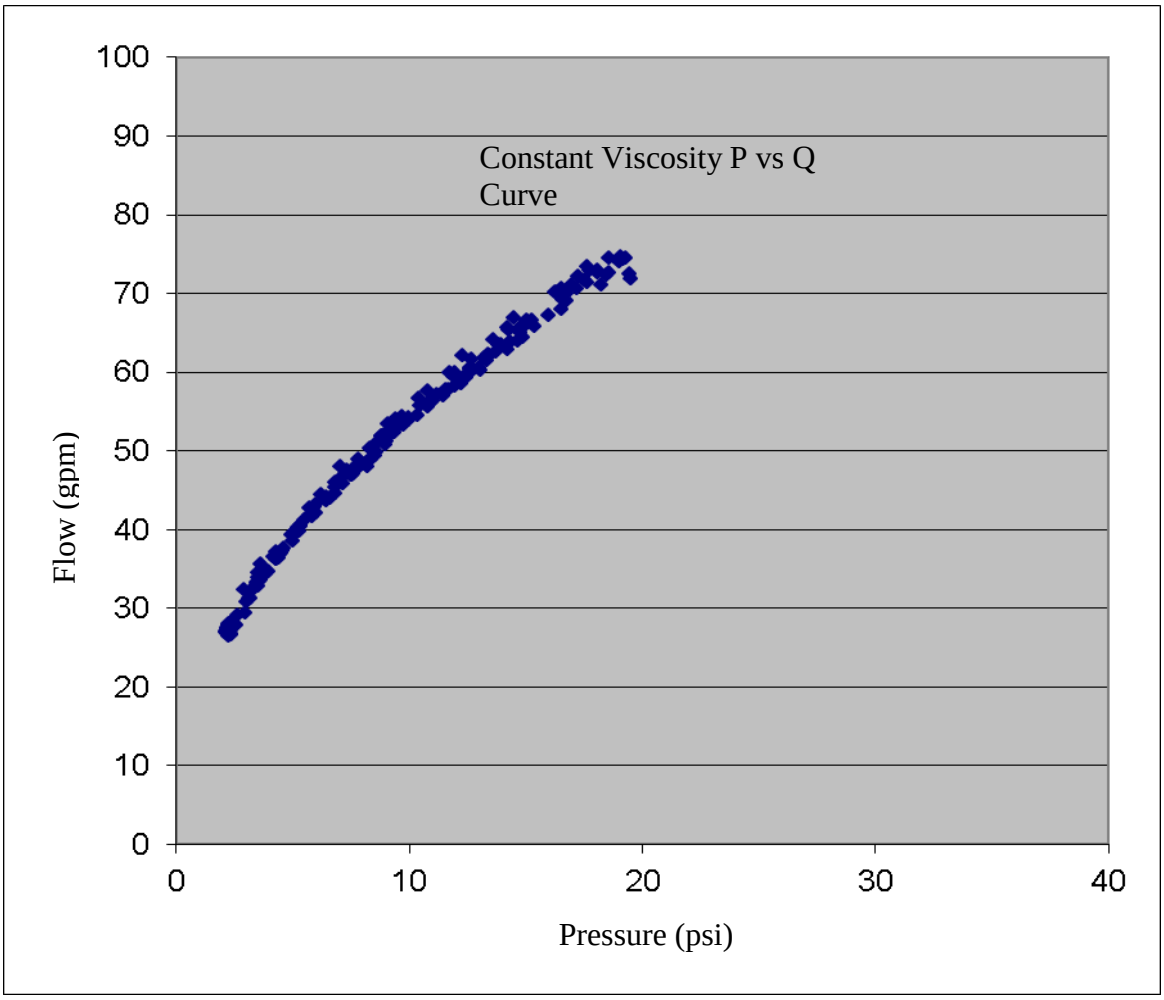

Figure 3.1. Constant viscosity concept curve adapted from previous study (Mullins and Winters, 2010)

3.1.2 Experimental Design and Set-up

To provide a broad range of flow versus pressure curves, five different viscosities were chosen for testing (30, 40, 45, 60 and >90 seconds). A falling head test system was designed and fabricated that could precisely reproduce the same conditions. As designed, the falling head system consists of a 115.25in long, 6in ID clear PVC tube (Figure 3.2) and a Marsh funnel and stopper latch system which was attached to the test tube using a 6in rubber coupler and 2 adjustable straps (Figure 3.3)

Figure 3.2. 115.25in tall falling head test column

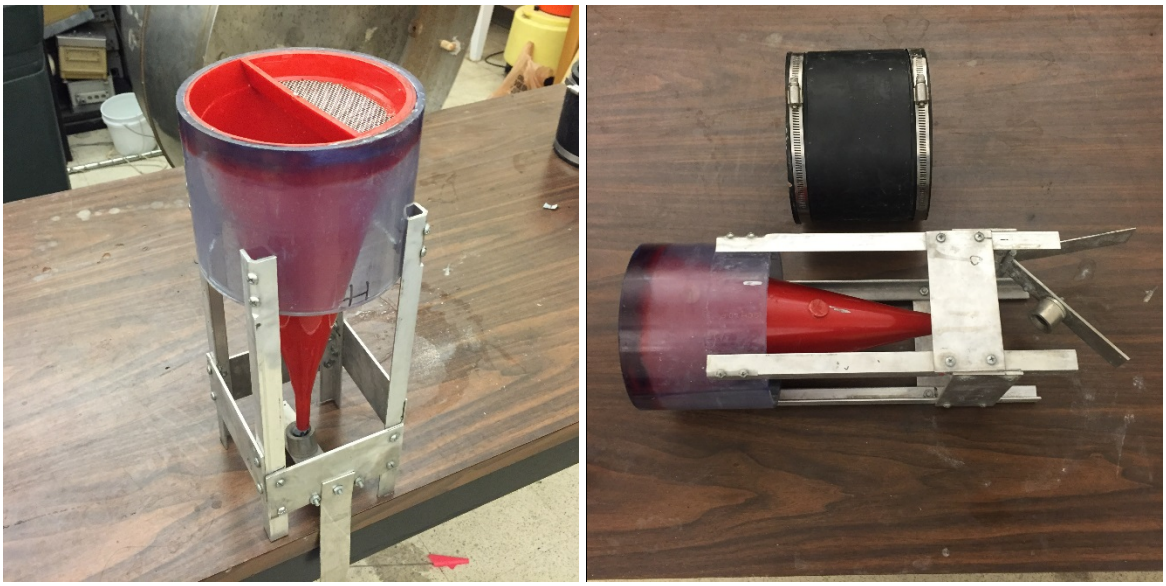

Figure 3.3. Marsh funnel attachment with stopper latch system and coupler

During an experiment, the stopper/latch system was locked shut and the PVC tube was filled to a fixed level with slurry. Once filled, the stopper/latch system was released, which allowed the slurry to discharge through the 3/16in diameter opening of the Marsh funnel.

The falling head test tube system was suspended from a 15 foot tall column using a 0.5in x 4in eye bolt attached to a 2in by 6in 0.5in thick steel plate system. Bolted through the steel are two 0.25in threaded steel rods which are mounted to the end of the falling head tube via 2 large screw clamps and a heavy-duty rubber PVC coupling (Figure 3.4).

Figure 3.4. Falling head test tube system suspended from 15 foot tall column

Instrumentation for the falling head system consisted of two components, one measuring the change in weight of the entire column with slurry as it discharged from the tube and the other to measure the changing head pressure of the slurry within the tube. An Omega LC105-500 S type dyne load cell was used to measure the weight of the falling head system. The LC105-500 has a 500lb capacity requiring 10Vdc excitation with a 3mV/V output (Figure 3.5). A flush mounted Honeywell model AB_HP 6 psi 100mV/5V pressure transducer was installed to

measure fluid head pressure. The transducer was located 4 inches from the bottom of test tube and a total of 18 inches above the 0.1875 inch diameter opening of the Marsh funnel (Figure 3.6).

Figure 3.5. Omega S type dyne load cell

Figure 3.6. Honeywell pressure transducer positioned 18 inches from bottom of Marsh funnel

Data from the instrumentation was collected and monitored by an Optim Electronics 5108AC Megadac acquisition system. (Figure 3.7)

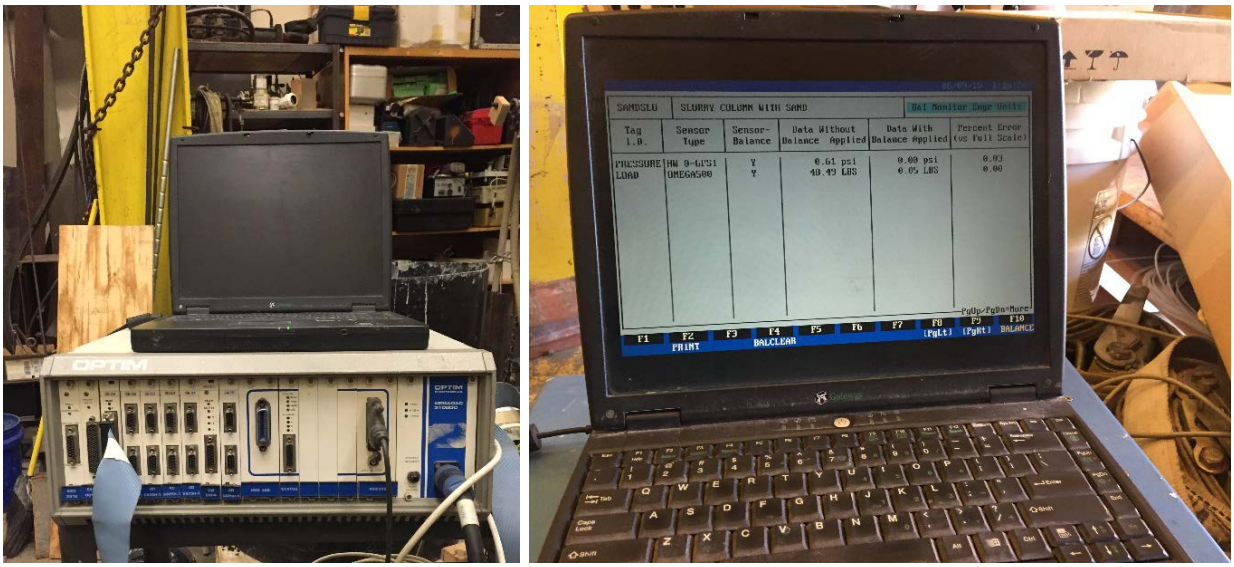

Figure 3.7. Megadac acquisition system with screen monitoring during test

In addition to the falling head system, it was also necessary to fabricate the slurry holding/mixing tank and piping system to delivery slurry the slurry column. The slurry tank was 31 inches in diameter and 36 inches tall with a side mounted 2in diameter outlet pipe and ball valve. The tank was connected to a Flowtec Thermoplastic 1.5 HP pump which is rated to flow at 45 gpm at 10ft of lift and 30psi. The pump discharged to a flexible 1in tube which could be attached to the slurry mixing/delivery piping system or used to mix slurry directly in the slurry tank (Figure 3.8).

Figure 3.8. Slurry mixing/delivery system with system discharging to holding tank

The slurry mixing/delivery piping system was constructed of 1in diameter schedule 40 PVC pipe. Slurry is pumped from the holding tank through the 1in diameter hose that is connected to a 1in PVC tee fitting. Flow rate and direction of the pumped slurry were then controlled by adjusting the ball valves located on both discharge arms of the tee fitting with one arm discharging downward to recirculating/mixing slurry back to slurry tank and the other arm routing the slurry upward to the top of the falling head tube (Figure 3.9).

Figure 3.9. Slurry mixing/delivery system flow valves and slurry discharge point at top of tube

3.1.3 Batch 1 Slurry Preparation and Testing

The first step of the Batch 1 slurry preparation process began with the mixing water. 50 gallons of water were placed in the slurry holding tank and the pH of the water was tested and found to have a pH of 7. 91 grams of CETCO Sodium Carbonate pH adjuster (soda ash) was added to the 50 gallons of tank water which brought the water to the target pH of 9. To maximize mixing efficiency, the soda ash was added to the water using a non-clog funnel-fed Hootonanny eductor (Figure 3.10).

Figure 3.10. Mixing water pH test before and after introduction of soda ash through Hootonanny eductor

The next step involved adding a predetermined amount of slurry powder to the mixing water to produce the desired 90-second viscosity. Using a mix ratio from previous test data, 50lbs of CETCO PUREGOLD GEL Bentonite powder was added to the 50 gallons of water. A rapid hydration Hootonanny was used to maximize the mixing hydration process. Directly after mixing, the viscosity of the slurry was tested using a Marsh Funnel and was determined to be 75sec/qt (Figure 3.11).

Figure 3.11. Addition of bentonite powder through Hootonanny eductor (left) and viscosity testing of slurry (right)

To ensure full hydration, the initial slurry mix was allowed to set for 24 hours before beginning the falling head tests. After the 24 hour set period, and before the first falling head test, the slurry was recirculated for 5 minutes. After being recirculated, the slurry had a viscosity of 113 sec/qt.

After the slurry recycling was completed, the flexible hose from the FlowTec pump was attached to the slurry mixing/delivery piping system tee fitting and the slurry was pumped into the falling head tube system using the previously described ball valve configuration to control the rate and direction of flow. The tube was filled to a preset level 9.5in from the top of the tube (Figure 3.12 and Figure 3.13).

Figure 3.12. Filling test tube with slurry

Figure 3.13. Filling test tube to level 9.5in from top of tube

At this level, the slurry was 119.5in above the end of the Marsh funnel and 101.5in above the Honeywell pressure transducer. Once the tube was filled, the stopper/latch system was released and the slurry freely discharged from the Marsh funnel until the tube was empty (Figure 3.14).

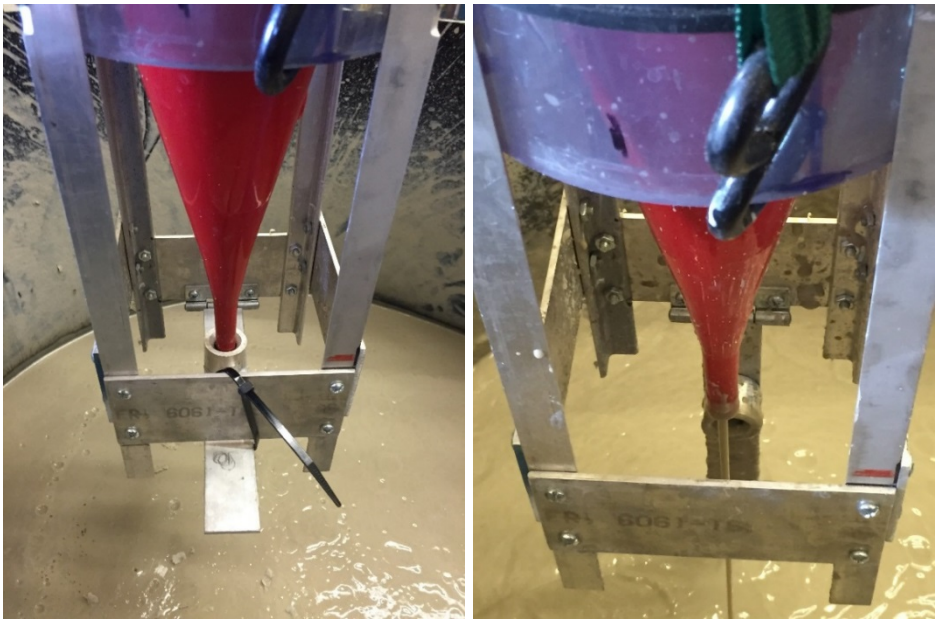

Figure 3.14. Stopper latch system in closed and open configuration

During these tests, changes in both weight and pressure head of the slurry were monitored and recorded. An example of the raw data collected is presented below in Figures 3.15 and 3.16.

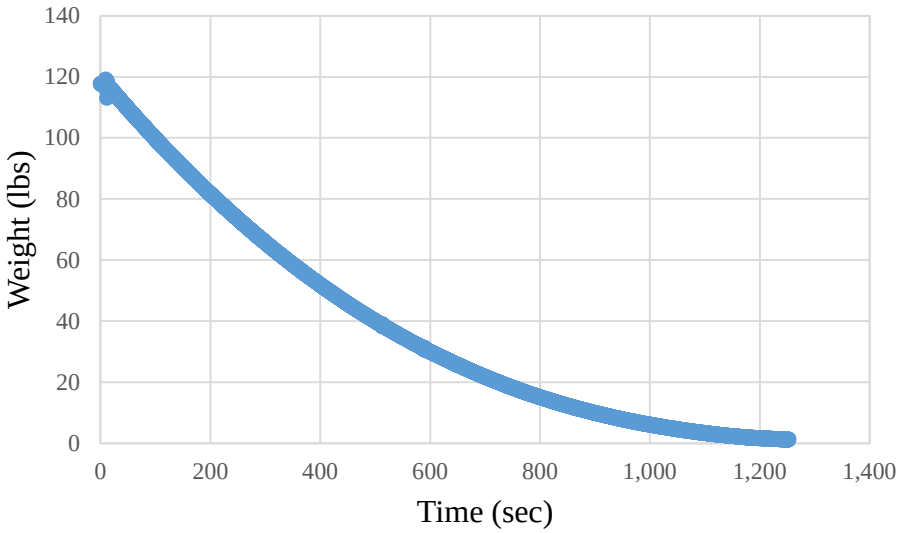

Figure 3.15. Batch 1 test 1 weight data

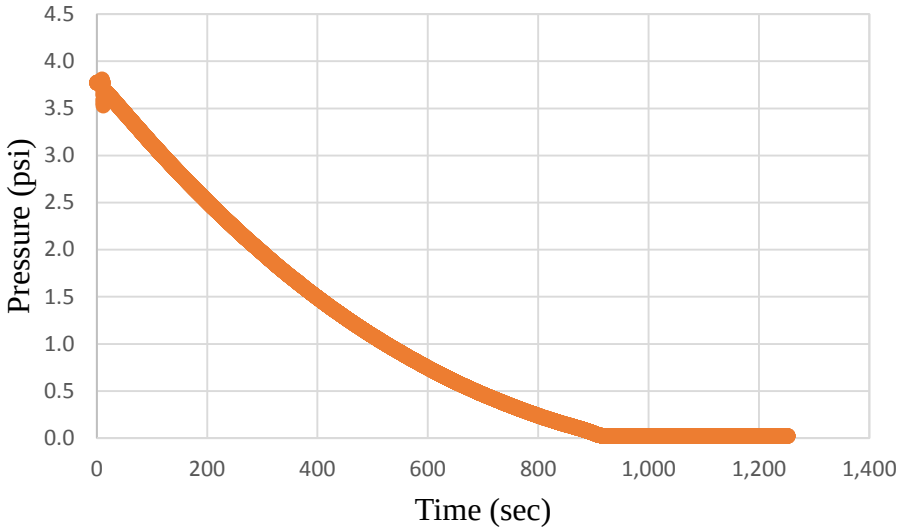

Figure 3.16. Batch 1 test 1 pressure data

It should be noted that the raw pressure data reached a zero value before the weight data. This was due to the location of pressure transducer being 18 inches above the discharge point of the falling head system. Therefore the transducer did not account for the pressure exerted by the last 18 inches of slurry as it discharged from the Marsh funnel.

The complete set of all the raw data graphs generated from Batches 1 through 5 may be found in Appendix A1.

Viscosity, density and sand content of the discharging Batch 1 slurry were also measured. Slurry viscosity was measured using a Marsh funnel. To confirm that the slurry was uniform throughout the entire process, viscosity of the discharging slurry was also taken at several different times/elevations during the course of each test (Figure 3.17).

Figure 3.17. Pulling sample for viscosity testing

Once the tube had completely drained, the outlet of the test tube Marsh funnel was fastened shut, the slurry column refilled and a second test started. Table 3.1 presents the viscosities for all three Batch 1 tests.

Table 3.1. Batch 1 viscosity test results

Test 1			Test 2			Test 3		
Time	Height	Viscosity	Time	Height	Viscosity	Time	Height	Viscosity
(sec)	(in)	(sec/qt)	(sec)	(in)	(sec/qt)	(sec)	(in)	(sec/qt)
0	109.14	86.72	26	104.29	87.03	2	107.88	91.97
293	60.76	89.28	198	74.72	94.62	207	72.54	95.87
506	35.78	93.07	460	40.34	99.22	435	42.69	98.56
723	18.07	95.84	682	20.87	101.32	674	21.20	105.07

Density was measured only once at the beginning of the first of the three Batch 1 tests with the test sample being taken directly from the discharge end of the falling head testing tube. The density of the Batch 1 slurry was 1054.3 grams/liter and was measured using a KIMAX 1000 mL volumetric flask and a Veritas L10001 precision scale in lieu of the field density balance (Figure 3.18).

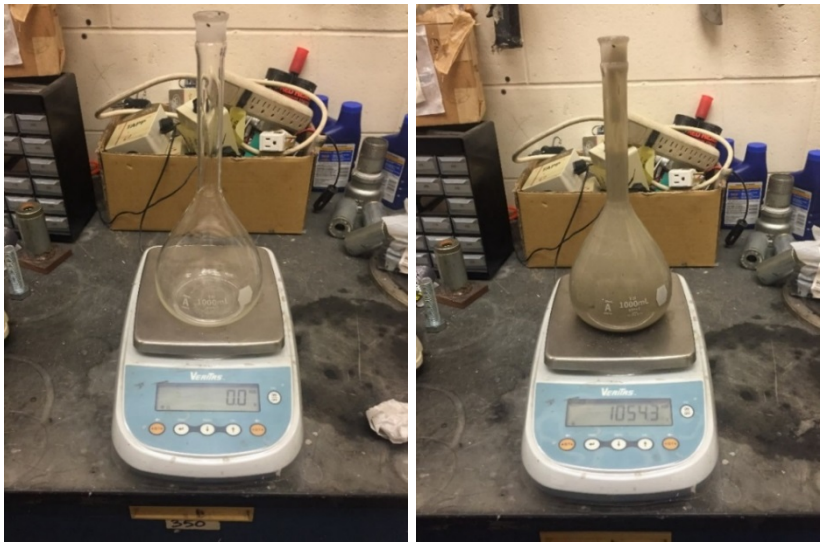

Figure 3.18. Measuring density of slurry sample.

Batch 1 sand content was also measured just once from a sample taken at the beginning of the Batch 1 test which had a value of 0.25%. The sand content was measured by performing test method FM 8-RP13B-3 sand content test with a sand content kit part no. 400010001EA (Figure 3.19).

Figure 3.19. Sand content kit and sand content testing

3.1.4 Batch 2 Slurry Preparation and Testing

Upon the completion of the three Batch 1 tests, 5 gallons of slurry were removed from the slurry holding tank and replaced with a like volume of pH corrected water; the net effect reducing the slurry viscosity for the next tests. The slurry/water combination was then pumped through the slurry mixing/delivery system for 5 minutes to thoroughly mix the combination while flushing any of the Batch 1 slurry from the test tube.

As with Batch 1, a total of 3 falling head tests were performed on the slurry measuring the changes in weight and pressure. An example of the Batch 2 raw data collected is presented in Figures 3.20 and 3.21

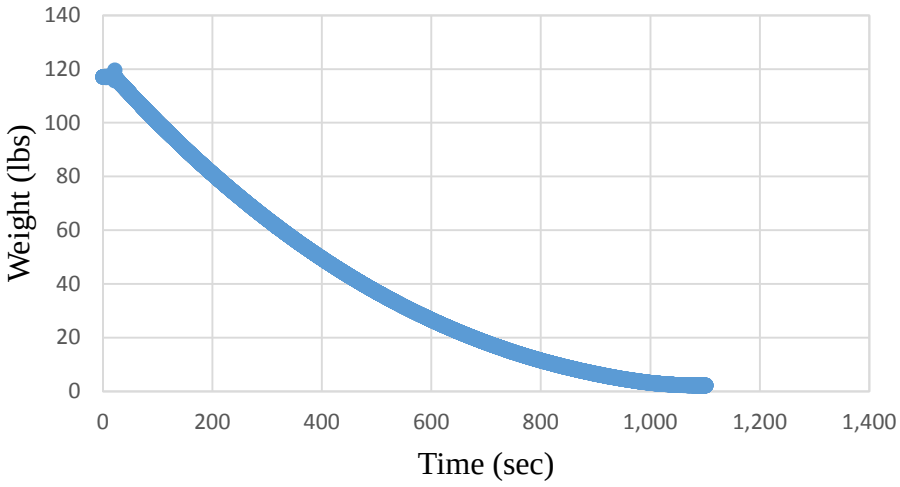

Figure 3.20. Batch 2 test 1 weight data

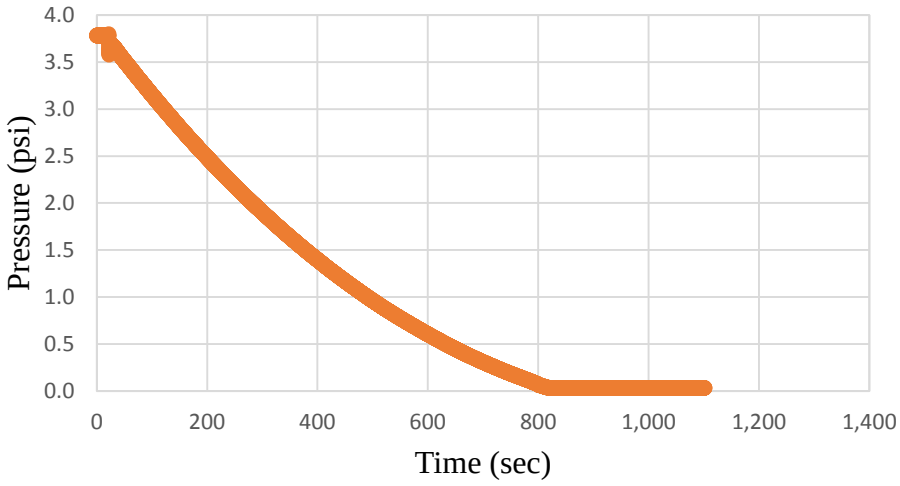

Figure 3.21. Batch 2 test 1 pressure data

Using the same tests and procedures performed during the Batch 1 test, both the density and sand content of the Batch 2 slurry were measured giving a density of 1046.6 grams/liter and a sand content of 0.25%.

Viscosity of the discharging slurry was also taken at several different times/elevations during the course of each of the three tests. The results of the tests are presented in Table 3.2.

Table 3.2. Batch 2 viscosity test results

Test 1			Test 2			Test 3		
Time	Height	Viscosity	Time	Height	Viscosity	Time	Height	Viscosity
(sec)	(in)	(sec/qt)	(sec)	(in)	(sec/qt)	(sec)	(in)	(sec/qt)
0	109.63	59.75	0	109.46	59.00	0	106.76	63.02
155	80.10	59.97	170	77.64	60.25	111	81.93	62.84
344	51.02	60.25	335	52.45	61.59	221	60.20	64.50
521	30.45	62.00	506	32.21	61.72	398	32.16	64.59

3.1.5 Batch 3 Slurry Preparation and Testing

Upon completion of the three Batch 2 tests, 5 gallons of slurry were again removed from the slurry holding tank and replaced with a like volume of pH corrected water. The slurry/water combination was then pumped through the slurry mixing/delivery system for 5 minutes to thoroughly mix the combination while flushing any of the Batch 2 slurry from the test tube.

As with Batch 2, a total of 3 falling head tests were performed on the slurry measuring the changes in weight and pressure. An example of the Batch 3 raw data collected is presented in Figures 3.22 and 3.23.

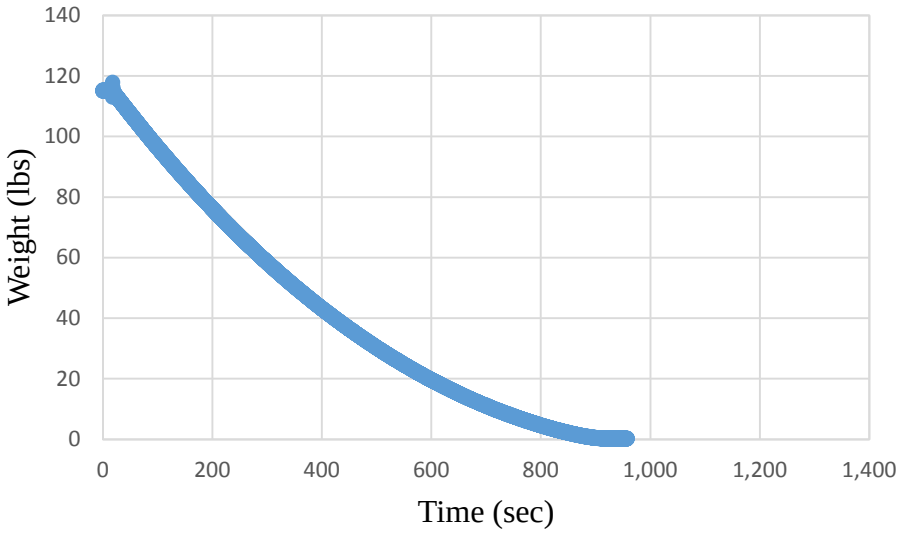

Figure 3.22. Batch 3 test 1 weight data

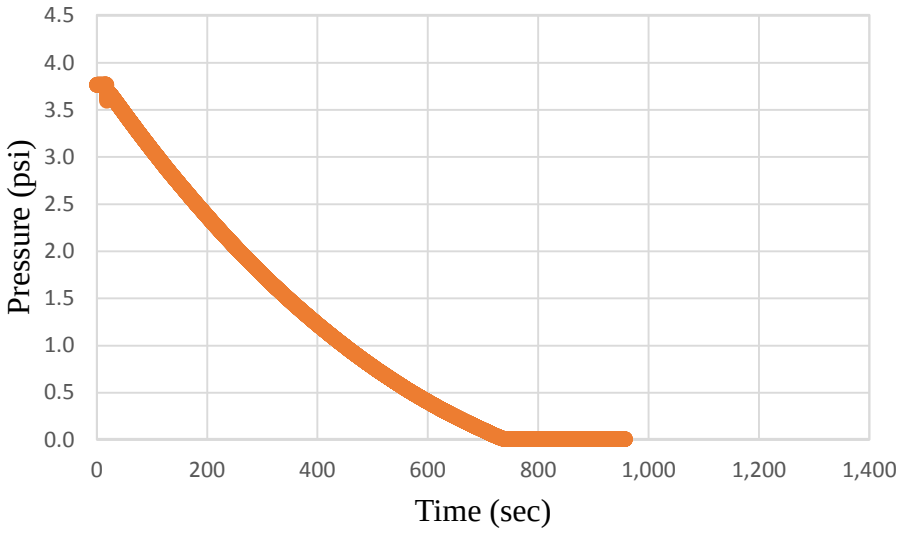

Figure 3.23. Batch 3 test 1 pressure data

Using the same tests and procedures performed during the Batch 1 test, both the density and sand content of the Batch 3 slurry were measured giving a density of 1041.9 grams/liter and a sand content of .25%.

Viscosity of the discharging slurry was also taken at several different times/elevations during the course of each of the three tests. The results of the tests are presented in Table 3.3.

Table 3.3. Batch 3 viscosity test results

Test 1			Test 2			Test 3		
Time (sec)	Height (in)	Viscosity (sec/qt)	Time (sec)	Height (in)	Viscosity (sec/qt)	Time (sec)	Height (in)	Viscosity (sec/qt)
16	106.20	44.69	27	105.88	43.97	24	105.24	44.03
150	84.57	43.84	145	81.75	45.00	146	85.37	44.35
264	68.59	43.97	273	59.19	45.06	285	65.80	45.41
394	52.63	44.53	430	40.52	44.72	430	48.11	45.41
733	23.49	45.81	571	21.14	44.59	701	23.66	44.97

3.1.6 Batch 4 Slurry Preparation and Testing

Upon completion of the Batch 3 tests, 5 gallons of slurry were once again removed from the slurry holding tank and replaced with a like volume of pH corrected water. The slurry/water combination was then pumped through the slurry mixing/delivery system for 5 minutes to thoroughly mix the combination while flushing any of the Batch 3 slurry from the test tube.

As with Batch 3, a total of 3 falling head tests were performed on the slurry measuring the changes in weight and pressure. An example of the Batch 4 raw data collected is presented below in Figures 3.24 and 3.25.

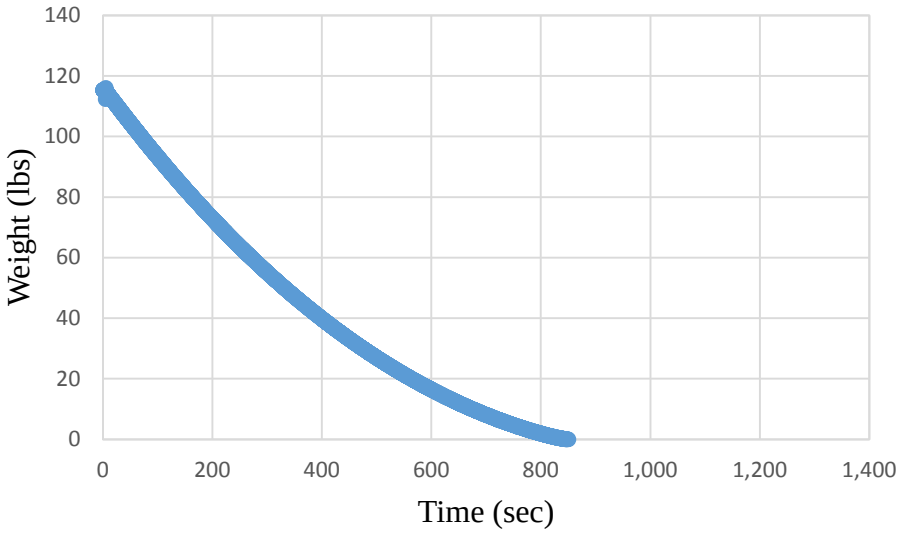

Figure 3.24. Batch 4 test 1 weight data

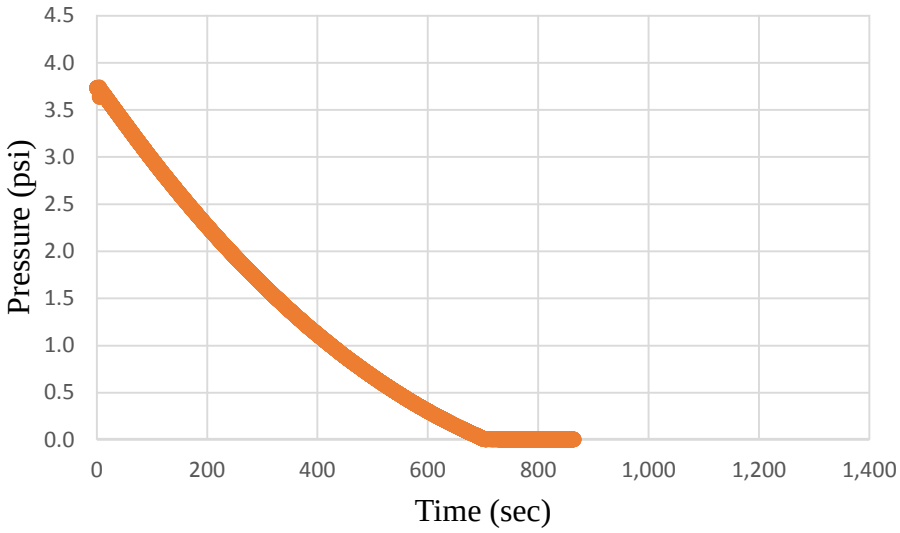

Figure 3.25. Batch 4 test 1 pressure data

Using the same tests and procedures performed during the Batch 1 test, both the density and sand content of the Batch 4 slurry were measured giving a density of 1038.1 grams/liter and a sand content of .25%.

Viscosity of the discharging slurry was also taken at several different times/elevations during the course of each of the three tests. The results of the tests are presented in Table 3.4.

Table 3.4. Batch 4 viscosity test results

Test 1			Test 2			Test 3		
Time (sec)	Height (in)	Viscosity (sec/qt)	Time (sec)	Height (in)	Viscosity (sec/qt)	Time (sec)	Height (in)	Viscosity (sec/qt)
19	105.68	38.75	0	108.21	39.63	9	107.00	39.72
161	82.22	40.13	140	84.90	39.57	127	81.14	40.57
324	59.28	40.22	290	63.19	40.00	226	63.68	40.15
485	40.82	39.28	455	43.40	39.97	284	54.15	40.62
718	20.31	40.53	673	23.65	40.97	514	23.60	40.44

3.1.7 Batch 5 Slurry Preparation and Testing

Upon completion of the Batch 4 tests, 15 gallons of slurry were removed from the slurry holding tank and replaced with a like volume of pH corrected water. The slurry/water combination was then pumped through the slurry mixing/delivery system for 5 minutes to thoroughly mix the combination while flushing any of the Batch 4 slurry from the test tube.

As with Batch 4, a total of 3 falling head tests were performed on the slurry measuring the changes in weight and pressure. An example of the Batch 5 raw data collected is presented in Figures 3.26 and 3.27.

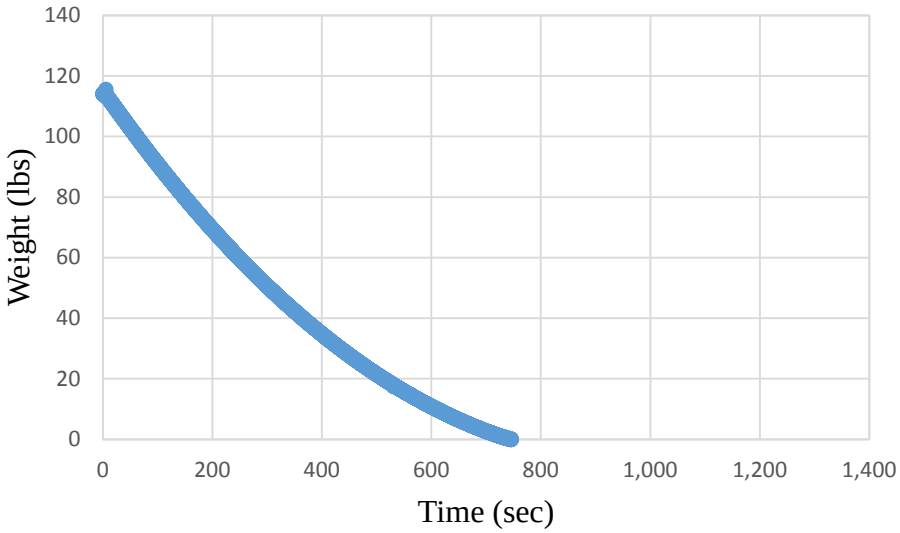

Figure 3.26. Batch 5 test 1 weight data

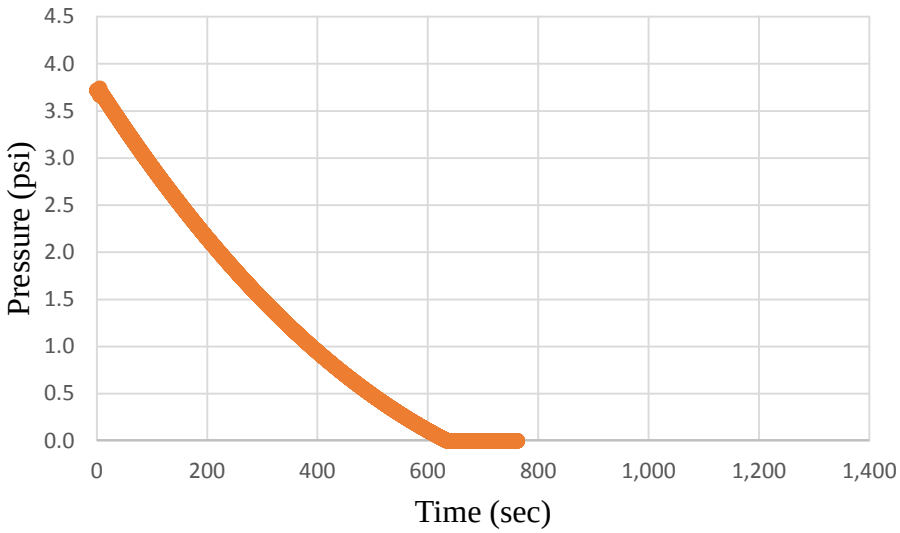

Figure 3.27. Batch 5 test 1 pressure data

Using the same tests and procedures performed during the Batch 1 test, both the density and sand content of the Batch 5 slurry were measured giving a density of 1029.2 grams/liter and a sand content of .25%.

Viscosity of the discharging slurry was also taken at several different times/elevations during the course of each of the three tests. The results of the tests are presented in Table 3.5.

Table 3.5. Batch 5 viscosity test results

Test 1			Test 2			Test 3		
Time	Height	Viscosity	Time	Height	Viscosity	Time	Height	Viscosity
(sec)	(in)	(sec/qt)	(sec)	(in)	(sec/qt)	(sec)	(in)	(sec/qt)
13	105.60	32.34	10	105.62	32.15	7	106.57	32.06
118	81.84	32.14	111	82.76	31.91	116	81.82	32.17
213	62.80	32.02	208	63.32	32.22	221	60.89	31.84
311	45.02	32.31	324	43.20	32.22	328	42.80	32.16
468	23.78	32.44	464	23.83	32.04	465	23.83	32.18

3.1.8 Development of Pressure vs Flow Curves

Upon completion of the falling head tests, pressure vs flow curves where developed for each of the individual tests. The methodology used involved several steps. The first step was to adjust the raw pressure data for each of the five batches/viscosities to account for the fact that the pressure sensor was located 18 inches above the point of discharge of the falling head test system. Using the density measurements taken for each of the individual batches, the pressure exerted from 18 inches of additional pressure of the five different viscosities was calculated using the following formula:

$$P_{Batch} = P_{Water} * {Density_{Batch}}/{Density_{Water}}$$

For example, the density of Batch 1 was 1054.3 grams per liter and the density of the water used to make Batch 1 was measured to be 995.6 grams/liter. The pressure head from 18 inches of water is equal to 0.65 psi, therefore the pressure adjustment for Batch 1 was:

$$P_{Batch1} = .65psi * \frac{1054.3grams}{liter} \Big/ \frac{995.6grams}{liter} = .6884psi$$

This pressure adjustment was then added to the raw pressure values collected from each of the individual Batch tests. This number was added to all raw pressure values collected from the three Batch 1 tests. The adjustment values for each Batch are presented in table 3.6.

Table 3.6. Pressure adjustment values

	Density	Pressure Correction
	grams/liter	Psi
Batch 1	1054.30	0.6884
Batch 2	1046.50	0.6833
Batch 3	1041.90	0.6803
Batch 4	1038.10	0.6778
Batch 5	1029.20	0.6720
Water	995.50	0.6500

The next step was to calculate flow from the existing weight data. This is accomplished by establishing the change in volume over a fixed period of time. The first step was to convert the weight data into volume data. Using the known density of the individual batches of slurry, the volume was calculated using the following equation:

$$Volume_{Batch} = {Density_{Batch}}/{Weight_{Batch}}$$

For example, the starting weight from the first Batch 1 test was 117.66 lbs. The density of Batch 1 was 1054.3 grams/liter which converts to 8.792 lbs/gal. Therefore the volume of Batch 1 is:

$$Volume_{Batch1} = {117.66lbs}/{\frac{8.792lbs}{gal}} = 13.38\ gallons$$

Once the volumes were determined, the flow rate was calculated using the equation:

$$Q = {\Delta Volume}/{\Delta Time}$$

where:

$$Q = flowrate\frac{gallons}{minute}$$

$$\Delta Volume = \left(V_{t_i+.5minute} - V_{t_i}\right)$$

$$\Delta Time = .5minute$$

The graph of the Batch 1 slurry pressure vs flow relation is below in Figure 3.28.

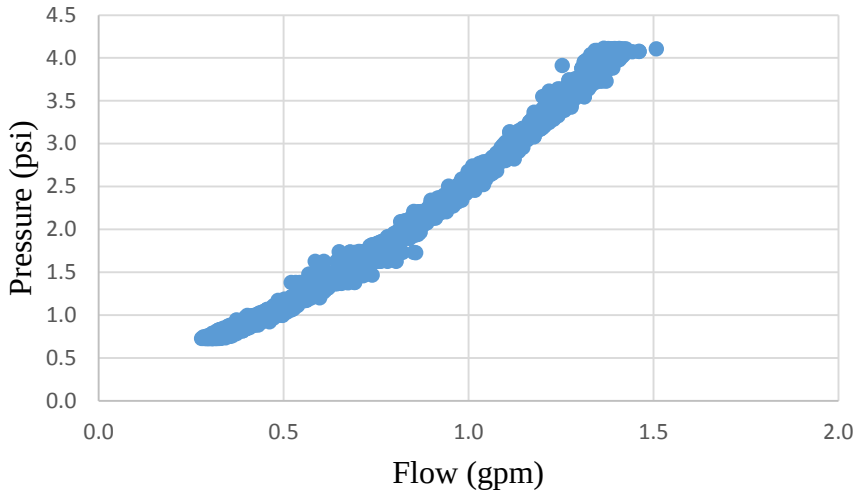

Figure 3.28. Batch 1 test 1 pressure vs flow curve for 91 sec/qt slurry

The complete set of curves for the individual tests from Batch 1 through 5 can be found in Appendix B1.

3.1.9 Uniqueness of the Pressure vs Flow Relationship "Proof of Concept"

As stated at the beginning of this thesis, the goal of the falling head test experiment was to verify the uniqueness of the "pressure versus flow" family of curves for a given series of viscosities. To this end, individual pressure versus flow curves developed from each of the five viscosities tested were plotted onto a single graph (Fig 3.29).

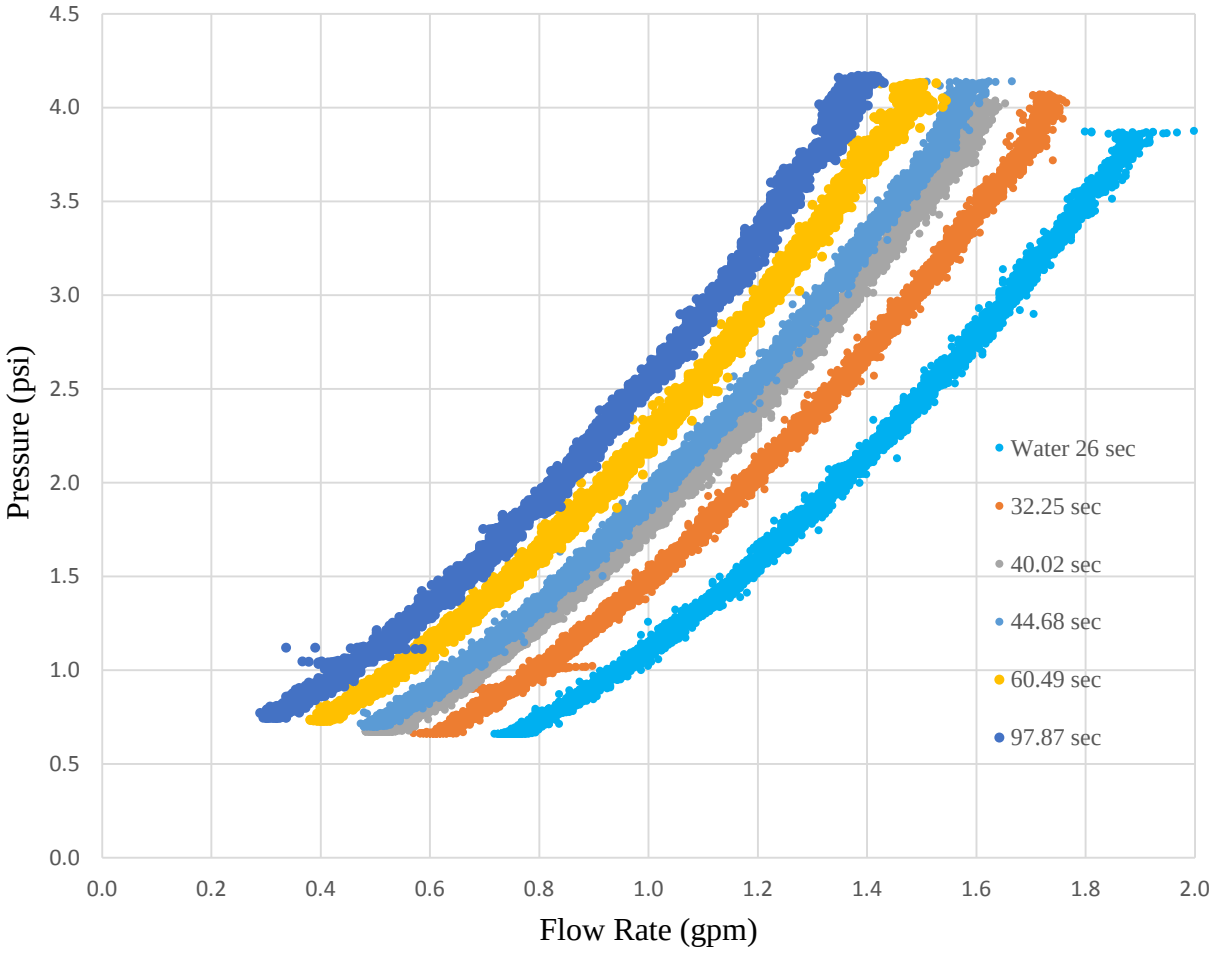

Figure 3.29. Pressure vs flow family of curves

Upon examination of the above graph, one notes that although the curves generated by the five different viscosities have similar overall shapes, the curves are clearly shifted along the flow rate axis with the higher viscosity slurry having lowest starting and finishing flow rates followed by the 60 viscosity curve and so on. Therefore, for any given pressure, there is a narrow range of corresponding flow rates which would be unique to that particular viscosity. To illustrate this point, the ranges of the x and y axis for the above graph have been limited to show the corresponding range of flow rates associated with each of the five test viscosities (Figure 3.30).

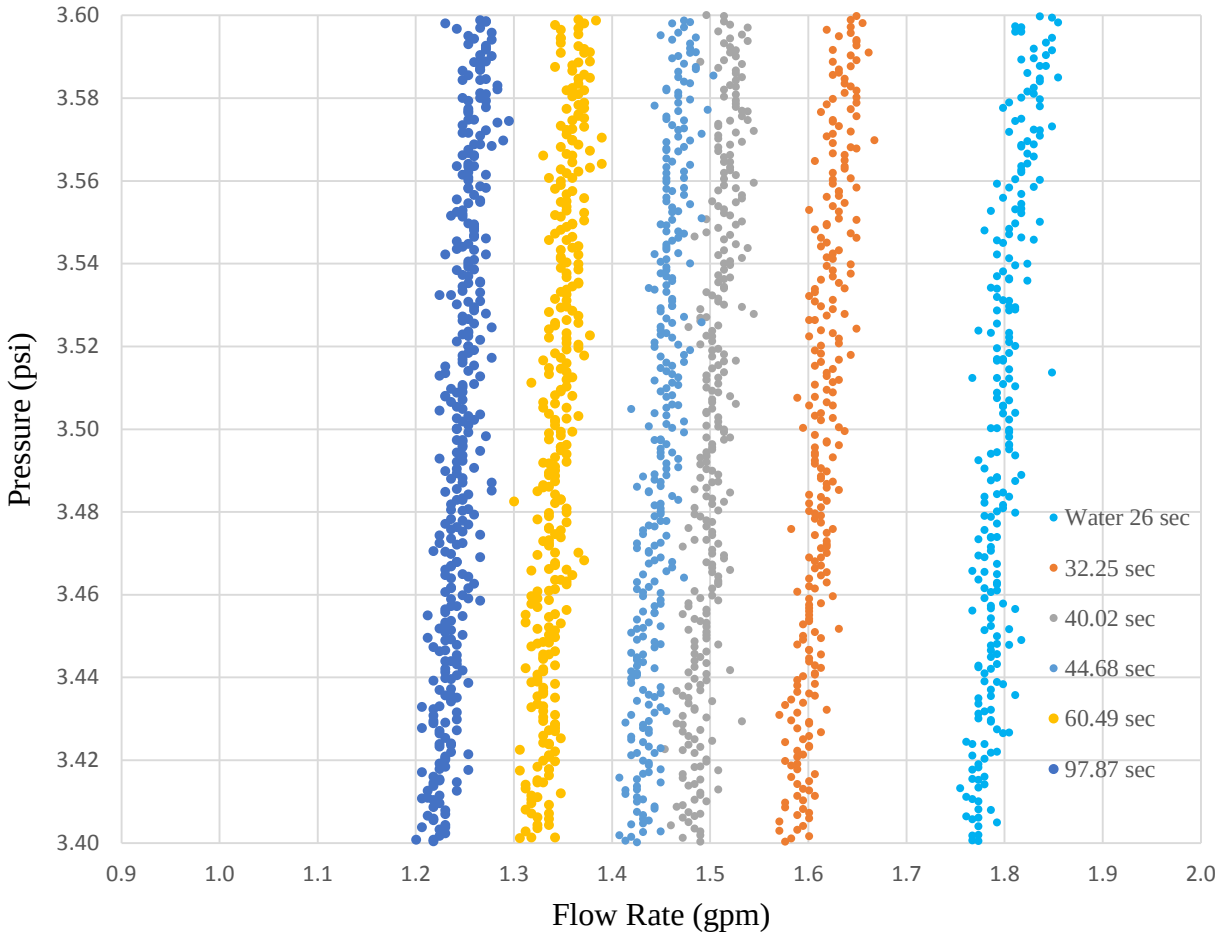

Figure 3.30. Exploded view of Figure 3.29 showing separation between individual curves

As shown in Figure 3.30, at any given pressure, each of the five viscosities generated a narrow range of flow rates with virtually no overlap in the flow rates between viscosity curves. In closing, the results of the falling head experiment clearly supports the premise that the pressure-flow rate relation of a given non-polymer slurry is a function of its viscosity.

3.2 Slurry Preparation for the High-Sand Content Slurry Assessment

A second series of slurry was prepared in order to test the possible effects of high sand content on the predicted viscosity (from P vs Q plots). It should also be noted that the initial volume of the second series of slurry differed from that of the first test where each used a full bag of bentonite, but the newer bags produced more effective slurry (less powder for the same viscosity). After the addition of 50lbs of CETCO PUREGOLD GEL Bentonite powder to the 50 gallons of pH 9 water via the rapid hydration Hootonanny, the viscosity was found to be in the 240 sec/qt range. In order to lower the viscosity to a the desired 90 sec/qt range, an addition 8 gallons of pH 9 water was added to the slurry mix for a total volume of 58 gallons.

In order to elevate the sand content of the second series slurry, which was consistently found to be 0.25%, a total of 60lbs of sand was added to the slurry during the 5 minute recirculation period just prior to the first of the high sand content Batch 1 tests. The sand content was again measured and found to be 10%. A sieve analysis of the sample of sand added to the slurry was performed and the results are presented below in Figure 3.31.

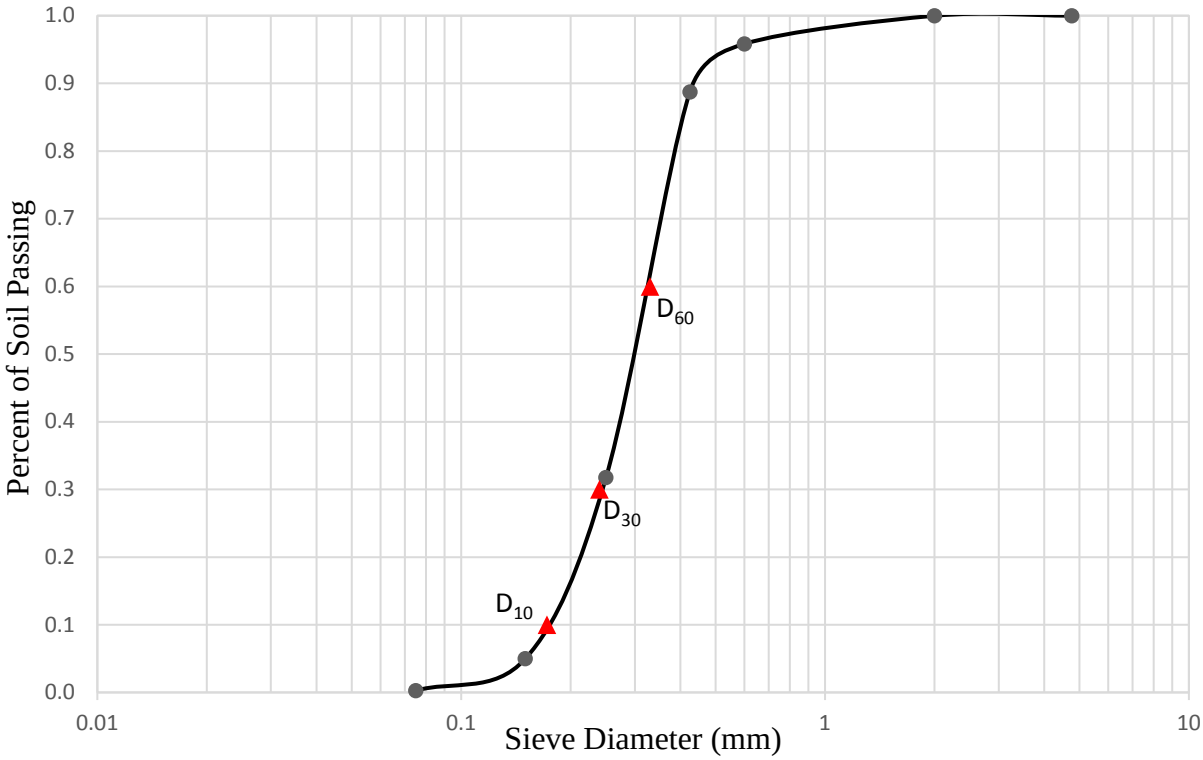

Figure 3.31. Sieve analysis of sand used for high sand content test

Using the sieve data, the sand was found to have a D_{10} of .17mm, a D30 of .23mm, a D60 of .33mm with a uniformity coefficient C_c of 1.94 and coefficient of curvature C_u of .94. Using the Unified Soil Classification System (ASTM D 2487), the sand would be classified as a SP or poorly graded sand. Using the AASHTO classification system, the sand would be classified as an A-3 with > 50% passing the No. 40 sieve and < 10% passing the No. 200 sieve.

3.2.1 High-Sand Content Slurry Testing

The testing of the slurry was performed using steps similar to those performed during the first series of slurry tests, with density being measured at the beginning of Test 1 for each of the five batches. In addition, the same amount of slurry was removed and replaced with pH correct water for each batch. With the volumes of slurry removed and water added, the resulting mix

ratios and test-averaged viscosity for each of the high sand content batches are presented in Table 3.7 and, as a point of reference, the values from the first test series presented in Table 3.8.

Table 3.7. High sand content slurry test mix ratios, densities and average viscosities

High Sand Content	Batch 1	Batch 2	Batch 3	Batch 4	Batch 5
Slurry Removed/ Water Added to Holding Tank	0	5 gal	5 gal	5 gal	15 gal
Lbs. Slurry/Gallon	0.82	0.79	0.72	0.66	0.49
Density Grams/Liter	1139.0	1119.9	1103.0	1093.1	1033.8
Density Lbs/Gal	9.506	9.345	9.201	9.122	8.629
Starting Viscosity	147.66	65.74	46.84	39.24	30.80

Table 3.8. First test series mix ratios, densities and average viscosities

Series 1 Test	Batch 1	Batch 2	Batch 3	Batch 4	Batch 5
Slurry Removed/ Water Added to Holding Tank	0	5 gal	5 gal	5 gal	15 gal
Lbs. Slurry/Gallon	1.00	.90	.81	.73	.51
Density Grams/Liter	1054.3	1046.5	1041.9	1038.1	1029.2
Density Lbs/Gal	8.801	8.733	8.695	8.633	8.628
Starting Viscosity	86.72	59.75	44.69	39.56	32.34

The high-sand content test procedures differed from those of Series 1 in the following ways. First, each viscosity was run twice (for repeatability) and not three or more. Second,the Marsh viscosity was measured three times per test now at predetermined slurry heights which were marked on the slurry column (Figure 3.32) as opposed to the Series 1 tests which were measured continuously until the column was empty which tended to be four to five times.

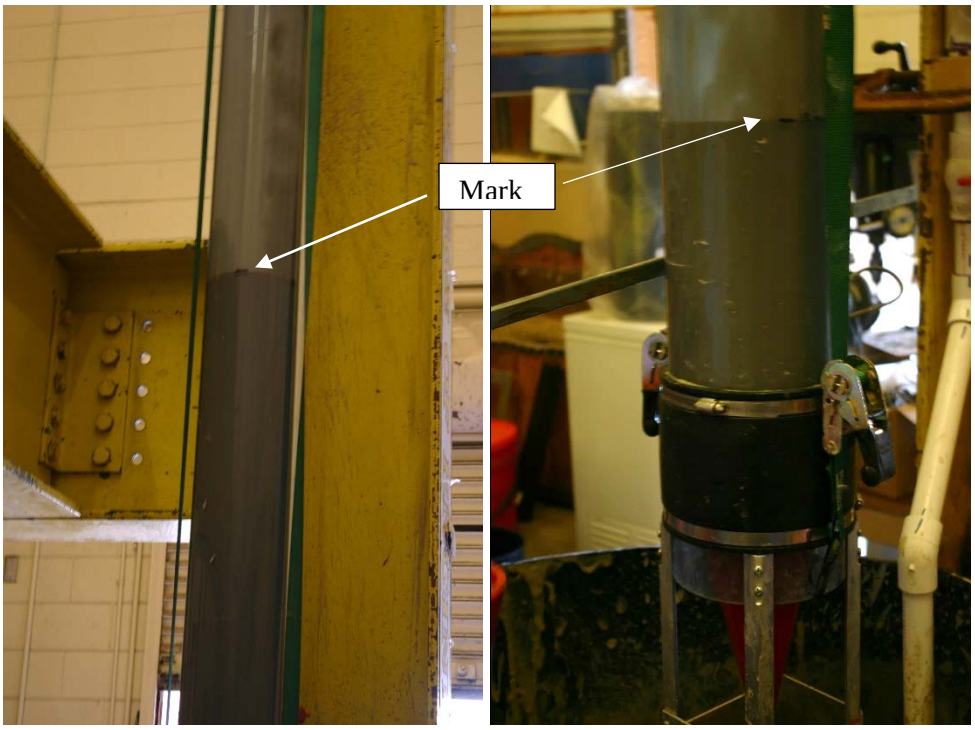

Figure 3.32. Test tube with marking for when to pull sample

A third difference was the amount of sand content tests that were performed in each trial run. This stemmed from the concern that sand may settle during the test and may not be uniformly distributed throughout the duration of the test. As a result, 3 sand content tests were taken which coincided with the other viscosity tests.

The results from individual viscosity and sand contents of the high-sand content tests are presented in Tables 3.9 to 3.18 below.

Table 3.9. Batch 1 viscosity test results

Test 1			Test 2		
Time	Height	Viscosity	Time	Height	Viscosity
(sec)	(in)	(sec/qt)	(sec)	(in)	(sec/qt)
64	105.37	134.65	27	104.34	133.41
376	66.75	139.44	371	66.75	143.53
820	26.00	166.63	817	26.00	168.30

Table 3.10. Batch 1 sand contents

Test 1			Test 2		
Time	Height	Sand Content	Time	Height	Sand Content
(sec)	(in)	(%)	(sec)	(in)	(%)
80	102.46	10.50	24	104.93	10.00
397	53.90	9.50	379	55.86	9.80
877	14.28	8.00	867	14.73	10.00

Table 3.11. Batch 2 viscosities

Test 1			Test 2		
Time	Height	Viscosity	Time	Height	Viscosity
(sec)	(in)	(sec/qt)	(sec)	(in)	(sec/qt)
18	106.50	61.35	25	105.28	63.04
300	66.75	66.00	300	66.75	64.35
677	26.00	70.06	679	26.00	69.62

Table 3.12. Batch 2 sand contents

Test 1			Test 2		
Time	Height	Sand Content	Time	Height	Sand Content
(sec)	(in)	(%)	(sec)	(in)	(%)
17	106.78	10.00	22	106.00	9.25
301	57.28	8.00	282	60.33	8.00
699	16.44	8.00	679	17.85	8.00

Table 3.13. Batch 3 viscosities

Test 1			Test 2		
Time	Height	Viscosity	Time	Height	Viscosity
(sec)	(in)	(sec/qt)	(sec)	(in)	(sec/qt)
15	107.95	46.16	26	106.56	45.69
277	66.75	47.02	283	66.75	46.35
623	26.00	48.12	624	26.00	47.65

Table 3.14. Batch 3 sand contents

Test 1			Test 2		
Time	Height	Sand Content	Time	Height	Sand Content
(sec)	(in)	(%)	(sec)	(in)	(%)
13	108.32	9.00	26	106.52	9.25
277	58.76	6.00	283	58.34	6.00
623	18.03	7.00	624	18.03	8.00

Table 3.15. Batch 4 viscosities

Test 1			Test 2		
Time	Height	Viscosity	Time	Height	Viscosity
(sec)	(in)	(sec/qt)	(sec)	(in)	(sec/qt)
17	107.48	39.15	17	107.66	38.54
270	66.75	38.47	270	66.75	39.06
589	26.00	40.28	590	26.00	38.94

Table 3.16. Batch 4 sand contents

Test 1			Test 2		
Time	Height	Sand Content	Time	Height	Sand Content
(sec)	(in)	(%)	(sec)	(in)	(%)
17	107.48	9.25	18	107.47	9.25
270	57.89	4.50	269	57.98	4.50
590	17.40	6.00	589	17.40	5.00

Table 3.17. Batch 5 viscosities

Test 1			Test 2		
Time	Height	Viscosity	Time	Height	Viscosity
(sec)	(in)	(sec/qt)	(sec)	(in)	(sec/qt)
18	109.24	30.96	25	108.30	30.38
255	66.75	30.66	260	66.75	31.40
544	26.00	30.53	549	26.00	30.90

Table 3.18. Batch 5 sand contents

Test 1			Test 2		
Time	Height	Sand Content	Time	Height	Sand Content
(sec)	(in)	(%)	(sec)	(in)	(%)
18	109.24	8.00	25	108.30	6.00
224	64.11	1.00	260	57.75	0.35
545	17.02	0.25	549	16.37	0.75

3.2.2 Development of Pressure vs Flow Curves

Upon completion of the falling head tests, pressure vs flow curves were developed for each of the individual tests. The methodology used was the same as that used for the first series of tests. As with the first test series, it was necessary to adjust the raw pressure data for each of the five Batches/viscosities to account for the location of the pressure sensor 18 inches above the point of discharge of the falling head test system. Using the density measurements taken for each of the individual Batches and the formula used in the first series of tests, a pressure adjustment for the five different viscosities was calculated and is presented in Table 3.19 below.

Table 3.19. Pressure adjustment values

	Density	Pressure Correction
	grams/liter	psi
Batch 1	1139.0	0.744
Batch 2	1119.9	0.731
Batch 3	1103.0	0.720
Batch 4	1093.1	0.714
Batch 5	1033.8	0.675

The next step was to calculate flow from the existing weight data. As with the first series of tests, this was accomplished by establishing the change in volume over a fixed period of time and was done using the same procedures for adjusting the pressure data, converting weight data

to volume and calculating flow rate using a 0.5 minute time step. An example of a high-sand content pressure vs flow curve is presented in Figure 3.33.

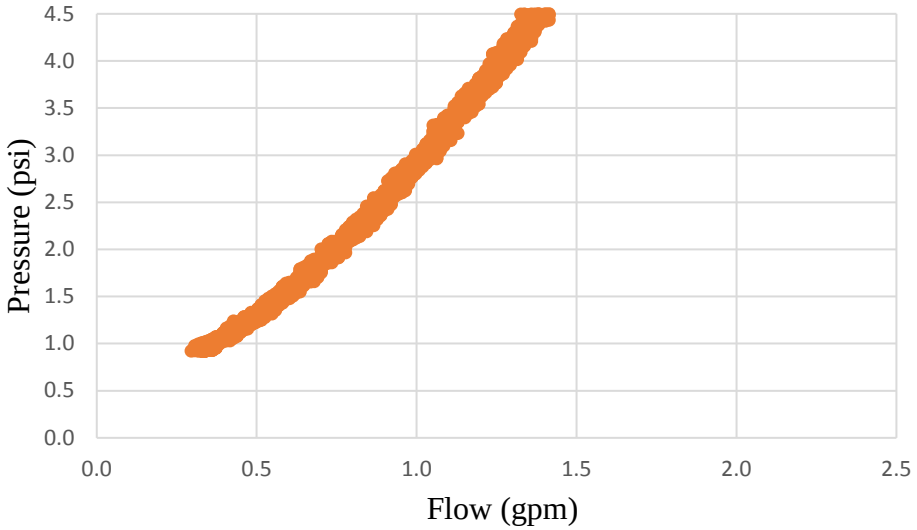

Figure 3.33. Batch 1 test 1 pressure vs flow for 146.91 sec/qt slurry

A complete set of the individual curves from Batches 1 through 5 from test series 2 can be found in Appendix B2.

3.2.3 Assessment of High-Sand Content on the Pressure vs Flow Relationship

To visually assess what, if any, impact high sand content levels might have on the unique pressure versus flow demonstrated in the first part of this experiment, pressure versus flow data from similar viscosities from both tests were plotted on the same graph. Unfortunately, exact viscosity matches were not achieved so the graphs do not align precisely. Examples from the five ranges of viscosities tested are presented in Figures 3.34 through 3.38 below:

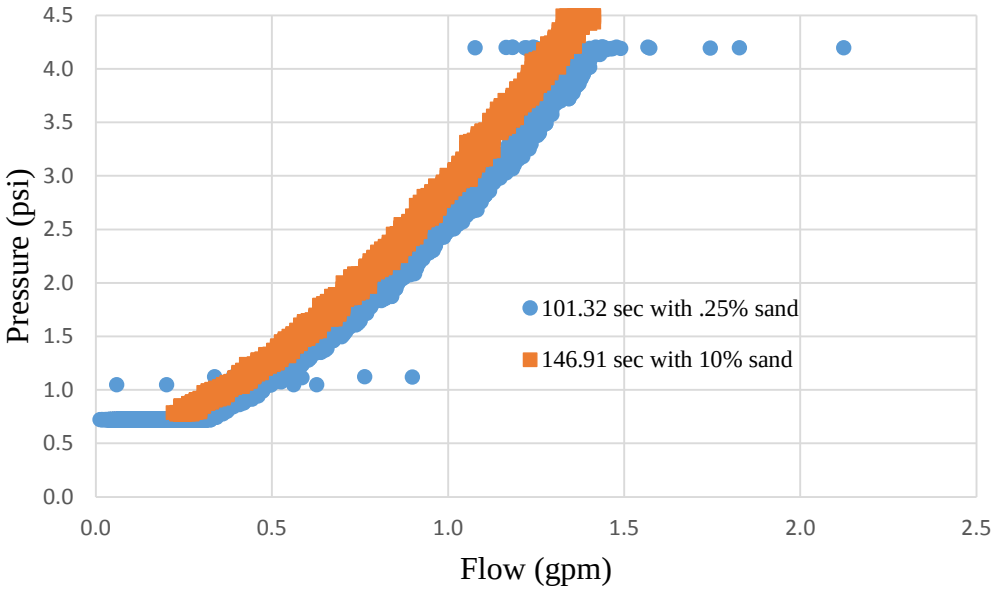

Figure 3.34. 90+sec/qt pressure vs flow response comparison

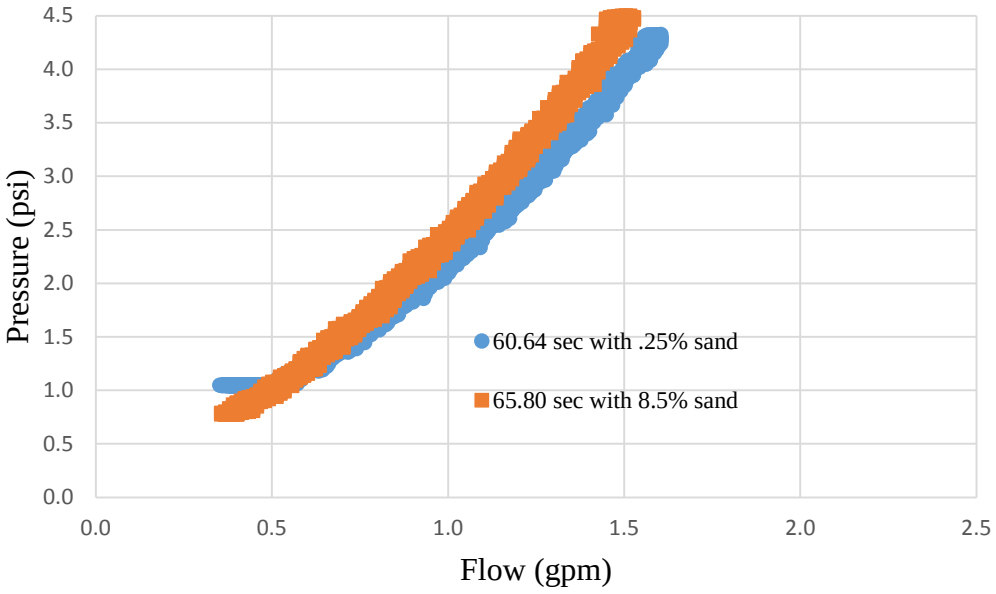

Figure 3.35. 60 sec/qt pressure vs flow response comparison

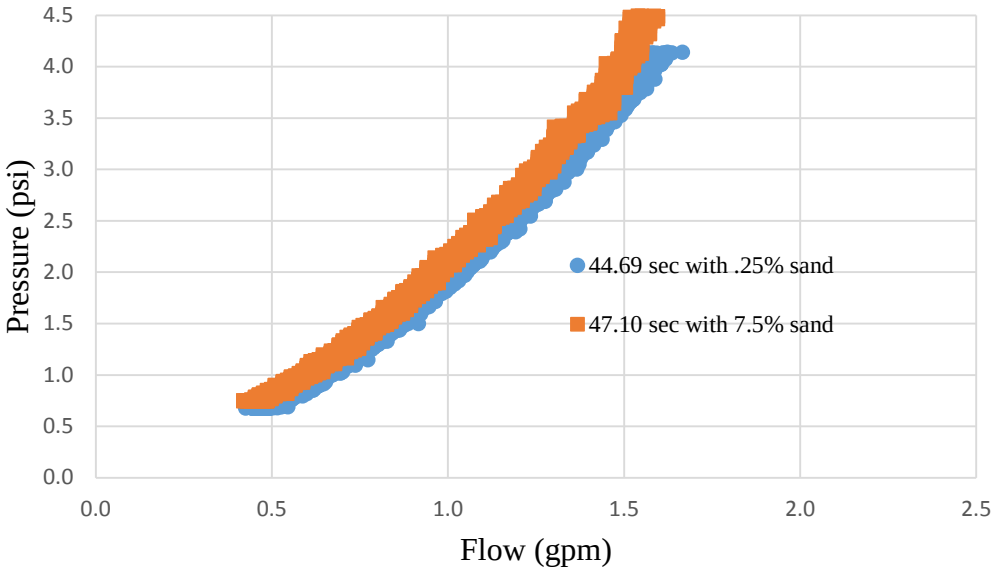

Figure 3.36. 45 sec/qt pressure vs flow response comparison

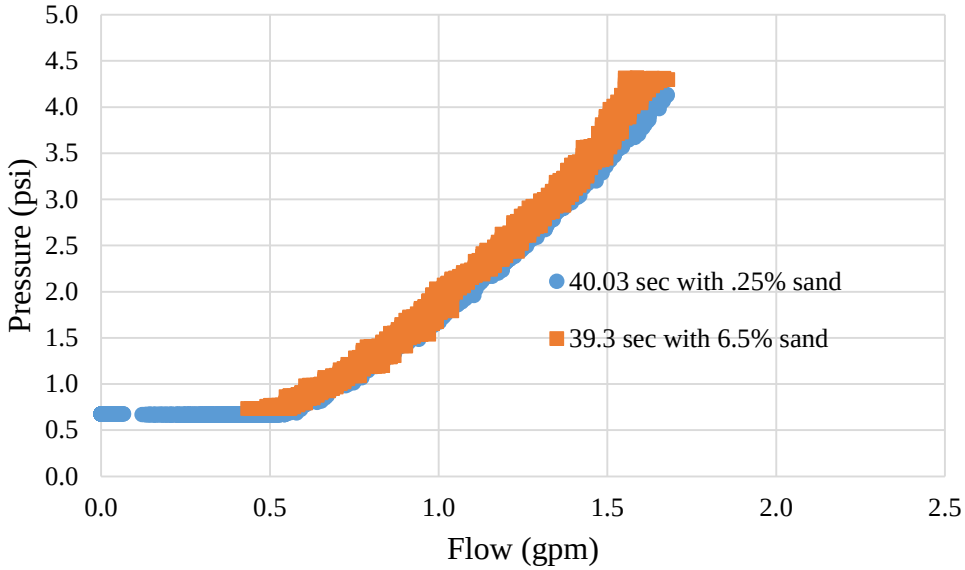

Figure 3.37. 40 sec/qt pressure vs flow response comparison

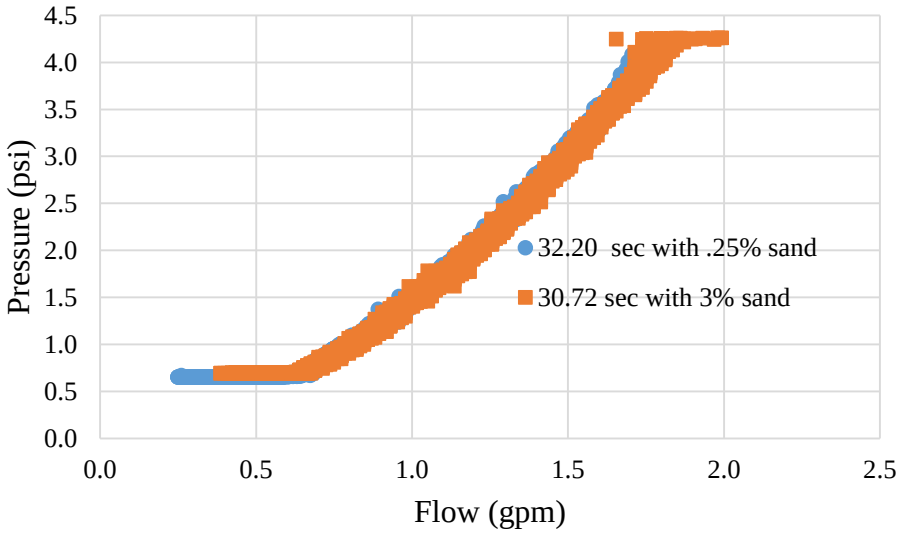

Figure 3.38. 30 sec/qt pressure vs flow response comparison

Upon examination of the above graphs, one can conclude that elevated sand content has little discernable effect on the pressure versus flow relationship of the slurries tested. Although not exactly the same viscosity, in all cases the slightly higher viscosity comparator had the highest pressure.

3.3 Design and Testing of the Slurry Pumping System

Section 3.3 is the design and construction of the viscosity monitoring component of the all-in-one monitoring system. The objective includes designing a slurry pumping system with instrumentation for monitoring flow rate, pressure and density which includes determining the optimum orifice diameter and length as it relates to the flow-pressure curves.

3.3.1 Preliminary Design and Testing of Slurry Pumping System

After the falling head testing, a pressurized system was built to allow testing of various orifices. The same 1.5HP Flowtec pump was used to pump slurry from the holding tank through a Toshiba GF630/LF620 electromagnetic flowmeter. In-line after the flow meter was an

Omegadyne PX209-100G5V 0-100 psi pressure transducer to measure the pressure developed from a 3/8 in ID nozzle / restriction. The test setup is shown in Figure 3.39.

Figure 3.39. Pump (left), flow meter, pressure transducer and nozzle (right)

Two 1in diameter flexible hoses, each with a valve, tee off from the pump. As seen in Figure 3.40, one hose directed flow through the orifice testing system while the other shunts excess flow from the pump back to the tank.

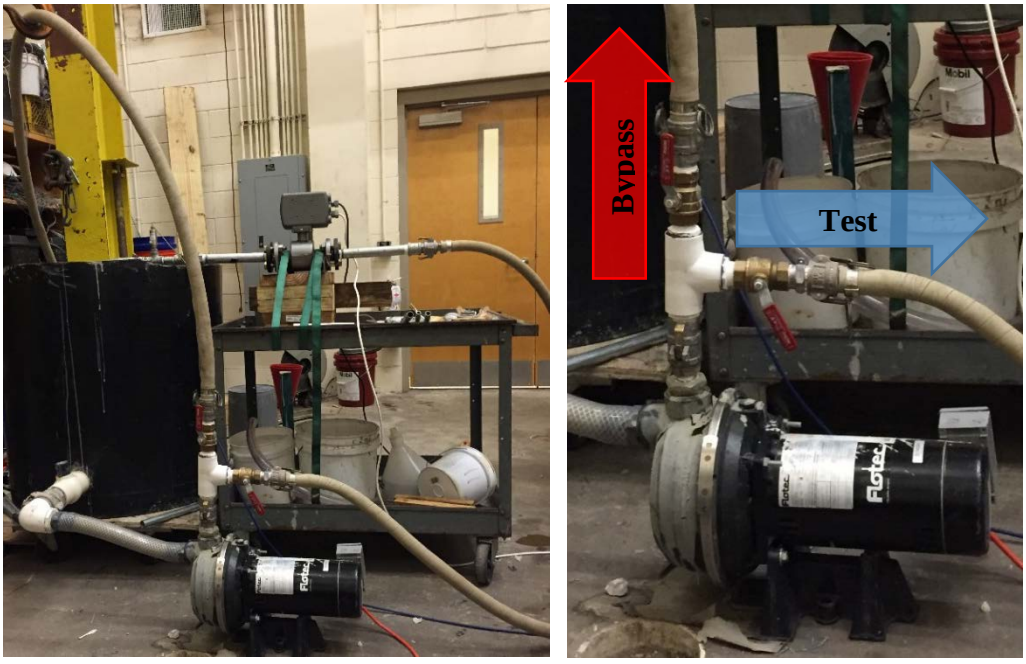

Figure 3.40. Valves to direct slurry flow

Using a hose clamp, a 2ft piece of flexible 1.125in ID tubing shown in Figure 3.41 was attached to return the slurry flow from the orifice to the tank and control overspray/mess.

Figure 3.41. Nozzle with slurry return tubing

A Megadac data acquisition system was used to monitor and record test data from the flow meter and pressure transducer (Figure 3.42).

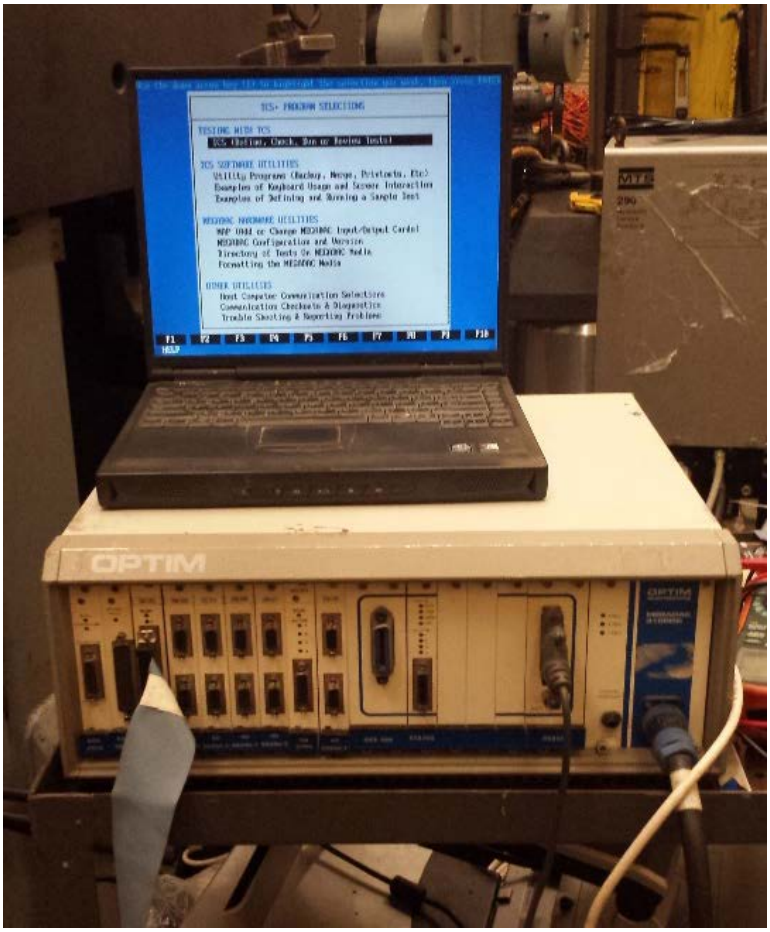

Figure 3.42. Megadac system and screen to monitor during testing

3.3.2 Testing Procedures

In the column tests, head pressure and flow were controlled by gravitational forces. This approach limited the range of testable pressures and flows. With the pump driven system, pressure and flow are modulated by adjusting the slurry flow control valve as seen in Figure 3.43. This allowed for more efficient testing as any range of flow rates could be tested more quickly.

Figure 3.43. Adjusting slurry flow control valve

In order to complete a test, pressure data was collected while the operator varied the flow from zero to maximum flow through the test bed. In order to achieve this, the test started with 100% of flow going through the bypass hose and 0% flowing through the test setup. Gradually, the test valve was opened until fully open (50% of flow to test, 50% to bypass), after which the

bypass valve was gradually closed resulting in all available flow being directed through the testing sensors.

In sequence, Figure 3.44 shows the flow resulting from these valve positions with blue indicating test setup flow and red indicating bypass flow. The process was then reversed until zero flow through the testing system was once again achieved, signaling the end of the test. Figure 3.44 displays the flow rate for the duration of one test. Part (a) of Figure 3.44 corresponds with (a) in Figure 3.45, which occurs at the beginning and end of a test. Valve position (c) causes the peak of the flow curve, and (b) is on both sides of the curve, between the (a) and (c) position.

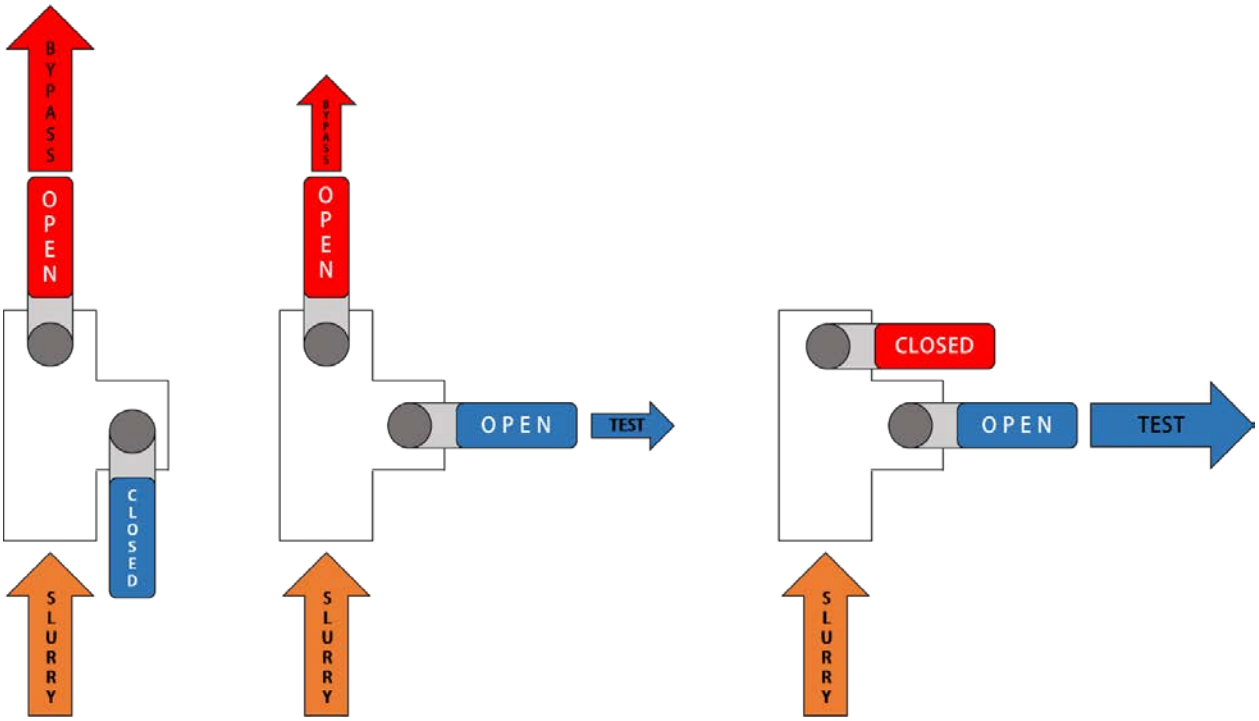

(a) (b) (c)

Figure 3.44. Flow resulting from different valve positions

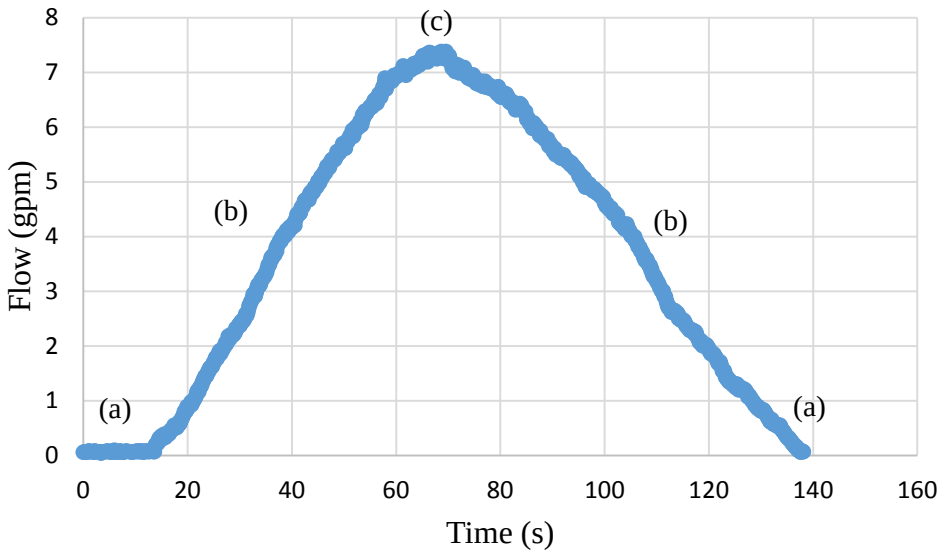

Figure 3.45. Flow vs time graph

After the test was completed, the data was reviewed on the Megadac system for any issues. A smooth, continuous curve similar in shape to that of Figure 3.46 is the result if no testing issues having occurred.

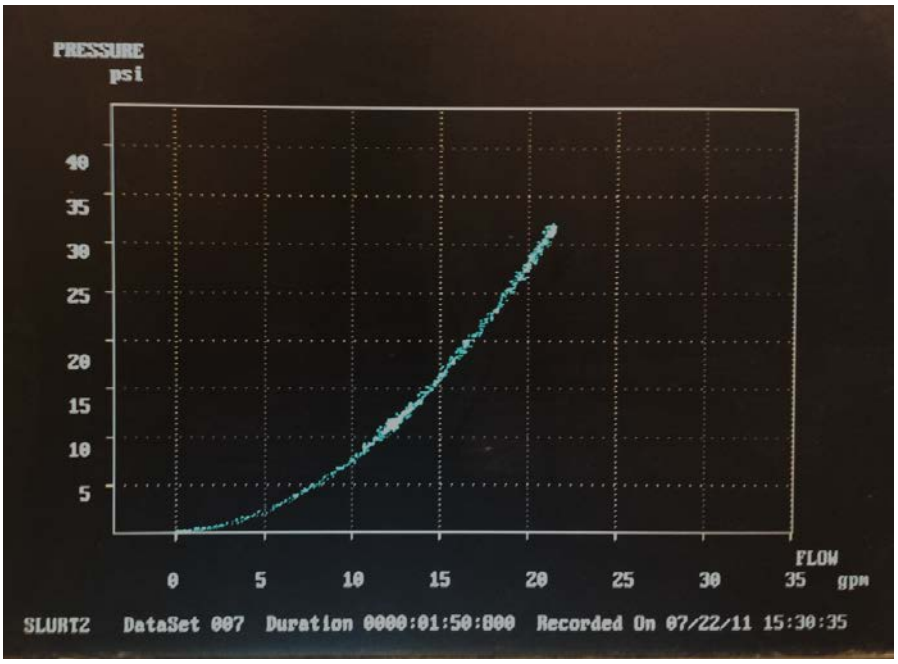

Figure 3.46. Sample of plotted raw data on Megadac

Testing was completed in order from high viscosity to low viscosity. After each batch was tested, 5 gallons of slurry were removed from the tank and replaced with 5 gallons of pH treated water. An exception occurred between the 4th and 5th batch where a 15 gallon water replacement was necessary to obtain a significantly lower viscosity. Less viscous bentonite slurries require more dilution than the highly viscous to obtain the same change in measured viscosity. The decreasing effect of a 5 gallon water replacement on batch viscosity is visible in Table 3.20 between batches 1 through 4.

Table 3.20. Properties of tested slurry batches

	Test #	Marsh (s)	Temp (°F)
Batch 1	001	127	77
	002	155.47	78
	003	146	78
	Average	143	77.7
5 gallons of slurry removed, 5 gallons of water added			
Batch 2	004	59.94	79
	005	58.78	79
	006	58.53	80
	Average	59	79.3
5 gallons of slurry removed, 5 gallons of water added			
Batch 3	007	46.72	80
	008	45.62	80
	009	45.65	80
	Average	46	80.0
Nozzle			
Batch 4	010	40.5	80
	011	39.72	80
	012	39.66	80
	Average	40	80.0
15 gallons of slurry removed, 15 gallons of water added			
Batch 5	013	31.09	80
	014	31.12	79
	015	31.6	79
	Average	31	79.3

3.3.3 Testing Results

Figure 3.47 shows that there was a clear differentiation between the curves, all of which follow the trend of higher viscosity slurry resulting in higher pressure developed. The degree of separation was very slight with a 0.6 psi difference between the 40 and 31 second slurries at 10 gallons per minute. The 31 and 40 second slurry mixes are similar to the 30-40 second range of acceptable bentonite slurry viscosities as stated by the 2016 Florida DOT Standard Specifications for Road and Bridge Construction. The least viscous fluid, water, is the bottom curve with the least pressure developed from the flow obstruction. The most viscous mix of 143 seconds sits atop the other curves as more energy (pressure) is needed to produce any chosen flow rate. All intermediate viscosities are layered between the most and least viscous solution curves. The full collection of raw data for this round of testing may be found in Appendix C.

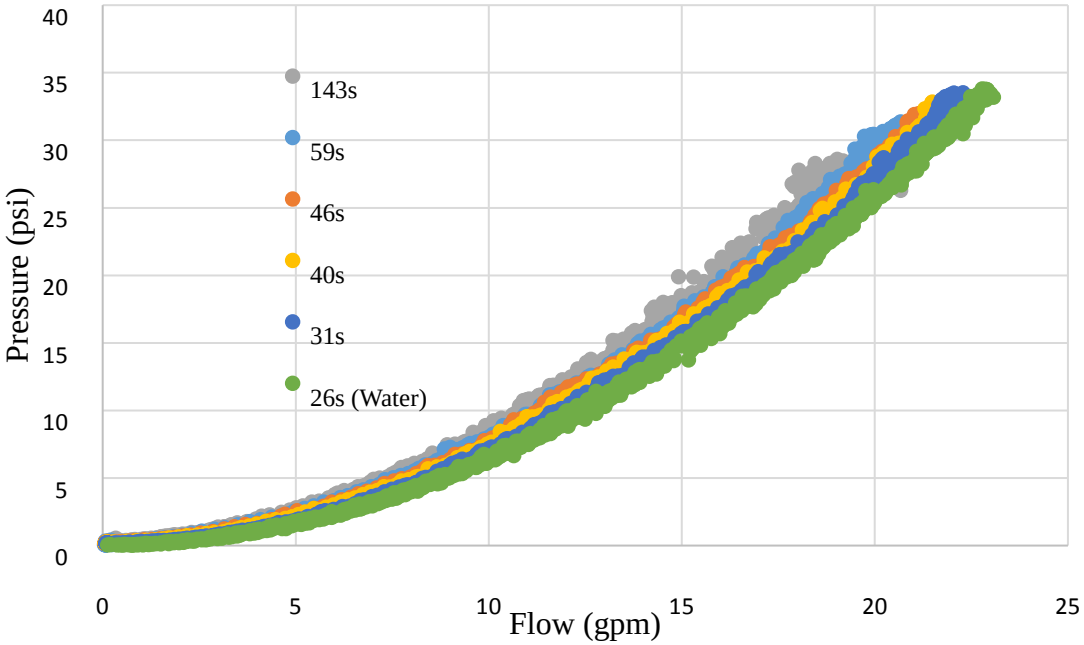

Figure 3.47. Curves from a range of different viscosities through 3/8 in. ID nozzle

While this test did show separation between curves, the difference was not very pronounced. Greater isolation between curves was desired for more precise identification of slurry viscosity. As viscosity is the measure of a fluid's resistance to shearing, an orifice that provides more internal shearing surface would maximize the effect of fluid viscosity on the pressure vs flow curve. By expanding the role of shearing stresses in these curves, greater separation between curves could be achieved.

A subsequent series of tests was then devised whereby testing a multitude of orifices with different properties, namely diameter and length, would provide insight into the most practical and effective orifice design. The significance was to use as large an orifice diameter as possible to reduce clogging potential while producing the most pressure variation (for a given flow rate) which provides the most sensitivity to the overall system performance.

3.3.4 Preliminary Orifice Testing

The test setup for orifice testing was identical to the previous test setup except that several orifices, shown in Figure 3.48, were tested instead of just one nozzle. Figure 3.49 shows the attachment point. The pipe nipples were either bought at the correct length or cut to length. The head loss from additional pipe length was the motivation for different lengths.

Figure 3.48. First round of orifice tests

Figure 3.49. Attaching orifice for testing

3.3.5 Preliminary Orifice Testing Procedure

The testing procedure was largely unchanged from the previous test, aside from testing two viscosities instead of many. Knowing that the range of P vs Q curves will be bookended by

the lowest and highest tested viscosity, only testing a high and low range allowed for more efficient testing.

First, all orifices were rotated through the test setup and tested using water as the low range viscosity. Next, the orifices were tested with a high range (49 second) slurry. These results were analyzed to find the orifice with the maximum difference in developed pressure between the low and high viscosities.

3.3.6 Preliminary Orifice Test Results

Taking the raw data and adjusting the pressure to eliminate the sensor offset, curves similar to Figure 3.50 were created. The full collection of raw data for this round of testing is presented in Appendix D1.

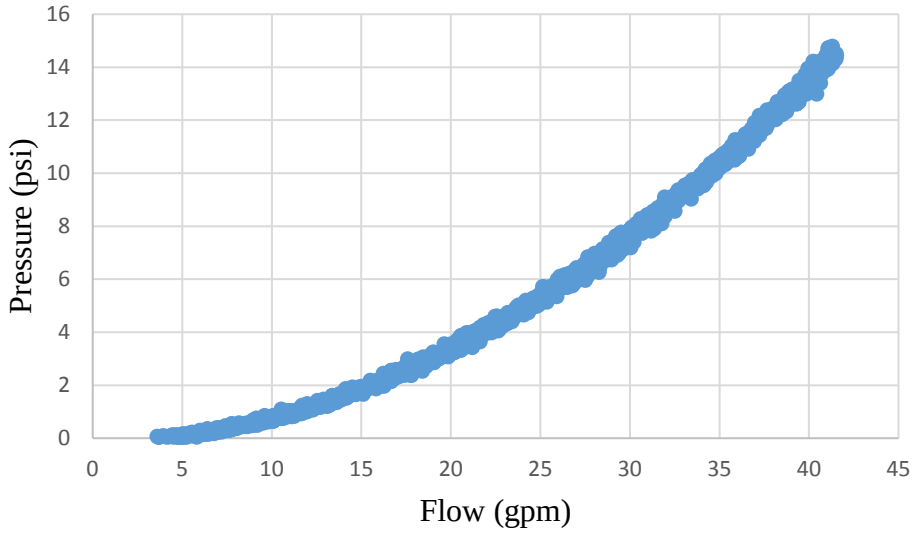

Figure 3.50. Orifice with 0.63in inner diameter, 6in length, water

Graphs for each orifice, with water and slurry data plotted simultaneously give a visual representation of the difference in developed pressure. Figures 3.51 and 3.52 are examples of this

type of graph. Figure 3.51 shows an orifice with little difference between slurry and water curves, while Figure 3.52 has significant curve separation. Note that the longer, narrower orifice provides more separation than wider, shorter orifices.

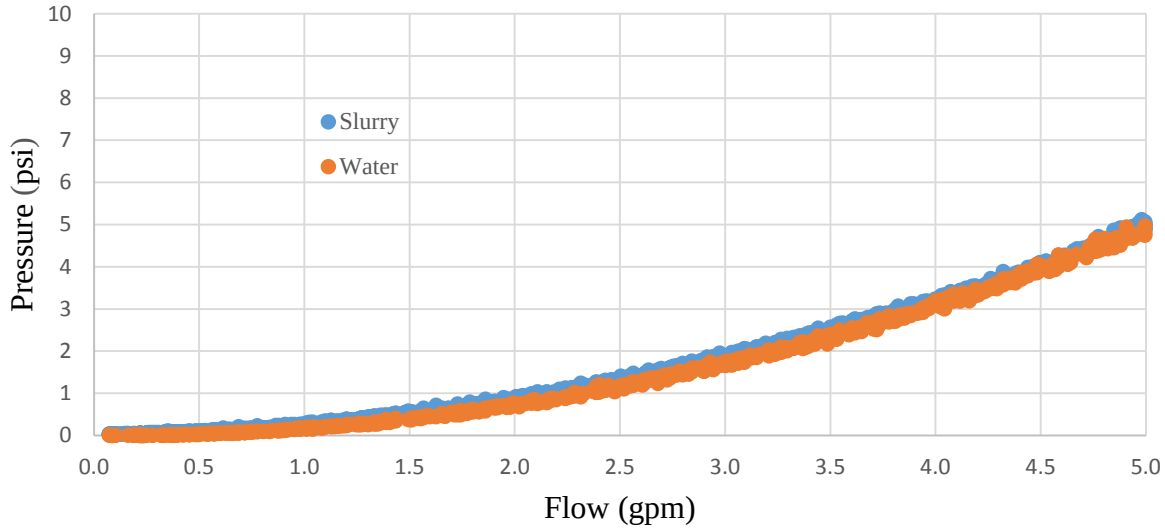

Figure 3.51. Orifice with 0.3in inner diameter, 1in length

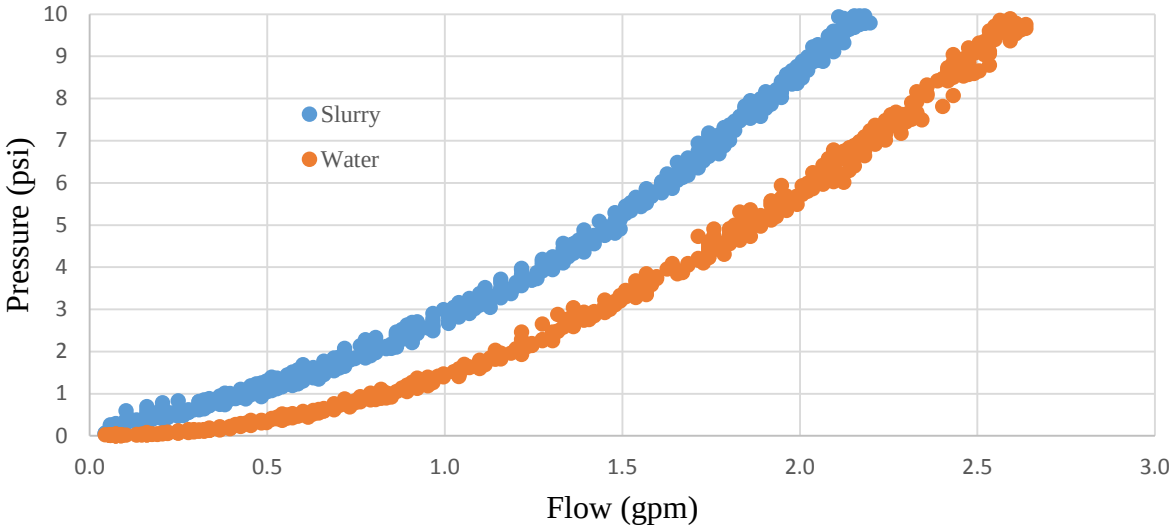

Figure 3.52. Orifice with 0.18in inner diameter, 6in length

Figure 3.53 shows the trend that as diameter decreases or length increases, pressure rises (as expected from head loss calculations). Curves paired by color designate matched diameters but different lengths, with the lighter color being the longer option.

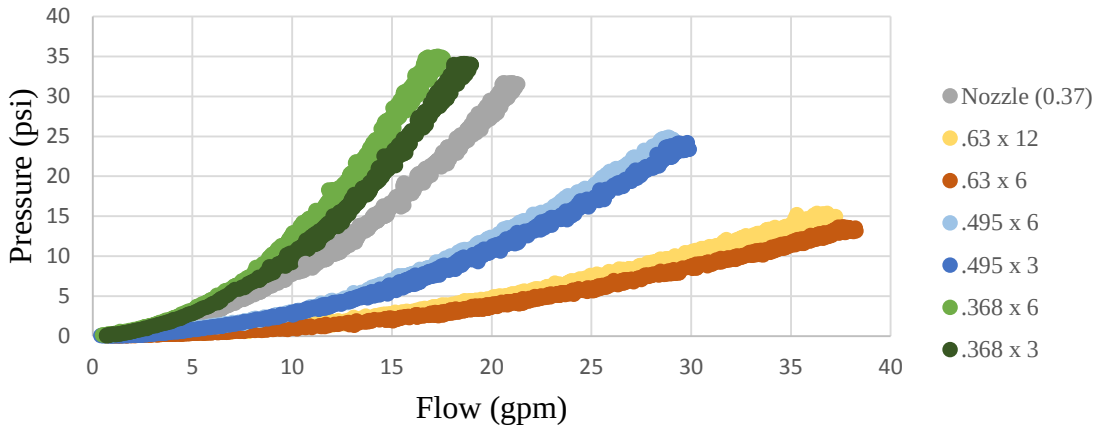

Figure 3.53. Batch representation of orifice testing with slurry (ID x Length)

3.3.7 Orifice Optimization Tests

For this round of testing, the test setup was revised for better accuracy and precision. To improve resolution and therefore accuracy, a pressure transducer with a 0-10 psi range (OMEGA PX81D0-010D5T) replaced the 0-100 psi transducer used previously. Precision was addressed by allowing the orifice to discharge into an overturned bucket, allowing the slurry flow to spin and fall into the tank thereby reducing the potential for any data-skewing backpressure at the discharge interface (from the splatter controlling hose). This method also let the flow lose energy before returning to the tank, reducing the opportunity for bubbles that if retained in flow, could affect sensor readings. Both features are shown in Figure 3.54, while Figure 3.55 shows the orifice inserting into the bucket.

Figure 3.54. Bucket to return discharge flow back into tank and 0-10 psi pressure transducer

Figure 3.55. Orifice and discharge flow collection

Further exploring the trends discovered in previous testing that result in curve separation, smaller orifices with a greater variety in length were tested. These orifices are presented in Table 3.21 and Figure 3.56. Actual diameter and length were measured using a caliper.

Table 3.21. Tested orifices

Test #	Nominal Diameter (in)	Actual Diameter (in)	Nominal Length (in)	Actual Length (in)
1	.375 OD	0.31	6	6.0625
2	.375 OD	0.3	5	4.914
3	.375 OD	0.3	4	4.05
4	.375 OD	0.295	3	3.018
5	.375 OD	0.29	2	1.984
6	.375 OD	0.295	1	1.134
7	.25 OD	0.19	6	5.9375
8	.25 OD	0.18	5	4.9375
9	.25 OD	0.177	4	3.985
10	.25 OD	0.183	3	3.04
11	.25 OD	0.19	2	2.045
12	.25 OD	0.18	1	1.074
13	0.125	0.28	4	3.966
14	0.125	0.275	3	2.935
15	0.125	0.245	2	2.01
16	0.125	0.247	1.5	1.498

Figure 3.56. Varying lengths and diameters of orifices

The orifices were cut to length from copper coils using a tubing cutter. This style of cutting may leave a metal edge that hangs into the cross section, reducing the diameter. To combat this, a deburring tool was used. All are pictured in Figure 3.57.

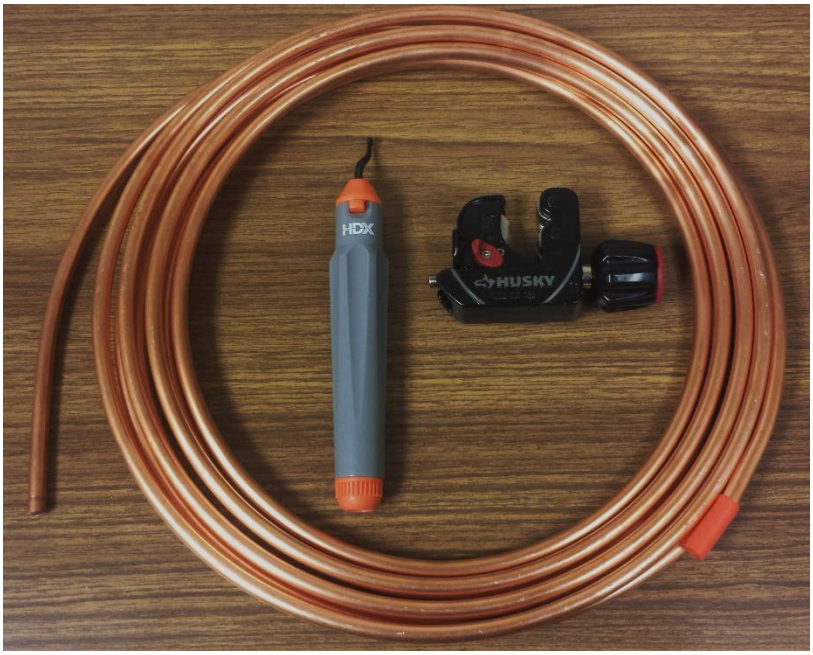

Figure 3.57. Copper coil, deburring tool and tube cutter

Like the previous tests, only a high and low range viscosity was tested for efficiency. All orifices were tested first with water, then with slurry (49 sec).

3.3.8 Final Optimization Testing Results

16 graphs (one per unique orifice design) were developed from this round of data. The full collection of raw data for this round of testing may be found in Appendix D2. By striking a vertical line through the curves, the difference between intercepted points is the pressure difference at that flow rate. Microsoft Excel aided this calculation as is shown in Figure 3.58.

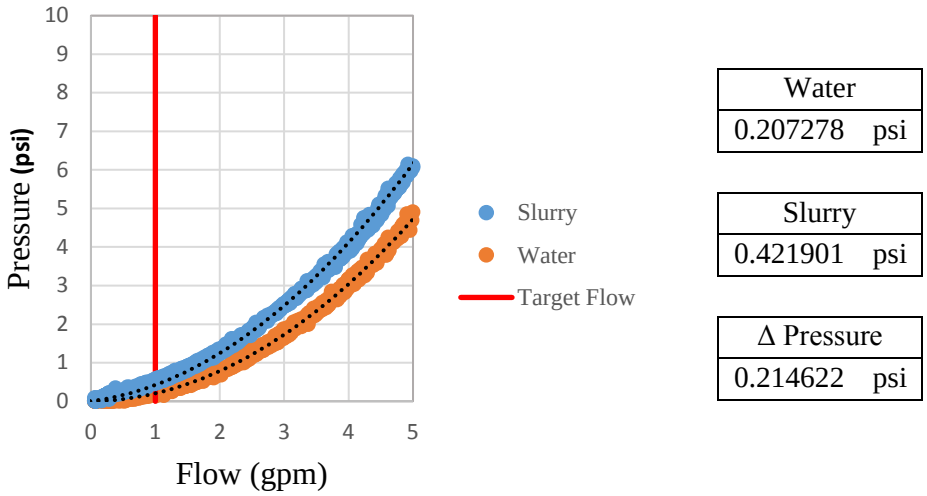

Figure 3.58. Microsoft Excel calculation of pressure difference using 0.3in diameter, 6in length

When all this information was obtained, a graph was produced comparing pressure differences between slurry and water flow vs length of orifice. Figure 3.59 shows these results for a 1 gpm flow rate. The four lines represent the four different internal diameters tested for this series of orifice testing.

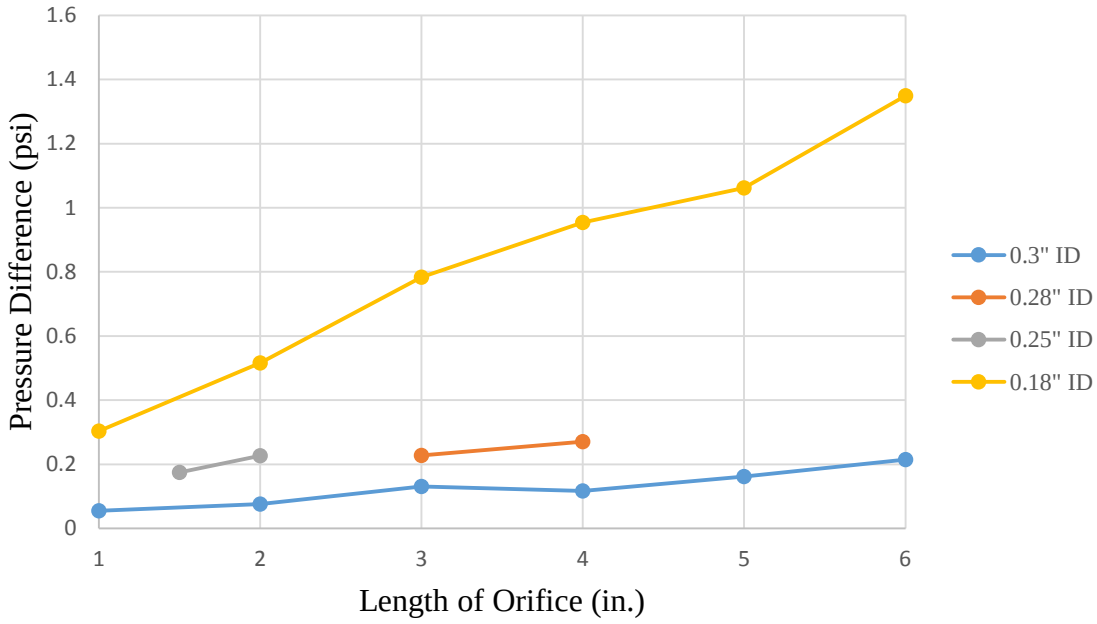

Figure 3.59. Pressure difference vs orifice length at 1gpm

Note that the 0.25in ID and 0.28in ID both claimed to be the same 0.25in diameter upon purchase, but the difference noted in the data led to further investigation of that claim. Figure 3.60 shows the 1 and 2in lengths and the 3in and 4in lengths from the two vendors. These results showed that the diameter had a larger effect than the change in length.

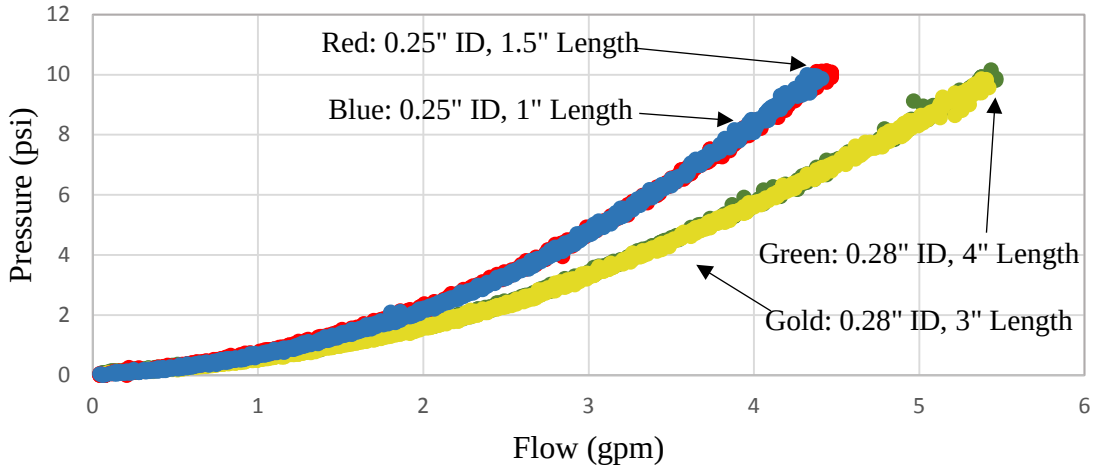

Figure 3.60. Anomaly in data due to inconsistent internal diameter in purchased materials

Further analyzation gives an opportunity for graphs to be made to aid in machine design later. For instance, striking a horizontal (for constant pressure) through the data points in Figure 3.61 and plotting the points provides a graph describing flow rate based on orifice diameter, as seen in Figure 3.62.

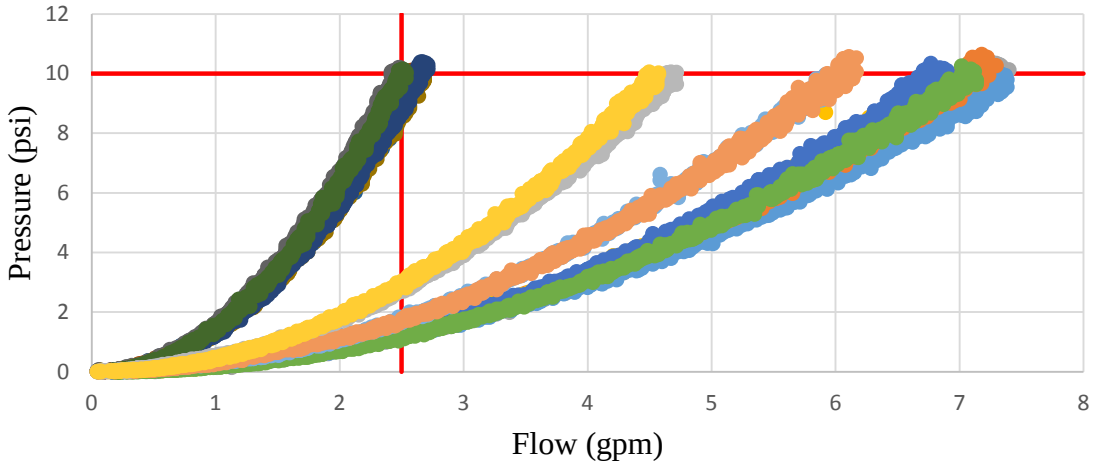

Figure 3.61. Orifice P vs F data including vertical and horizontal guidelines

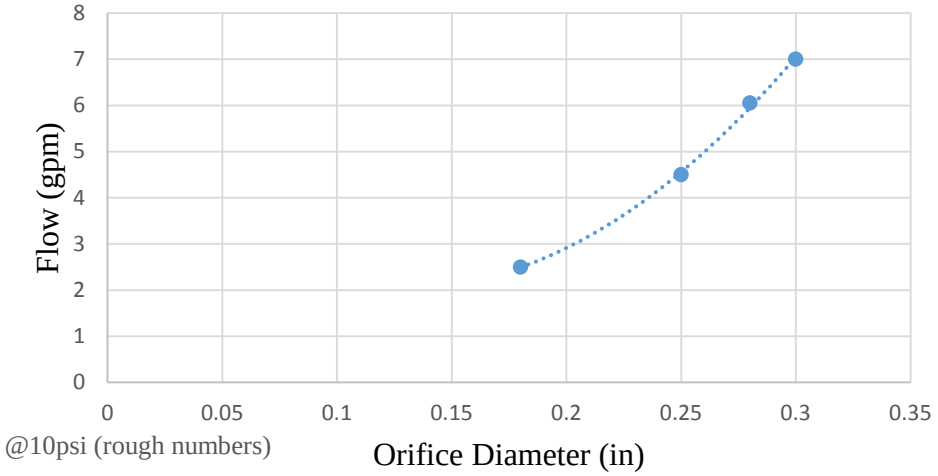

Figure 3.62. Flow rate vs diameter at 10 psi

Alternatively, as seen in Figure 3.63 a pressure vs diameter graph at a constant flow rate may be made using the red vertical guideline seen in Figure 3.61.

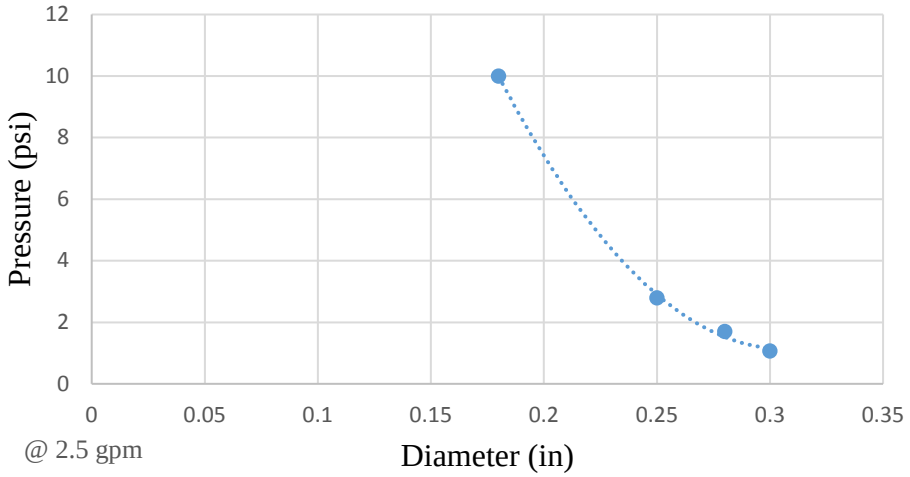

Figure 3.63. Pressure vs diameter at 2.5gpm flow rate

The design curves led the selection of a 3/16in ID orifice with a 6in length and a flow rate in the area of 2 gpm. This develops adequate pressure while keeping flow rate relatively low. Being able to use a low flow rate lowers the power requirements of the pump, thereby keeping the final product from becoming excessively heavy and cumbersome.

3.4 All-in-one Slurry Testing System

Early concepts for an all-in-one slurry testing system gave consideration to two disparate approaches: (1) a down-hole self-contained “dive bell” wherein pressure, flow, and density would be monitored at the depth of the unit and where depth would be tracked by a top-side depth encoder wheel, or (2) a top-side based slurry monitoring system where only a pickup hose would be lowered down the excavation, a top-side pump would pull slurry from the excavation, the depth of the pickup hose tip would be tracked by depth encoder wheel, and where a tracking

system would compute the slurry properties and assign it to the correct depth based on travel time up the hose. The accessibility of the second option was intriguing, but the size of the hose required to minimize fluid flow head losses made the overall system too large to meet the anticipated goals of the thesis. While the top-side concept can still be made to work, a smaller and much more mobile down-hole system was sought. Figure 3.64 shows a computer generated rendering used to size components and the enclosure/housing.

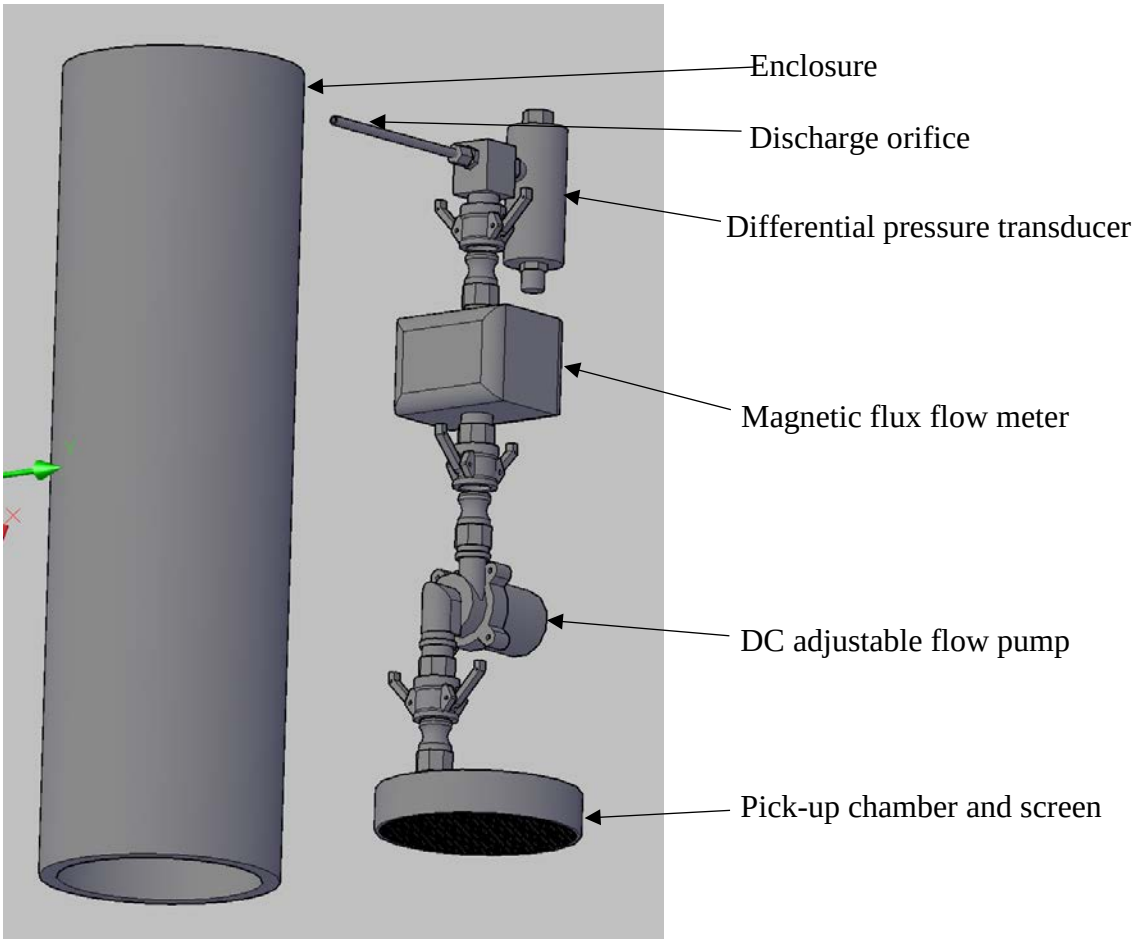

Figure 3.64. Rendering of primary P, Q monitoring system.

Components of the system stemmed from the search of available equipment and the flow rate versus pressure relationships that provided the most significant separation in the individual curves.

- Filter Screen. The components include a large diameter pickup screen (Figure 3.65) attached to a chamber to assist the filtered slurry flow to the pump. The filter screen opening size (no. 10 sieve) was selected to prevent clumps of slurry that might clog the system, similar in concept to that which is provided on a Marsh funnel.

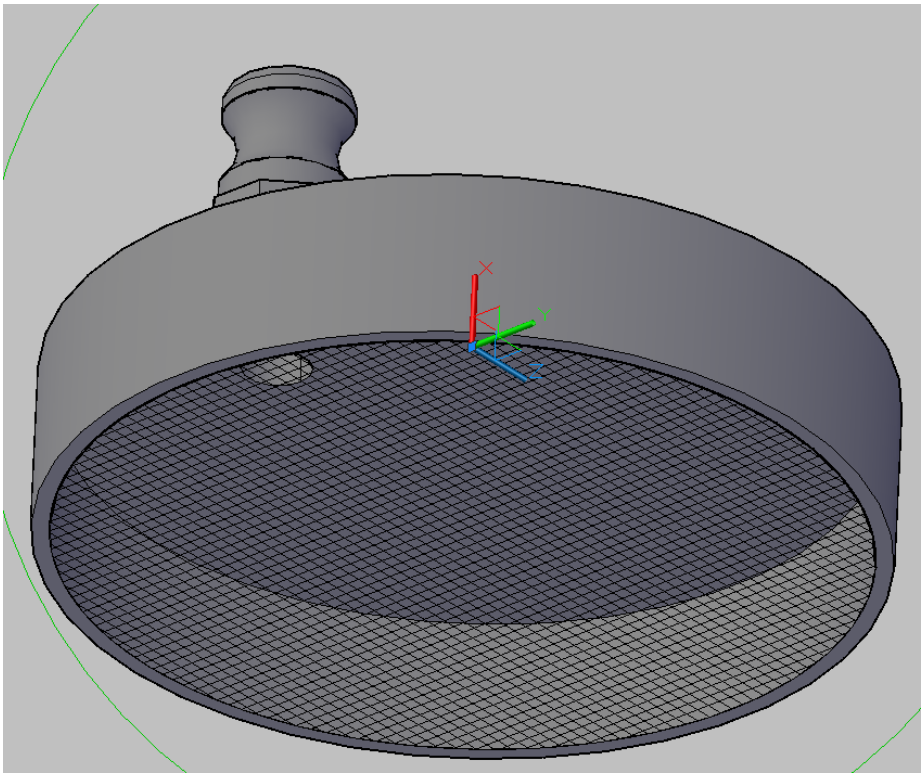

Figure 3.65. Pickup chamber and filter screen (No. 10 sieve).

- Pump. Several compact pumps were found to work well, but a low flow, DC powered, adjustable flow rate pump (Model DC50C) from ZKSF was selected which was coupled to both the pickup chamber and to the flow meter (Figure 3.66).

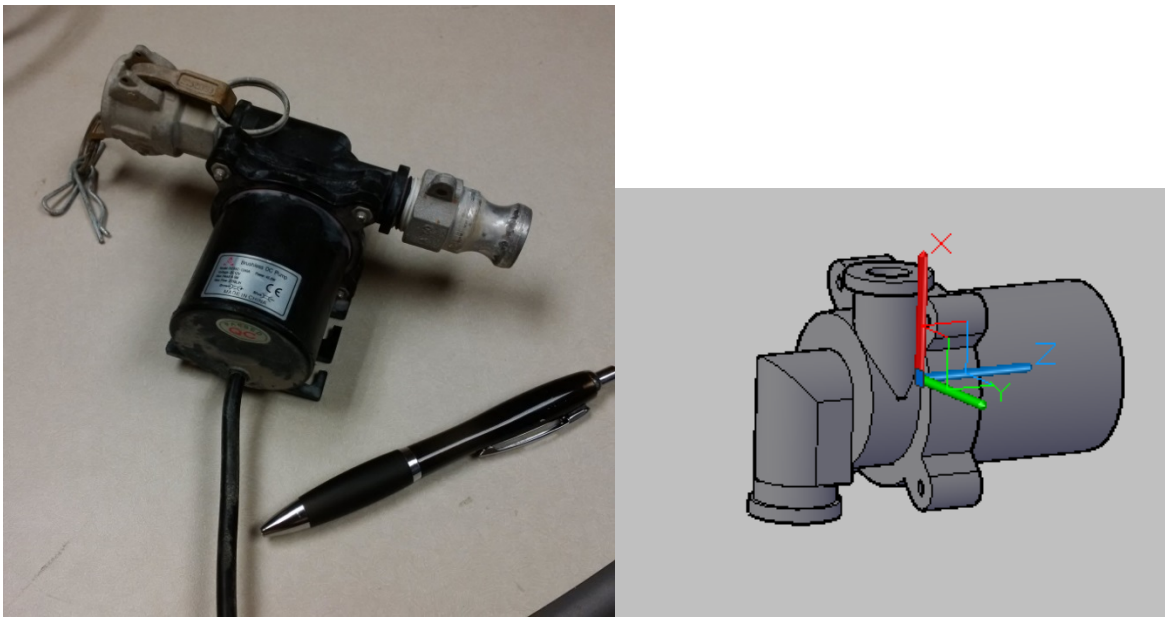

Figure 3.66. Model DC50C brushless DC adjustable flow pump.

- Flow Meter. While Doppler type meters are well suited to fluids with suspended solids, magnetic flux flow meters were found to be the most robust flow meter (no internal moving parts), would be not vulnerable to wear, and provided the best resolution and accuracy. Figure 3.67 shows the low flow magnetic flux meter selected for the all-in-one system.

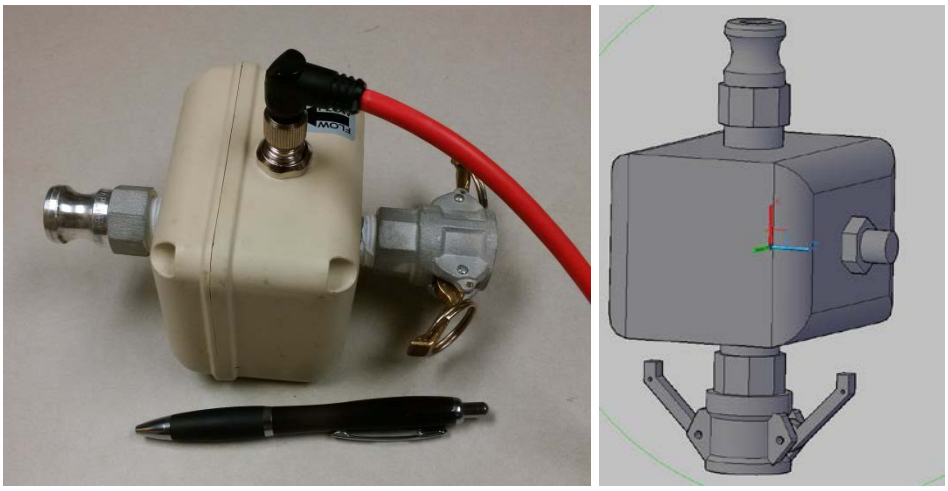

Figure 3.67. Model FMG82A magnetic flux flow meter from Omega.

- Pressure Transducer. To increase resolution a low pressure range differential transducer was selected. The advantage of a differential transducer is two-fold: firstly, as all slurry P vs Q curves are based on the

pressure across the nozzle, the differential transducer simultaneously tracks the increasing outflow pressure as slurry depth increases. Secondly, the transducer range is only required to withstand the pressure caused by the pump and not the high pressure that accompanies great excavation depths (i.e. 200ft excavation ≈ 90 psi; pressure across nozzle ≈ 1 to 2psi). In this way, the resolution of the transducer can be fully focused on a small pressure range without worries of damaging the pressure sensitive membrane. Figure 3.68 shows the Omegadyne Model PX81D0-010D5T differential pressure transducer selected for use. This device has a 10psi maximum pressure range, but even smaller ranges are available.

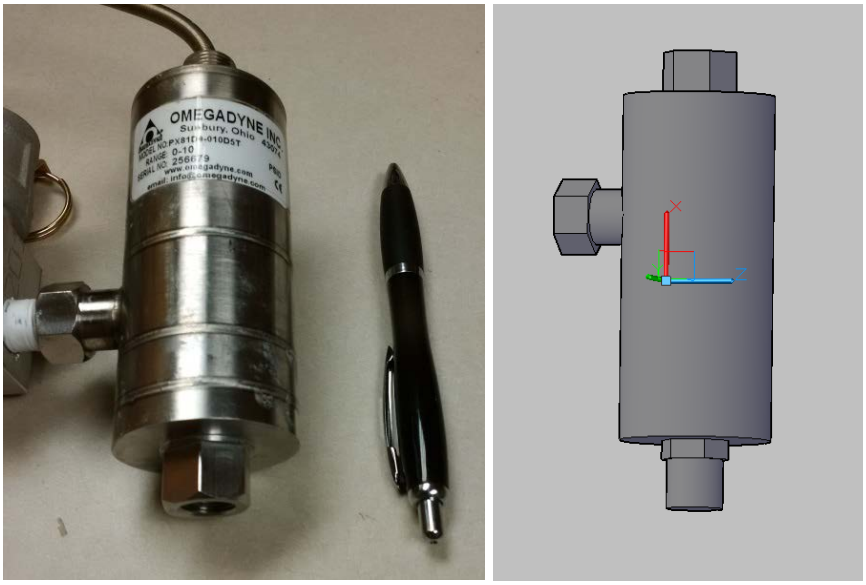

Figure 3.68. Omegadyne Model PX81D0-010D5T differential pressure transducer.

- Discharge Nozzle. Finally, the dimensions of the discharge nozzle were set based on experiments discussed earlier. While a longer discharge nozzle may be selected in future lab and field tests to further increase viscosity measurement delineation, a 6in long, 3/16in ID tube was selected (Figure 3.69). This nozzle was coupled to the pressure transducer and the flow meter via a junction block as shown in Figure 3.69. At this point, the discharge nozzle exited the system enclosure through the side and is sealed to the enclosure walls with a gland fitting. Future exit locations out the top of the enclosure were under consideration.

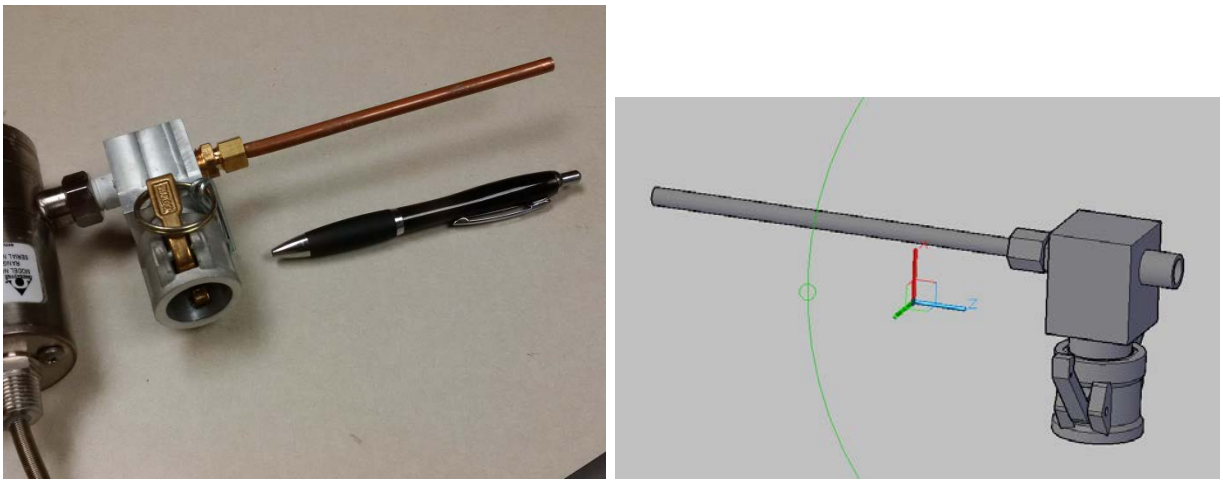

Figure 3.69. Discharge nozzle assembly that exits the enclosure through the side.

All flowing components are coupled with cam-lock quick-connect fittings to aid in both assembly and service. An advantage of a top-exit discharge nozzle (noted above) is to further facilitate assembly and service but is not intended to increase system performance.

3.5 System Calibration

Calibration of the P versus Q relationship to viscosity is a multi-part exercise that involves both laboratory testing and curve fitting. Calibration of the all-in-one slurry "viscometer" component forms an important part of the chapter 3 efforts, but an example has been presented based on the earlier falling head tests.

As each viscosity has a unique P vs Q curve, the data was fitted to determine the best fit function (Figure 3.70). At this point, the data can be sorted by lines of constant pressure or flow rate using an equation; the intersections of each constant flow rate line is then plotted versus the viscosity intersected by these lines. Figure 3.71 shows the viscosity versus pressure for lines of constant flow rate. Using a simple conversion to verify a hyperbolic relationship, the pressure /

viscosity data showed a strong regression fit (Figure 3.72) and functions for these curves were then developed. The slope (m) and intercept (b) are then specific to a given flow rate.

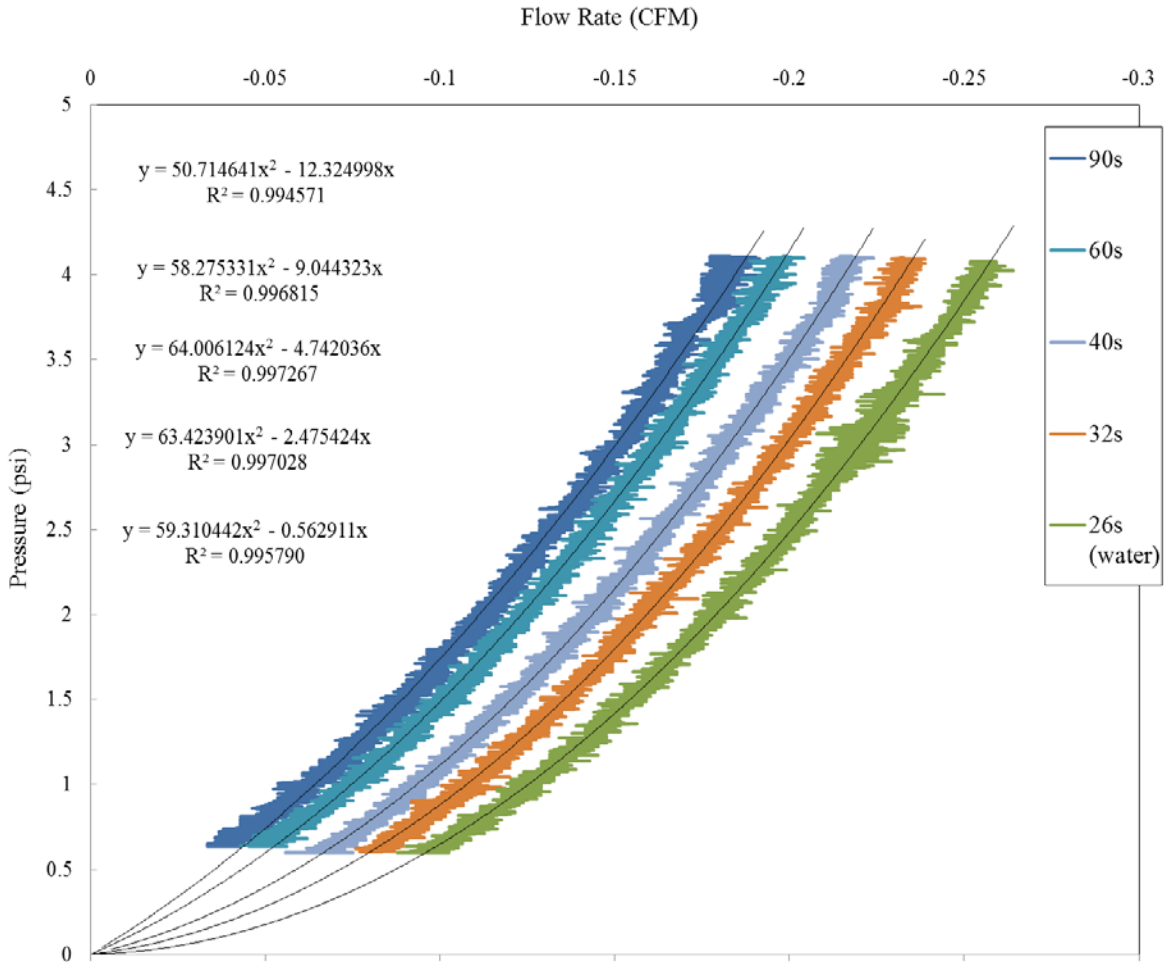

Figure 3.70. Fitted P vs Q curves for wide range of viscosity.

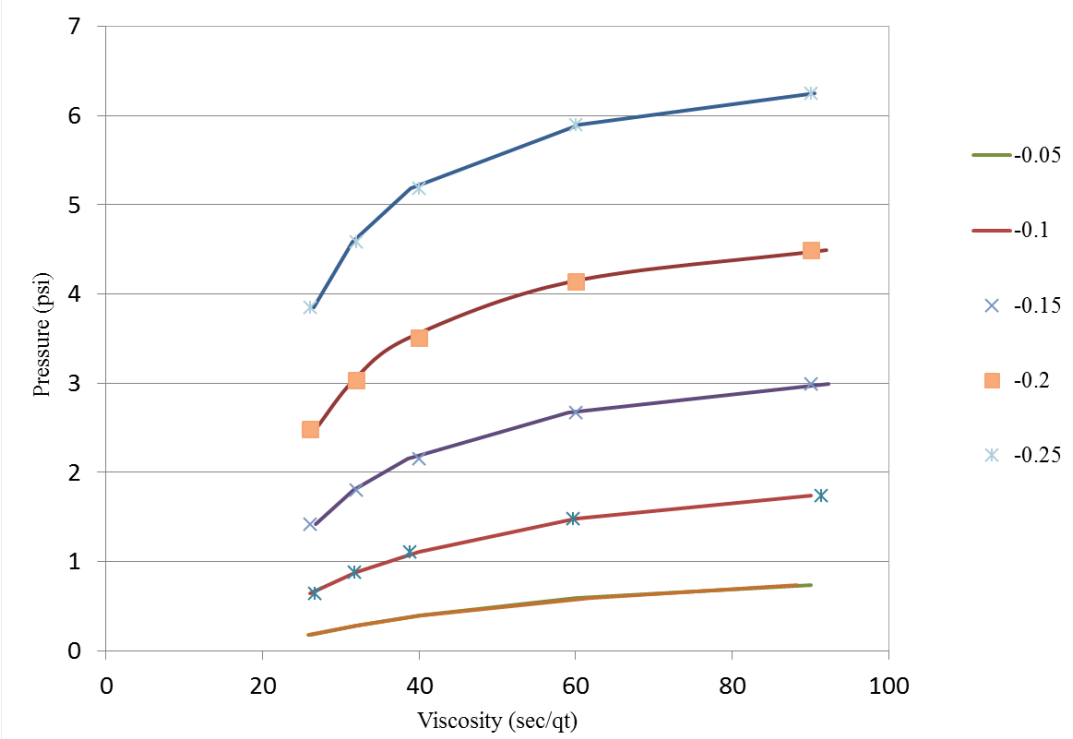

Figure 3.71. Pressure vs Viscosity curves from lines of constant flow rate (in gpm).

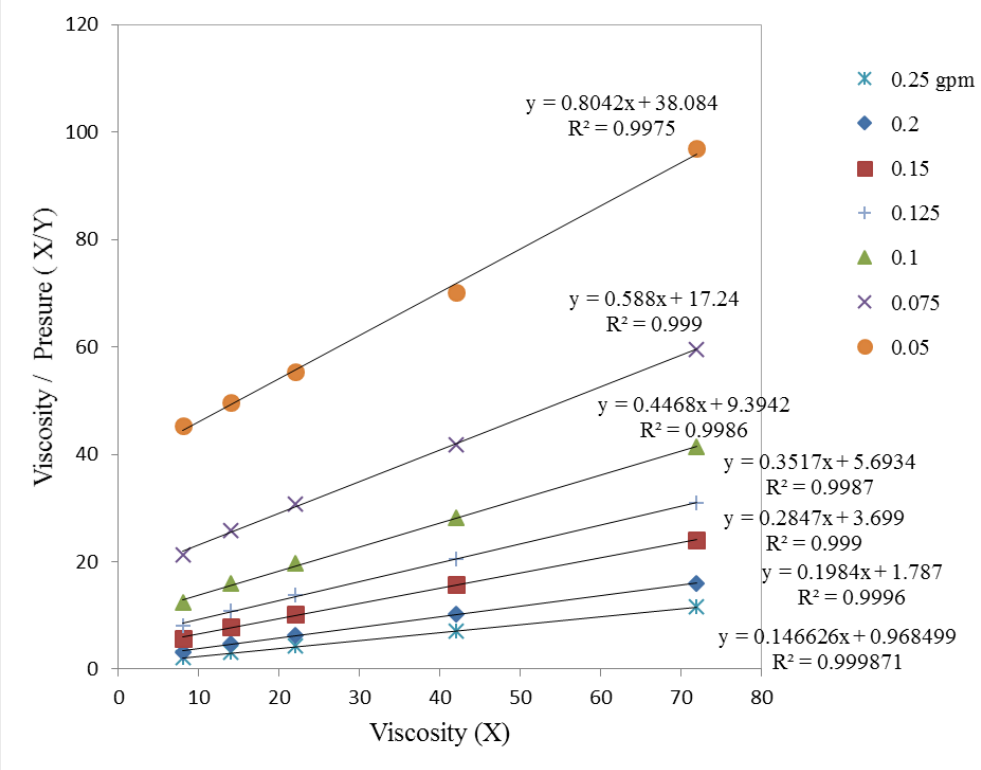

Figure 3.72. Linearization confirming hyperbolic relationship.

The linear coefficients from Figure 3.72 where then plotted vs the flow rate and a second set of regressions were performed (Figure 3.73).

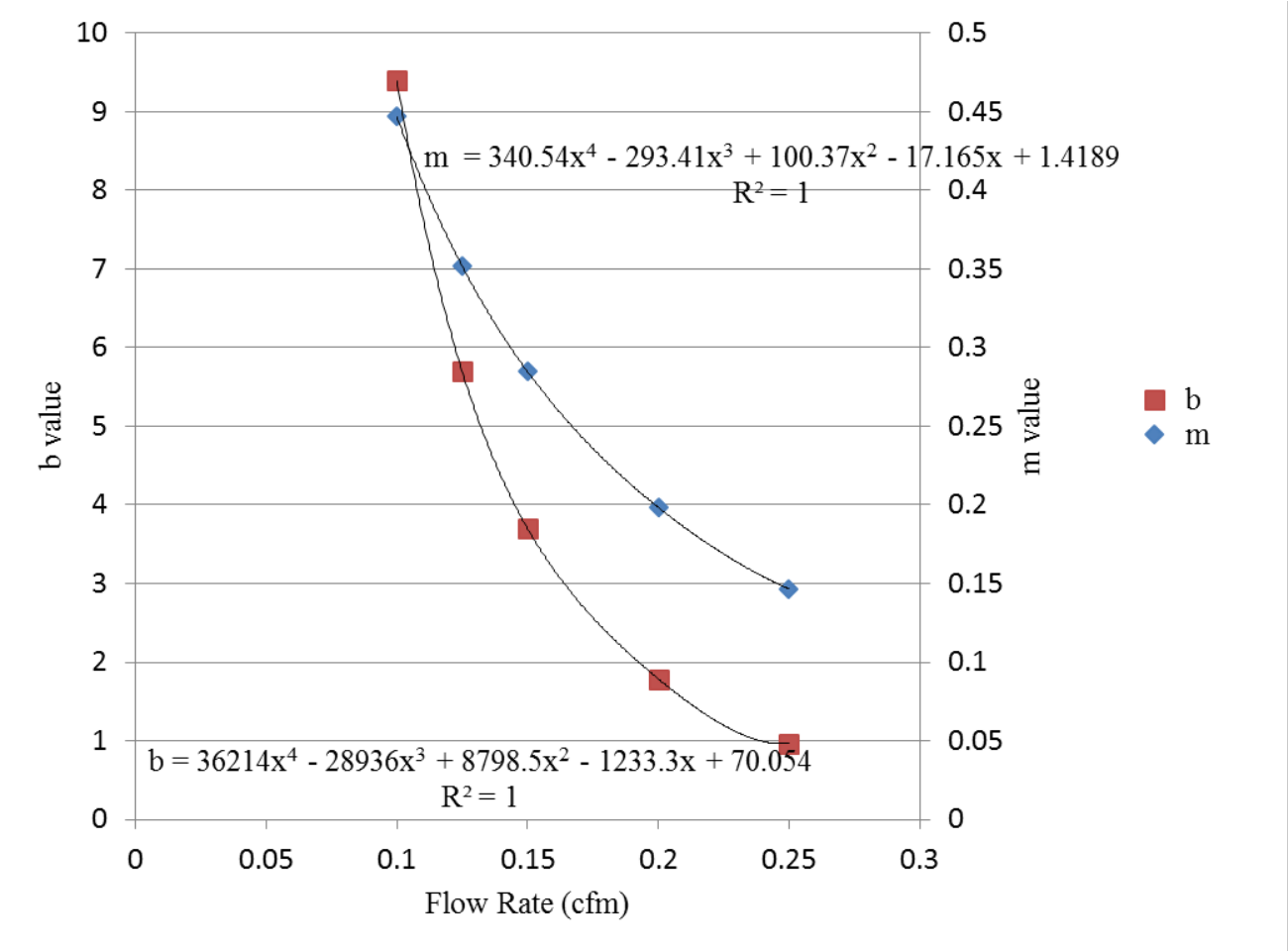

Figure 3.73. Linear fit parameters m and b vs flow rate.

Using this approach, the flow rate is input to select the m and b coefficients that define the appropriate P vs Viscosity hyperbolic relationship. Then the pressure is input into the inverse form of the Viscosity vs P equation to predict the instantaneous viscosity. In this way, the viscosity is a function of both P and Q.

Remember the hyperbolic relationship was identified using the linearized form

$$\frac{Visc}{P} = mVisc + b$$

Solving for viscosity gives the revised form as a closed form solution

$$Viscosity = Pb/(1 - Pm)$$

Using this approach, P and Q data from Series I were from 90sec, 40sec, and 26sec tests to show the stability of the predictive equation (Figure 3.74).

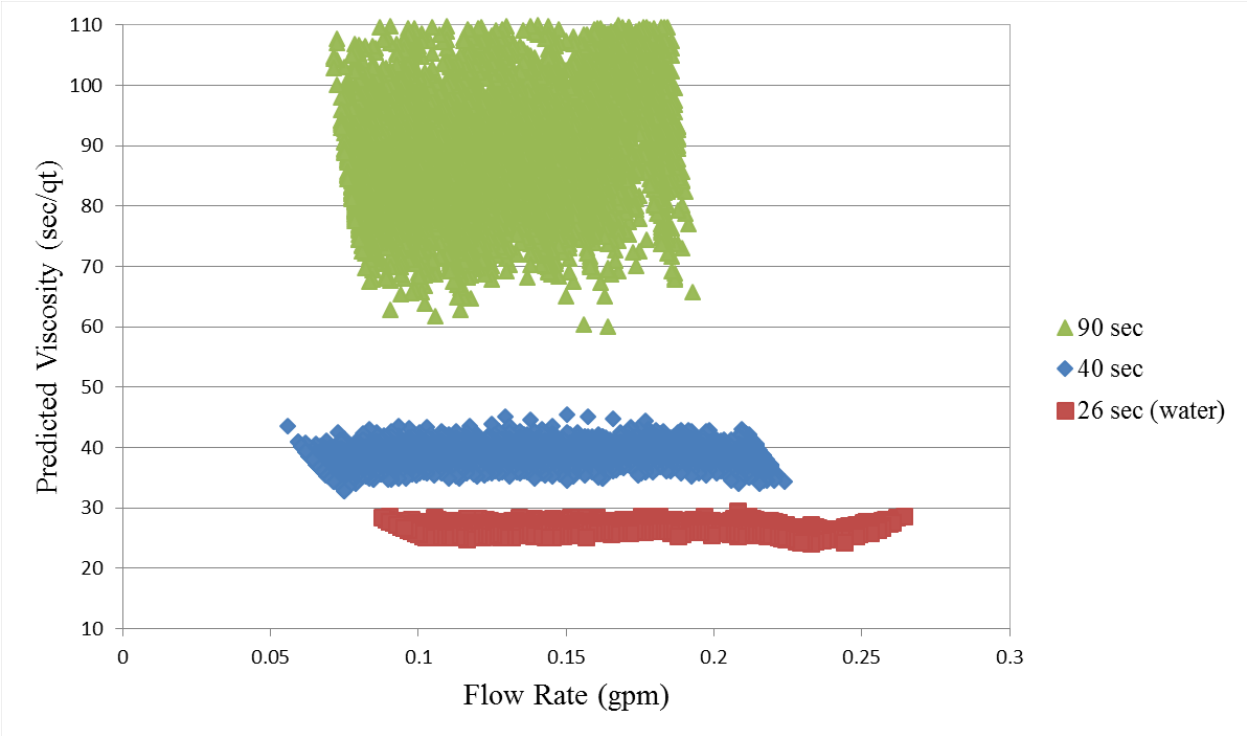

Figure 3.74. Instantaneous viscosity from predictive algorithm.

The instantaneous nature of the example data and prediction is based on samples taken at a sampling rate of 10Hz. The flow rates were based on time-dependent weight measurements where the change in slurry weight per time was converted to equivalent volume of flow and hence a flow rate. Such approaches are inherently sensitive to small time steps and often produce erratic results. The slower emptying (falling head) 90sec slurry was more affected as two successive measurements would have had similar weights. The system algorithm implements an averaging scheme which produces output at a user defined depth interval (e.g. 1ft). This will reduce the observed scatter in the predictions. Regardless, the average viscosities predicted and shown were 91, 39 and 27sec for the Marsh funnel measured slurries of 90, 40, and 26sec, respectively. The all-in-one system uses magnetic flux flow measurements which are far less noisy and do not incorporate small time step division errors.

While the specific regression presented was not for the finalized system, the same process was followed to calibrate a prototype all-in-one-system discussed in Chapter 4. Although not mentioned in this Chapter, measurement of slurry density and predictions of sand content are also incorporated in the all-in-one-system. Sand content determination using the prototype system is in essence computational but thorough testing of these concepts and algorithms are discussed in Chapter 4 as well.

CHAPTER 4: LABORATORY TRIALS

4.1 Overview

While the concept and procedures for calibration were thoroughly discussed in Chapter 3, the as-built device required several changes which made all previous calibrations void (e.g. nozzle length and shape change the losses during flow). This chapter outlines the fabrication and laboratory testing to calibrate the all-in-one slurry testing system. It also includes performance tests conducted to demonstrate system battery life as various components are interchanged with alternate components.

4.2 Design Changes / Fabrication

Each of the components illustrated in Figures 3.64 – 3.69 were scrutinized for practical aspects of assembly and maintenance prior to fabrication. Several of these parts were found to need altering to fit the enclosure housing (Figure 3.64) or to facilitate assembly. For instance, the discharge nozzle was originally designed to exit through the side of the housing which complicated disassembly / assembly. As a result, the finalized design opted to exit the discharge through the top cap. Also not shown in the concept assembly (Figure 3.64) was the density measurement components. Figure 4.1 shows an updated layout of the down-hole unit (DHU) complete with battery packs and a second differential pressure transducer used for density determination.

The density gage works simply on the difference in pressure over a known difference in depth. The design length of the assembly (approximately 30in) would then produce a registered differential pressure of approximately 1psi for water. However, the internal plumbing to these interfaces must be fluid filled with a fluid type of known density that can be sealed within the lines and not be free to exchange during routine testing. This translated into a design change that needed to incorporate interface membranes that would isolate the internal gage fluid from the slurry yet accurately transfer the pressure. Both differential pressure transducers required these isolators to protect the gage from fouling from repeated exposure to slurry. The density transducer required two isolators, while the flow/pressure gage required one relative to the outside slurry pressure into which the discharge would occur. Both the top and bottom caps of the system were redesigned with 3/4in diaphragm isolation chambers as shown in Figure 4.2. Figure 4.3 shows the fabricated components.

The housing for the entire assembly was selected to be a transparent 6in ID PVC pipe. Both ends of the pipe were cut square and polished to a smooth surface to promote a satisfactory seal with O-rings. This meant that O-ring grooves were cut into both the top and bottom caps. Four full length 1/4in stainless steel rods were cut and threaded to serve as tension rods that compress the top and bottom caps onto the smooth housing end faces.

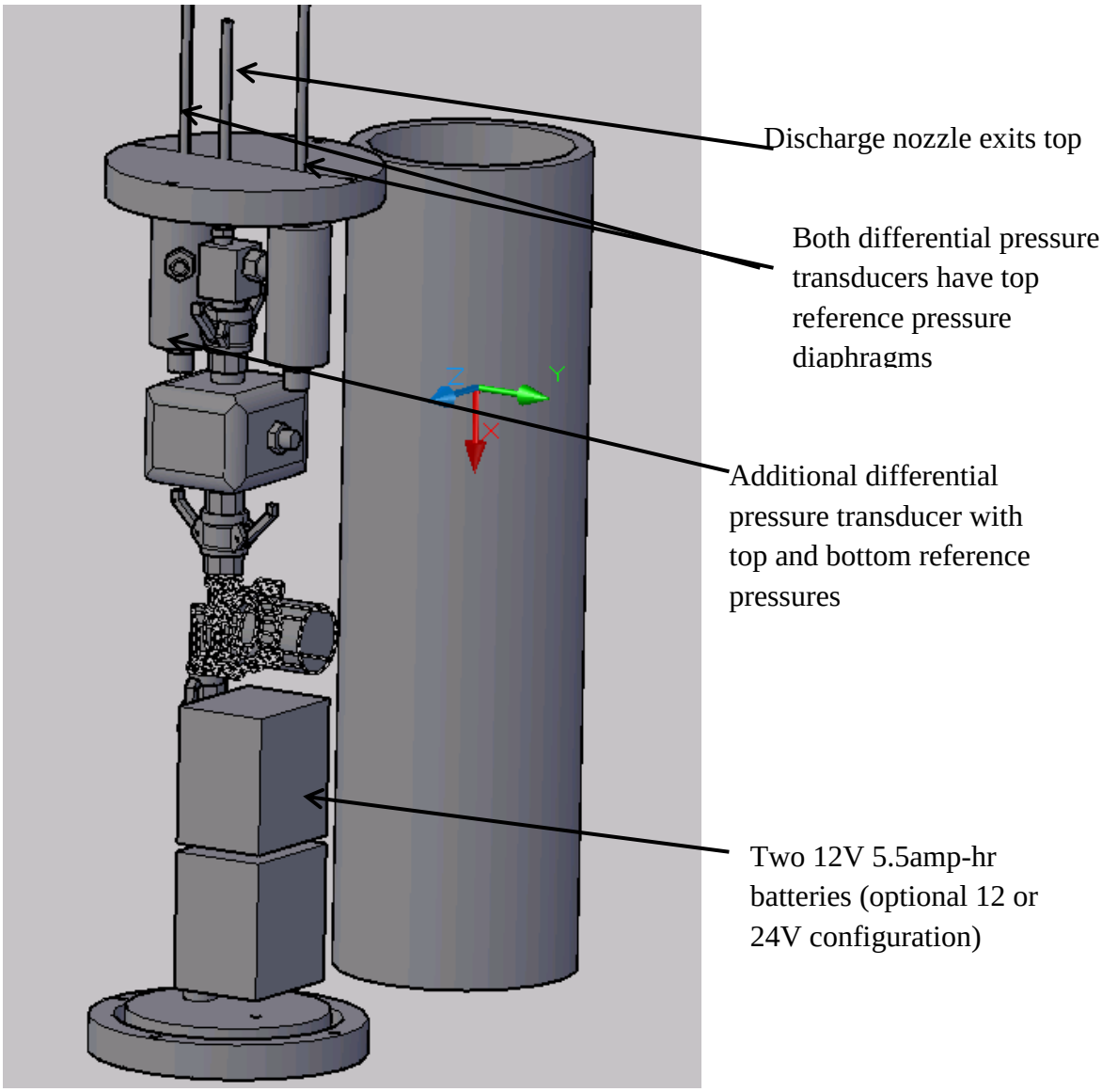

Figure 4.1. Updated design drawings of the down-hole unit to include exit ports.

The finalized design provided for disassembly of the system by removing the tension rods and then removing the eight bolts that seal the pump pickup plate to the bottom end cap. At this point, the end cap falls away from the entire unit and the top cap and all the components down to the pump pickup plate slide upward out of the housing in one piece. This further allowed all differential pressure fluid lines to maintain their internal / isolation fluid (50/50 glycerin water mix).

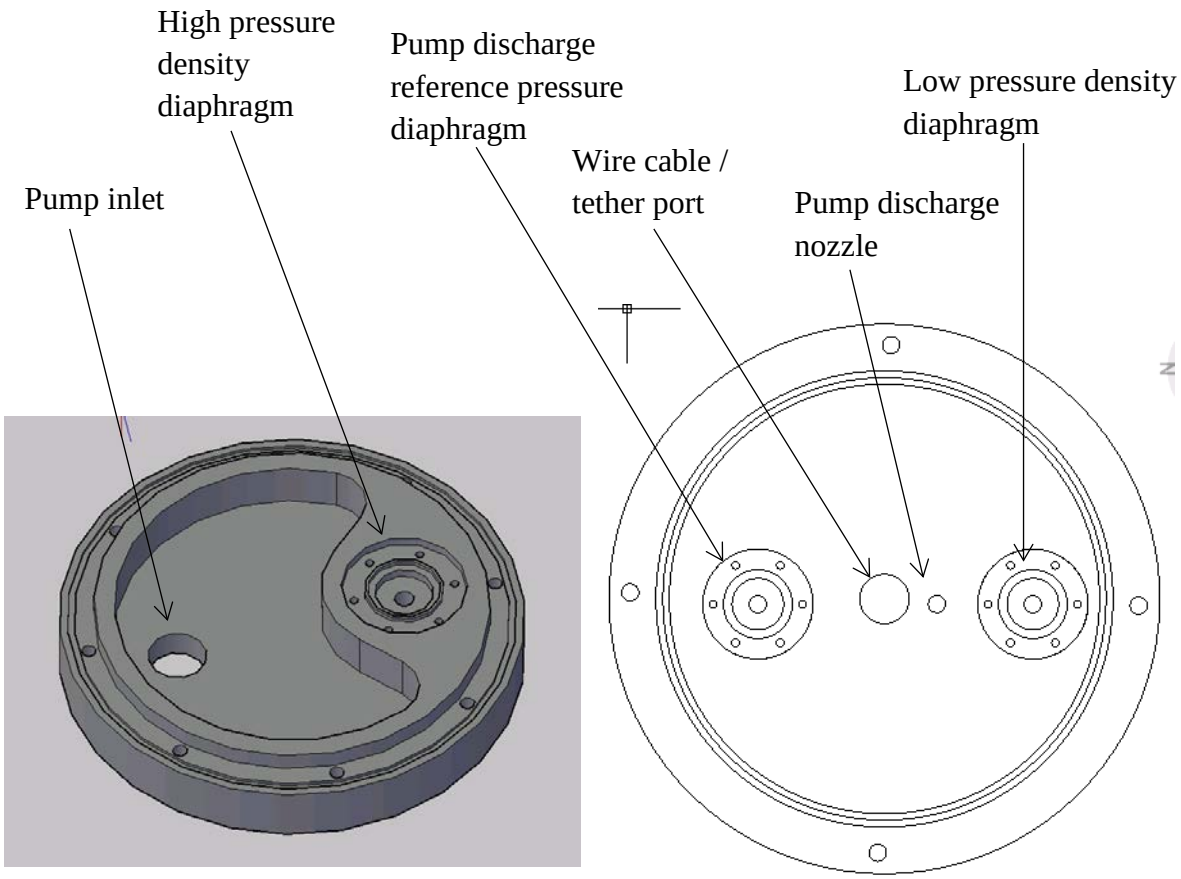

Figure 4.2. Pump pickup plate (left) and top cap (right) complete with diaphragm interface chambers.

Figure 4.3. Fabricated components: 8in diameter top cap (lt), 5-3/4in diameter pump pickup (ctr), and 8in diameter bottom cap with recesses for housing and pickup plate (rt).

Note that the pump pickup and bottom cap share an 8 bolt hole pattern to secure them together, and both the top and bottom caps have 4 holes outside the housing lip for the tension rods.

4.3 Power Considerations and Cabling

Component selection discussed in Chapter 3 did not address the individual power requirements of each device. For instance, depending on which pump was selected (from all the acceptable models tested), AC or DC voltage may be used and the current demand of each pump is accompanied with wire size requirements. 110 AC voltage was eliminated from further consideration for multiple reasons. However, if a 12VDC pump with a 4 amp draw is supplied from the top down a 150ft tether cable, two 5AWG conductors would be required (with a 5% acceptable voltage drop). The copper only would weigh 30lbs and there would still be need for all the instrumentation wiring. As a result, on-board batteries were selected to control the cable/tether size and weight. This aided in other practical aspects such as the self-weight of the assembly needed more weight to submerge and the cable/tether needed to be pliable enough to bend over the depth encoder assembly at the top (which tracks the assembly depth).

Power requirements varied by component and presented a challenge in satisfying all needs without having excess weight/complexity. The flow meter requires 10-15 VDC, while the pump can use 12 or 24 VDC and the pressure transducers use 24-32 VDC. Table 4.1 shows the individual components of the system, the associated power needs and the number of conductors needed to be within the cable/tether.

Table 4.1. Power and conductor requirements.

Description	Power Requirement	Reqd. No. Cable / Tether Conductors	Output Type
Pump	12 or 24VDC	None for operation	N/A
Pump relay	12VDC triggered by computer system	2	N/A
Flow meter	10-15VDC	2 or 4 (for both output)	4-20mA current or digital counts
Nozzle pressure	24-32VDC	2	0-5VDC
Density pressure	24-32VDC	2	0-5VDC
Battery Charge	12 or 24VDC top to bottom feed	2	N/A
Battery Monitor	N/A	2	N/A
Pump Speed Control	N/A	3	N/A

Immediately apparent is that neither battery configuration (12 or 24V) fully satisfied all the instrumentation and pump voltage needs. Initial use of additional battery sets (e.g. 3 – 9VDC batteries in series) were thought to be needlessly complicated, so a simplified single supply source was sought. With the pump being the highest current demand, the single primary source was set to satisfy the pump. This still left two choices as the pump options could be 12 or 24V.

Supplying lower voltage from a higher source is relatively easy using readily available, inexpensive voltage regulators; the opposite is more challenging. However, newer technology DC voltage boosters are now readily available especially for low amperage requirements. A model RRLM25961.23-30V boost converter from RioRand was selected that could boost DC voltage from 3 to 35 volts (Figure 4.4) which satisfied the higher voltage needs of the pressure transducers.

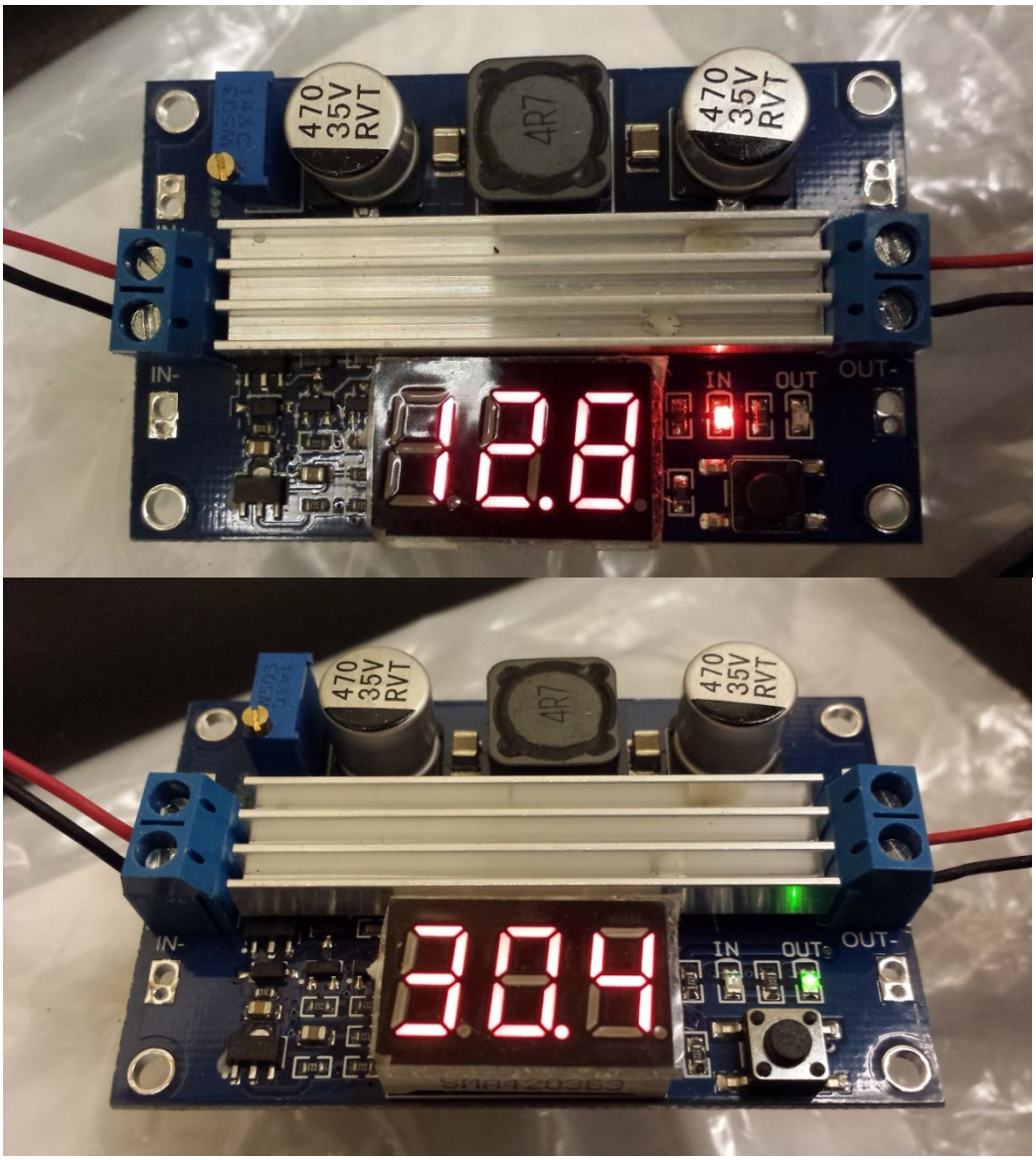

Figure 4.4. Boost converter showing input (12.8) and output (30.4) voltage.

The boost converter output was slightly affected by input voltage, so in the event of supply battery voltage decay, the boosted voltage could also drop. Setting the boost converter output voltage well above the minimum required (24 - 32V) by the pressure transducers protected from this condition and kept the transducers from being underpowered. To see how low power input affected the pressure transducers, a simple test was performed where a pump was connected to a high capacity RV/Marine grade deep cycle battery to keep pump flow and

pressure near constant. Figure 4.5 shows the effects of low supply source voltage on the registered pressure. No actual drop in flow rate or pressure was observed during the course of the test.

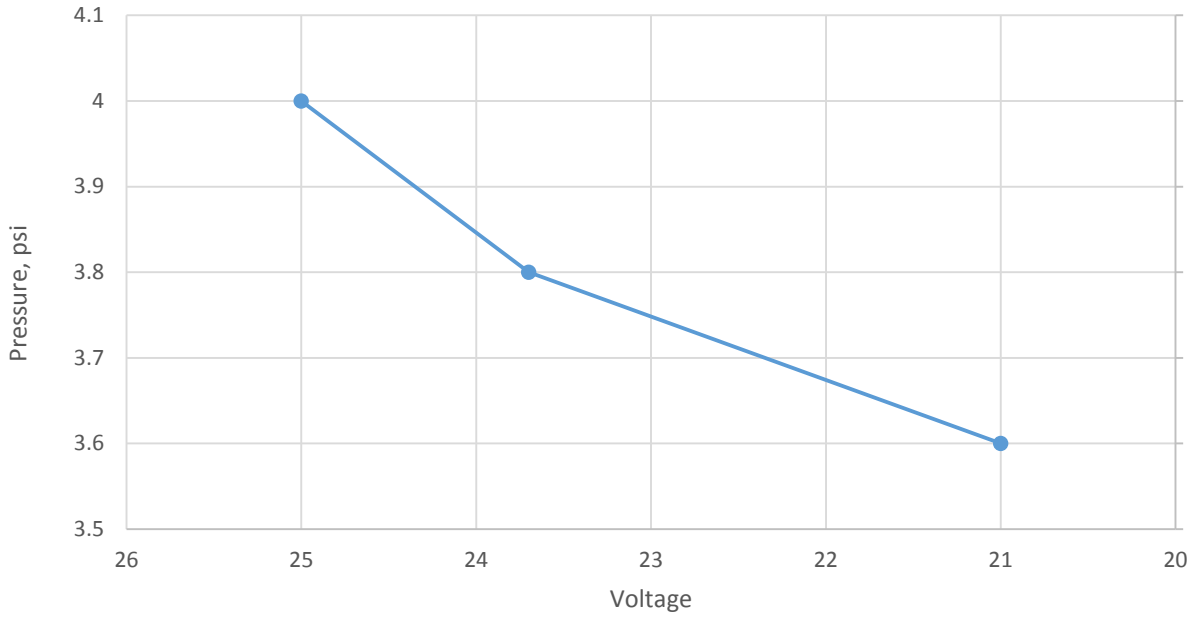

Figure 4.5. Transducer reading drop from inadequate input power.

While using one 12V battery may be able to power the system, adding the second battery doubles the amp-hour capacity and introduces the ability to provide 24V power if wired in series. This provided flexibility to run the pump at 12 or 24 volts while satisfying all the instrumentation requirements. Two 12V 5.5Amp-hr lead acid batteries were selected with dimensions that fit the available space within the system housing (Figure 4.6).

Figure 4.6. 12 volt batteries with common 9 volt for size reference.

4.4 Battery Life / Pump Performance Testing

The prototype all-in-one slurry testing system needed to maintain a practical amount of field service life to be a viable unit. Despite calculations that showed the draw and Amp-hr specifications would be sufficient, the actual performance was tested under different slurry conditions including clear water to thick slurry. These tests were run with varied pump type and battery supply voltage configurations. This flexibility stemmed from the selected pump coming with various performance features (i.e. high pressure low flow rate, high flow low pressure, 12V, 24V or 12/24V, etc.). All of these pumps are variable flow pumps controlled by a potentiometer type controller. Figure 4.7 shows the test setup with the pump submerged and the system flow meter and pump nozzle assembly recirculating back to the pickup reservoir. Figure 4.8 shows the results of these tests performed on different pumps and supply voltages.

Three configurations shown are: the 24V pump run at 24V, the 12V pump run at 12V, and the 12/24V pump run at 12V. For comparison purposes, the average of the two battery voltages is shown instead of the total supplied voltage. In this way the 24V and 12V supplies could be better assessed. Naturally, flow rate and pressure both dropped with battery life. Figure 4.9 shows one of the tests along with flow and pressure. Also the flow rate and pressure from the three configurations were not the same. The 24P@24V pumped at a maximum flow rate of 1.6gpm, 12P@12V at 1.4gpm and the 24P@12V at 1.2gpm. All fell within the range tested in the first calibration exercise discussed in Chapter 3 for the falling head Marsh funnel tests.

Figure 4.7. Battery life / pump performance tests.

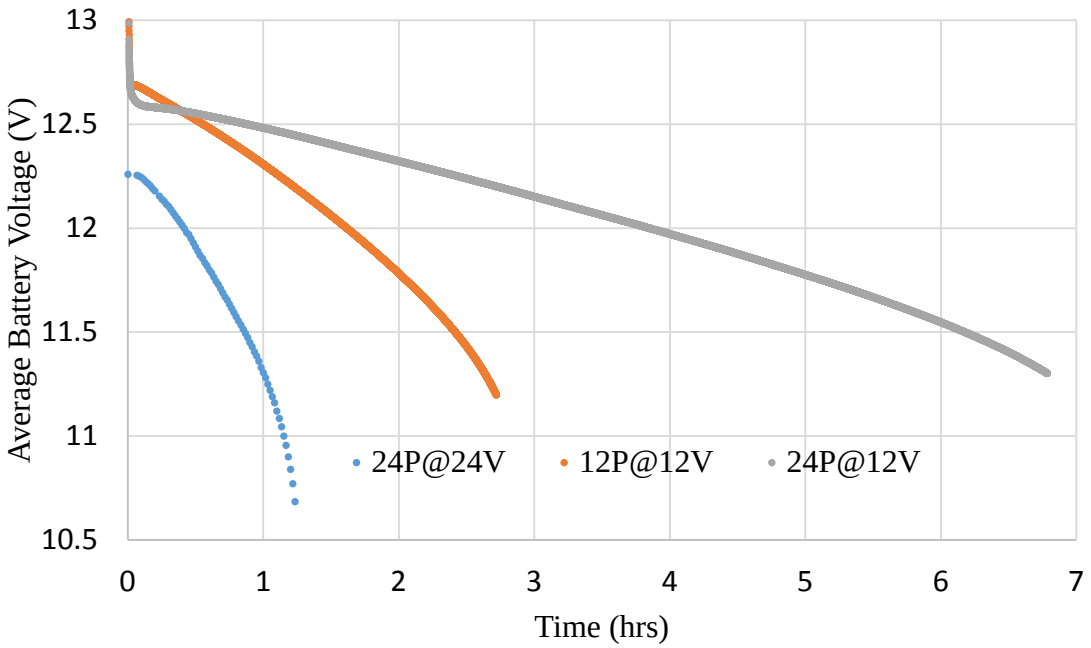

Figure 4.8. Battery life tests from various pump and voltage setups running at full capacity pumping clear water.

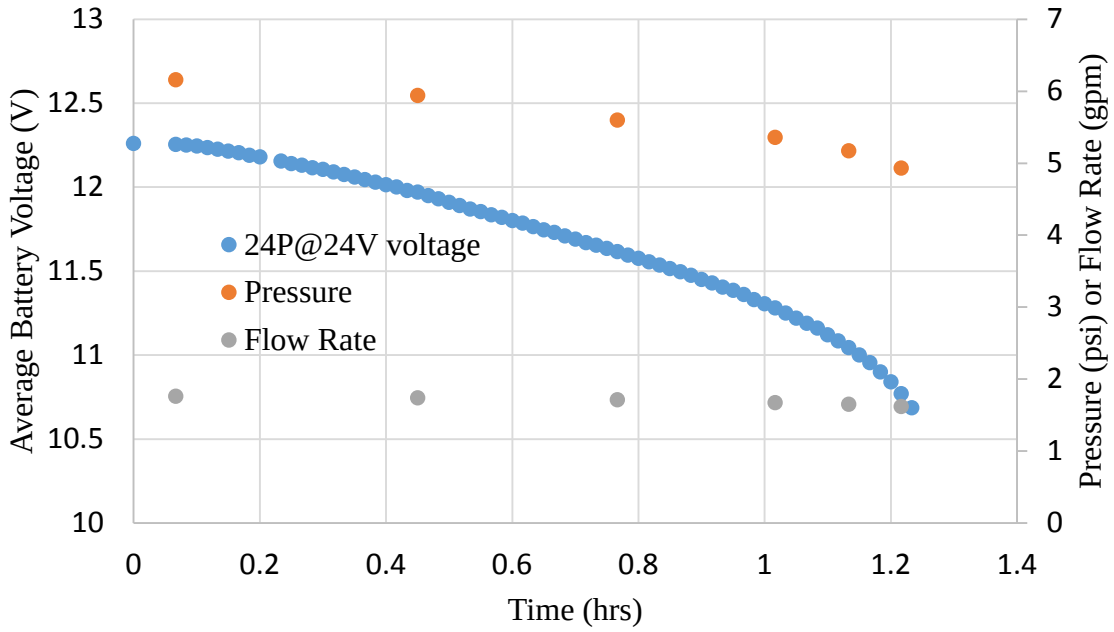

Figure 4.9. Flow and pressure drop relative to voltage and time of testing for 24P/24V configuration running at full capacity pumping clear water.

4.5 System Assembly

Several steps were required in the initial assembly of the all-in-one slurry testing device. Where the pump, flow meter, nozzle and pressure transducer had all been tested in concert with each other, the density transducer had not. Likewise, the new longer discharge nozzle through the top cap and all diaphragm features had not been incorporated. The following steps were required when assembling the down-hole device for the first time.

(1) The top cap was prepared to receive three ferrule type tube seals through which the reference pressure ports and discharge nozzle could exit the top cap.
(2) The pump pickup plate was similarly fitted with one ferrule type fitting for the high pressure density diaphragm port. A 1/2in NPT cam-lock fitting was also attached to the inside face of the plate which provided quick-connect ease to the pump intake port.
(3) The pump pickup plate was bolted to the bottom cap. At this point the entire unit was assembled from bottom to top.
(4) The pump, flow meter and nozzle were all already prepared with similar cam-lock fittings. This conveniently allowed for assembly and precise component alignment without having to spin together threaded pipe fittings.
(5) An extension pipe was also fitted with cam-lock fittings and secured to the pickup plate and the intake port of the pump. The additional length provided by the extension pipe provided additional space in the housing to secure the two batteries.
(6) The flow meter and nozzle assembly were next connected to the pump using the same cam-lock fittings.
(7) At this point the low pressure ports of the differential pressure transducers were extended with copper tubing with sufficiently long lengths that would completely pierce the top plate. The discharge nozzle was similarly extended.
(8) The transparent PVC housing was then lowered over and around all component and fitted into the bottom plate recess thereby sitting on the lower O-ring seal. At this point three copper tubes extended from the top of the assembly.
(9) The three copper tubes extending from the top where then threaded through the ferrule fittings in the top plate and the plate was lowered until the O-rings on the underside of the top cap were in contact with the transparent PVC housing.

(10) The tubes extending from and out of the top cap were then marked to show the precise length of the entire system, the top cap was removed and two pressure transducer tubes were cut to length.
(11) The transparent PVC housing was then removed, the top cap reinstalled over the copper tubes and all ferrules were secured into the prescribed position set by the cut lengths.

Note that at this point (and here forward) the system must be assembled and disassembled by sliding the entire assembly through the housing complete with the pump pickup plate. The device is then comprised of three basic pieces: Part (1) all the internal components attached to the top cap complete with pump pickup plate, Part (2) the transparent PVC housing, and Part (3) the bottom plate.

(12) With Part (1) upright and top cap facing upward, both the upper diaphragm seal in the top cap were then flooded with a 50/50 glycerin solution until all air was expelled from the lines and a nitrile rubber membrane was placed over the filled chamber and secured with a collar and protective grill.
(13) With Part (1) laying horizontally and the higher pressure density transducer port facing upward, the transducer was flooded with the glycerin solution and a copper tubing extending to the pump pickup plate was attached. Recall the pickup plate is also equipped with another diaphragm chamber that supplies high pressure readings to the density transducer.
(14) With Part (1) inverted and the pickup plate facing upward, the copper tube running to the density transducer was flooded with the glycerin solution, nitrile rubber membrane was installed and the collar and grill components secured. At this point Part (1) is completed.
(15) Wiring to all sensors, relay, and battery were then fed through the top cap through a wire restraining waterproof gland assembly (Hubbell Deluxe Cord Grips). All electrical connections were then made. Wiring details are discussed later.
(16) Final assembly then can be accomplished in several ways. One convenient method starts with Part (1) inverted (secured without damaging the discharge nozzle or cable/tether), Part (2) is lowered over pickup plate and the inner components until it rests securely on the top cap O-rings, and the place Part (3) on to Part (2) making sure that the four tension rod holes align with the top cap as well as ensuring that the eight pickup plate bolt holes also align.

(17) The eight pickup plate bolts should be tightened in a crossing and alternating pattern such that only a small torque is applied, repeating the pattern until no further movement is observed at the low subtle torque levels. At no time should the applied torque exceed 18in-lbs.

(18) Install the four tension rods that extend through the top and bottom caps and tension the rods again uniformly to prevent uneven force in the O-rings or tilting. At no time should the applied torque in the tension rods exceed 75in-lbs.

(19) Using two of the four tension rods where the threads extend beyond the nuts securing the bottom plate, secure the pump filter screen components.

Figures 4.10 and 4.11 show the device being assembled.

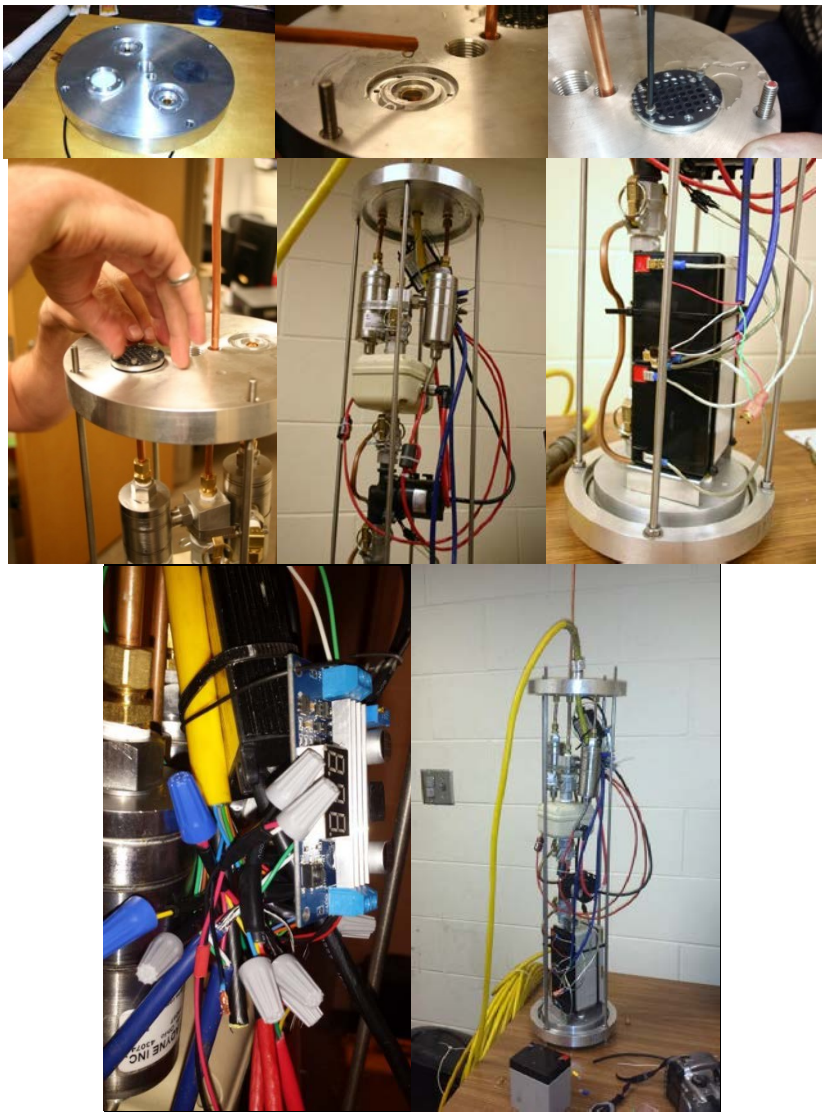

Figure 4.10. Internal component assembly.

Figure 4.11. Assembly of the three primary components.

4.6 Computerized Data Collection System (CDS)

The instrumentation within the system were all connected to an off-the-shelf data collection system from Omega (Model OMB-DAQ-55) which accommodates 5 differential (or 10 single ended) analog inputs and 2 digital pulse counters. Drivers for the hardware are available for other data acquisition software, but free data collection software is available from Omega that can either take data independently as a standalone, or can be called via EXCEL programming.

The DAQ unit was housed in a water proof protective enclosure (Pelican 1600) along with a miniature computer, 13.2V gel cell battery and military type connections for the down-hole unit as well as a top-side depth encoded wheel body. As the DHU has on-board batteries, charging is facilitated via connection to the computer system where external AC to DC chargers are connected. This prevents unnecessary disassembly of the DHU. The 12V battery in the computer case is used to trigger the downhole system relay and can be used to prolong the miniature computer life. Figure 4.12 shows the computer and DAQ enclosure.

The DHU cable/tether provides all conductors required (Table 4.1) which in turn are coupled to the DAQ unit in the enclosure. The wiring diagram for all aspects of the system is shown in Figures 4.13 and 4.14.

Figure 4.12. Computerized DAQ System (CDS).

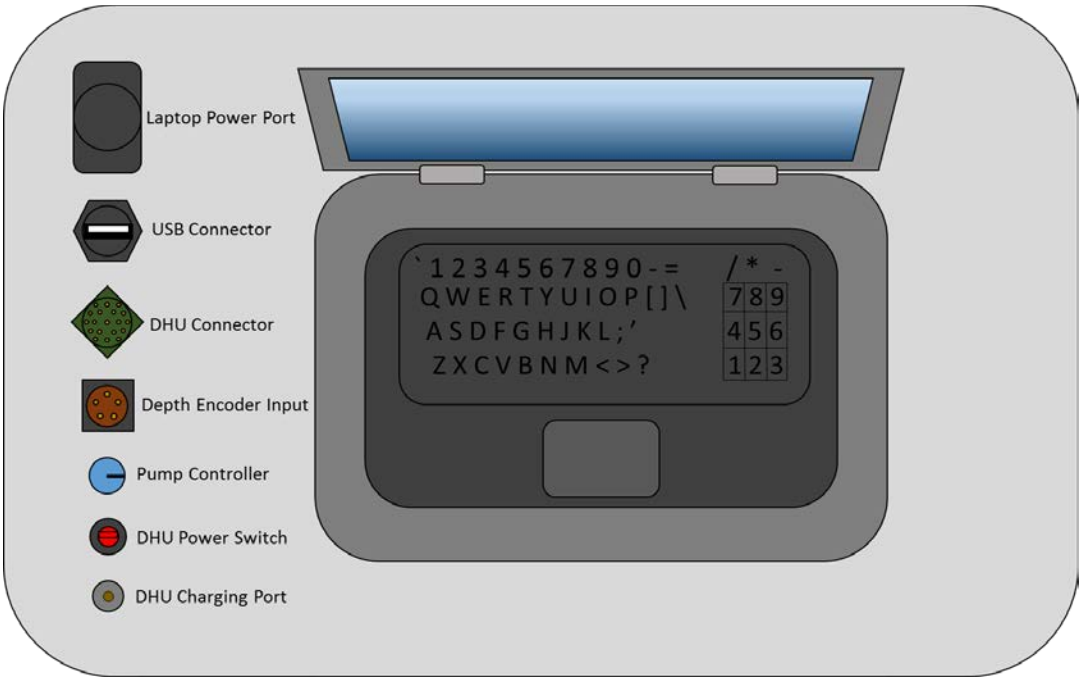

Figure 4.13. CDS panel, connectors and ports.

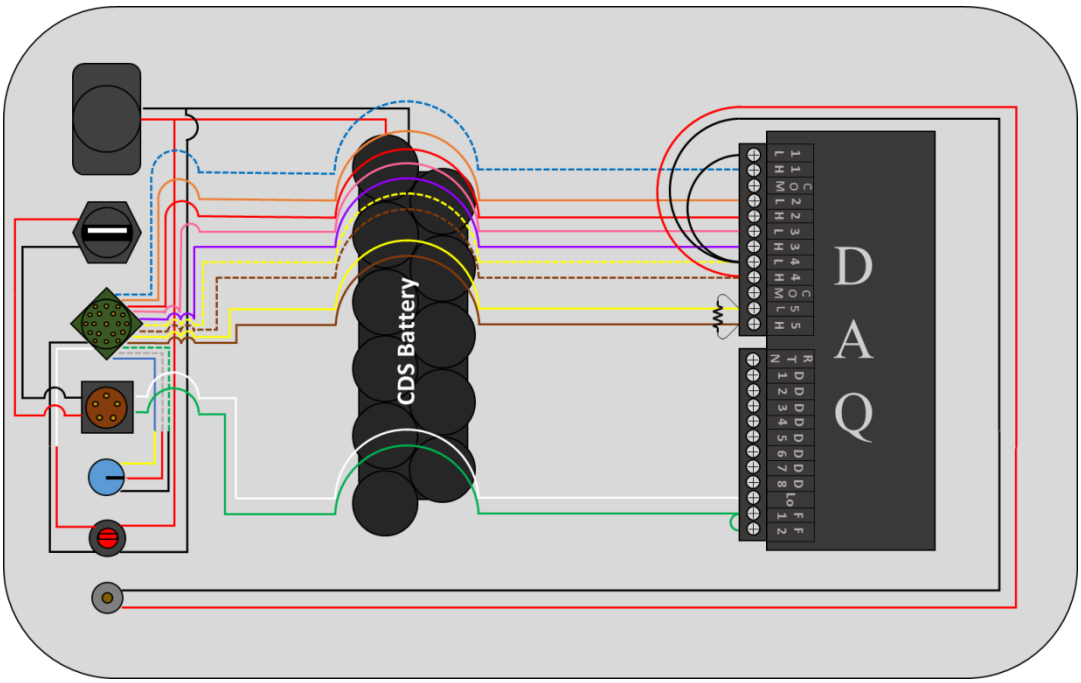

Figure 4.14. Internal wiring of CDS unit.

As seen in the previous figure, wire color transitions are shown where sensor wiring splices into the wiring harness. For completeness, the accompanying wiring diagram for the DHU is provided in Figure 4.15.

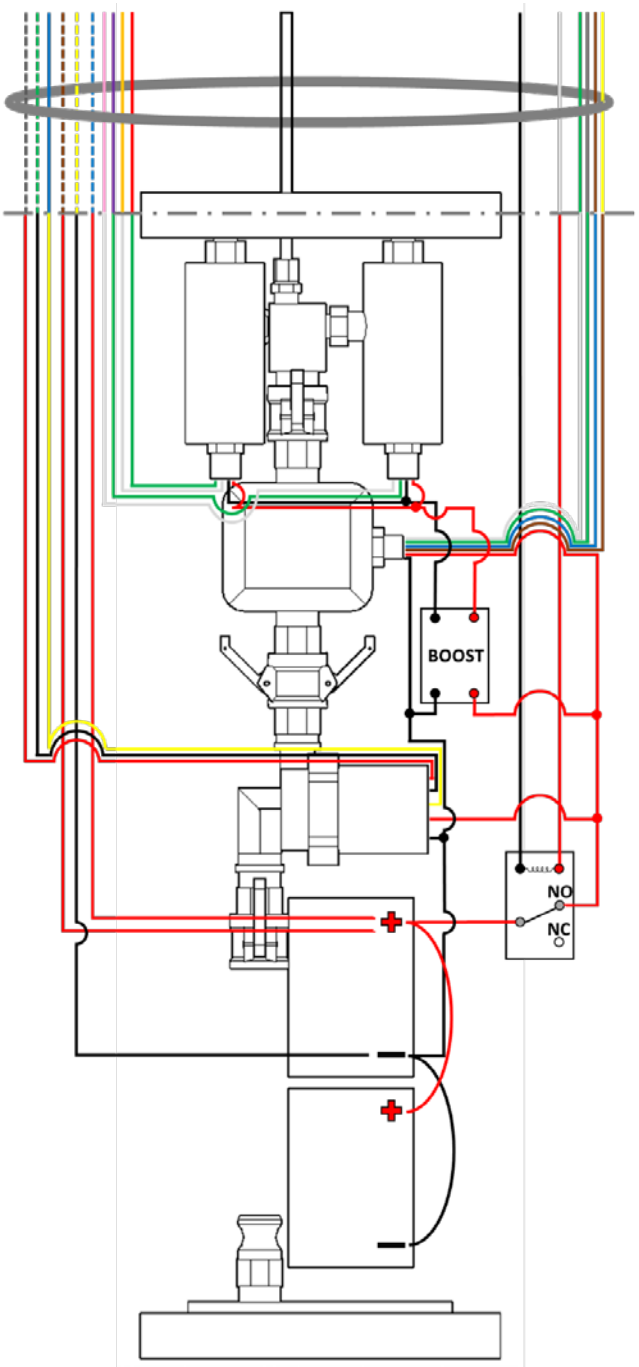

Figure 4.15. DHU wiring diagram.

4.7 Calibration Tests

The DHU was calibrated using the same basic procedures outlined in Chapter 3 where the pump flow and nozzle pressure were monitored while different viscosity slurries were pumped through the system. In theory a single flow rate could be used for all slurry tests from which the resulting pressure would be correlated to the viscosity. But having the flexibility of running the pump at any flow rate provides a more robust algorithm. Using the variable pump speed option the pump was swept through its full range of flow rates for viscosities of slurry tested.

A 4ft tall, 12in diameter PVC vessel was partially filled with water such that the added volume of the DHU would not overflow when submerged and the DHU was inserted to test the actual buoyancy. As noted earlier, additional weight was needed to offset the buoyancy from displaced water and even more weight would be needed for the full range of anticipated higher slurry densities in the field. The power relay in the DHU was triggered from the CDS and the variable flow rate pump control was adjusted to produce the first calibration curve. This process was repeated for varied degrees of suspended bentonite clay content (viscosity ranges from 26 to 73sec/qt). Figures 4.16 – 4.17 show the DHU submerged in calibration vessel in clear water and bentonite. Figures 4.18 - 4.19 show the results of all calibration tests.

Figure 4.16. DHU submerged in clear water for buoyancy and first P vs F calibration test.

Figure 4.17. Slurry placed and stirred in calibration chamber (top); DHU partially submerged in bentonite during calibration (bottom).

Using the variable pump control feature, each calibration test was performed over the widest range the pump would supply for the given slurry. Thicker slurry was not able to flow as quickly and therefore show a smaller range of flow rate. While the flow meter can register flow rates as low as 0.03gpm, no data below 0.1gpm were used to calibrate the DHU in the given configuration.

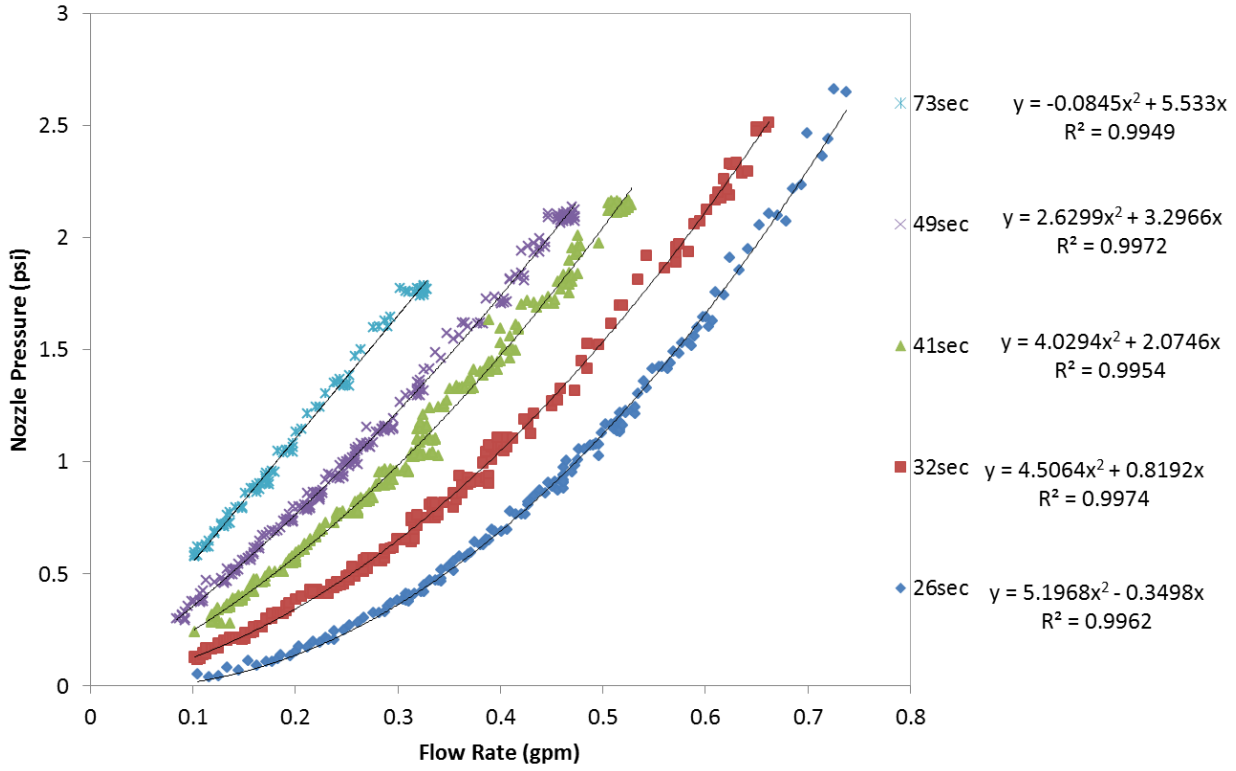

Figure 4.18. Calibration curves from DHU in different viscosity slurries.

Using the numerical fitting exercise outlined in Chapter 3, viscosity prediction equations were developed for the DHU configuration and then used to predict the viscosity of the tested slurries. Figure 4.19 shows the predicted slurry for each of the 5 slurry batches tested. The calibration equations were only valid for flow rates experienced by all tests so flow rates were limited to less than 0.3gpm.

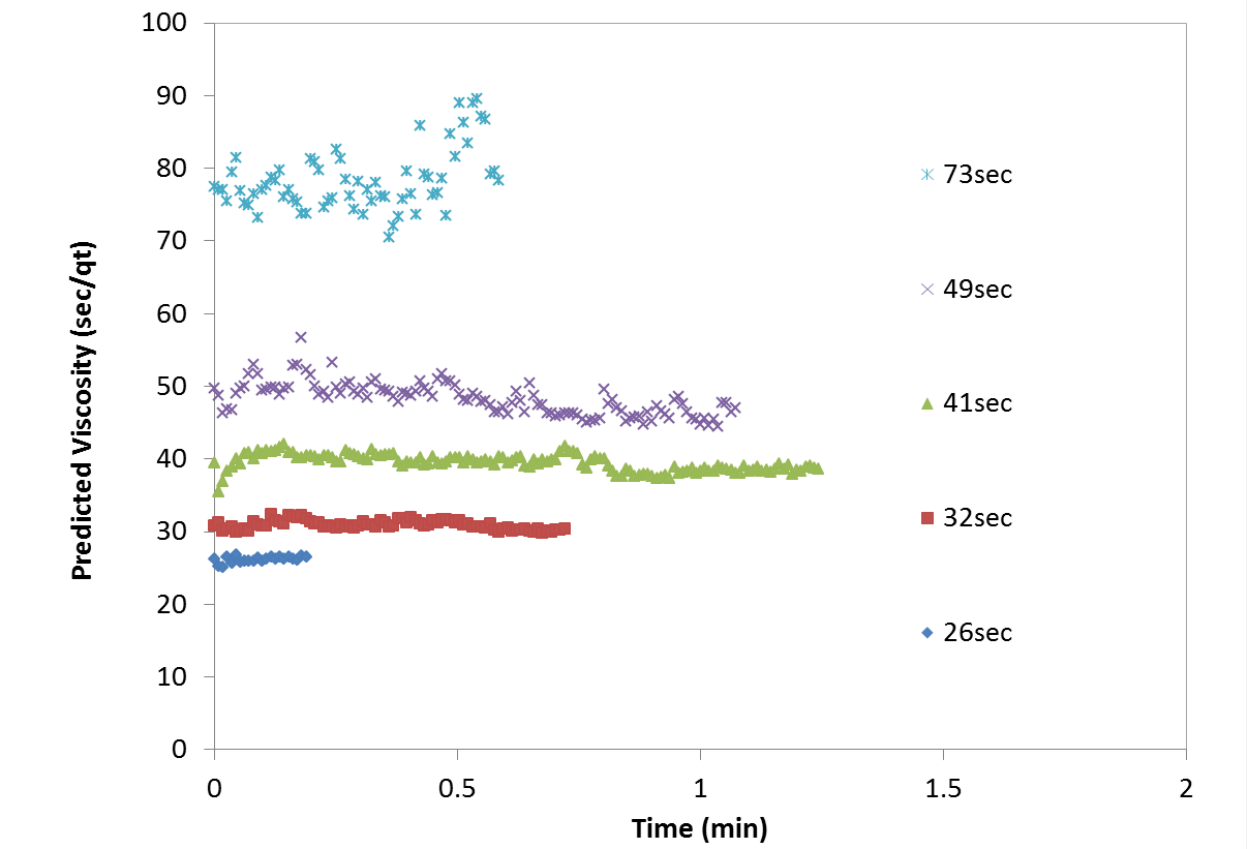

Figure 4.19. Predicted viscosity from calibration equations.

4.8 Sand Content Tests

The premise of the sand content determination method used in the all-in-one slurry testing system stemmed from the measured response of viscosity versus sand content. In previous tests, increased suspended solids (sand which provides no gel strength) was shown to have no effect on the measured viscosity. Therefore, for a given slurry, the addition of sand only increased the measured density. However, the efficiency of different slurry products varies and may require more or less mineral clay product to produce the same viscosity and as a consequence will have different clean slurry densities. This is referred to as yield by the API standards. API Section 13a Section 9 and 10 bentonite products are stated to yield 80-90bbls of

slurry when 2000lbs of dry slurry is mixed with water; high yield products produce 200bbls again for 2000lbs of dry slurry powder. This translates into mix ratios of 0.52 and 0.24lbs per gallon of slurry for pure and high yield slurries, respectively. Using the results from a past study (Figure 4.20) these mix ratios for the two product types equate to a common viscosity of 32-33sec/qt (Mullins and Winters, 2010).

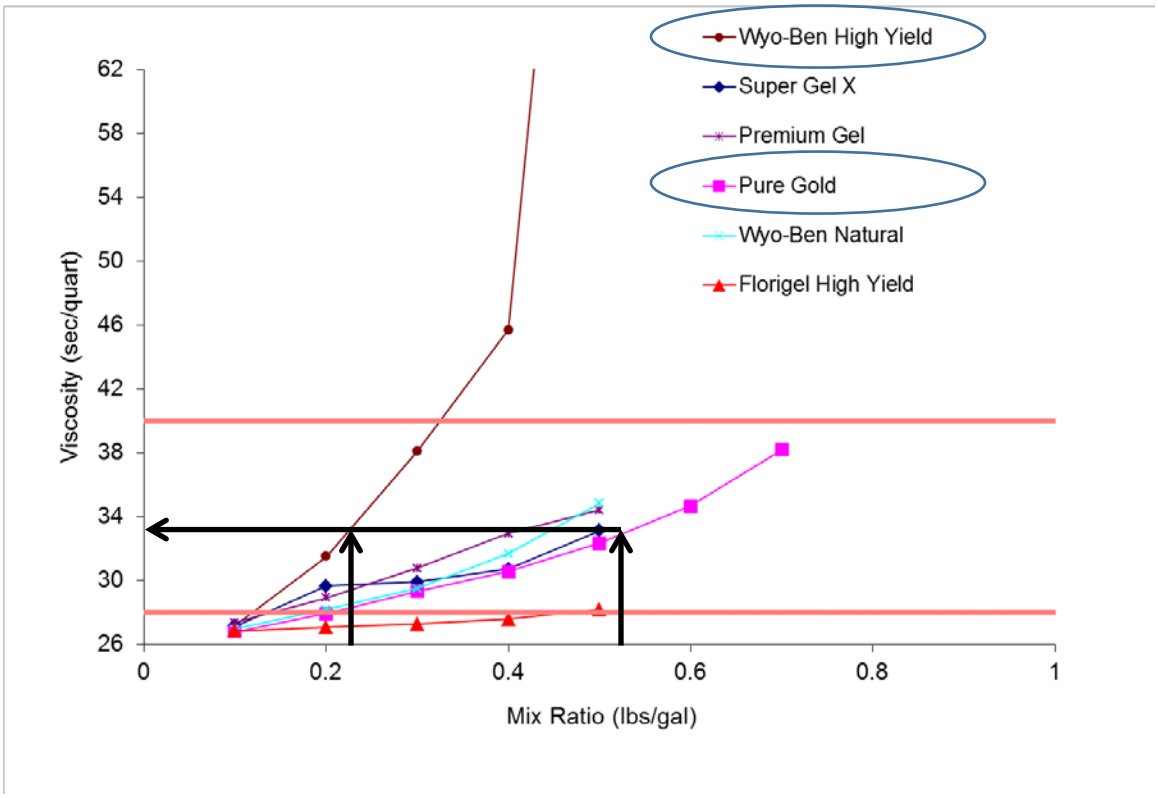

Figure 4.20. The effect of mix ratio on viscosity for various mineral slurry products.

These variations in effectiveness mean that the true concentration of clean slurry in the measured density and the suspended sand content cannot be simply assigned on the basis of weight. Figure 4.21 shows the relationship between density and viscosity for several clean (0% sand content) slurry products including: pure bentonite, high yield bentonite, attapulgite, and a polymer.

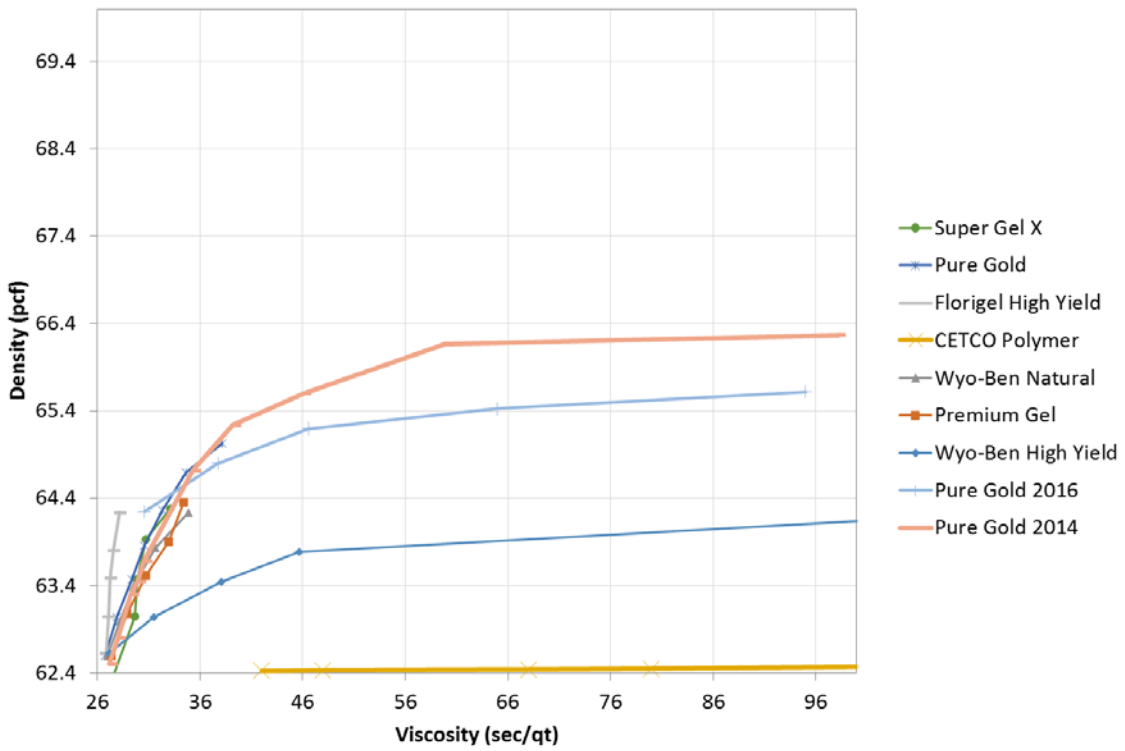

Figure 4.21. Density versus viscosity for a wide range of clean slurry products.

Review of the density vs viscosity relationship shows that pure bentonite slurries (90bbl yield) are the densest, polymer is essentially the same as water, and high yield (polymer blended bentonite) are roughly half way between. Most importantly, it shows that some knowledge of the slurry product must be known to distinguish between suspended sand and bentonite clay powder when looking at density from a given viscosity reading.

To provide further insight into the variables that define how sand content can be determined from density and viscosity, a series of tests were performed using varied suspended solid compositions from pure mineral slurry to heavily laden sandy slurry.

4.8.1 Slurry Preparation

Slurry preparation for the sand content tests was performed using the similar steps described in Chapter 3. Therein, a bulk sample (52gal) of high viscosity slurry (>>90sec/qt) was mixed by adding 45.82lbs of CETCO PUREGOLD GEL bentonite powder to the 50 gallons of pretreated pH 9 water via the non-clog Hootonanny eductor with a vacuum tube pick-up feed seen in Figure 4.22.

Figure 4.22. CETCO PURE GOLD GEL being mixed with Hootonanny eductor with vacuum tube feed.

To ensure complete hydration, the slurry was allowed to set for 24 hours at which time the viscosity was tested and found to be in the 180sec/qt range. In order to lower the viscosity to the desired 90 sec/qt range, 5 gallons of slurry were removed from the bulk slurry holding tank and replaced with 5 gallons of pH 9 water. The slurry was then recirculated for a period of 5 minutes. Following recirculating, the viscosity was retested and found to be 95 sec/qt.

4.8.2 Sand Content Testing

Testing protocol for the second phase of sand content investigations varied from the initial sand content test. Instead of adding sand directly to the clean 90 sec slurry and then diluting the total volume by removing slurry and adding water, individual 3 gallon samples of slurry were blended using the appropriate ratio of freshly made clean 90 sec slurry to pH corrected water to attain the desired range of viscosities (30-90sec/qt). To provide a baseline data set, the viscosity, density and sand content of the each clean 3 gallon sample was measured before sand was introduced. This measured the amount of natural sand that accompanied the bentonite powder from the manufacturer.

The mixing proportions of 90sec/qt slurry and water for each of the 5 viscosity ranges tested is presented below in Table 4.2. Also included is the dry slurry to water mix ratio, slurry density, measured viscosity and sand content for each of the viscosities.

Table 4.2. Baseline slurry mix ratios, densities, viscosities and sand content.

Base-Line Values	90 sec	60 sec	50 sec	40 sec	30 sec
90 sec slurry (gal)	3	2.7	2.43	2.13	1.53
Water (gal)	0	0.3	0.57	0.87	1.47
Lbs. Slurry/gal of water	0.82	0.74	0.67	0.59	0.42
Density (g/l)	1051.4	1049.5	1044.30	1038.00	1026.5
Density(lbs/ft$^{3)}$	65.64	65.51	65.19	64.80	64.08
Viscosity (sec/qt)	95.00	64.97	46.56	37.75	30.62
Sand Content (%)	.4	.4	.3	.25	.15

To further quantify the possible impact of sand content on slurry viscosity, a broad range of sand content values was tested for each of the five viscosities. Each of the 3 gallon samples were tested immediately after they were mixed, with the 90sec/qt slurry being first followed by the 60, 50, 40 and 30sec/qt samples. The target sand contents chosen were 2%, 4%, 8% and 16%. The methodology used during the sand content testing of each the five viscosities consisted of the following steps:

(1) After blending the prescribed volumes of 90sec slurry and water, the 3 gallon sample is mixed using a drill and paddle for a period of 3 minutes at which time sand content, viscosity and density of the slurry are measured.

(2) Immediately afterwards, a predetermined amount of sand was added to the 3 gallon sample to increase its sand content to approximately 2% and was mixed again for 3 minutes (Figure 4.23).

Figure 4.23. Adding sand to increase sand content to 2% then remixing slurry.

(3) Following mixing, a small sample of the slurry was pulled for the sand content test (Figure 4.24). The 3 gallon sample was then mixed for 2 more minutes at which time both viscosity and density were measured (Figure 4.25).

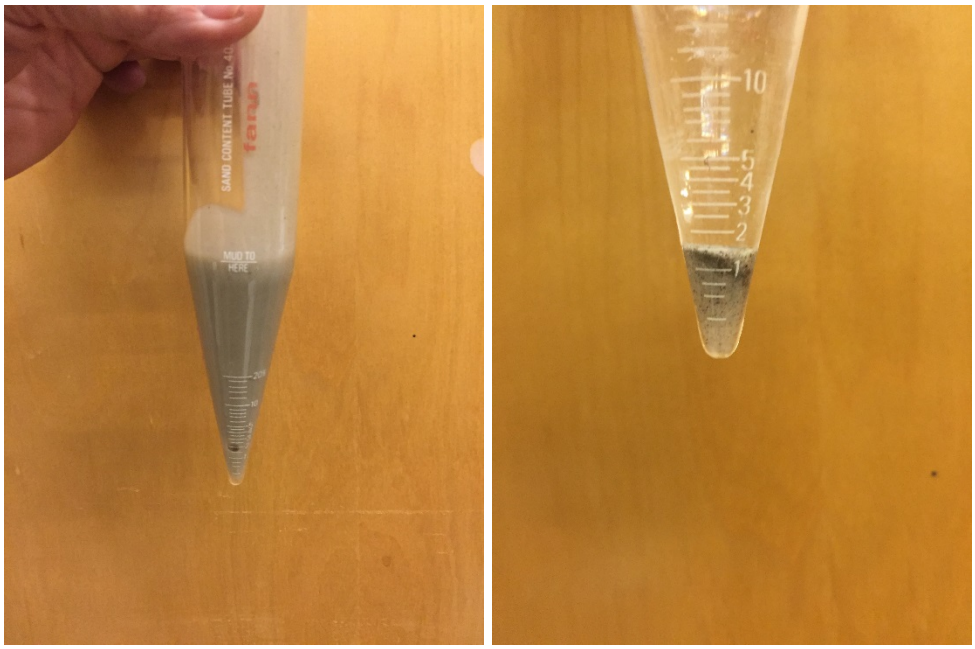

Figure 4.24. Sand content sample and measured sand content for 2% sand content test.

Figure 4.25. Viscosity and density testing of 2% sand content slurry.

(4) Upon completion of the 2% sand content test, the sand content of the 3 gallon sample was raised to 4% and mixed for 3 minutes and Step 3 was repeated.

(5) Upon completion of the 4% test, the sand content of the 3 gallon sample was raised to 8% and all tests were repeated.

(6) Finally, the sand content was raised to 16% and all tests repeated.

The results of the sand content tests for each of the 5 viscosities are presented in Tables 4.3 through 4.7.

Table 4.3. 90 sec/qt slurry sand content test results

	Normal	2%	4%	8%	16%	16%
Sand Added (g)	0	163.5	327.8.	650.3	1141.3	2812.9
Total Sand Added (g)	0	163.5	491.3	1141.6	2282.9	2812.9
Density of Sand Added (lb/ft3)	0	.90	2.70	6.27	12.55	15.46
Measured Sand Content (%)	.4	1.5	3.4	8.2	14	17
Density(g/l)	1051.4	1063.5	1082.2	1117.3	1176.9	1184.7
Density (lb/ft3)	65.63	66.39	67.56	69.75	73.47	73.96
Viscosity (sec/qt.)	95	112.8	102.53	103.62	104.25	101.46

Table 4.4. 60 sec/qt slurry sand content test results

	Normal	2%	45	8%	16%
Sand Added (g)	0	327.4	358.6	685.6	1305.9
Total Sand Added (g)	0	327.4	686	1371.6	2677.5
Density of Total Sand Added (lb/ft3)	0	1.80	3.77	7.54	14.72
Measured Sand Content (%)	.4	1.7	4	8.7	16
Density(g/l)	1049.5	1062.3	1088.4	1126.2	1191.8
Density (lb/ft3)	65.52	66.32	67.95	70.31	74.40
Viscosity (sec/qt0	64.97	63.57	66.72	64.41	66.06

Table 4.5. 50 sec/qt slurry sand content test results

	Normal	2%	45	8%	16%
Sand Added (g)	0	348.9	349.5	699	1400
Total Sand Added (g)	0	348.9	699.3	1398.3	2798.3
Density of Sand Added (lb/ft3)	0	1.92	3.84	7.69	15.38
Measured Sand Content (%)	.3	2.2	4	9	17
Density(g/l)	1044.3	1061.3	1080.9	1118.2	1190.4
Density (lb/ft3)	65.19	66.25	67.48	69.80	74.31
Viscosity (sec/qt)	46.56	48.69	48.87	49.31	48.32

Table 4.6. 40 sec/qt slurry sand content test results

	Normal	2%	45	8%	16%
Sand Added (g)	0	350.1	349.4	699.3	1404
Total Sand Added (g)	0	3501.	699.5	1398.8	2802.8
Density of Sand Added (lb/ft3)	0	1.92	3.84	7.69	15.40
Measured Sand Content (%)	.25	2.2	3.8	8.2	12.5
Density(g/l)	1038	1053.7	1072.4	1111.4	1176.6
Density (lb/ft3)	64.8	65.78	66.94	69.38	73.45
Viscosity (sec/qt)	37.75	39.53	38.94	40.43	40.59

Table 4.7. 30 sec/qt slurry sand content test results

		2%	45	8%	16%
Sand Added (g)	0	349.1	349.5	699	1301.7
Total Sand Added (g)	0	349.1	698.6	1397.6	2701.3
Density of Sand Added (lb/ft3)	0	1.92	3.84	7.68	14.84
Measured Sand Content (%)	.15	.8	.25	.5	.5
Density(g/l)	1026.5	1031.5	1031.5	1041.6	1055.9
Density (lb/ft3)	64..08	64.39	64.39	65.02	65.91
Viscosity (sec/qt)	37.75	39.53	38.94	40.43	40.59

The results of the sand content test matrix are also shown in Figure 4.26 which provides both qualitative and quantitative meaning to sand content determination from viscosity and density measurements. This plot shows several points of interest:

- Low viscosity slurry does not have the capability/gel strength to hold an appreciable amount of sand in suspension.
- Increased polymer content slurry (data not shown) is less capable of suspending solids. This is denoted by a progressively lower slope of the maximum suspension line.
- When determining sand content, the clean slurry density curve should be known from which a given viscosity can be used to identify the density baseline above which all additional density can be attributed to sand content.

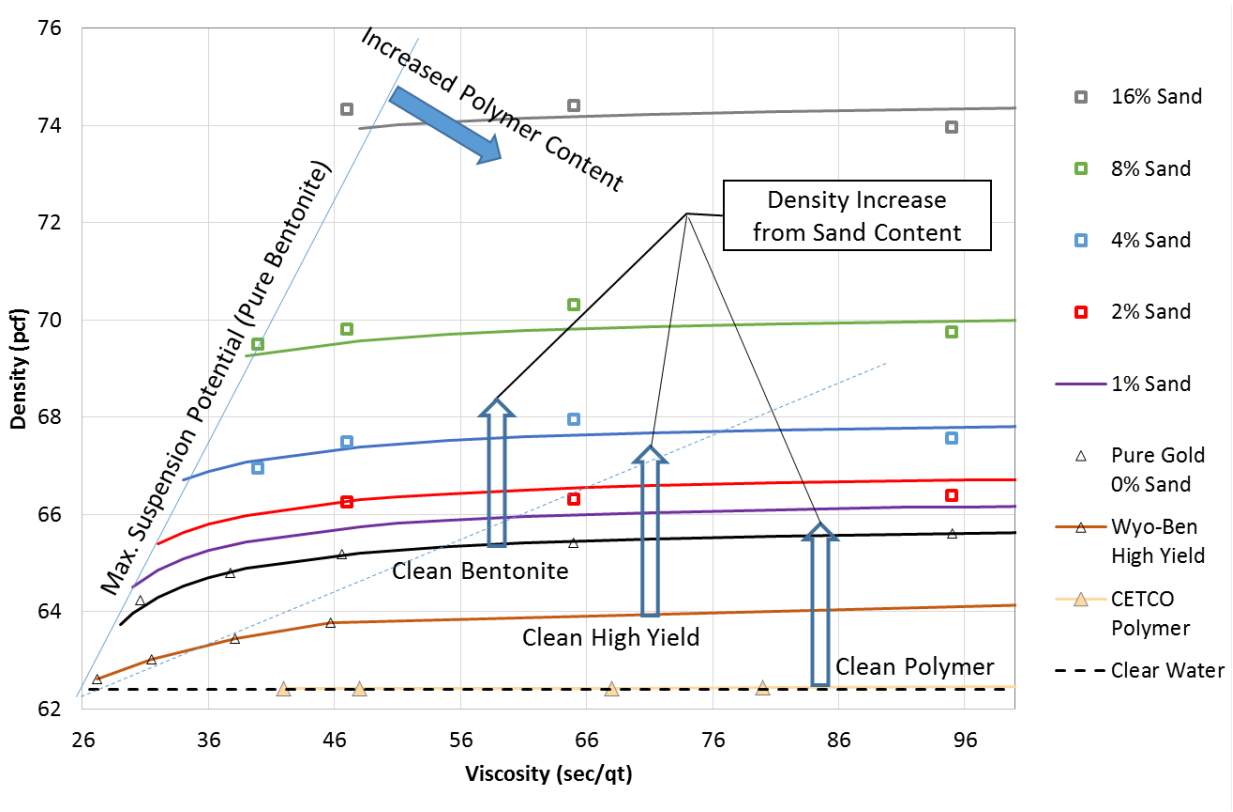

Figure 4.26. Sand content from viscosity and density measurements.

Using these findings, a simplified equation was developed for pure bentonite to calculate sand content (SC) from viscosity and density.

$$SC = \frac{(\gamma_{meas} - \gamma_{clean})}{(\gamma_w S_g e - \gamma_{meas})} x\ 100\%$$

where

γ_{meas} is the measured density of the soil laden slurry

Sg is the specific gravity of sand, 2.65

e is the void ratio of very loose sand in the sand content vial, 0.8 and

γ_{clean} is the density of the clear slurry at a given viscosity which can be estimated for pure bentonite slurry to be

$$\gamma_{clean} = \frac{V - 21}{0.015(V - 21) + 0.004}$$

and V is the viscosity in sec/qt.

Similar equations for γ_{clean} for high yield products can be prepared as well. The weight contribution of polymer slurry can most likely be fully ignored making all additional weight the by-product of suspended sand content / cuttings.

4.9 Chapter Summary

The assembly and calibration of the all-in-one slurry testing system were successfully concluded which involved pressure testing the DHU, processing several different slurry viscosities, and making predictions of a slurry viscosity from pressure and flow rate. Refinement of the calibration process to provide a more robust prediction algorithm is envisioned and discussed later. Ultimately, the calibration equations form a surface like that shown in Figure 4.27 which in concept is helpful, but the closed-form solution of the surface is the only way to quickly predict slurry properties. This also applies to the equation to produce sand content from density and viscosity inputs.

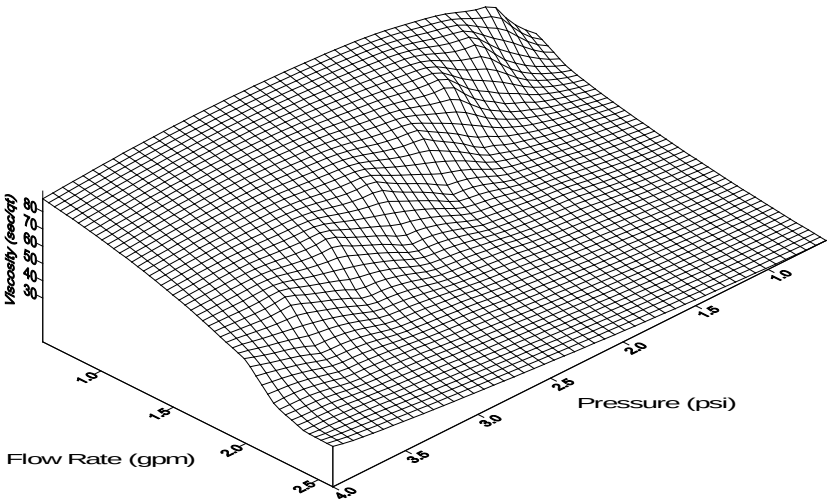

Figure 4.27. Viscosity surface based on various flow rates and pressures.

CHAPTER 5: FIELD TESTING

5.1 Overview

This chapter describes testing with the all-in-one slurry testing system in ways that cannot be easily replicated in the laboratory. Specifically, this involves field setup logistics, incorporation of depth tracking and operating the system in high hydrostatic pressure conditions. This included the creation of field simulation apparatus in which realistic conditions may be found as well as on-site testing. Given this is the first such prototype, this chapter outlines both the successes and failures of the field trials.

5.2 Field Simulation Test Setup

Depending on the particular drilling and slurry management philosophy of the contractor, field slurry tests may never show slurry properties that test the limits of the developed all-in-one slurry testing system. Therefore, to produce a wide range of slurry conditions that might possibly exist and even exceed the state specified slurry limits that are likely to be avoided in the field, a series of field simulation tests were performed.

Shaft lengths and the associated depths of excavation can range from 25ft for miscellaneous structures to hundreds of feet deep. Shafts for bridge structures typically range from 50 to 150, where the hydrostatic pressure at a given depth is the summation / incremental increase associated with the slurry density. The system must be capable of withstanding this

pressure. Practically, for the field simulation tests, a 45ft target vessel depth was selected based solely on the height of the Kopp Engineering building at the University of South Florida where much of the structures and foundation research is conducted. The test apparatus was comprised of a 45ft long, 12in diameter SCH40 PVC pipe complete with one end cap, valves, couplers, a slurry mixing tank, a recirculation tank, a pump and associated hoses. Figure 5.1 shows the pipe assembly and it being hoisted into place alongside the building. Figure 5.2 shows the simulation vessel in position secured to the wall with a welded steel bracket.

The weight of the slurry filled vessel was supported by a welded base frame through which 2in ID pipe fittings were connected to the bottom of the 45ft column. All fittings were outfitted with cam-lock fittings to facilitate multiple pumping configurations. Figure 5.3 shows the basic connections with the assorted tanks.

Figure 5.1 Assembly and erection of 45ft field simulation vessel

Figure 5.1. (continued)

The basic operation of the test setup involved mixing slurry to a prescribed viscosity, pumping the slurry from the mixing tank into the excavation simulator (PVC column) from the bottom up until it slips over into the 2in ID return line located 1ft from the top of the column. The return line was routed into the recirculation tank in which sand could be added and then recirculated back into the column. Pumping from the bottom up was designed to suspend the cuttings and unify the column of slurry until pumping was terminated. At that time, the suspended solids would then settle or be supported in the slurry depending on the viscosity/gel strength of the slurry.

With time, a given slurry column may then develop a non-uniform sand content distribution as well as bentonite concentration and density distribution. By performing downhole tests at various wait times after discontinuing pumping another parameter of construction could be replicated. In all, the excavation simulator could be filled with clean or soil laden slurry of different gel strengths and demonstrate the effects of time on slurry properties. Therein, most slurry columns in field conditions do not have uniform slurry properties throughout.

Figure 5.2. Final positioning and fastening bracket bolted to top of building.

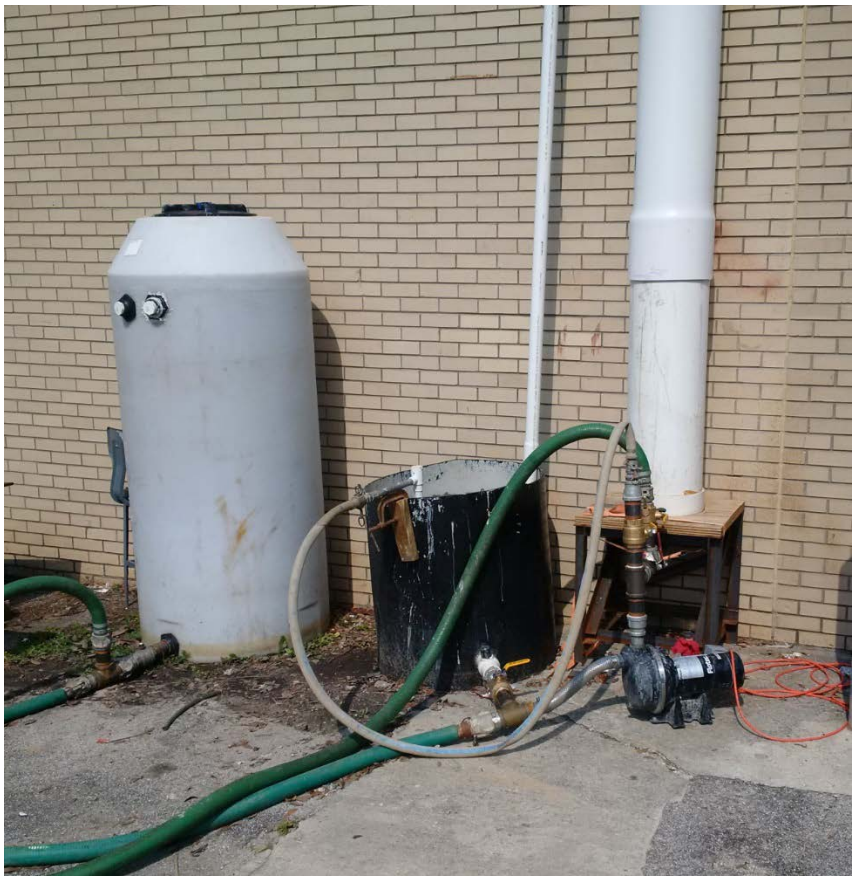

Figure 5.3. Mixing / holding tank (left), recirculation tank (middle), simulated excavation vessel (right) all connected to the pump via cam-lock fittings with hoses.

5.3 Field Simulation Tests

While Chapter 4 used a short calibration vessel to define the unique flow versus pressure relationship for slurry viscosity ranging from 26 to 73sec/qt, the effects of deep excavation pressures were not demonstrated. The field simulation setup provided this condition.

Tests were initially performed using clear water where only system pressure would change and not the slurry properties with depth; slurry was not dependent on time (e.g. settling cuttings). These tests repeated calibration type tests by monitoring flow versus pressure by varying flow but the trials were performed at different depths. This increased the pump inflow

pressure which would in turn increase the output pressure. However, the reference diaphragm on the low side of the differential pressure transducer (for nozzle pressure) reduced the effective pressure on the system so that the high sensitivity of a low range transducer could be used even at very high depths and the associated hydrostatic pressures. Figure 5.4 shows the raw pressure and flow data for this data set.

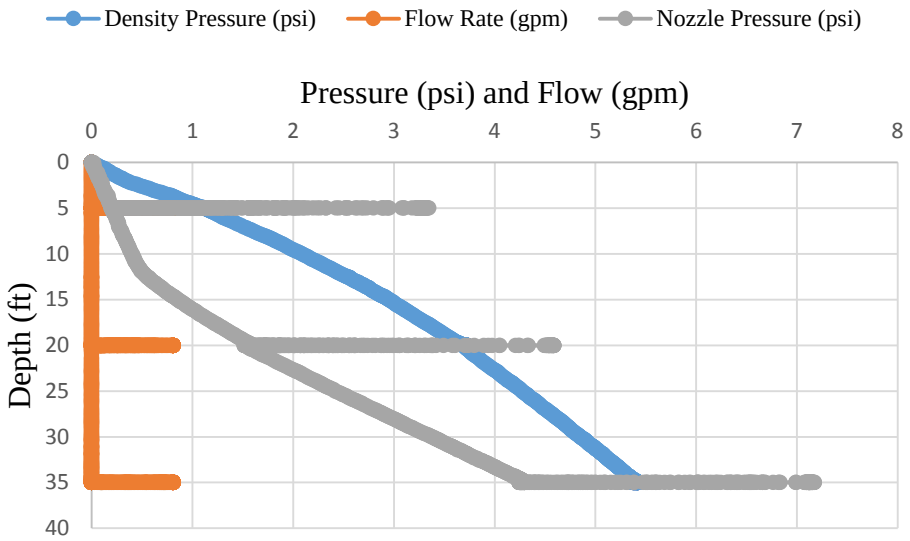

Figure 5.4. Pressure vs depth data with three calibration flow vs pressure sets.

The flow rate was slowly increased similar to the process used in the calibration tests so that the magnetic flux type flow meter could stabilize. This was repeated at depths of 5, 20, and 35ft (Figure 5.5). The starting pressures were all different starting at 0.3, 1.6 and 4.3psi, respectively. However, note that the actual hydrostatic starting pressure would have been 2.2, 8.7, and 15.2psi, again respectively, but without the offsetting effects of the reference diaphragm port. This showed that the reference port was having a positive effect, but not the intended completely neutralizing/offsetting effect which would make the nozzle pressure independent of depth. Another observation was that the same increment of hydrostatic increase from 20 to 35ft

had a larger increase in the baseline pressure when compared to that observed from 5 to 20ft. This indicated that the glycerin filled lines were not fully bled clear of all air. All three diaphragm lines were vacuum bled several times for up to 20min and until no further air bubbles could be drawn out.

The pressure versus depth of both the density transducer and the nozzle pressure transducer showed a non-linear or bilinear response which again supported the need to bleed the lines of remaining air.

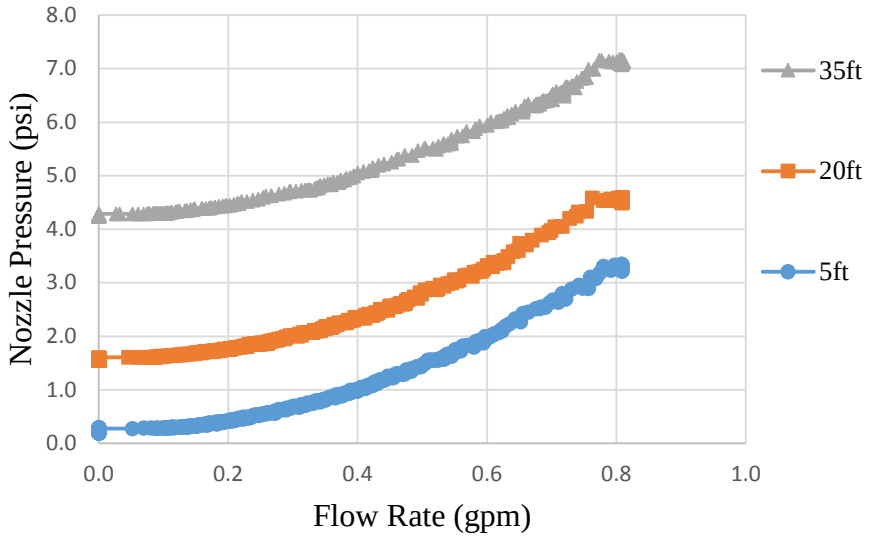

Figure 5.5. Nozzle pressure vs flow rate at progressively higher hydrostatic conditions.

However, and as predicted, when the starting pressure was subtracted from the pressure vs flow tests, all three sets of data aligned with the calibration tests shown in Figure 4.18 (clear water, 26sec/qt) as shown in Figure 5.6. While every effort to remove the depth/pressure dependent offset is beneficial, it is possible to simply correct for the offset by properly structuring the testing procedure to identify and remove the offset prior to converting the measurements into viscosity values.

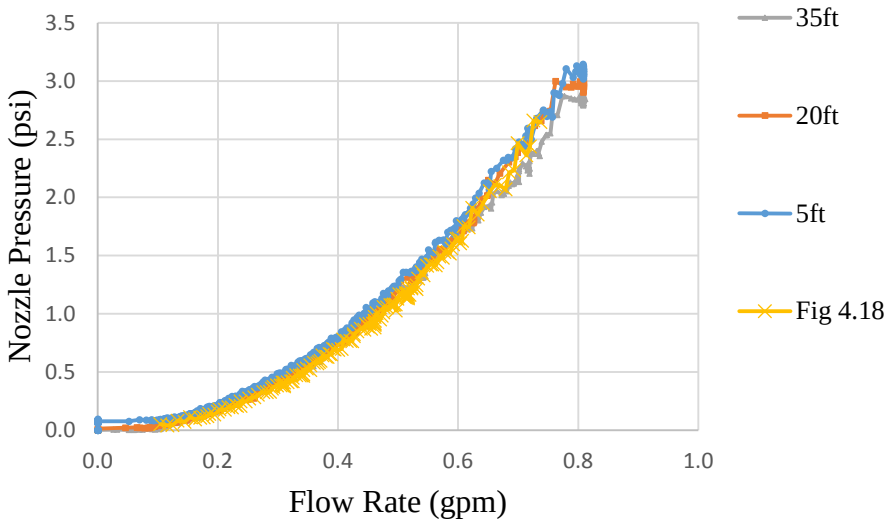

Figure 5.6. Pressure vs flow rate corrected for starting pressure condition.

Several additional deep pressure tests were performed, bleeding the lines after each test until very little effect of remaining air could be detected. Figure 5.7 shows the density low pressure port before and after the final purging of entrapped air.

Figure 5.7. Vacuum purging of low pressure density pressure port with glycerin solution; initial (left), after 15min under vacuum (right).

Erratic results persisted which were thought to be the effects of the chamber pressurizing which implied that the transducer bodies may be sensitive to external pressure. Figure 5.8 shows the effects of pressure head the DHU readings for density and nozzle pressure. Note the two independent pressure transducers (same model and pressure range) responded with an identical change in pressure due to the increased surrounding hydrostatic pressure.

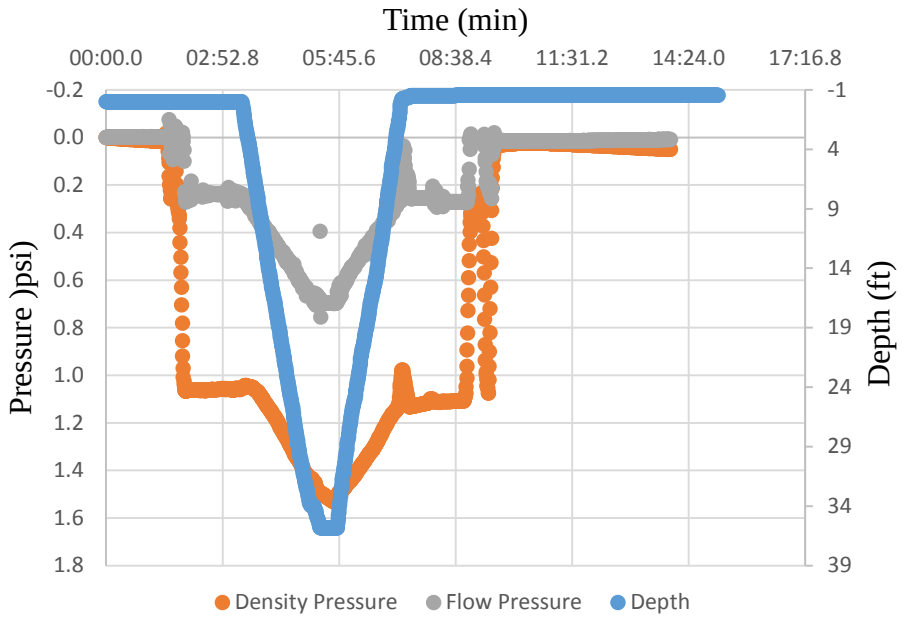

Figure 5.8. Pressure transducers sensitive to external pressure on DHU chamber.

Looking into these effects, an ambient air pressure relief tube was installed to maintain a uniform internal pressure relative to the top side atmospheric pressure and possibly remove this effect. With the chamber vented and the density transducer purged once again, the density gage was fully stabilized. Figure 5.9 shows the results from a slurry test run at 5ft intervals in clear water indicated by steps in the depth traces. The pressure head remained constant throughout. Spikes in the nozzle pressure are due to activating the pump at each depth interval. However, the nozzle pressure still showed sensitivity to depth to the same degree as before.

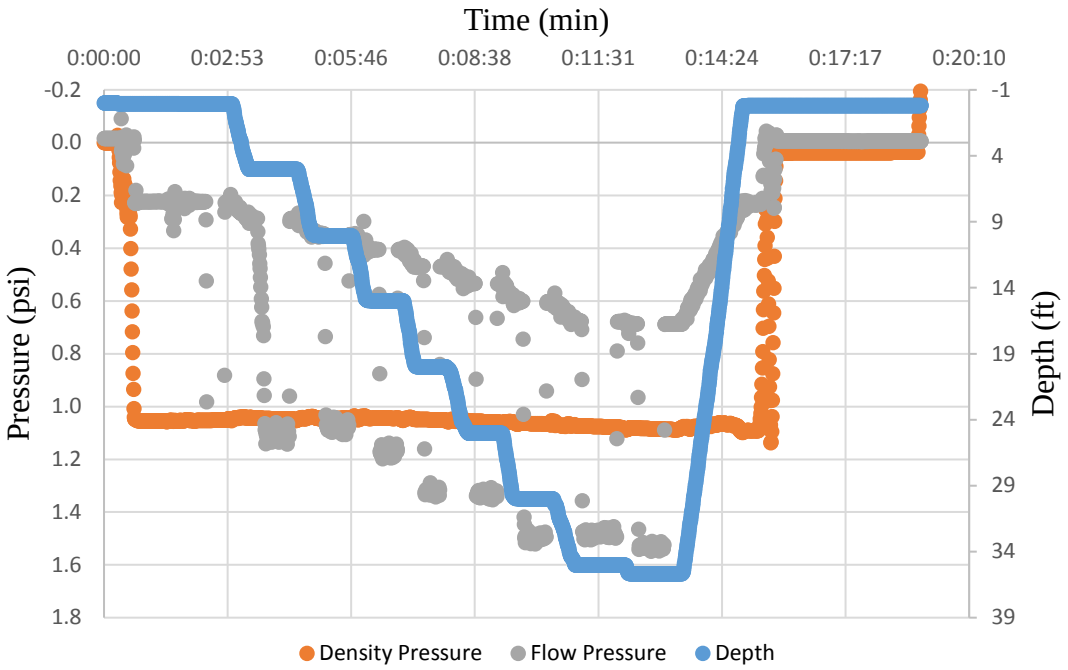

Figure 5.9. Density pressure transducer stabilized but nozzle flow pressure was still sensitive to depth.

With the nozzle pressure transducer still experiencing depth sensitivity, the same procedure used on the density transducer was repeated for the nozzle pressure transducer. This type of vacuum purging has been cited in manufacturer literature wherein multiple steps are required.

5.4 Testing Protocols

Several aspects of the prototype testing system were scrutinized to determine the most reliable testing procedure. Ideally, the test would/could be run by simply lowering the DHU while the pump was activated and all measurements were recorded on-the-fly like many other QA/QC integrity test methods. However, several aspects of the DHU required the procedure to be tailored to accommodate these features.

5.4.1 Density

The high pressure (bottom) pressure port of the density pressure transducer if exposed to downward motion might sense the velocity head similar to a pitot tube that measures velocity in an airplane. Likewise, the low pressure port (upper) could experience a vacuum/eddy effect if the downward DHU velocity was significant. If the descent is maintained at a low enough rate then on-the-fly density measurements could be made. Computations show that the descent rate below which no more than a 0.1pcf error would occur is 0.02ft/sec. This based on the stagnation pressure that occurs in an incompressible fluid. Where periodic pauses at prescribed depth intervals can be used in concert with faster descents, the DHU is equipped with lead plates (for ballast) that cover the entire bottom surface and blocking this type of velocity effects. Regardless, a decent rate no greater than 0.4ft/sec was established and is recommended so that on-the-fly density data will be meaningful.

5.4.2 Viscosity

The pressure versus flow rate relationships used to determine the instantaneous viscosity are based on zero flow producing zero pressure, so the starting pressure (if non-zero) must be known. If the nozzle pressure increases with depth irrespective of viscosity, then the amount of non-zero offset may not be determined with certainty. Option 1 is to pause at prescribed depth intervals, note the zero flow pressure offset and then measure the rise in pressure caused by a measured flow. This effect was shown in Figures 5.4 and 5.5 for uncorrected and corrected pressure versus flow curves, respectively.

Option 2 is if the nozzle pressure offset is stable with depth, then on-the-fly measurements of flow and pressure could be recorded and converted to viscosity directly using

equations from Chapter 4. However, the design location of the reference pressure port on the prototype DHU relative to the nozzle pressure transducer membrane (on which strain gages are mounted to detect pressure) gives a pressure gradient based on the approximate 6in difference between. Therefore, as density changes so does the offset. A design change to compensate and remove the offset involves orienting the nozzle pressure transducer horizontally and having the discharge and reference port located on opposite sides of the system housing.

At present, the prototype DHU must use Option 1.

5.4.3 Sand Content

Recall sand content determination requires knowledge of the suspended clay content (slurry products) in order to separate increases in density caused by suspended cuttings and slurry products. Pure bentonite can add up to 2pcf to a density measurement at a viscosity of 40sec/qt and 4% suspended cuttings can add an additional 2pcf (Figure 4.26). Without knowing the slurry product component of the density, all increases in density can only be designated as suspended solids and not differentiated into components. Until the user can confidently differentiate the components with a library of various slurry products, it is advised to spot check the viscosity, sand content and density for a given project. For instance, the equation provided in Chapter 4 computes clean slurry density as a function of viscosity for Pure Gold Gel, pure bentonite. The software used in the CDS incorporates suggested values for pure bentonite, high yield bentonite and polymer slurries.

The considerations presented above were scrutinized over the span of the field tests to develop a recommended procedure (discussed later).

5.5 Simulated Field Tests

Three different slurry conditions were tested starting with water and then staying within present state specifications of 30sec and 40sec pure bentonite slurry. Mixing was performed in the mixing / holding tank using the non-clog eductor which was plumbed directly into the system of valves and hoses shown in Figure 5.3. Once the slurry achieved the target viscosity, the valves were changed to permit inflow into the bottom of the excavation vessel, the column was filled and recirculation was afforded via a 2in overflow pipe positioned 1ft from the top of the vessel. By recirculating upward, suspension of the mineral clay particles was promoted as well as any sand content that may be from the slurry product or from cuttings.

Column tests with water were used for verification while tests with 29-30 sec/qt and 35-36 sec/qt bentonite slurry made up the second two slurry consistencies.

5.5.1 Slurry Preparation

Preparation of the slurry for the first field simulation tests involved making 250gal of 30 sec/qt viscosity slurry. The slurry was mixed in the 100gal recirculation tank in 50gal batches using a rapid hydration Hootonanny with the vacuum tube option to blend the dry CETCO PUREGOLD GEL bentonite powder with pH corrected water. The ratio of dry powder to water was 0.4lb/gal with a total of 20lb of bentonite powder added to each 50gal batch. Upon completion of the powder/water mixing, the slurry was recycled for 5min and then pumped into the 300gal slurry storage tank. This procedure was repeated until a total of 250gal of slurry was produced. At the time of testing, the slurry was pumped from the holding tank into the 45ft tall excavation vessel from bottom up until full and overflowed the upper drain pipe.

For the second test, the slurry was prepared by draining approximately 50gal of slurry from the excavation vessel into the 100gal slurry recirculation tank. The slurry was then recirculated for 10min while an additional 13lb of additional dry slurry powder was added, again using the vacuum tube. Once the slurry was thoroughly mixed, it was then pumped to the 300gal slurry holding tank. The procedure was repeated two more times and then the rest of the slurry remaining in the excavation vessel was also pumped into the 300gal holding tank at which time the contents of the storage tank were mixed for an additional 15min. At the time of testing, slurry was again pumped from the holding tank up into the test excavation.

Soil cuttings were introduced into the slurry after clean slurry tests had been performed by slowly adding sand to the recirculation tank while the system was being recirculated into the test excavation. This pumping/recirculation process was continued until 160lb of sand had been introduced (approximately 4% by volume). Once all sand was in the system, the system was recirculated for 30min (Figure 5.10).

Figure 5.10. Increasing sand content by adding sand during slurry recirculation cycle.

These tests in essence served as extended calibrations where density measurements were inconsistent. As sand content is computed from density, these too were in error. Figures 5.11 – 5.13 show sample results from water, 30sec/qt and 36sec/qt tests, respectively. Results from all tests are included in Appendix E.

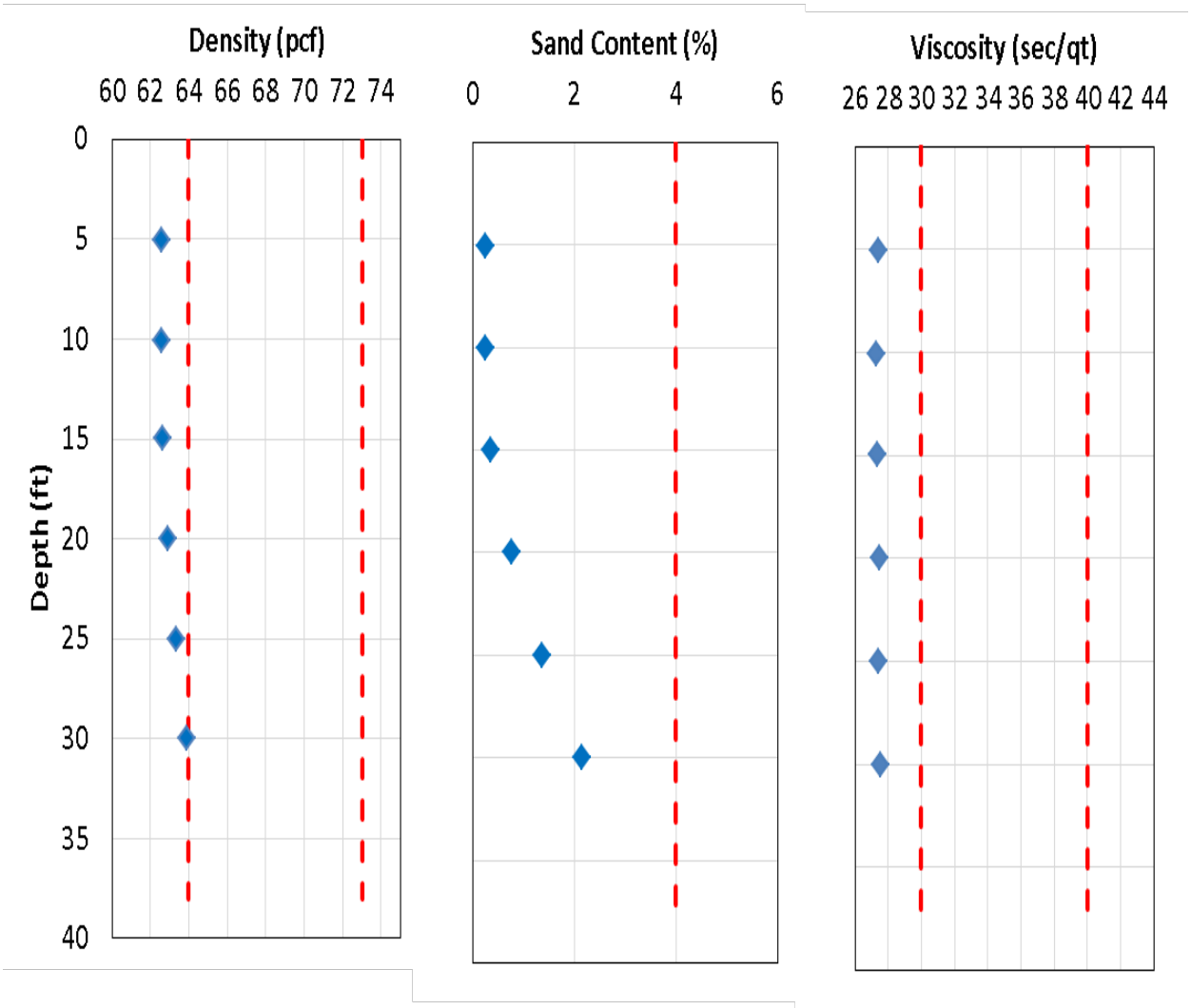

Figure 5.11. Sample data from clean water tests showing density measurement error.

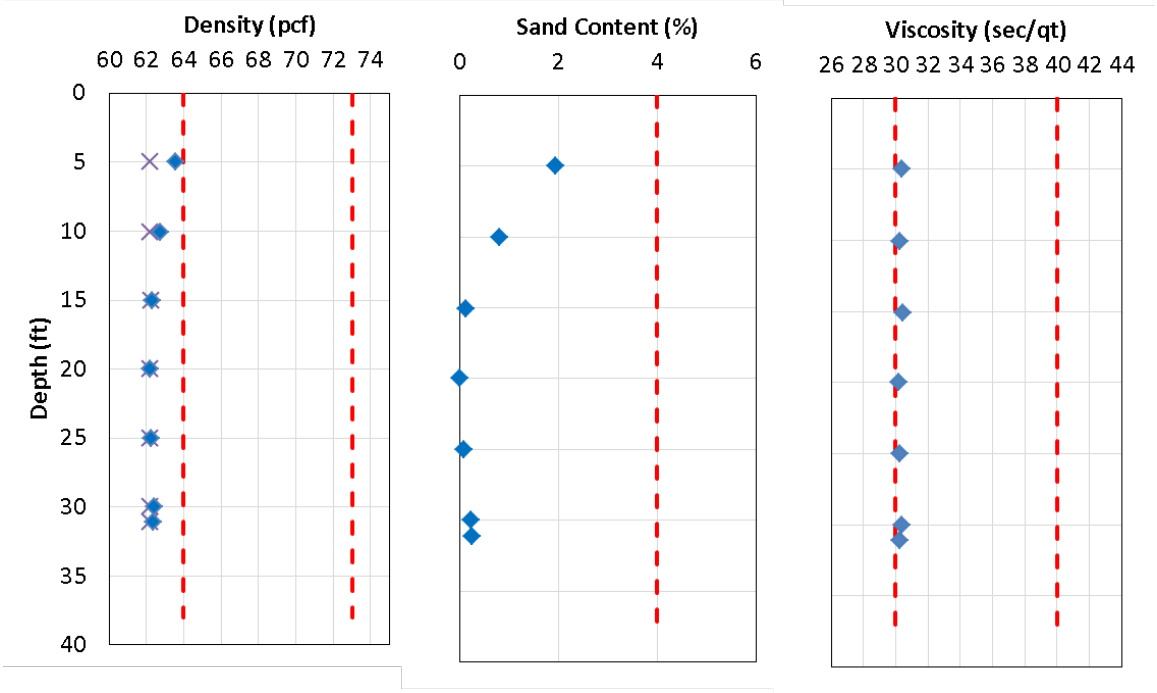

Figure 5.12. Sample data from clean slurry (no sand) test, 30sec/qt Marsh funnel; X marker denotes computed clean slurry density from viscosity measurements.

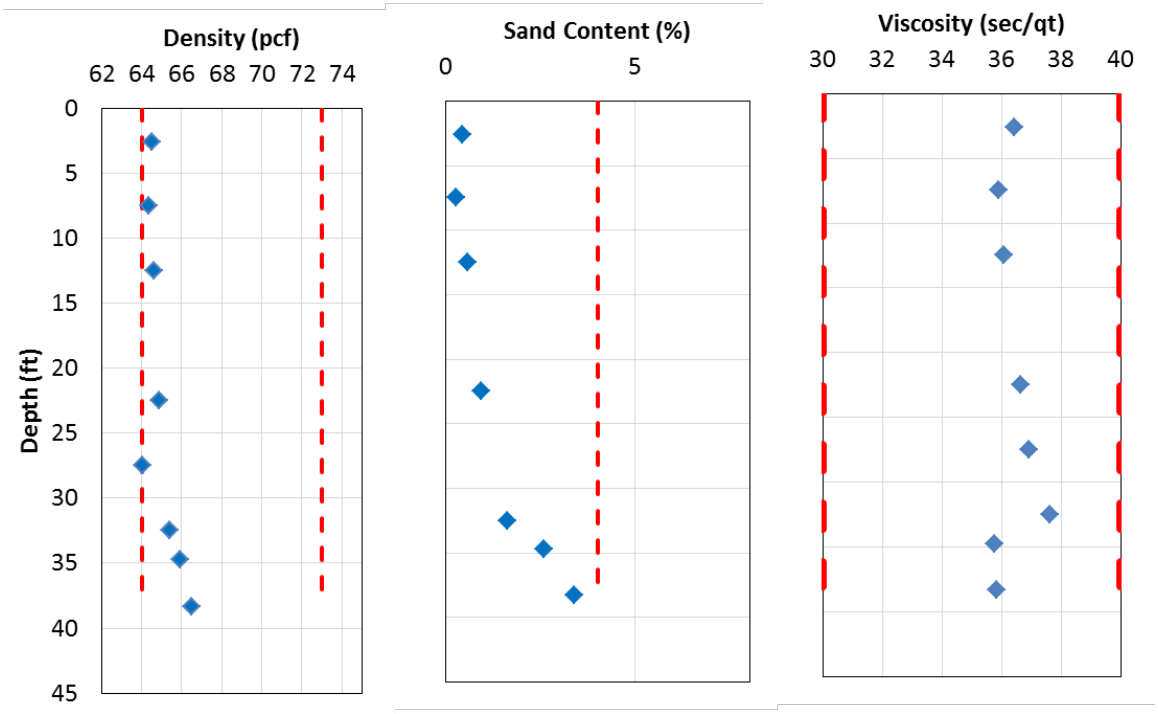

Figure 5.13. Sample data from clean slurry (no sand) test, 36sec/qt Marsh funnel.

As anomalous density results were encountered, the pressure ports / diaphragms were vacuumed, re-purged and re-sealed. For example, Figures 5.11 and 5.12 show a decreasing pressure trend with depth. Figure 5.13 shows more reasonable results.

5.6 Field Tests

Field testing was performed at sites identified by District I engineers where active drilled shaft construction operations were underway. This cooperation was essential to gain access to the sites, but reasonable accommodations also require that the data collection did not impair the construction sequence.

The first field test was on I-75 from Harborview Road to Sumter Boulevard. This project was located near the Charlotte and Sarasota County Line along the I-75 corridor in south Florida. The subject shaft was 54in diameter and 31ft long including the above ground portion. The actual depth of slurry tested was approximately 3.5ft less (27.5ft submerged). As this was not a primary bridge structure, the contractor was permitted to use polymer slurry per FDOT specifications. The polymer product was POLY-BORE manufactured by Baroid Industrial Drilling Products.

Construction logs indicate the excavation process spanned an elapsed time of 4hrs through sandy, silty sandy soil. The target viscosity used was 35 to 40sec/qt. Although clean polymer slurry is clear, the slurry after drilling contained suspended solids that made it appear light brown. Tactile examination easily detected coarse sand even near the surface.

Testing followed Option (1) discussed above where the basic steps were:

(1) Start data collection and verify the beginning baseline pressure values
(2) Lower the DHU until just submerged

(3) Route cable/tether over depth wheel
(4) Allow all pressures to stabilize
(5) Activate the pump and wait until measured flow rate stabilized
(6) Turn off pump and lower to the next depth increment (5ft)
(7) Repeat steps 4 through 6
(8) Continue process until the bottom of excavation is encountered

The entire process for this relatively short shaft took 6 minutes. Figure 5.14 shows the on-site testing. Samples of the slurry were immediately taken at each depth interval where data was collected and stored for conventional field testing, but in laboratory conditions that provide for refined density and viscosity determination. Sand content tests in the laboratory followed the exact field process with the exception that any slurry stored in the container was stirred to restore any suspended solids that were originally captured in the slurry. Often, field tests that slightly delay the sand content process do not capture the same concentration of suspended solids, especially in polymer slurries. By re-suspending the solids, the samples were more representative of that which the DHU encountered. Table 5.1 contains the results of all laboratory/conventional slurry tests from the samples collected from the site. Also a sample of the clean slurry in the supply tank is provided as a baseline.

Table 5.1. Slurry properties of field collected samples from Harborview Rd site.

Depth	Density (pcf)	Viscosity (sec/qt)	Sand Content (%)
0	62.45	41.2	0.75
5	62.52	42.0	1
10	62.55	38.8	2
15	62.72	38.5	3
20	62.68	37.7	3
25	62.81	36.8	5.5
Clean Slurry	62.16	44.2	0

Given the DHU is 2.5ft long and pulls slurry from the bottom end, the depth of reading is associated with the bottom of the unit. This depth is precisely correct for the viscosity and sand

content readings, but the density when positioned at that depth would be the average density over the top to bottom depths (e.g. 1.25ft density measurement location when bottom of DHU is located at 2.5ft).

Figure 5.14. Slurry testing at I-75 Harborview Rd high mast light foundation.

Test results from the DHU test are shown in Figures 5.15 - 5.17. Figure 5.15 shows the raw data versus time of test.

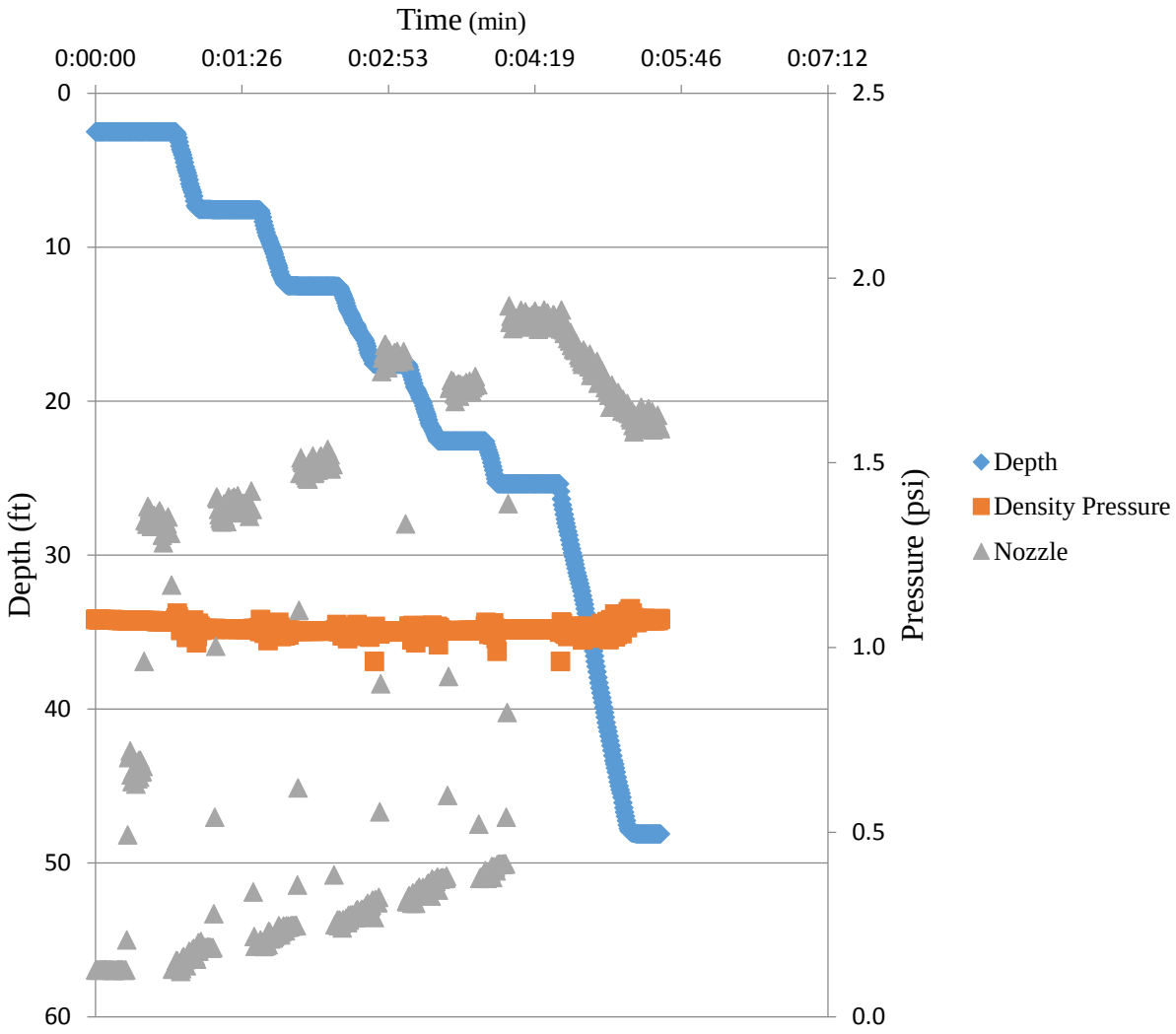

Figure 5.15. Raw data collected during slurry testing at Harborview Rd site.

All data was collected continuously, but the actual tests were performed on 5ft intervals and matched well with the calibration curves from Chapter 4 (Figure 5.16). Subtle variations in the arbitrarily selected pump flow setting show similar flow vs pressure trend for a constant viscosity slurry.

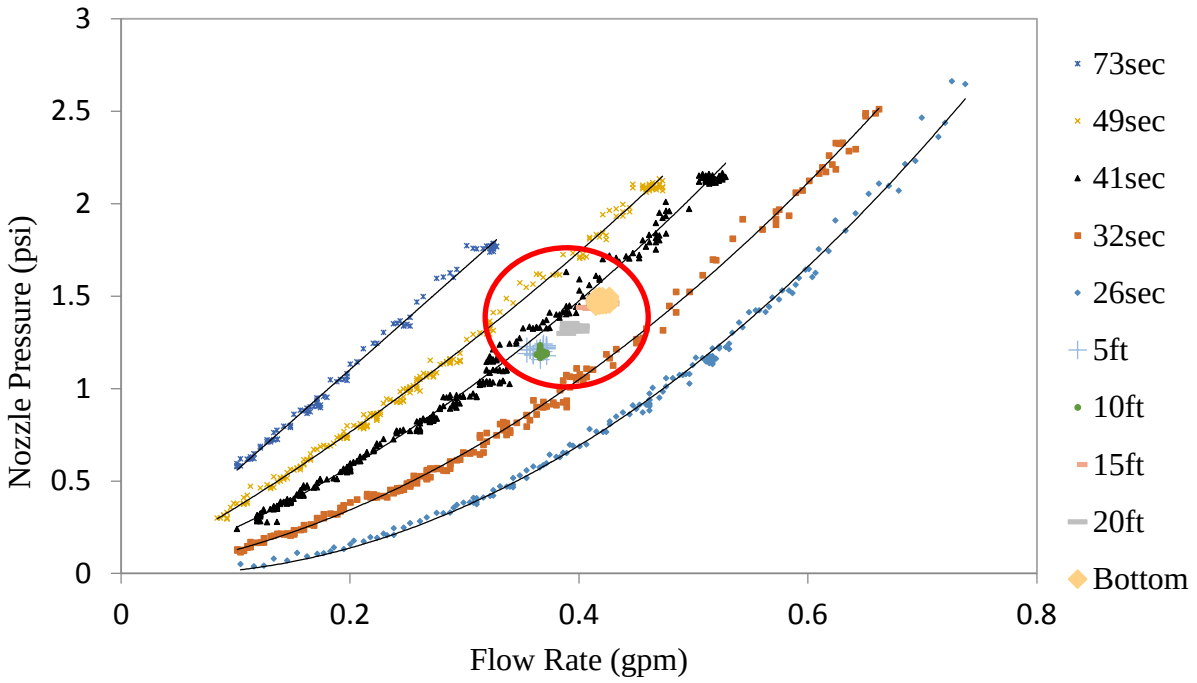

Figure 5.16. Flow and pressure data aligned just below the 41sec calibration curve indicating a near 40sec/qt Marsh funnel viscosity.

Figure 5.17 shows the computed slurry properties versus depth along with the Table 5.1 values. Given the short time duration required to sample at each depth, a tighter sampling interval could have been used without disrupting construction.

At the selected depth intervals, the Option (1) test procedure lowers the DHU to the prescribed depths, obtains a density and baseline nozzle pressure, the flow is increased, and data is collected until stable readings are obtained. Figure 5.17 also shows the results of manually performed tests (conducted in lab conditions) superimposed. Table 5.2 shows the data excerpted from the construction logs from the inspection team on-site during excavation and just prior to concreting.

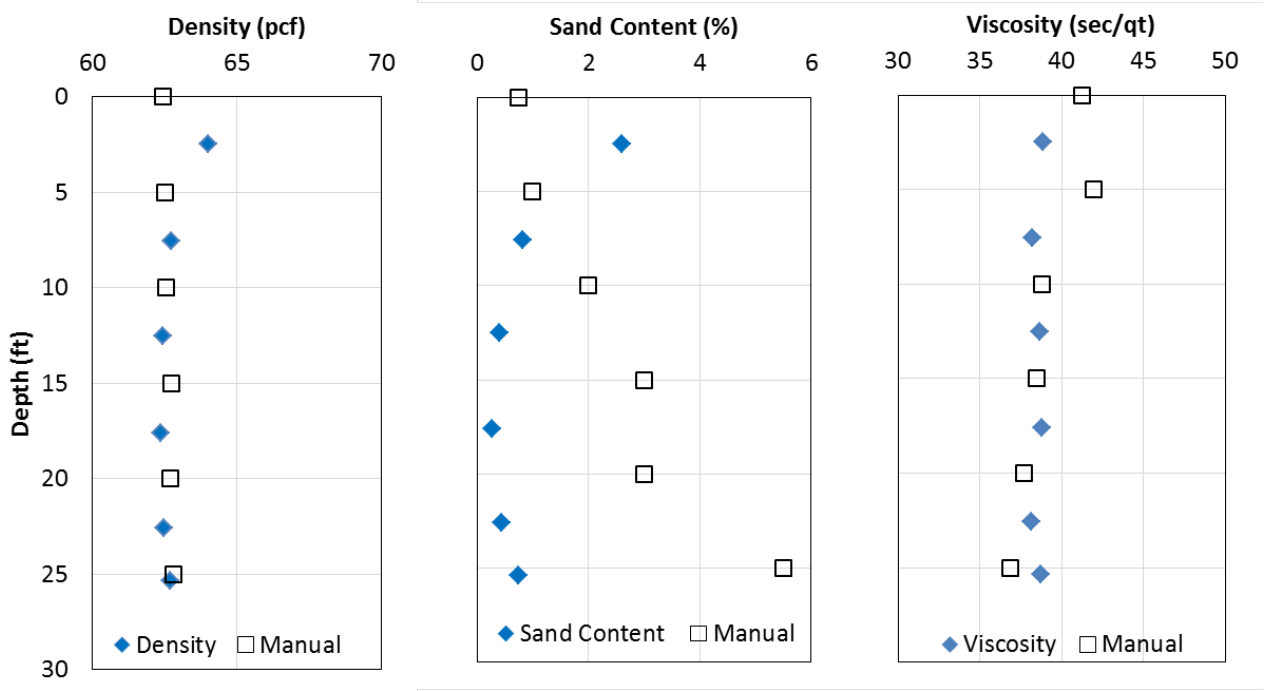

Figure 5.17. Automatically collected slurry property data vs depth (blue) and manually collected data tested in lab (open squares).

Table 5.2. Slurry properties measured on-site by inspection team.

Time	Density (pcf)	pH	Viscosity (sec/qt)	Sand Cont (%)	Comments
7:40	63	9	45	0	New slurry mix from inside tank.
8:30	63	9	34	0	Depth 10.0'
9:20	63	9	35	0	Depth 15.0'
10:00	63	9	38	0	Depth 20.0'
12:30	63	9.5	42	0	Depth 29.50'
After excavation prior to cage placement and concrete					
12:40	63	9.5	41	0	Depth 2ft (top)
12:40	63	9.5	42	0	Depth 29.5 (bottom)

Upon removal of the DHU from the excavation, a layer of sand was observed to have collected on the top cap even in the short duration of exposure which supported the laboratory results (higher sand content values than field results). The procedures used in the field were not

reviewed so no comment supporting or disputing those findings can be made. However, the lab technician at USF noted the process of washing the polymer slurry from the sand was not near as easy as that for bentonite slurry. If not careful it is conceivable that suspended sands could be inadvertently discarded if perceived to be only part of the slurry gel.

While some variation in density is expected, especially when sand content varies, the field density measurements mimicked the same trends noted in the simulations where density slightly decreased with depth and then increased. Figure 5.18 shows one of the simulated data sets along with field collected data. Density measurements from collected samples did not show significant changes yet the sand content did. The complication is that the same sample used for sand content may not be the same used for density despite efforts to make them same or similar.

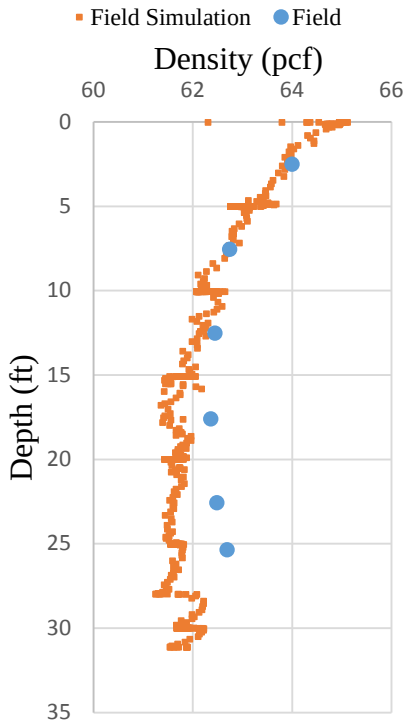

Figure 5.18. Unusual density trend that may indicate instrumentation errors.

An increasing trend with the differential density system (when in a constant density fluid) indicates the upper reference port (diaphragm seal) is not responding as much as it should. This was noted earlier in Figure 5.8. In this case, a decreasing trend (if the fluid is assumed to be constant density) would then indicate the lower diaphragm seal is not responding one to one with the applied pressure. Therefore, once again, the lower pressure diaphragm was purged and then resealed but at this time a slight modification to the protective screen was implemented which domed the screen to provide relief/room for the rubber diaphragm to bulge slightly outward when securing the membrane over the fluid surface. This removed the trend (Figure 5.19).

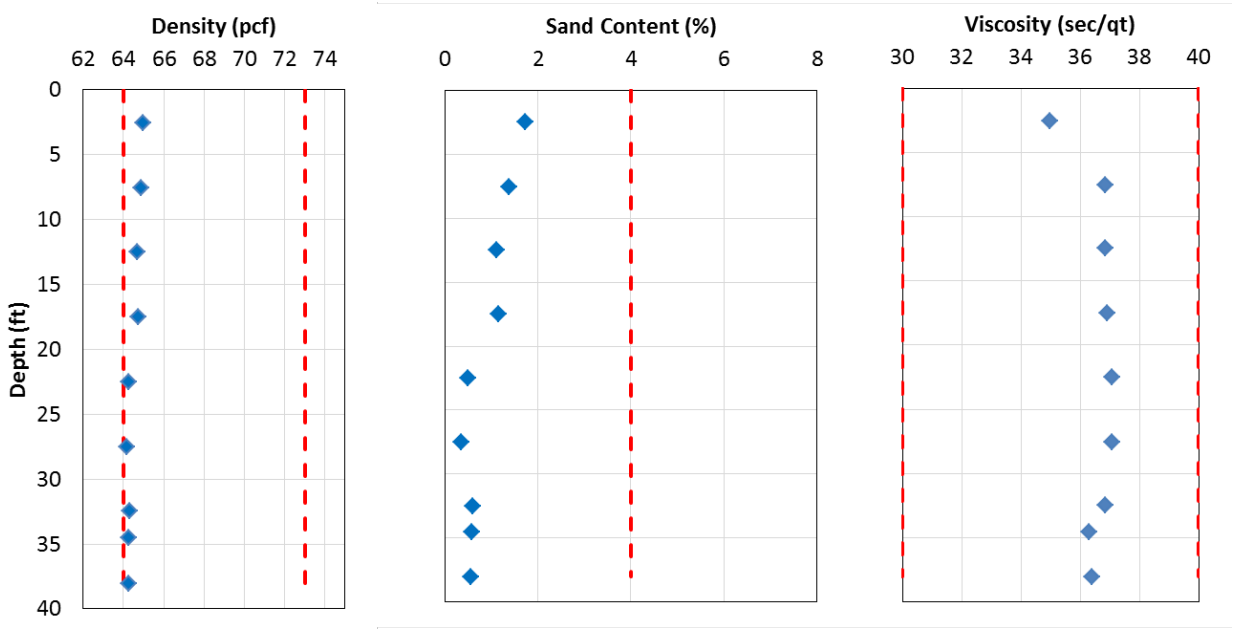

Figure 5.19. Corrected depth diaphragm

5.7 Recommended Testing Procedure

Revisions to the testing equipment and regression algorithms resulted in a recommended testing procedure. One change involved adding an extra data channel to provide a marker in the data sets indicating one of three conditions: (1) 0 volts; data that is not used in regression, i.e. descent data, (2) 5 volts; DHU is stationary where density and the nozzle pressure offset is

recorded, and (3) 12 volts: flow rate has increased until stable and data with this marker is used to compute viscosity. Figure 5.20 shows the additional three position switch on the CDS panel. Push left to take density readings (also nozzle pressure baseline), middle position is to descend or to start flow, and right to take viscosity data after flow is stabilized (pressure and flow). The addition of this switch stemmed from time consuming analysis of the field data which was caused by sorting active testing from less important steps. Density baseline measurements should always be taken before lowering the DHU into the slurry.

Summarizing, the following steps define the test procedure:

(1) Secure depth wheel assembly in appropriate location over the excavation, preferably as centered a possible.
(2) Connect depth wheel and DHU cables to CDS panel.
(3) With DHU oriented in a vertical position, start data collection software and confirm a stable density pressure reading is obtained. Begin data storage and collect several seconds of information.

Note that the exact zero base-line for density is not important but it is prudent to note variations that may indicate system damage. The recorded baseline is used in the regression software to refine the initial density measurements.

(4) Lower DHU into slurry until top of unit is flush with surface of slurry.
(5) With cable engaged in wheel assembly lower probe 0.5ft to first depth location.
(6) When nozzle pressure has stabilized from movement (one or two seconds), switch data marker to the density position and allow several seconds (e.g. 5 seconds) of data to be collected. This both takes a stable density measurement and provides the offset required to adjust the pressure vs. flow data as noted in Figures 5.5 and 5.6.
(7) Move data marker switch to the central position.
(8) Increase flow rate until between 0.3 and 0.4gpm.
(9) When flow rate has stabilized, move the data marker switch to the right position and again wait several seconds to collect data.
(10) Return data marker switch to center.
(11) Turn off pump.
(12) Lower DHU to next depth interval and repeat steps (6) through (11).

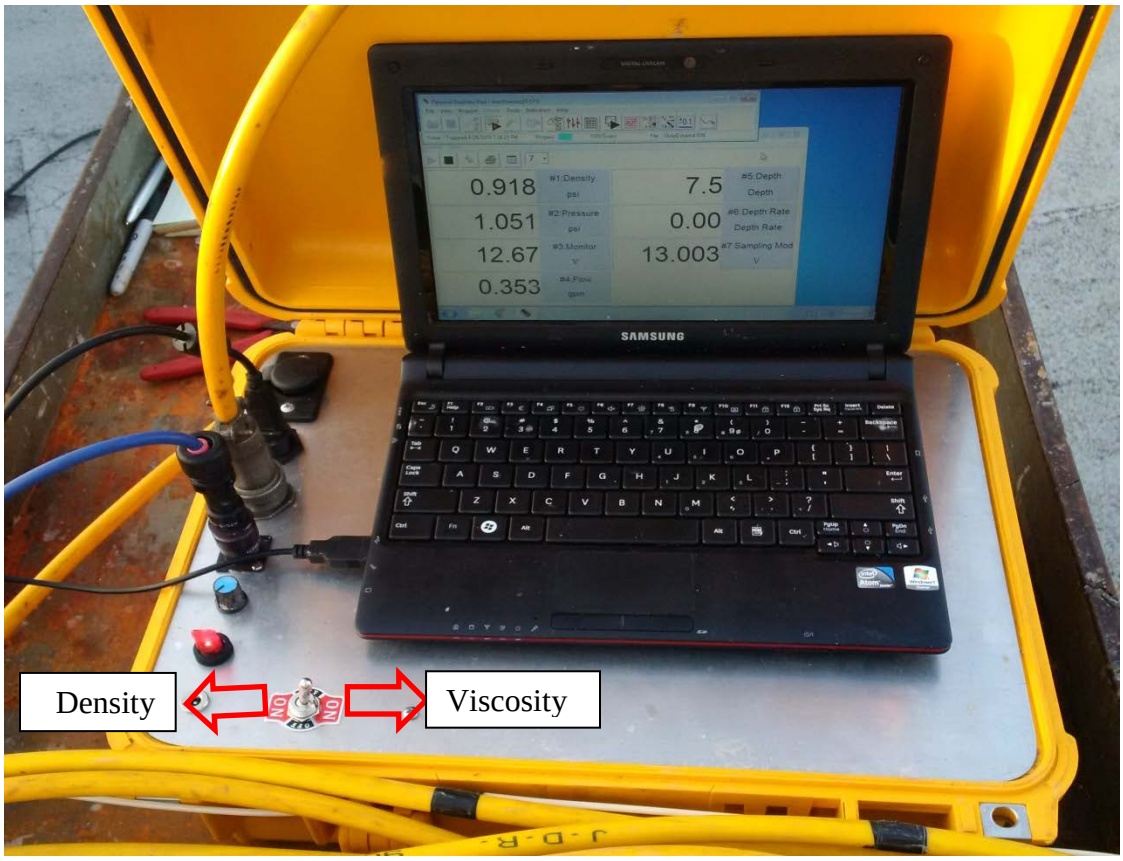

Figure 5.20. Revised version of CDS panel with data marker switch.

5.8 Chapter Summary

Slurry testing was performed in both field and simulated field conditions to similar depths. Uncertainty surrounding the density measurements also affects sand content determination due to the dependent computations. Comparing both field and simulated density measurements, the same trend was noted which implied a stray variable in the instrumentation which requires further evaluation. The basis of the density measurement was the difference in pressure over a set spacing between pressure ports. This methodology was thought to be less prone to error, but the interface between the slurry and glycerin filled transducer lines may continue to be the problem. An alternate device has been designed that uses Archimedes buoyancy principles, but this device was not tested with the DHU.

Lessons learned from the field testing component of this thesis include:

- Data analysis. The present data collection system is time based taking samples at 2Hz. Post processing requires a demarcation in the data that defines the test that is being performed. The added data marker switch removes user decision in analysis. This also means that data can be collected and directly analyzed while the test is being performed.
- Instrumentation. Purging transducer fluid lines is difficult and even when calibration is accurate in the laboratory, high pressures from field conditions reveal errors.
- Clean up. System clean out protocols need to be developed to prevent inadvertent clogging from drying slurry products. This is similar to proper maintenance of Marsh funnels and associated slurry testing equipment.
- Calibration. Chapter 3 calibration procedures involved slowly increasing the flow controller such that the instantaneously responding pressure nozzle reading would correspond well to the more sluggish responding flow meter. Use of data markers from the added switch on the CDS panel removed any data that had not achieved steady state conditions.
- Troubleshooting. High pressure calibration is essential to confirm transducer performance. Identification of error modes helped to facilitate proper cell readiness. Several modes are shown in the raw data results in Appendix E.

CHAPTER 6: CONCLUSIONS AND RECOMMENDATIONS

Excavation stability is perhaps the most important aspect of drilled shaft construction followed closely by concreting. Many contractors avoid open excavations altogether by using full length temporary casing thereby removing the need for drilling slurry and many of the associated complications. However, slurry excavation often requires smaller equipment and tends to be less expensive making it a common choice. The effectiveness of slurry excavation relies largely on proper performance of the slurry which in turn is maintained by assuring the density, viscosity, pH, and sand content stay within specified limits. These limits have been set either by past experience, research findings and/or by manufacturer recommended values. However, field slurry testing can be time consuming as all measurements are manually performed. This thesis focused on the development of an automated slurry testing system that both decreased time of testing and increased overall data quality documenting the slurry properties.

In the process of developing an automated down-hole slurry testing system, several tasks were undertaken including: a thorough literature search, component testing, prototype design and fabrication, laboratory trials and field testing of the developed system.

6.1 Prototype Design and Testing

Where the thesis objectives were to develop a field ready automated slurry testing system, the first steps were to verify the concept and perform a series of proof-of-concept tests. This involved several types of tests whereby pressure and flow rate relationships were generated for a wide range of slurry viscosities both with and without suspended solids. The basis of the concept stemmed from the simplicity of the Marsh funnel test: specifically, a fixed volume of slurry flows at rates inversely proportional to viscosity. Lower viscosity fluid flows more quickly and vice versa.

When considering the FDOT (and nationwide) specifications, this translates into flow rates of 0.38 to 0.5gpm for viscosities of 40 and 30sec/qt, respectively. The driving force for flow is the falling head pressure of the emptying funnel (approx. 17in to 13in) and where the density may be higher or lower depending on suspended solids content. Pressure therefore might range from 0.47 to 0.78psi again depending on slurry density. However, as each viscosity produced a unique pressure versus flow curve, the flow rate (and pressure) could be pushed beyond that observed during Marsh funnel testing. Further, as the Marsh funnel presently serves well to assess slurry in production settings, the ID of the funnel orifice was ultimately selected for the automated system.

With this information as a framework, pumps, flow meters and pressure transducers were selected to stay within this order of magnitude. The equipment design revolved around off-the-shelf transducers and was ever conscious of the field restrictions / obstacles that a field engineer might encounter. Component specifications for the selected devices were:

- Magnetic flux flow meter: 0.3-3gpm
- Pressure transducer: 0-10psi
- Pump: 0-2gpm @ 0ft of head (variable)
- Nozzle orifice: 3/16in ID (same as Marsh Funnel)

The equipment was tailored to stay light, setup quickly, and run at a target rate of 0.5 to 1ft/sec of descent. This equates to several minutes to test a 100ft excavation. The design weight of the down-hole component, however, was almost entirely based on the weight of the displaced slurry volume; the weight of the chosen devices and fixtures were actually too light so additional weight was required to make it sink. Smaller volume alternative designs are being considered at the time of this report.

6.2 Calibration

The uniqueness of the pressure / flow relationship for a given viscosity was confirmed both in laboratory falling head and pumped slurry tests. Falling head tests involved a 15ft tall, 6in diameter slurry column sealed/fastened to a conventional Marsh funnel. This provided a means to both extend the normal pressure limits of a Marsh funnel (from < 1psi to > 4psi) while also precisely recording flow and pressure for a given slurry viscosity.

Pumped slurry tests were performed at flow rates up to 42gpm through nozzle diameters up to 5/8in ID. Recall, higher flow rates were originally considered on the basis of a top side slurry processing system where only a pickup hose would be lowered into the excavation. Numerous aspects of this concept made it impractical.

Lower flow rates through smaller diameter nozzles were found to be more sensitive to changes in viscosity, hence the selected prototype component list. Figure 6.1 shows the calibration curves for the prototype design system. Flow rate through the system nozzle is less than 0.8gpm at its fastest at a maximum pressure less than 3psi.

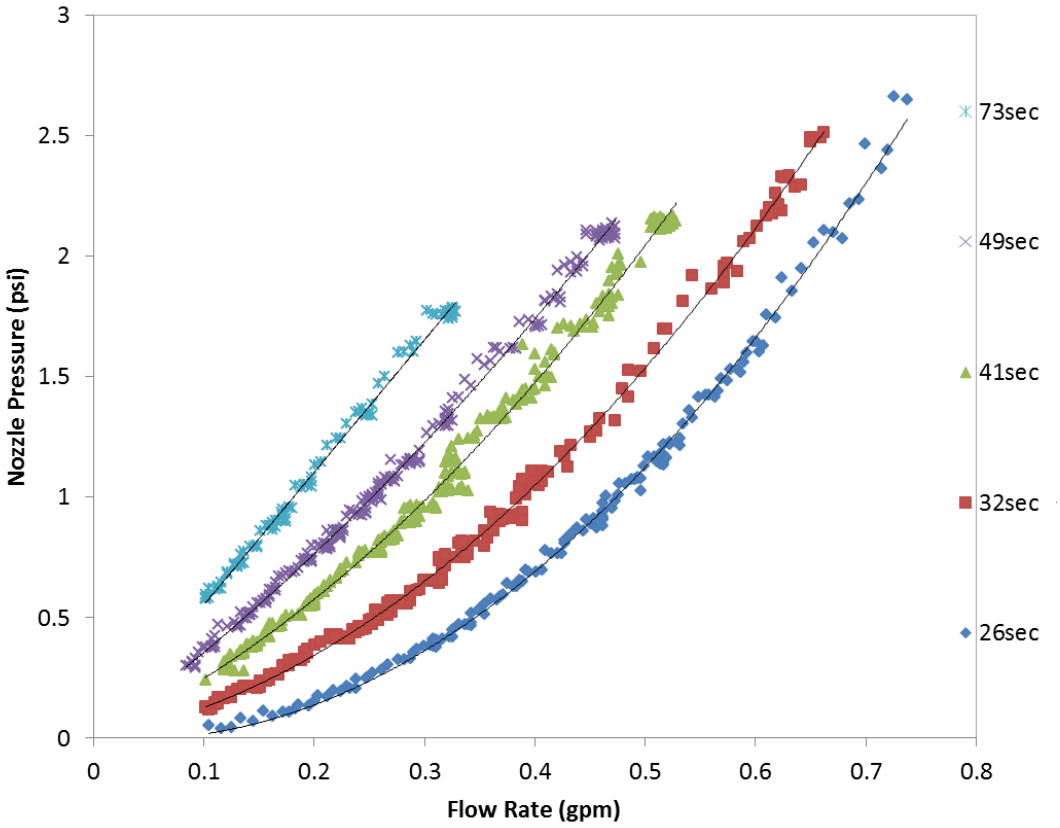

Figure 6.1. Calibration curves for slurry viscosities ranging from 26sec/qt water to 73sec/qt bentonite.

Improvements in the data collection system via data markers allowed for refined calibration procedures that semi-automated the process and provided a means to verify system performance quickly before and/or after field testing. In general, by inputting nozzle pressure and flow rate for a known viscosity like water, the unique point on a 3-D surface can be verified (Figure 6.2), but via a closed form solution.

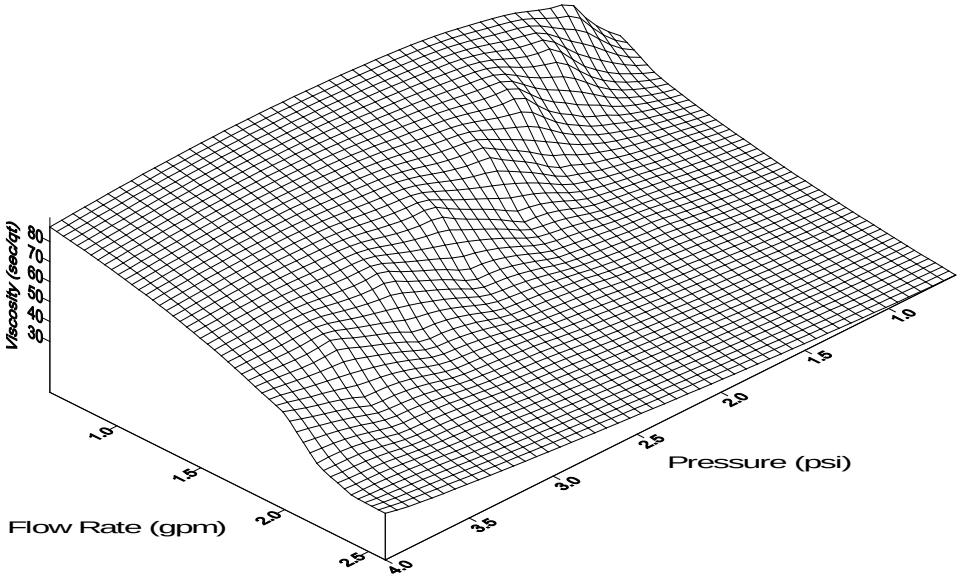

Figure 6.2. Viscosity surface based on various flow rates and pressures.

6.3 Field Testing

Field testing was broken into two types of conditions including on-site and simulated field conditions. Experience from on-site testing showed the entire system to be surprisingly easy to use despite the size of the prototype; simulated field tests were actually more difficult to perform due to the restricted access to the top of the simulated excavation column. Testing procedures evolved over the span of all tests which refined output. In short, data collection intervals (depth increments) are user defined, but even at seemingly tight intervals, the time of testing is expected to be less than manual testing methods.

While efforts to permit continuous non-stop data collection will continue, the incremental method noted above is recommended which includes:

(1) Start data collection and verify the beginning baseline pressure values
(2) Lower the DHU until just submerged
(3) Route cable/tether over depth wheel
(4) Allow all pressures to stabilize
(5) Activate the pump and wait until measured flow rate stabilized
(6) Turn off pump and lower to the next depth increment (5ft)
(7) Repeat steps 4 through 6
(8) Continue process until the bottom of excavation is encountered

The time required to collect data from each depth increment is about 10-15sec. When considering the added to time to descend to the next interval, data from each depth (including viscosity, density and sand content) should take no more than 1min.

Field testing revealed irregularities in density measurements which also affect sand content determinations. These were found to be a by-product of the protection screen placed over the diaphragm slurry/glycerin interface. By removing this screen, data became more in-line with expected. Improvements to the quality of these measurements continue to be made which includes an alternate density measuring system using Archimedes buoyancy principles and a submersible load cell.

6.4 Summary

The prototype all-in-one slurry testing system that was developed uses the same principles as that of the Marsh funnel to predict the same parameter which is an indication of true viscosity. The units of measure (sec/qt) are not real viscosity units (shear stress/velocity) but are understood empirically through field experience. While this was originally thought to be the hardest of the three to measure, it turned out to be the most robust. Continued use of the new

device will aid in further refinements and ultimately acceptance. The system is expected to speed the testing process and provide higher quality results.

REFERENCES

Alicat Scientific, (2015). http://www.alicat.com/wpinstall/wp-content/uploads/2012/05/doppler-flow-meter.gif

FDOT, 2016. Standard Specifications for Road and Bridge Construction, http://www.dot.state.fl.us/programmanagement/Implemented/SpecBooks/January2016/Files/116eBook.pdf

Hoffman & Hoffman, Ltd., (2015). http://www.hw-well.com/imageBank/Brochure_SandSense%20SWD-3.pdf

IESMAT, S.A., (2015). http://www.iesmat.com/iesmat/upload/file/Malvern/Productos-MAL/REO-Viscometer%20or%20Rheometer.%20Making%20the%20decision.pdf

Mullins, G., and Winters, D., (2010). "Rapid Hydration of Mineral Slurries for Drilled Shafts" Final Report, FDOT Project No. BDK-84-977-03, University of South Florida, Tampa, FL.

Omega Engineering,
(2015d). http://www.omega.com/literature/transactions/volume4/images/09_Fig_01_l.GIF

Omega Engineering, (2015e). http://www.omega.com/literature/transactions/volume4/T9904-09-ELEC.html#elec_4

Omega Engineering, (2015g). http://www.omega.com/literature/transactions/volume4/T9904-10-MASS.html#mass_2

Omega Engineering, (2015j). http://www.omega.com/pptst/FDT-40.html

Omega Engineering, (2015i). http://www.omega.com/pptst/FMG90.html

Omega Engineering, (2015b). http://www.omega.com/pptst/KFH.html

Omega Engineering, (2015a). http://www.omega.com/pptst/LC101.html

Omega Engineering, (2015k). http://www.omega.com/pptst/PHE558020_559020.html

Omega Engineering, (2015c). http://www.omega.com/pptst/PX01-MV.html

Omega Engineering, (2015f). http://www.omega.com/techref/table1.html

Rutgers, (2015). http://genchem.rutgers.edu/litmus.html

Smart Measurement, Inc., (2015). http://www.smartmeasurement.com/LinkClick.aspx?fileticket=3U-pygjoIJ0%3d&tabid=144

Universal Flow Monitors, (2015). http://www.flowmeters.com/magnetic-technology

Wyo-Ben, Inc., (2014). http://www.wyoben.com/media/magentothem/productpdf/MudBalance.pdf

APPENDIX A1: SERIES ONE WEIGHT AND PRESSURE RAW DATA

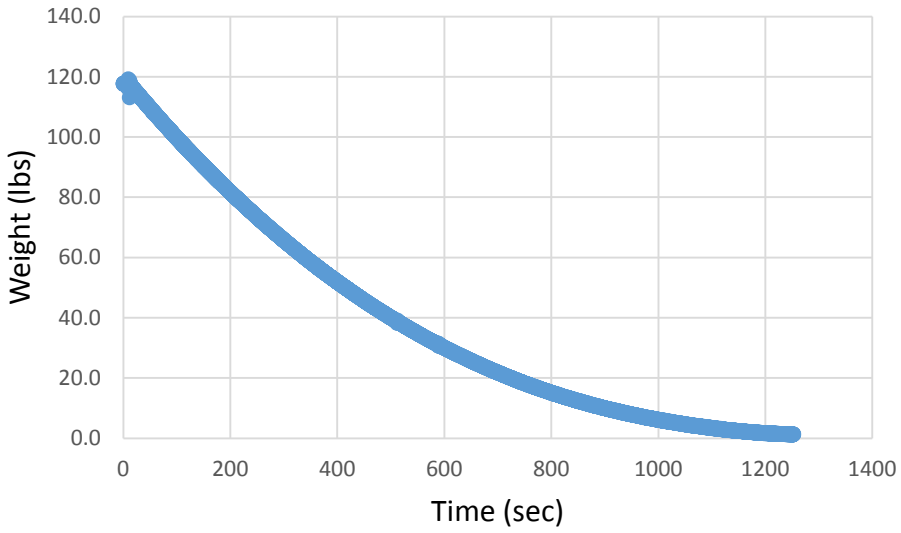

Figure A1.1. Batch 1 test 1 91.23 sec/qt viscosity weight data

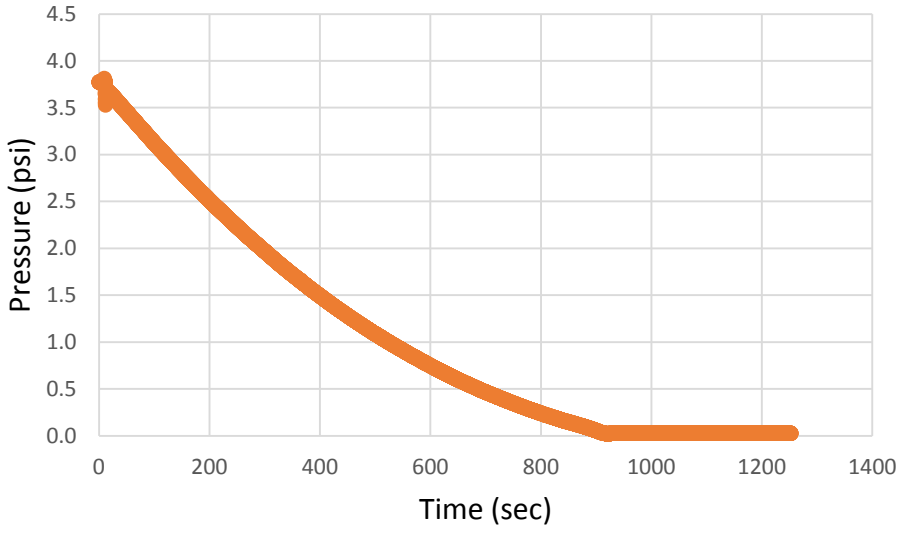

Figure A1.2. Batch 1 test 1 91.23 sec/qt viscosity pressure data

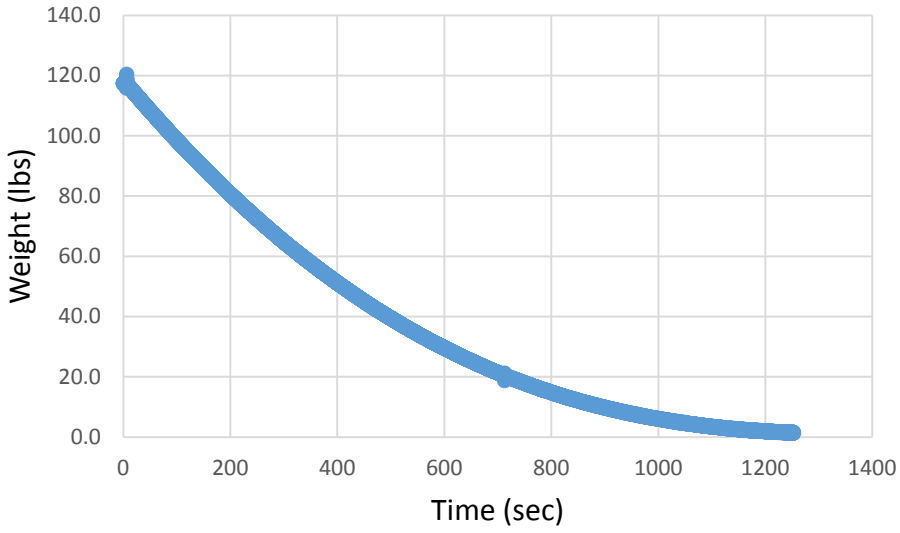

Figure A1.3. Batch 1 test 2 96.3 sec/qt viscosity weight data

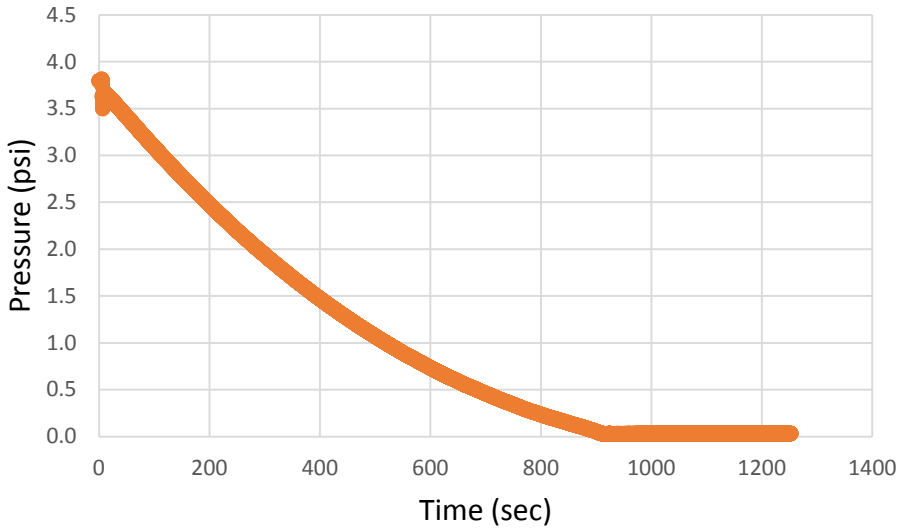

Figure A1.4 . Batch 1 test 2 96.3 sec/qt viscosity pressure data

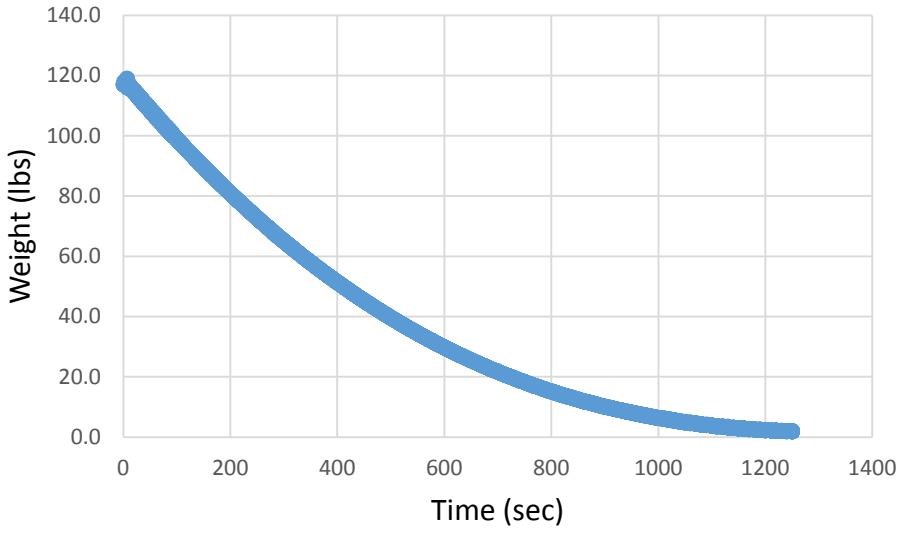

Figure A1.5. Batch 1 test 3 97.9 sec/qt viscosity weight data

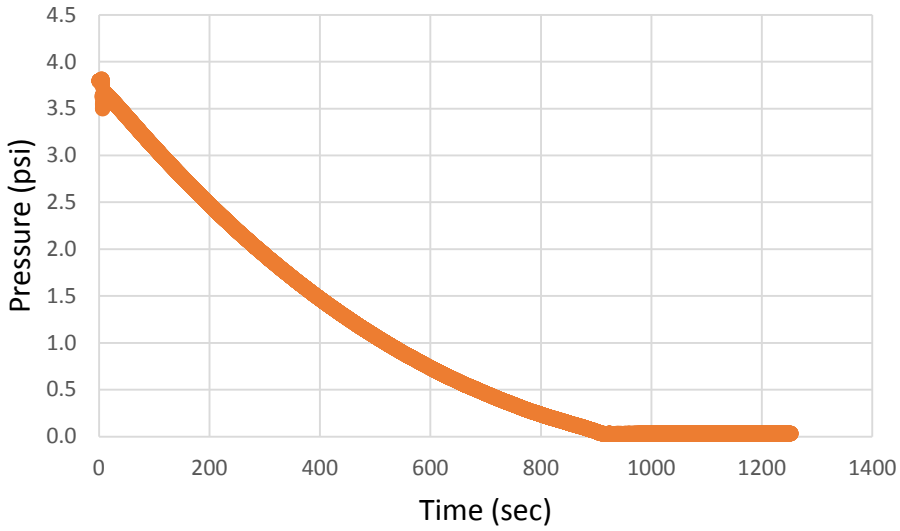

Figure A1.6. Batch 1 test 3 97.9 sec/qt viscosity pressure data

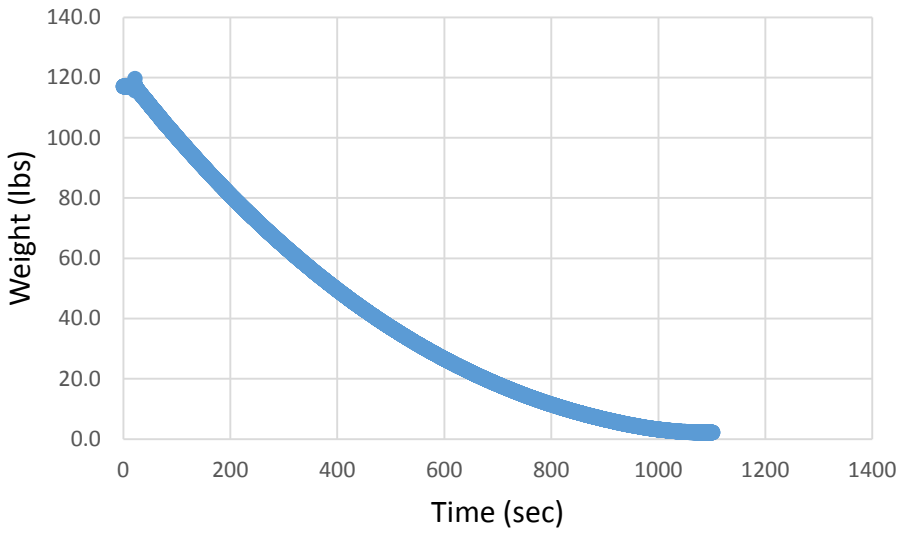

Figure A1.7. Batch 2 test 1 60.49 sec/qt viscosity weight data

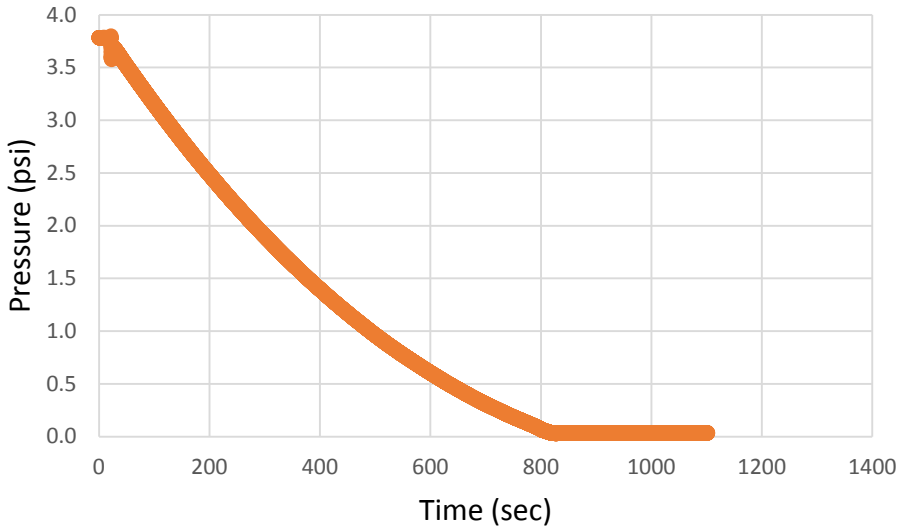

Figure A1.8. Batch 2 test 1 60.49 sec/qt viscosity pressure data

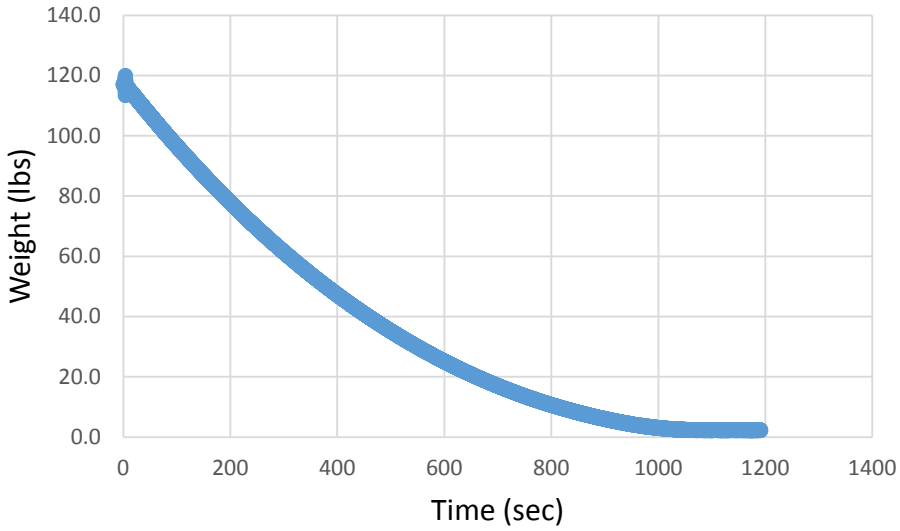

Figure A1.9. Batch 2 test 2 60.64 sec/qt viscosity weight data

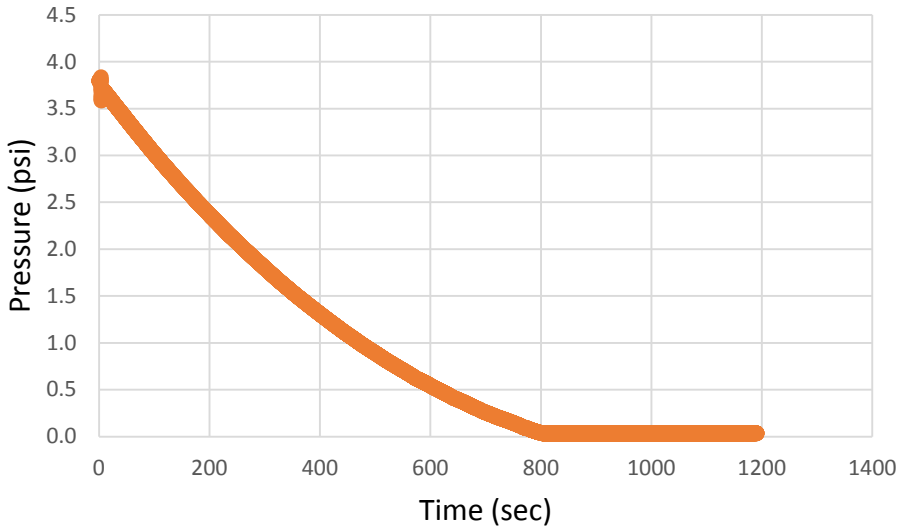

Figure A1.10. Batch 2 test 2 60.64 sec/qt viscosity pressure data

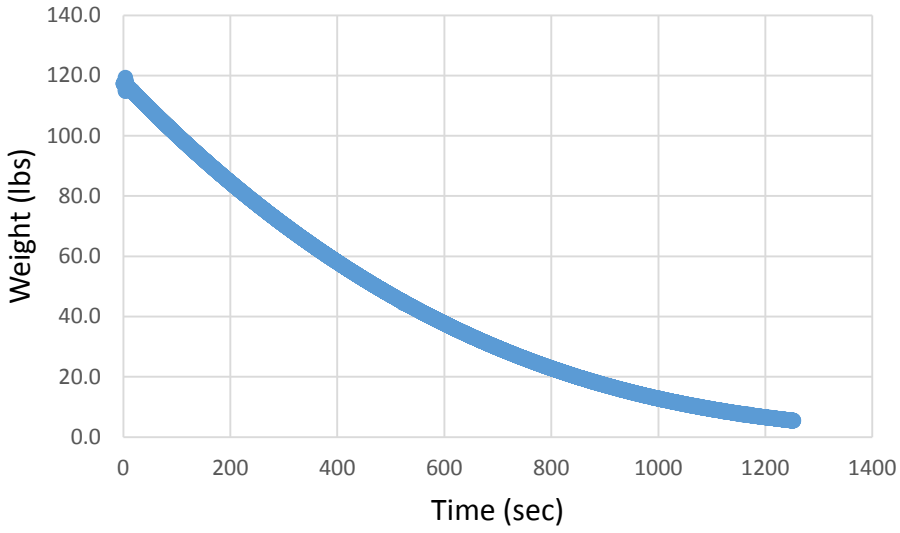

Figure A1.11. Batch 2 test 3 63.78 sec/qt viscosity weight data

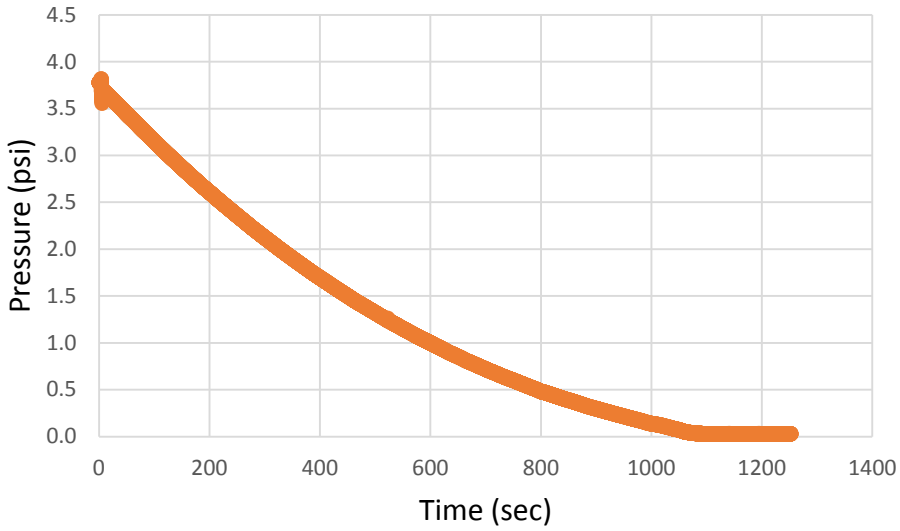

Figure A1.12. Batch 2 test 3 63.78 sec/qt viscosity pressure data

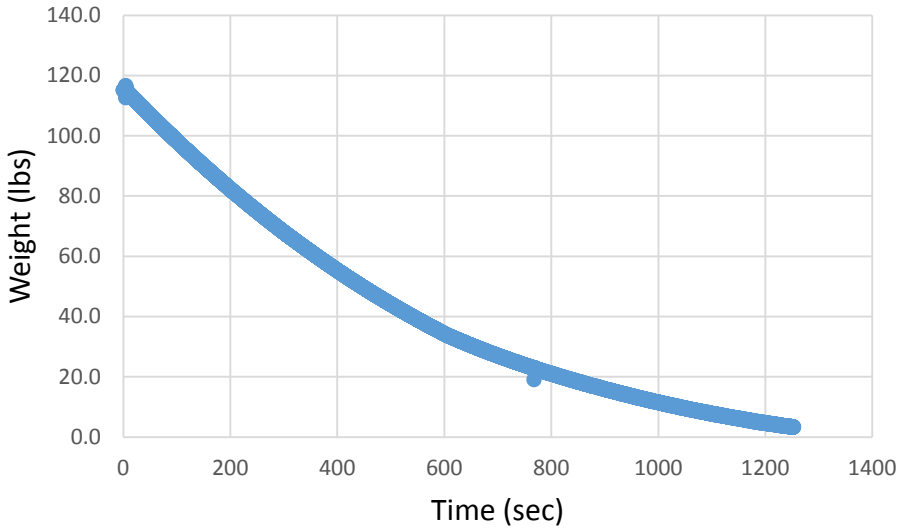

Figure A1.13. Batch 3 test 1 44.26 sec/qt viscosity weight data

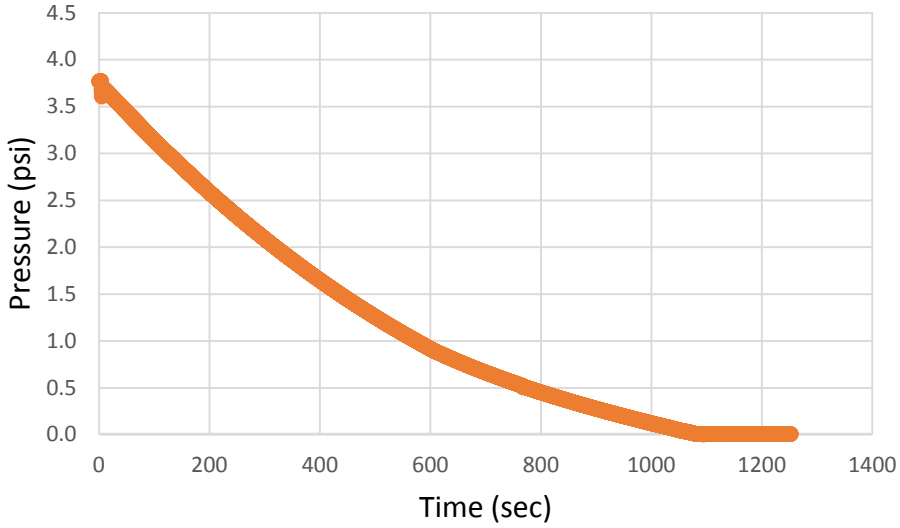

Figure A1.14. Batch 3 test 1 44.26 sec/qt viscosity pressure data

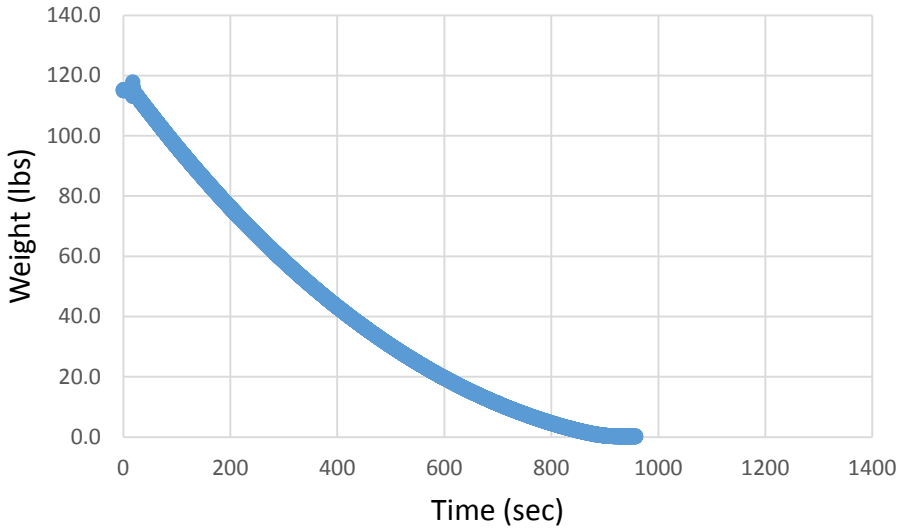

Figure A1.15. Batch 3 test 2 44.69 sec/qt viscosity weight data

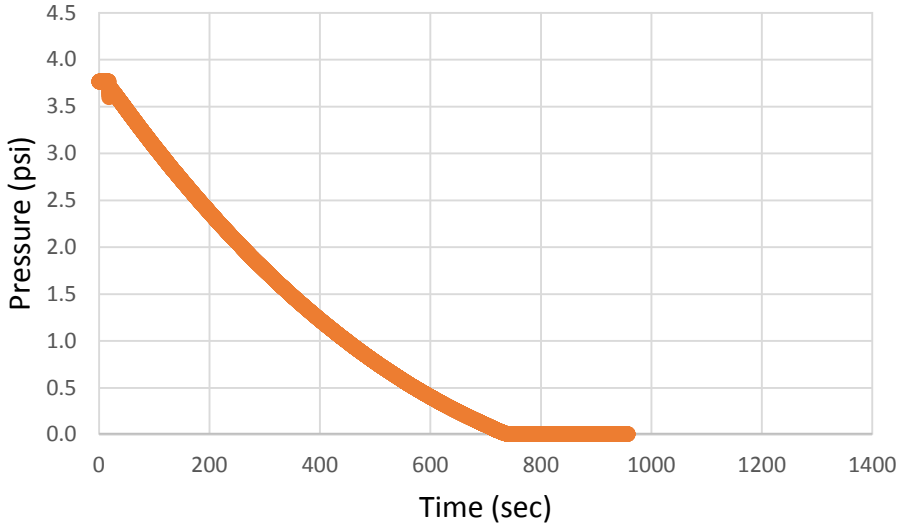

Figure A1.16. Batch 3 test 2 44.69 sec/qt viscosity pressure data

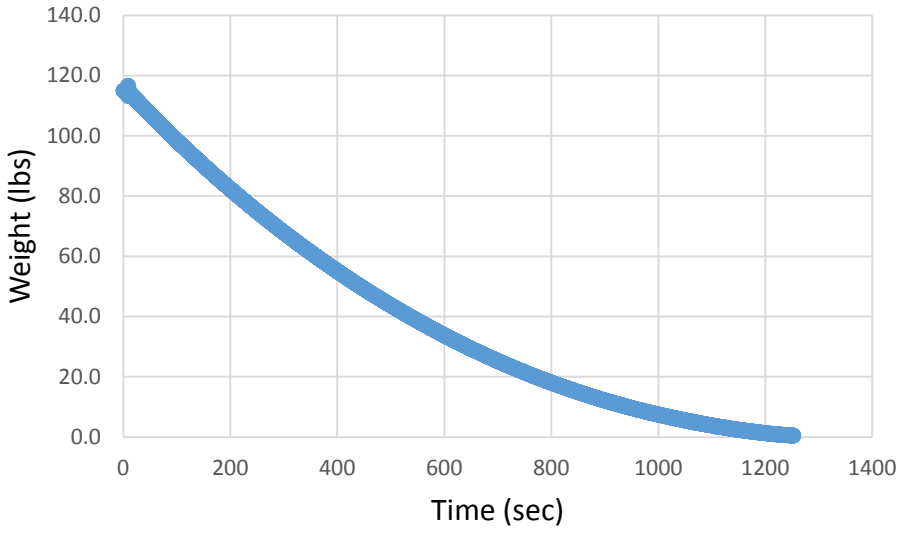

Figure A1.17. Batch 3 test 3 44.80 sec/qt viscosity weight data

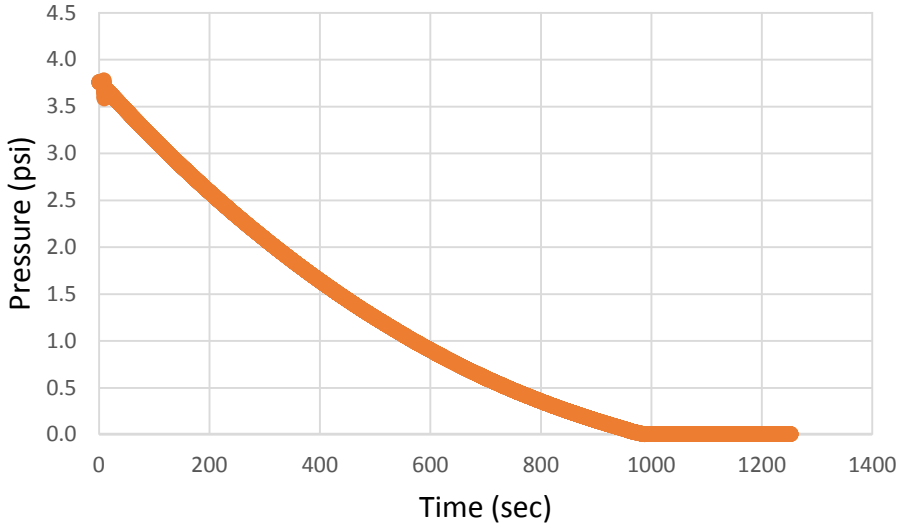

Figure A1.18. Batch 3 test 3 44.80 sec/qt viscosity pressure data

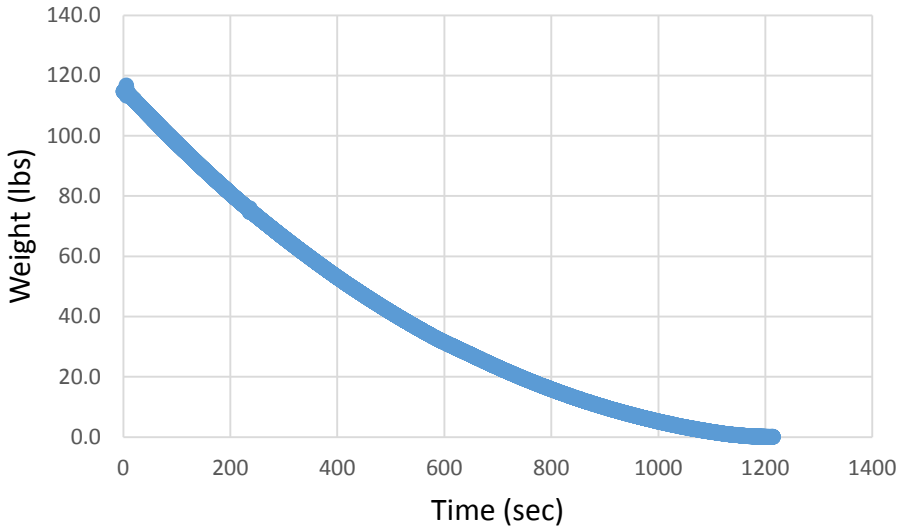

Figure A1.19. Batch 4 test 1 40.10 sec/qt viscosity weight data

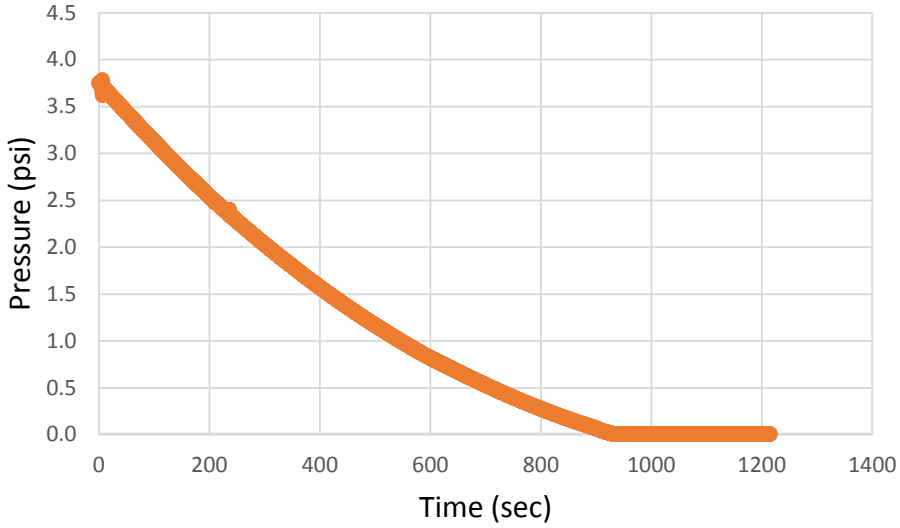

Figure A1.20. Batch 4 test 1 40.10 sec/qt viscosity pressure data

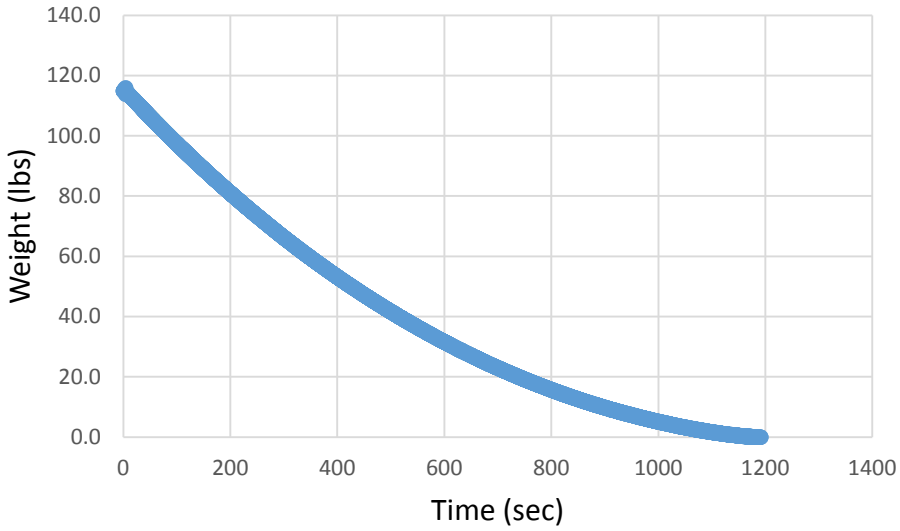

Figure A1.21. Batch 4 test 2 39.96 sec/qt viscosity weight data

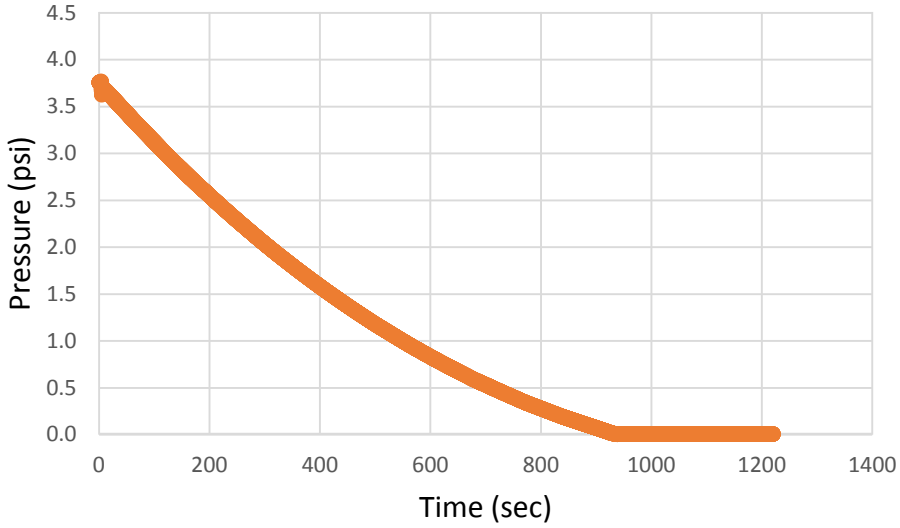

Figure A1.22. Batch 4 test 2 39.96 sec/qt viscosity pressure data

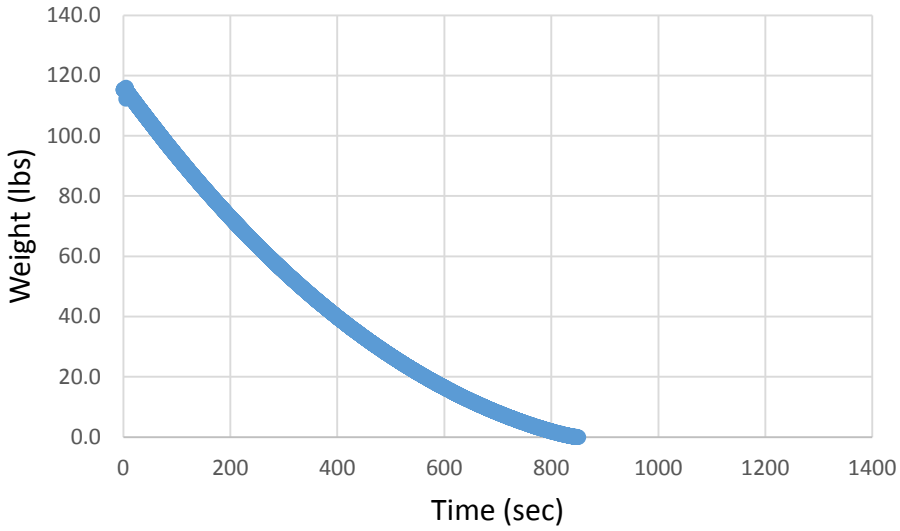

Figure A1.23. Batch 4 test 3 39.60 sec/qt viscosity weight data

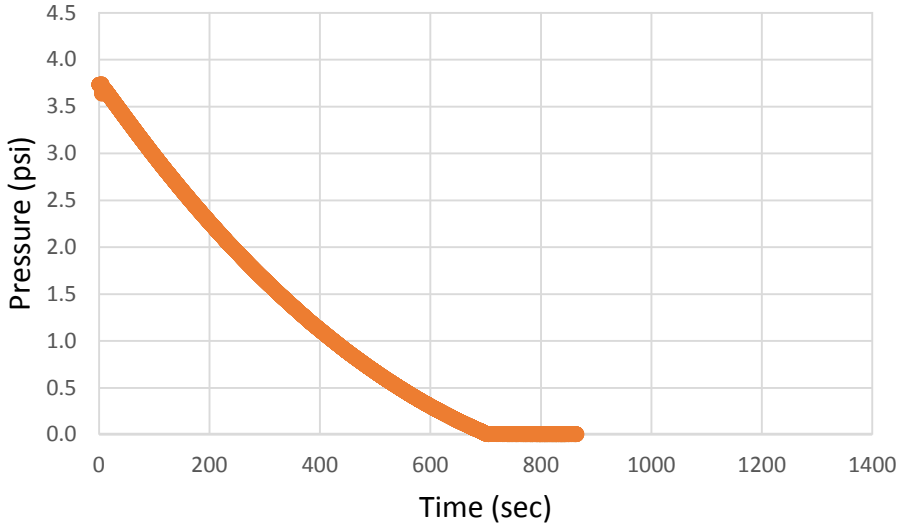

Figure A1.24. Batch 4 test 3 39.60 sec/qt viscosity pressure data

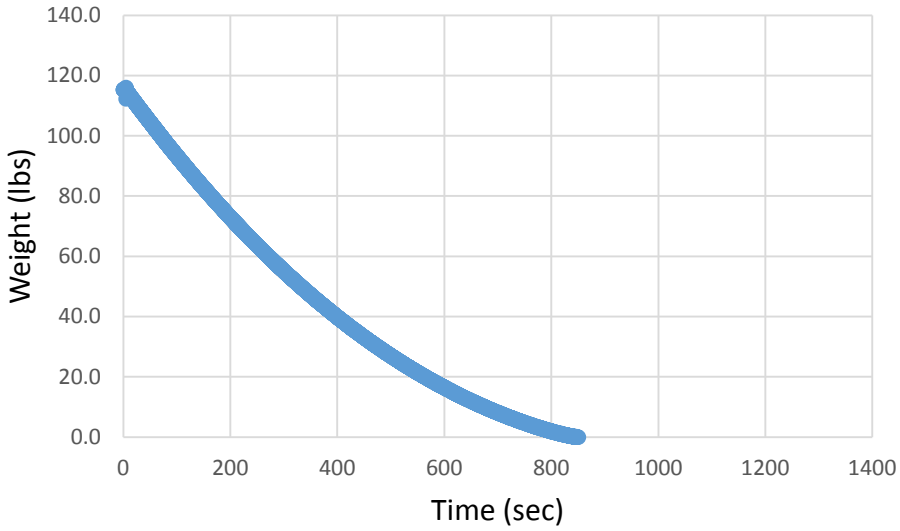

Figure A1.25. Batch 4 test 4 39.79 sec/qt viscosity weight data

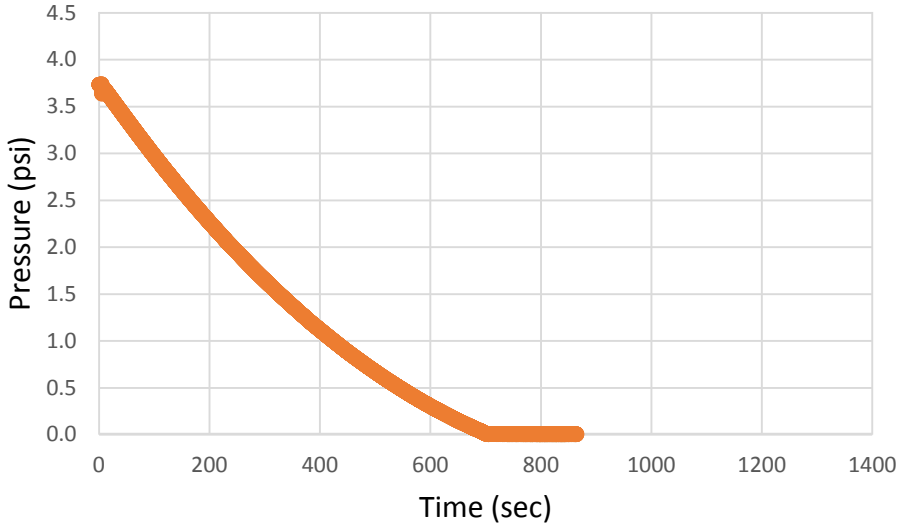

Figure A1.26. Batch 4 test 4 39.79 sec/qt viscosity pressure data

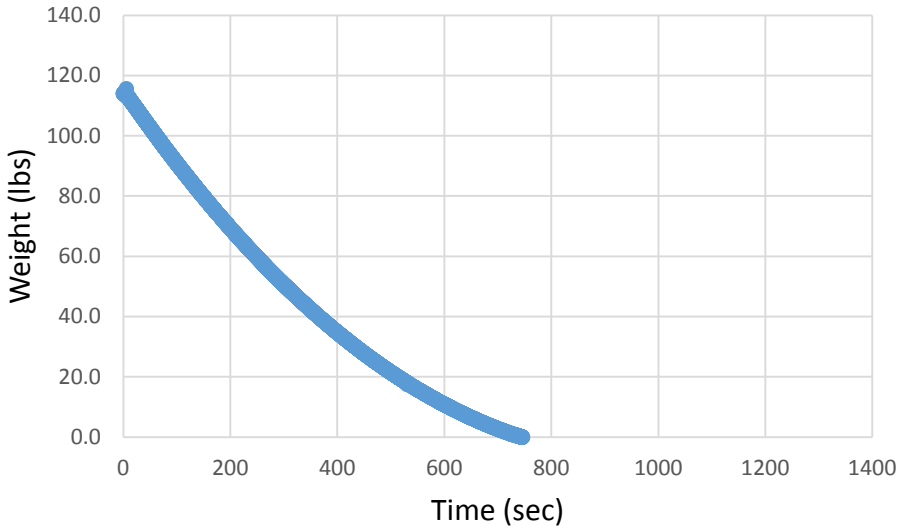

Figure A1.27. Batch 5 test 1 32.20 sec/qt viscosity weight data

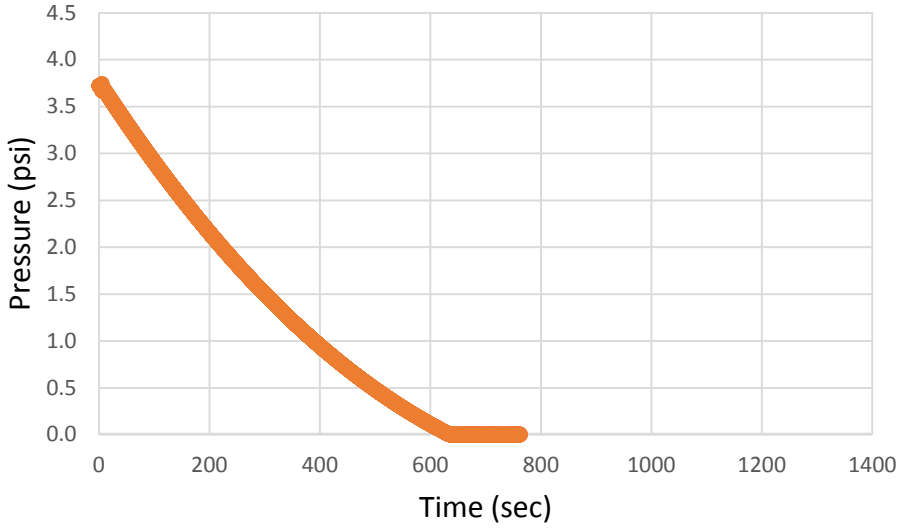

Figure A1.28. Batch 5 test 1 32.20 sec/qt viscosity pressure data

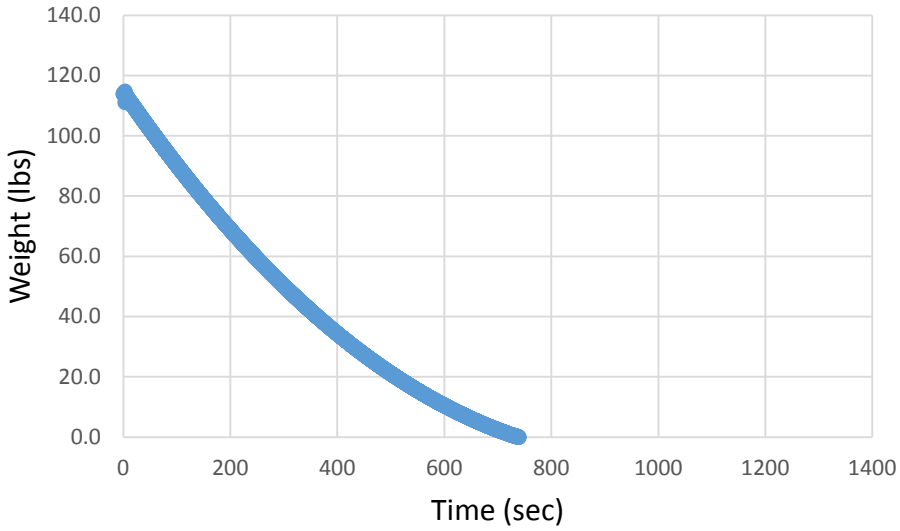

Figure A1.29. Batch 5 test 2 32.13 sec/qt viscosity weight data

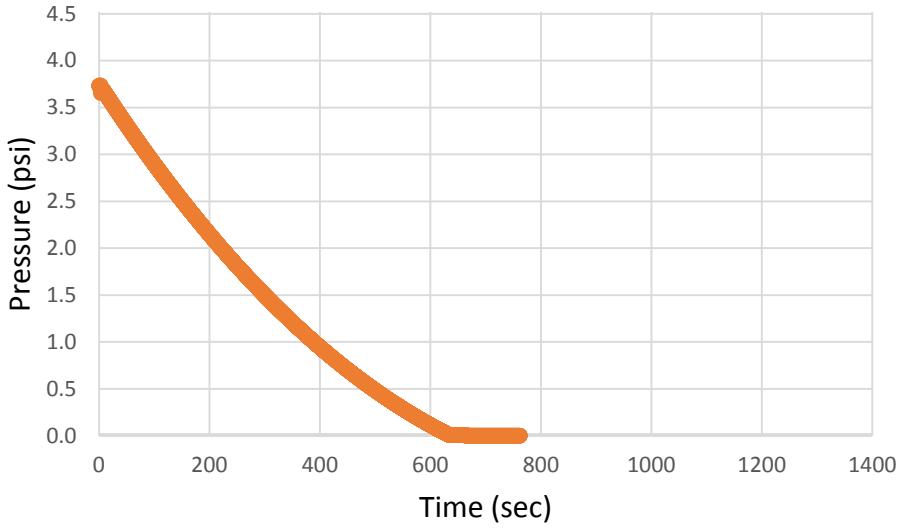

Figure A1.30. Batch 5 test 2 32.13 sec/qt viscosity pressure data

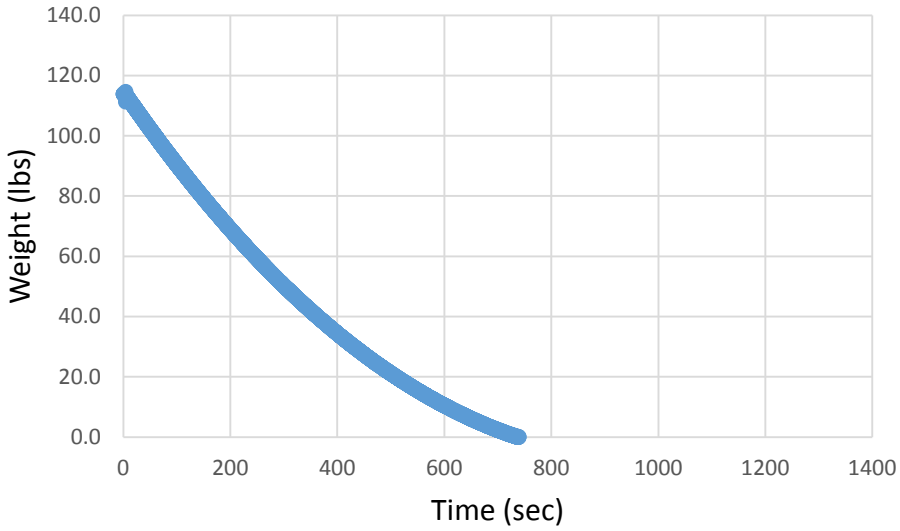

Figure A1.31. Batch 5 test 3 32.06 sec/qt viscosity weight data

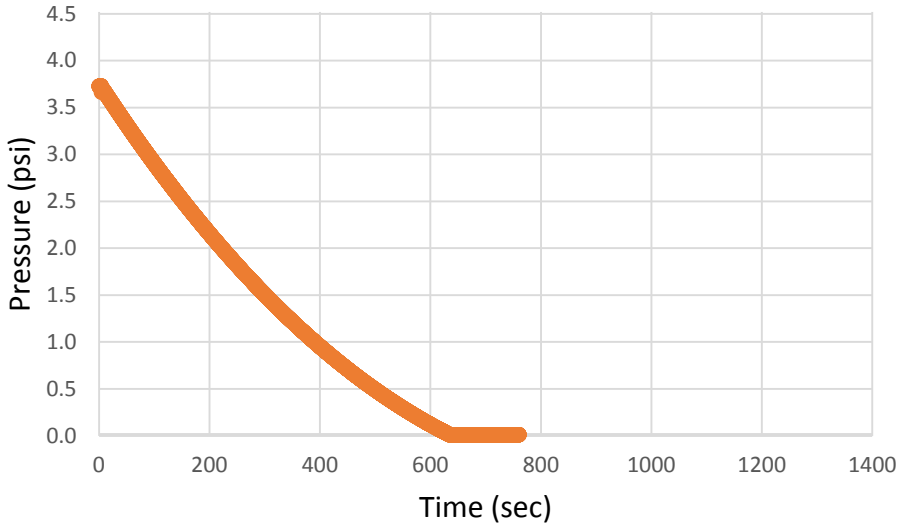

Figure A1.32. Batch 5 test 3 32.06 sec/qt viscosity pressure data

APPENDIX A2: HIGH SAND-CONTENT WEIGHT AND PRESSURE RAW DATA

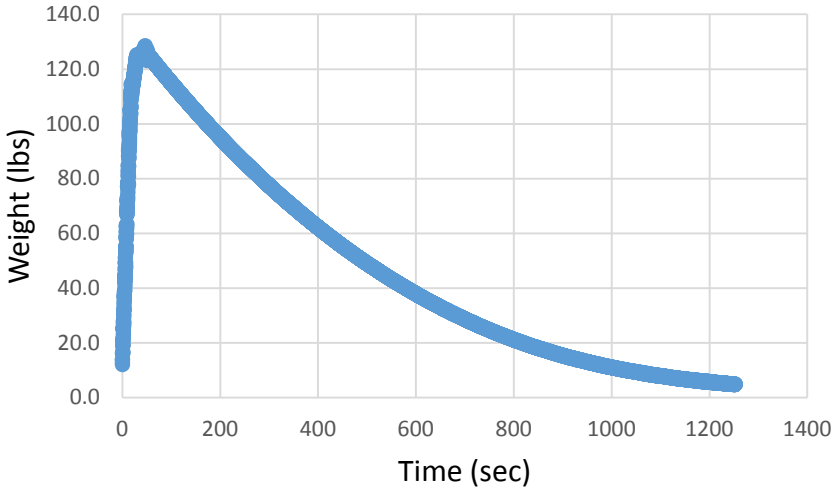

Figure A2.1. Batch 1 test 1 146.91 sec/qt viscosity weight data

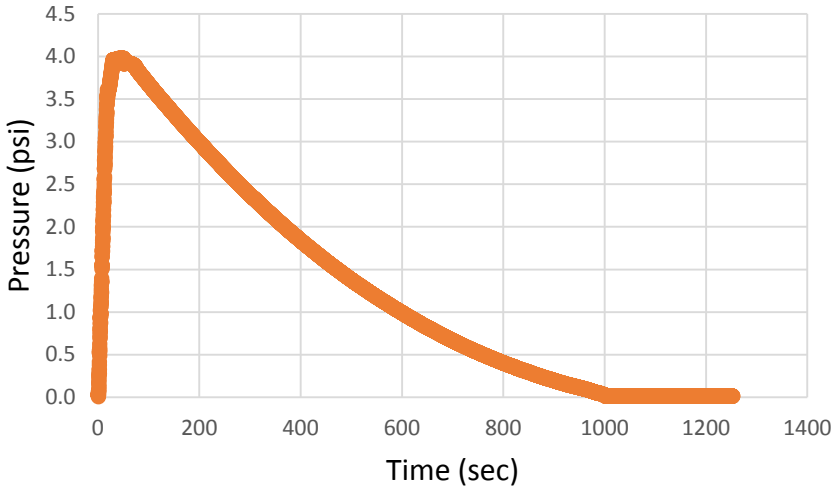

Figure A2.2. Batch 1 test 1 146.91 sec/qt viscosity pressure data

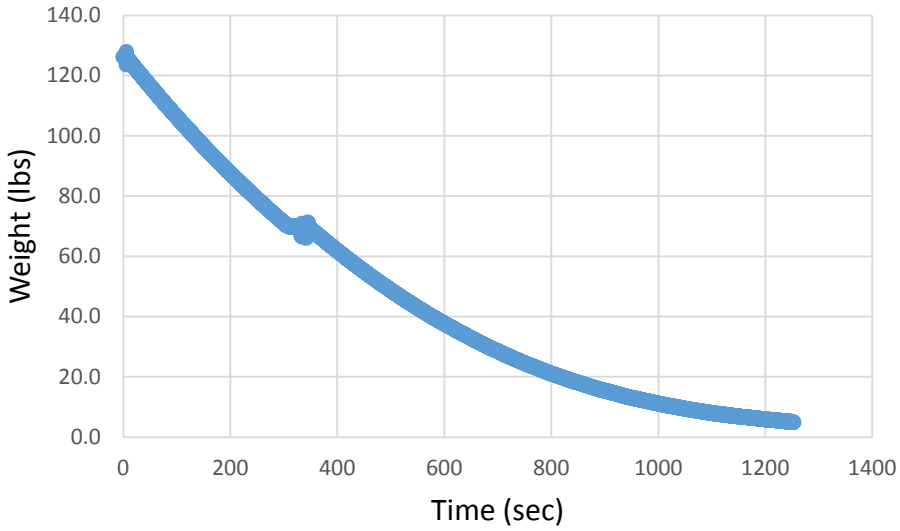

Figure A2.3. Batch 1 test 2 148.41 sec/qt viscosity weight data

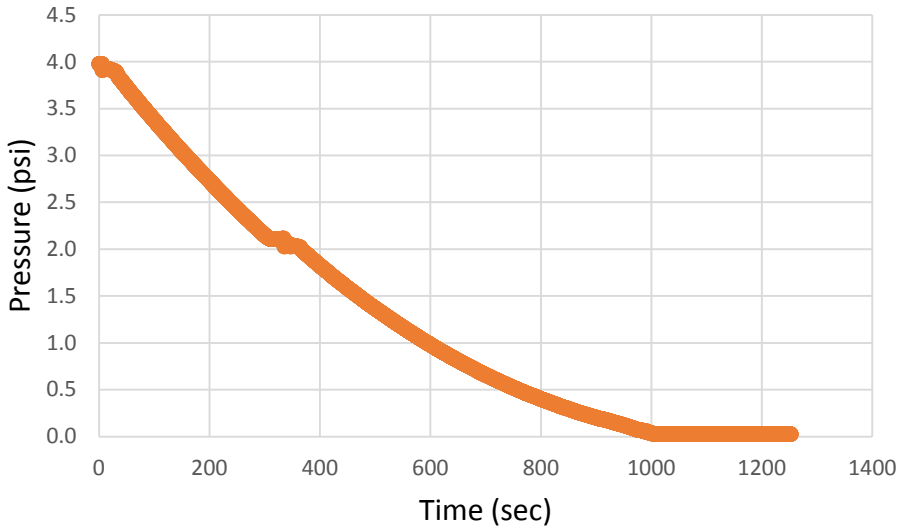

Figure A2.4. Batch 1 test 2 148.41 sec/qt viscosity pressure data

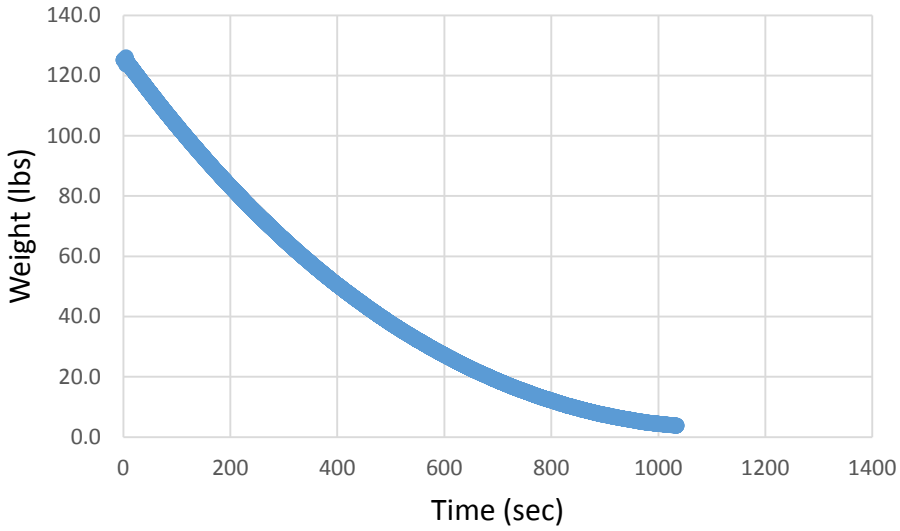

Figure A2.5. Batch 2 test 1 65.8 sec/qt viscosity weight data

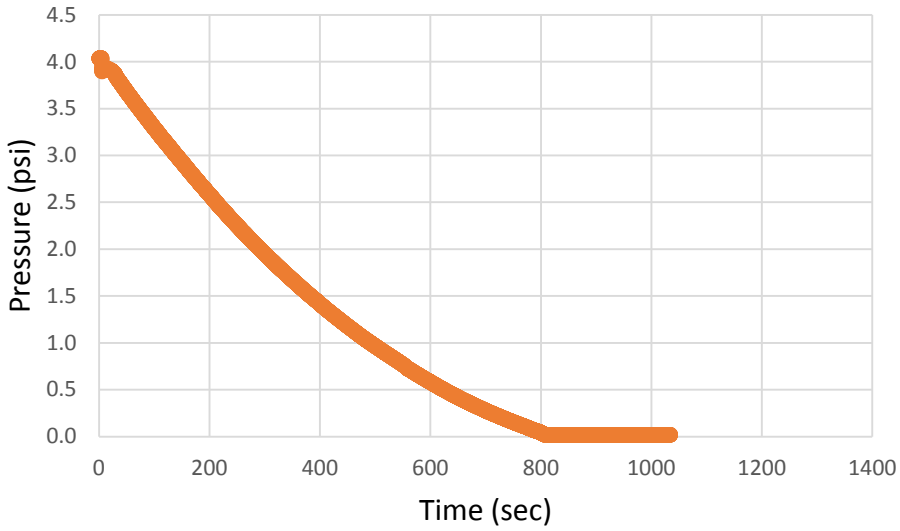

Figure A2.6. Batch 2 test 1 65.8 sec/qt viscosity pressure data

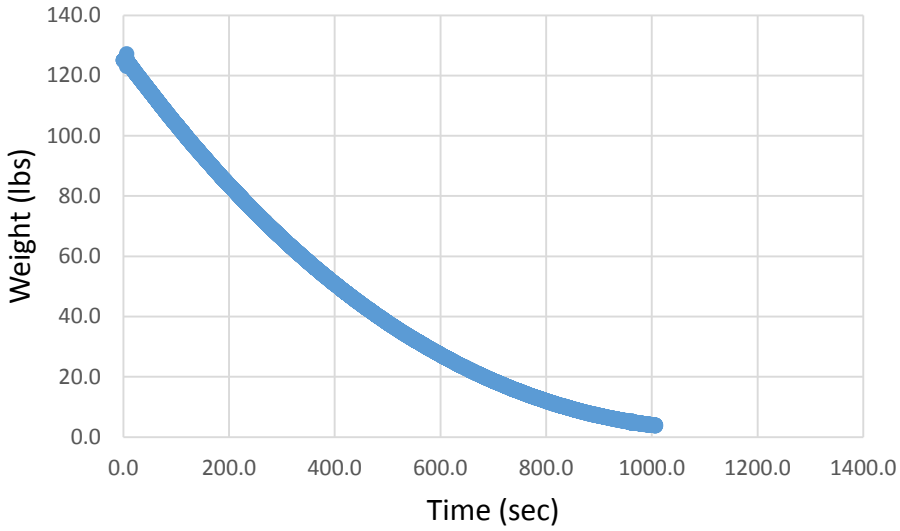

Figure A2.7. Batch 2 test 2 65.67 sec/qt viscosity weight data

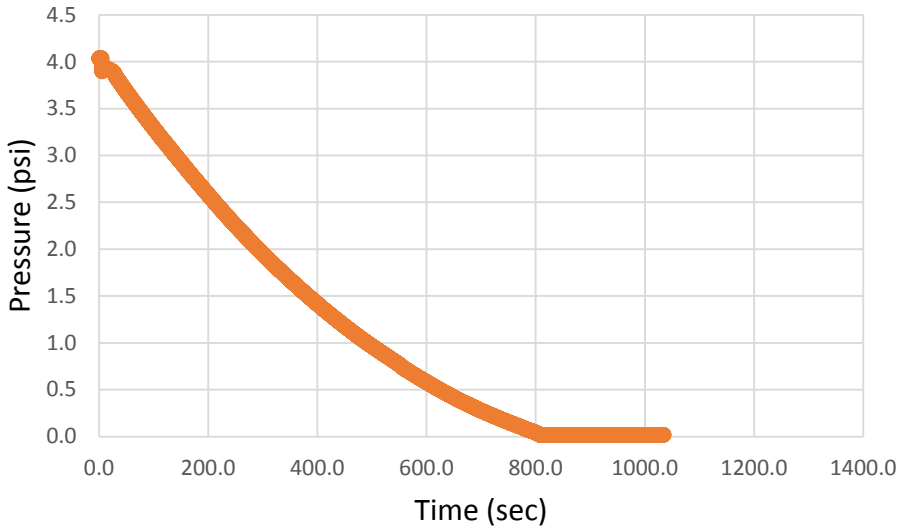

Figure A2.8. Batch 2 test 2 65.67 sec/qt viscosity pressure data

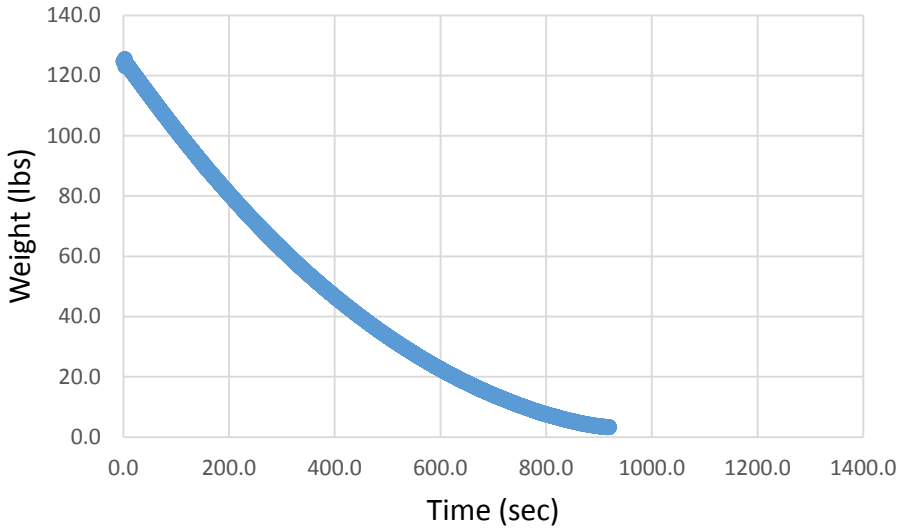

Figure A2.9. Batch 3 test 1 47.12 sec/qt viscosity weight data

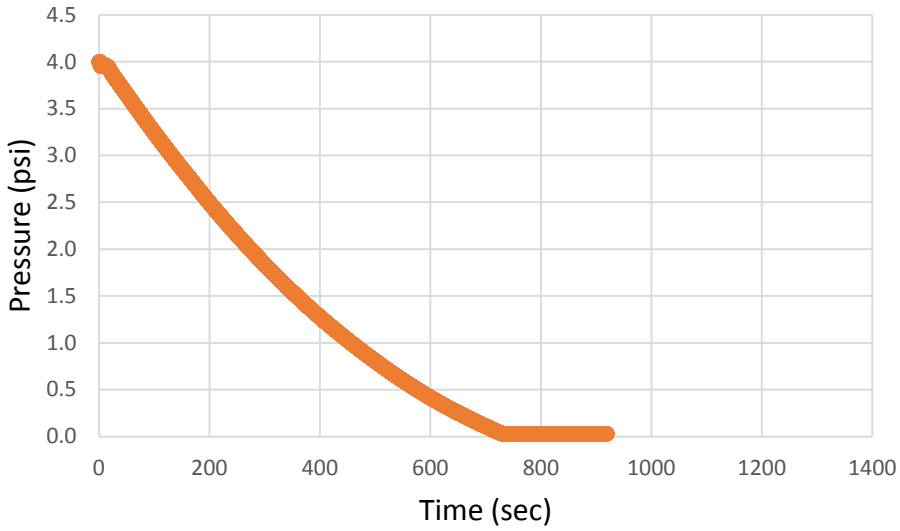

Figure A2.10. Batch 3 test 1 47.12 sec/qt viscosity pressure data

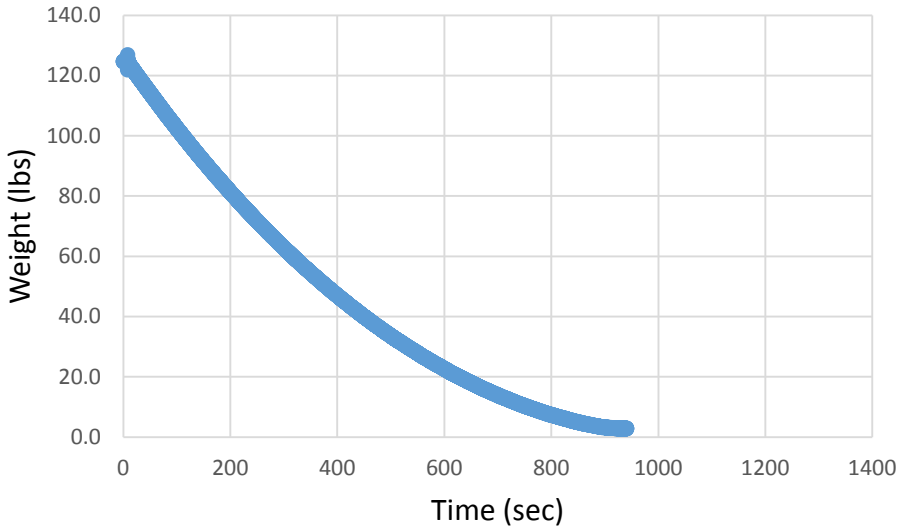

Figure A2.11. Batch 3 test 2 46.56 sec/qt viscosity weight data

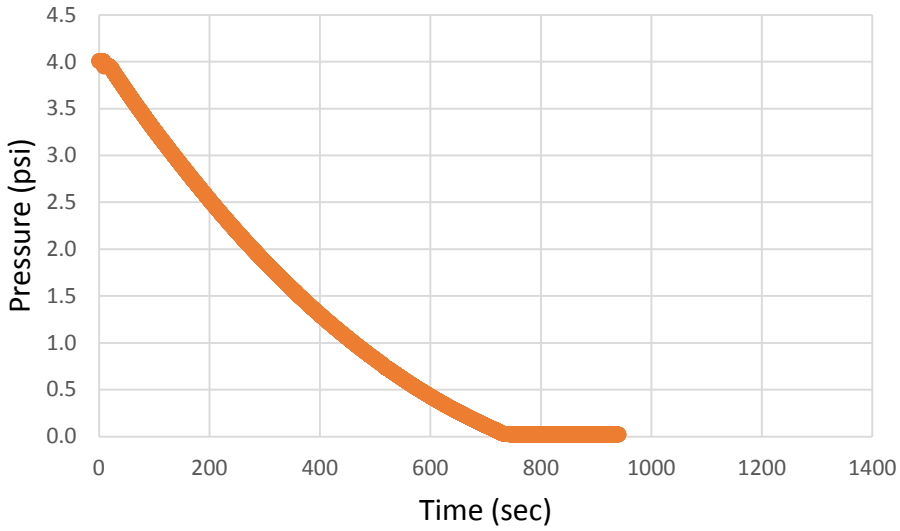

Figure A2.12. Batch 3 test 2 46.56 sec/qt viscosity pressure data

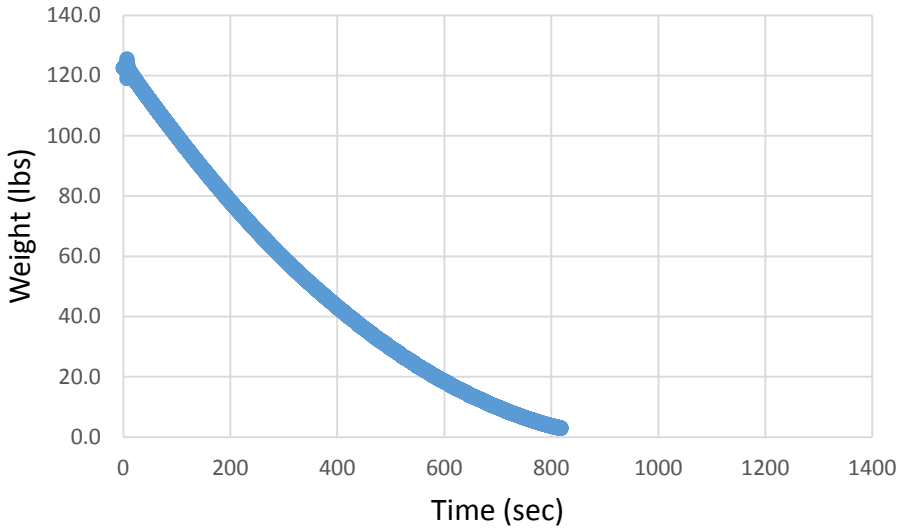

Figure A2.13. Batch 4 test 1 39.30 sec/qt viscosity weight data

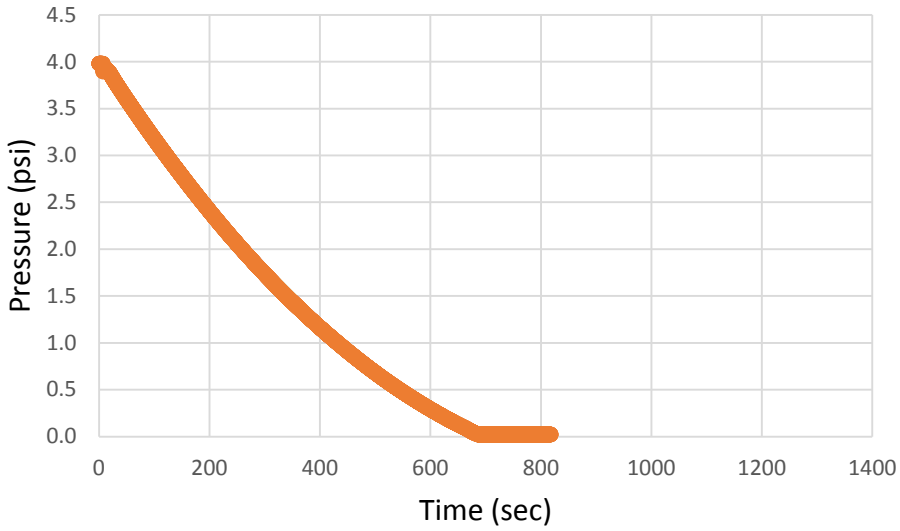

Figure A2.14. Batch 4 test 1 39.30 sec/qt viscosity pressure data

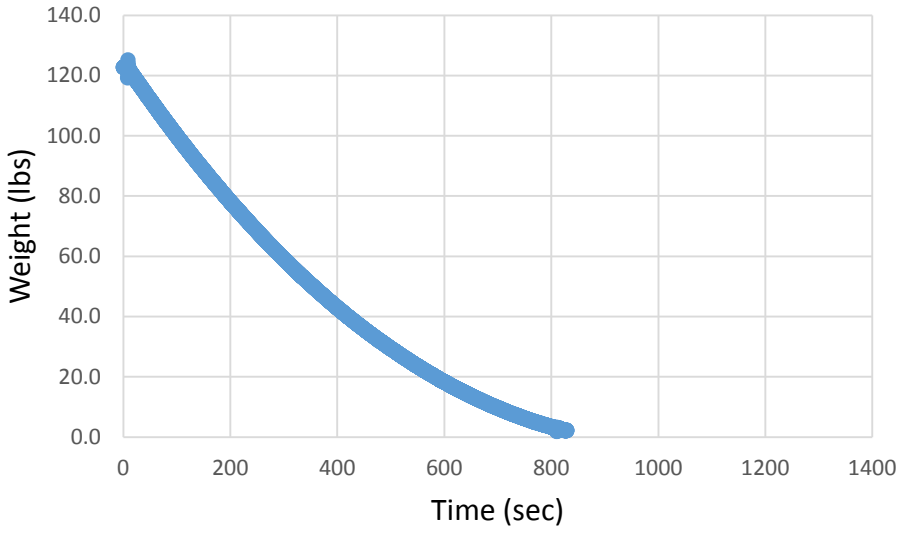

Figure A2.15. Batch 4 test 2 38.85 sec/qt viscosity weight data

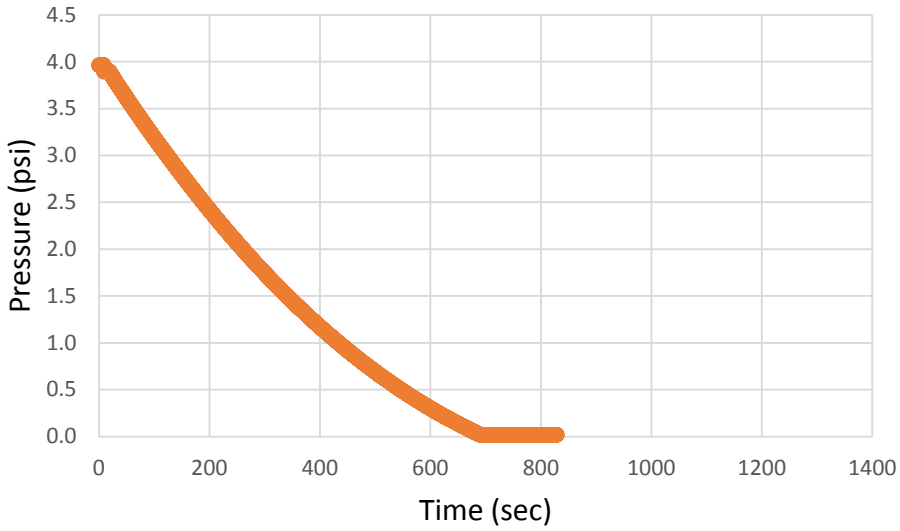

Figure A2.16. Batch 4 test 2 38.85 sec/qt viscosity pressure data

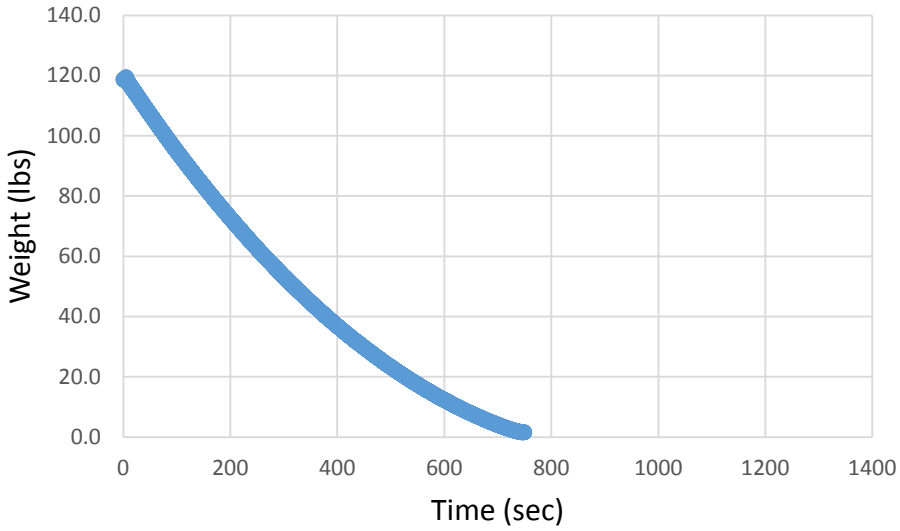

Figure A2.17. Batch 5 test 1 30.72 sec/qt viscosity weight data

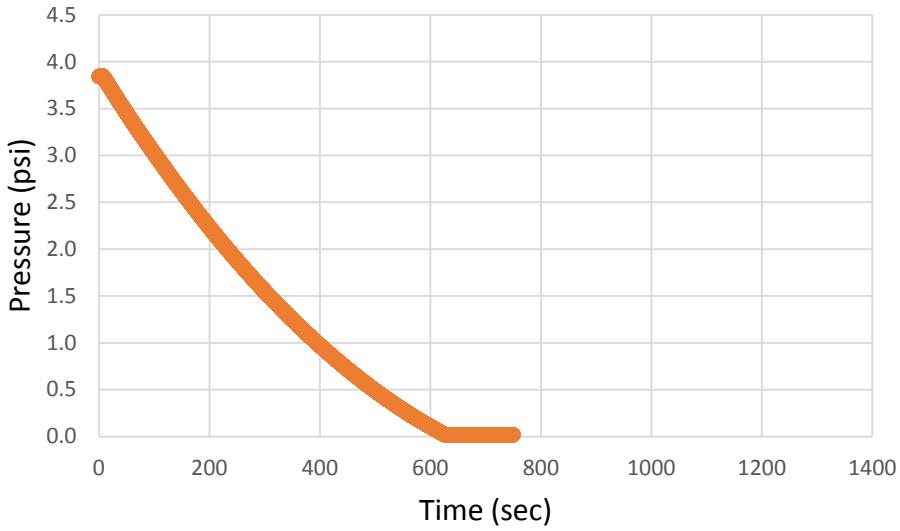

Figure A2.18. Batch 5 test 1 30.72 sec/qt viscosity pressure data

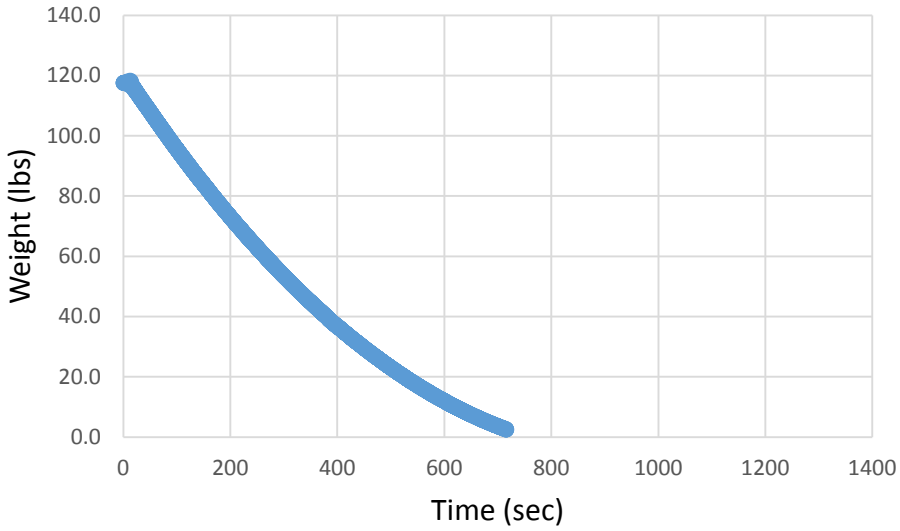

Figure A2.19. Batch 5 test 2 30.89 sec/qt viscosity weight data

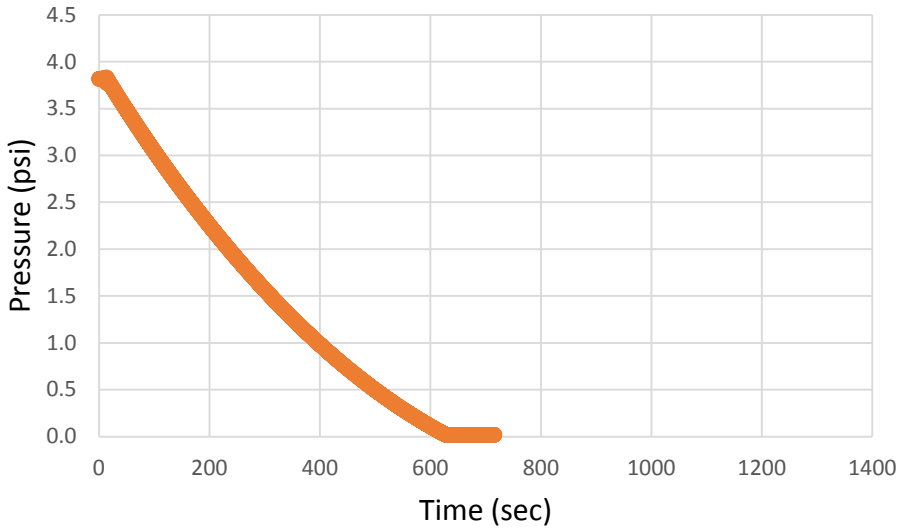

Figure A2.20. Batch 5 test 2 30.89 sec/qt viscosity pressure data

APPENDIX B1: SERIES ONE PRESSURE VS FLOW CURVES

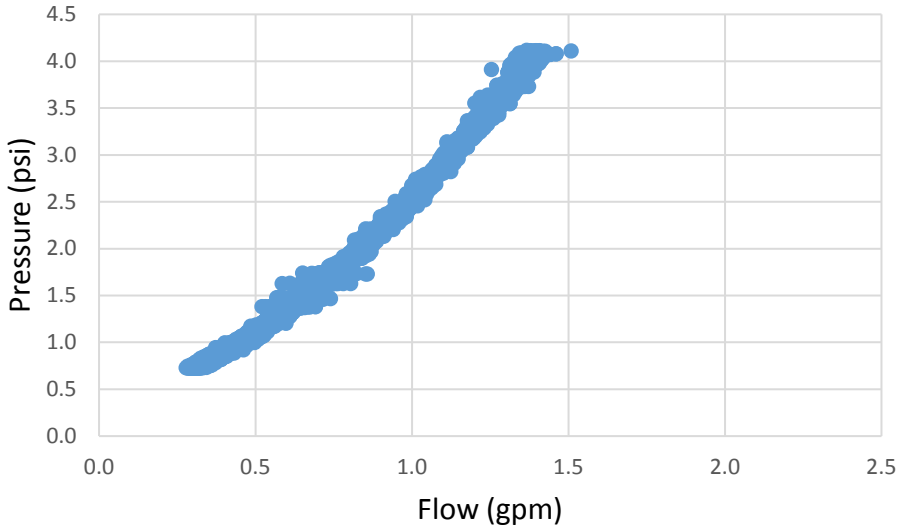

Figure B1.1. Batch 1 test 1 91.23 sec/qt pressure vs flow

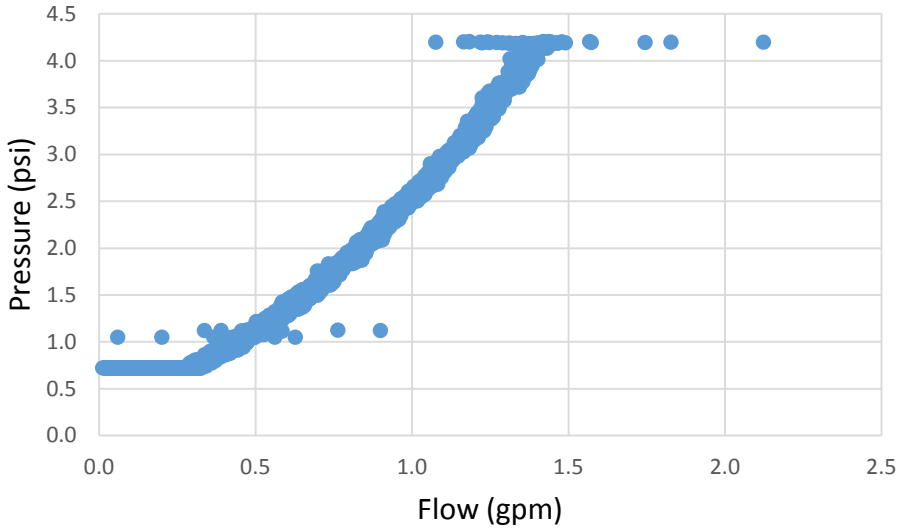

Figure B1.2. Batch 1 test 2 96.3 sec/qt pressure vs flow

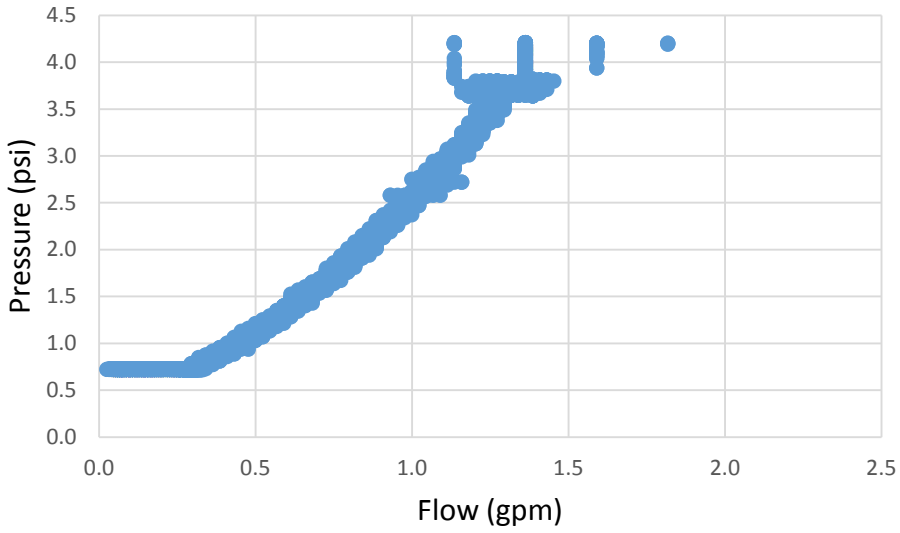

Figure B1.3. Batch 1 test 3 97.9 sec/qt pressure vs flow

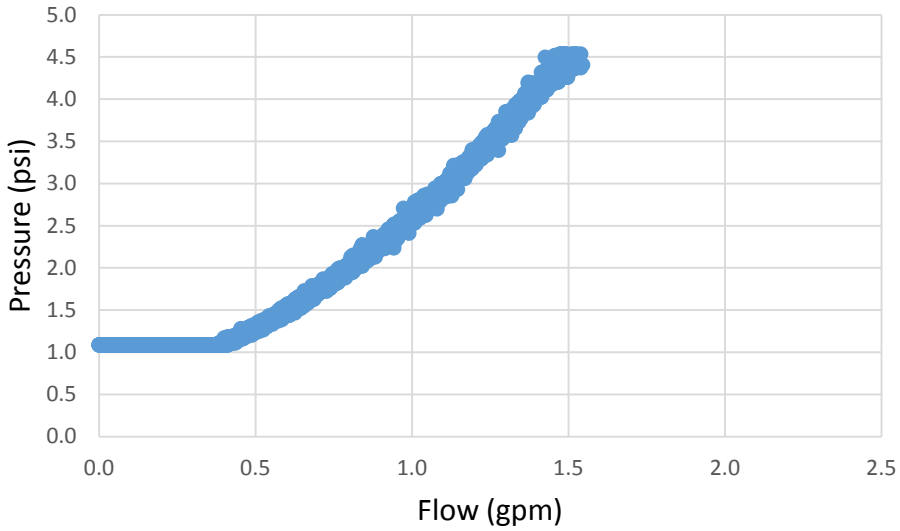

Figure B1.4. Batch 2 test 1 60.49 sec/qt pressure vs flow

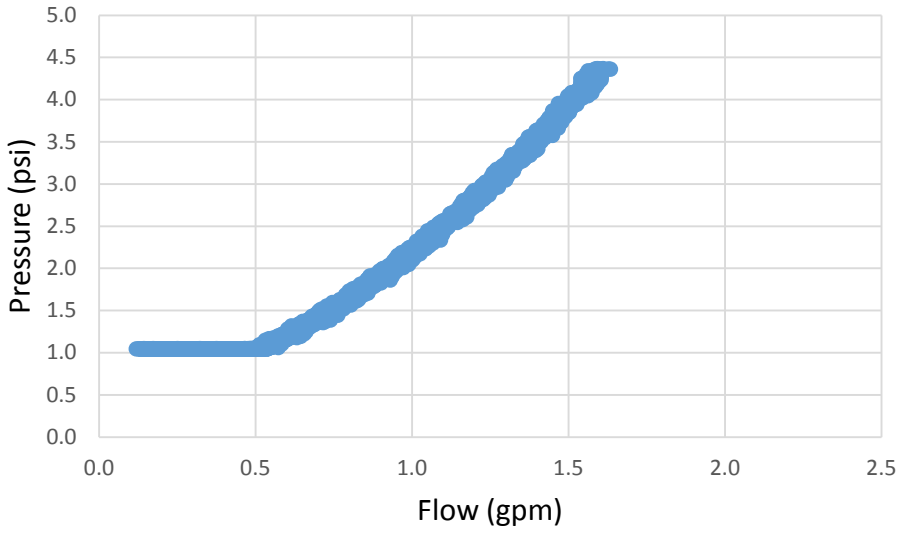

Figure B1.5. Batch 2 test 2 60.64 sec/qt pressure vs flow

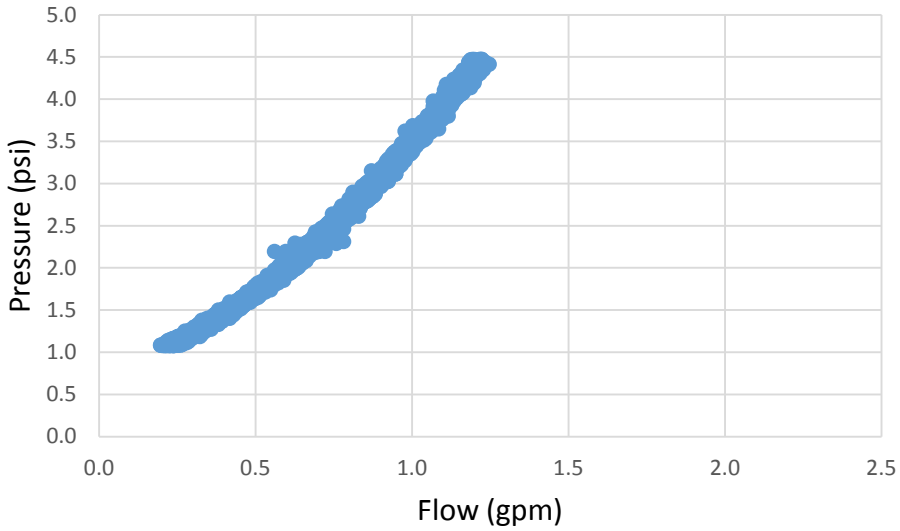

Figure B1.6. Batch 2 test 3 63.78 sec/qt pressure vs flow

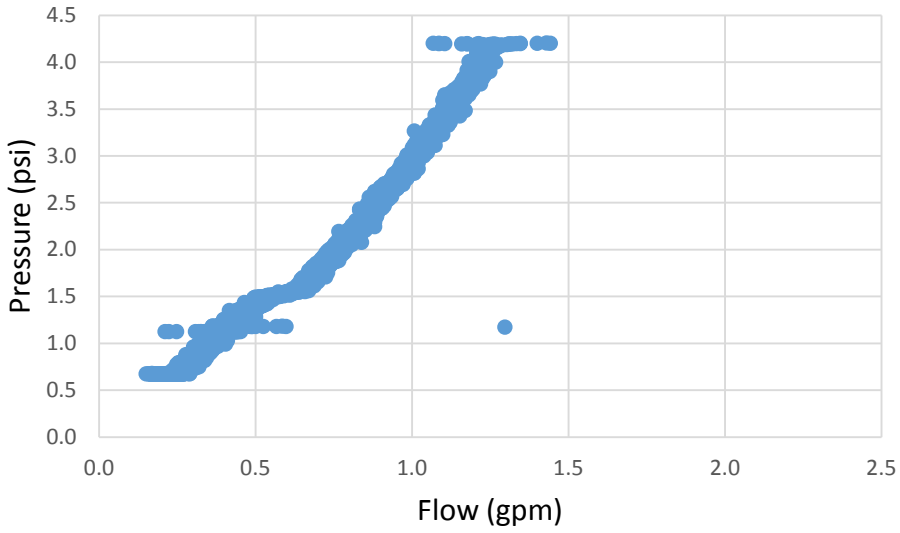

Figure B1.7. Batch 3 test 1 44.26 sec/qt pressure v flow

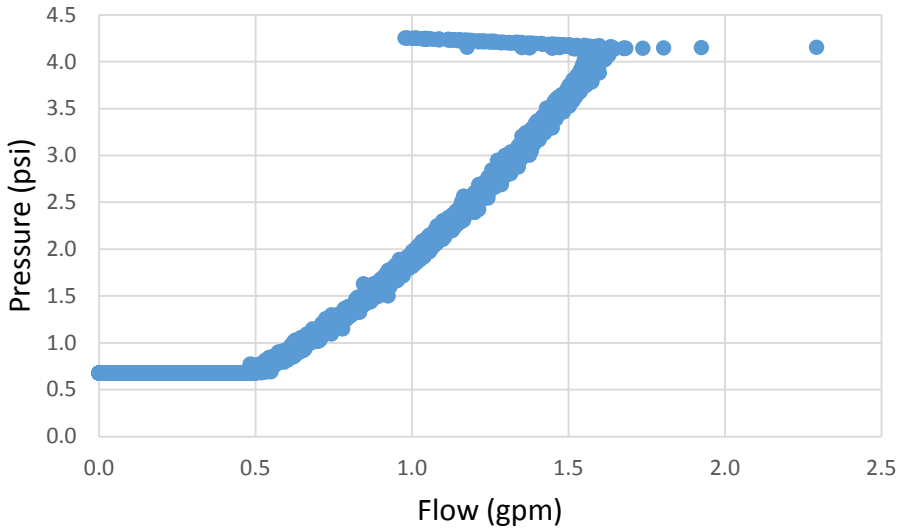

Figure B1.8. Batch 3 test 2 44.69 sec/qt pressure vs flow

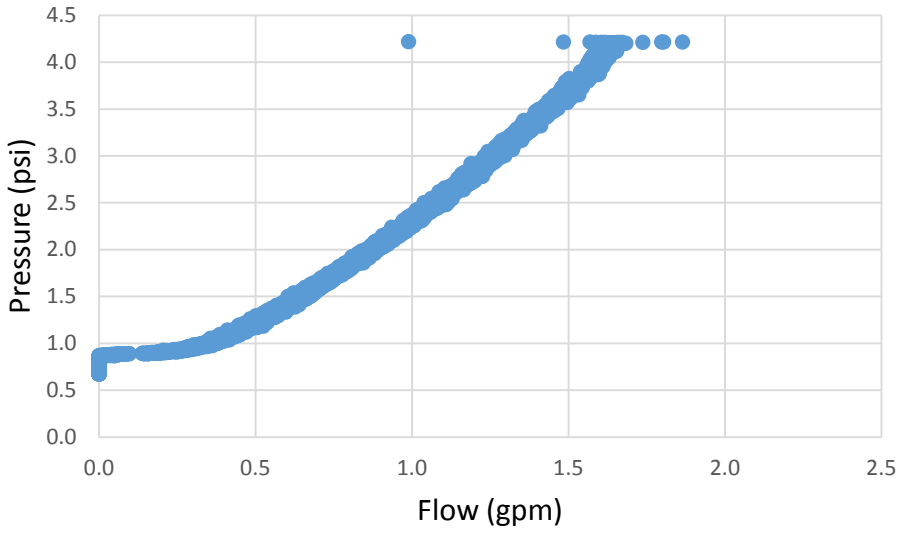

Figure B1.9. Batch 3 test 3 44.80 sec/qt pressure vs flow

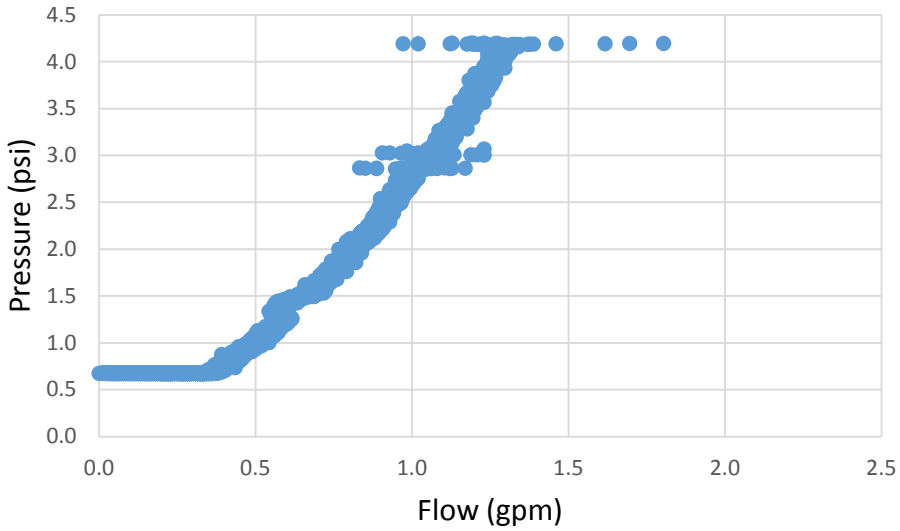

Figure B1.10. Batch 4 test 1 40.10 sec/qt pressure vs flow

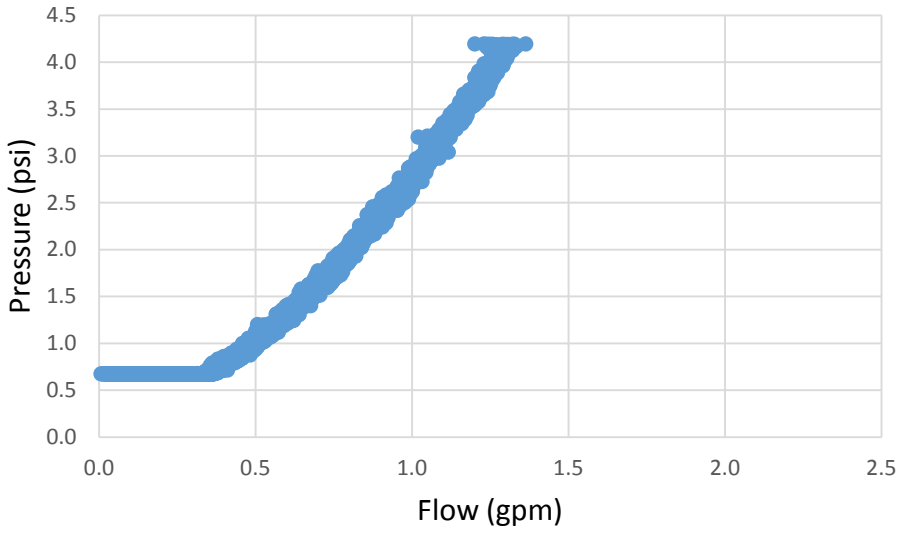

Figure B1.11. Batch 4 test 2 39.96 sec/qt pressure vs flow

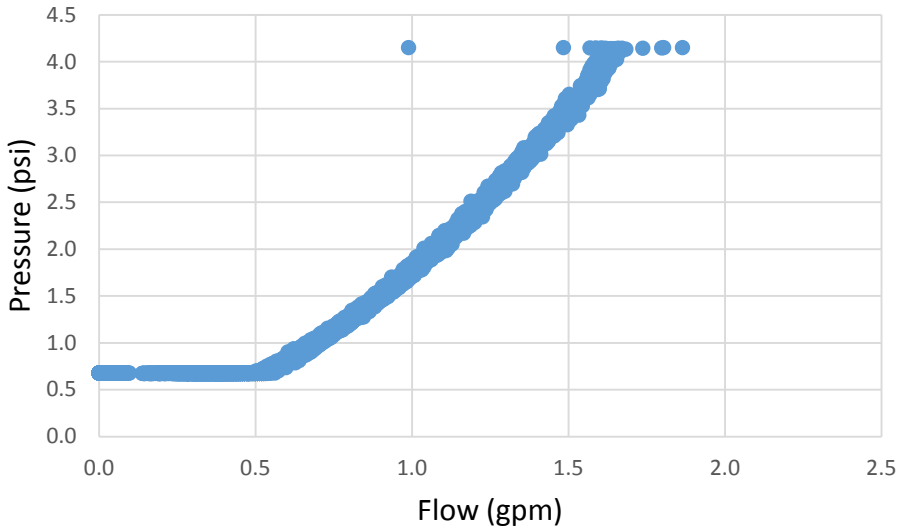

Figure B1.12. Batch 4 test 3 39.60 sec/qt pressure vs flow

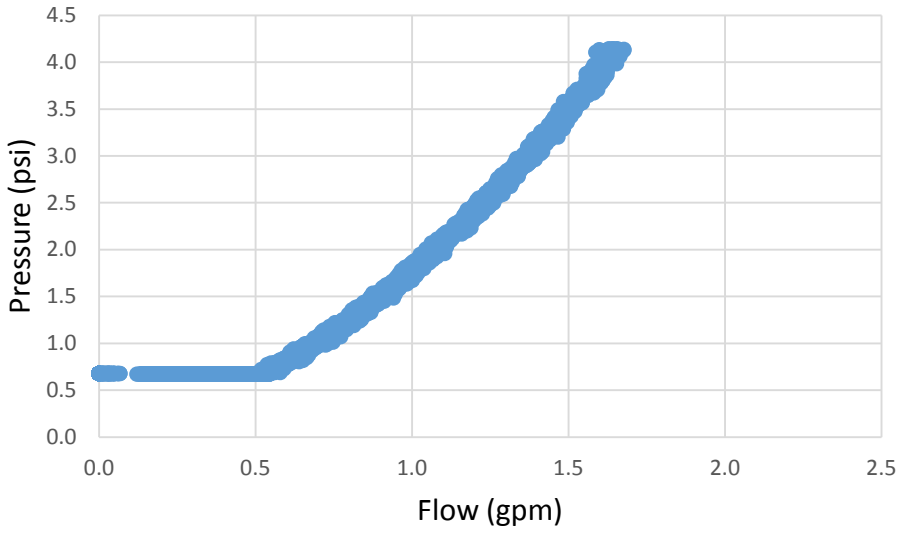

Figure B1.13. Batch 4 test 4 39.79 sec/qt pressure vs flow

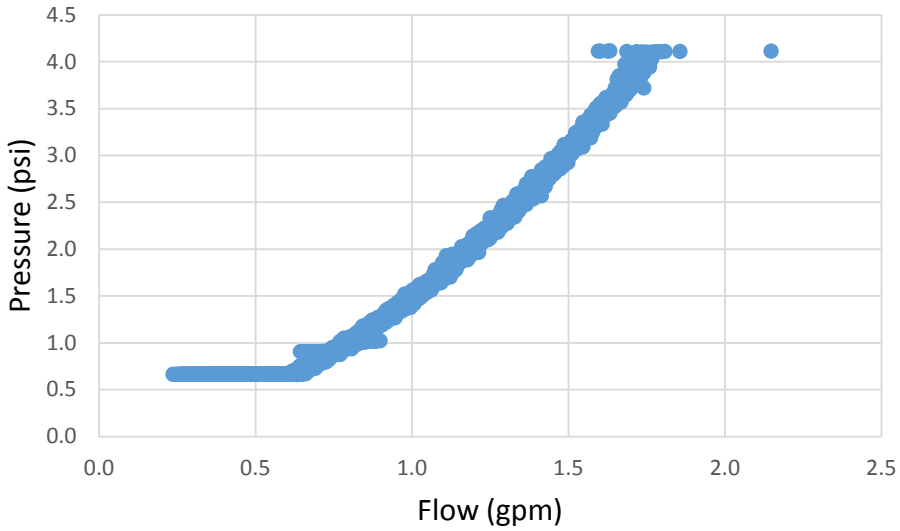

Figure B1.14. Batch 5 test 1 32.20 sec/qt pressure vs flow

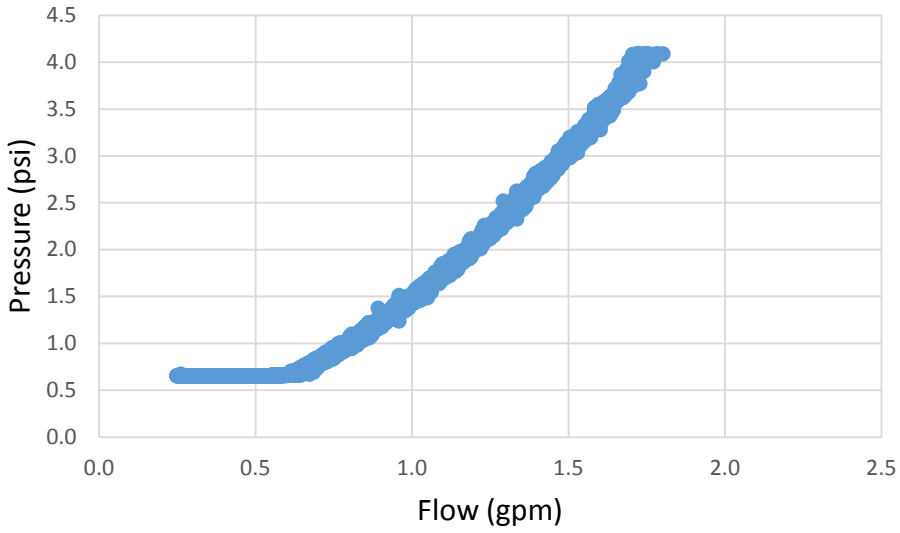

Figure B1.15. Batch 5 test 2 32.13 sec/qt pressure vs flow

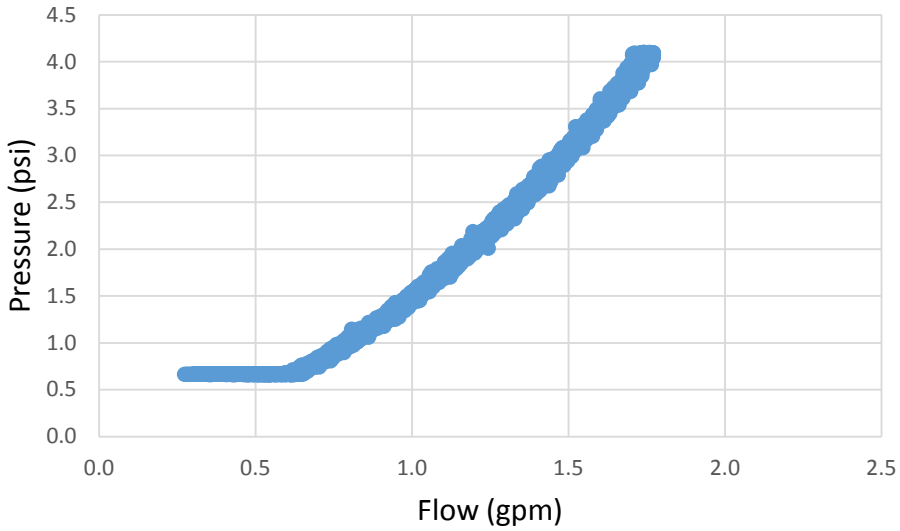

Figure B1.16. Batch 5 test 3 32.06 sec/qt pressure vs flow

APPENDIX B2: HIGH SAND-CONTENT PRESSURE VS FLOW CURVES

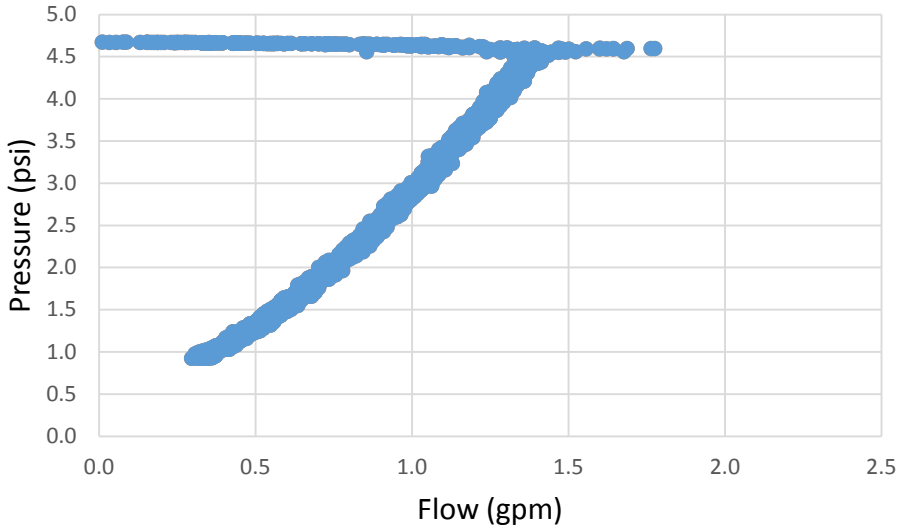

Figure B2.1. Batch 1 test 1 146.91 sec/qt pressure vs flow

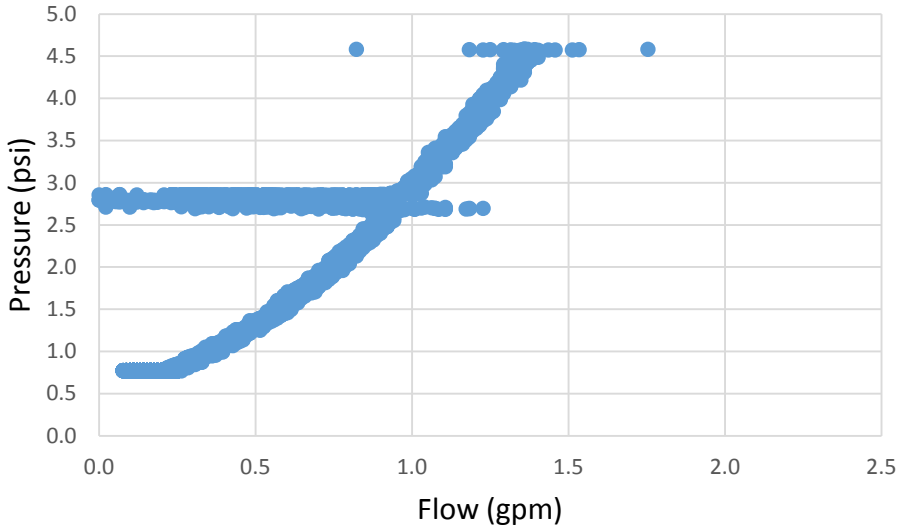

Figure B2.2. Batch 1 test 2 148.48 sec/qt pressure vs flow

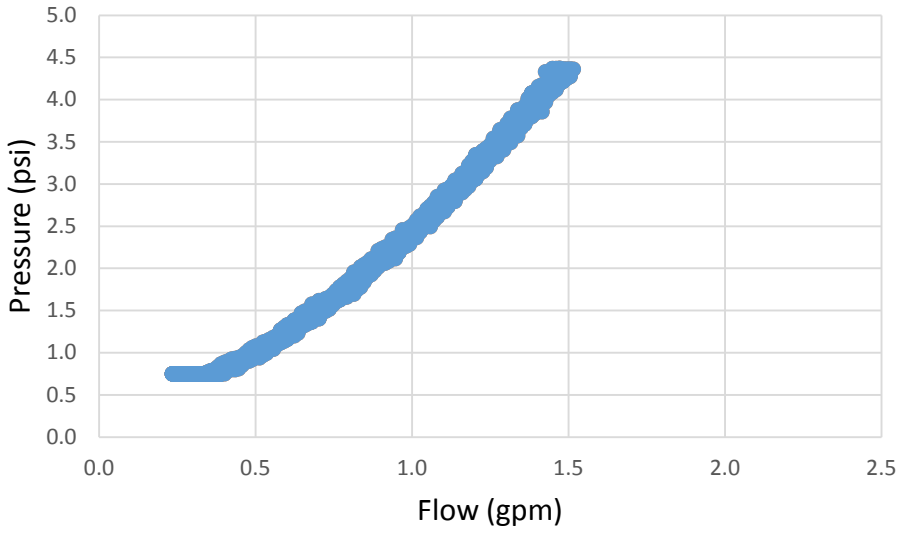

Figure B2.3. Batch 2 test 1 65.80 sec/qt pressure vs flow

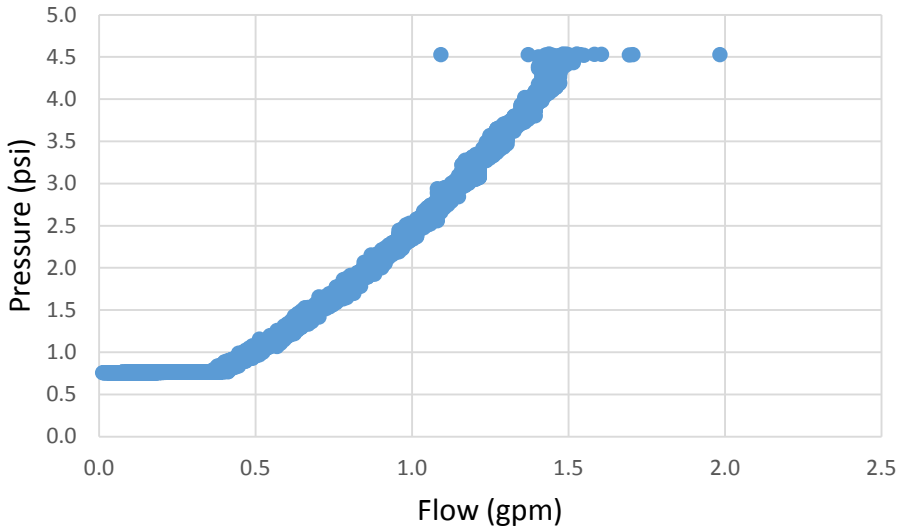

Figure B2.4. Batch 2 test 2 65.67 sec/qt pressure vs flow

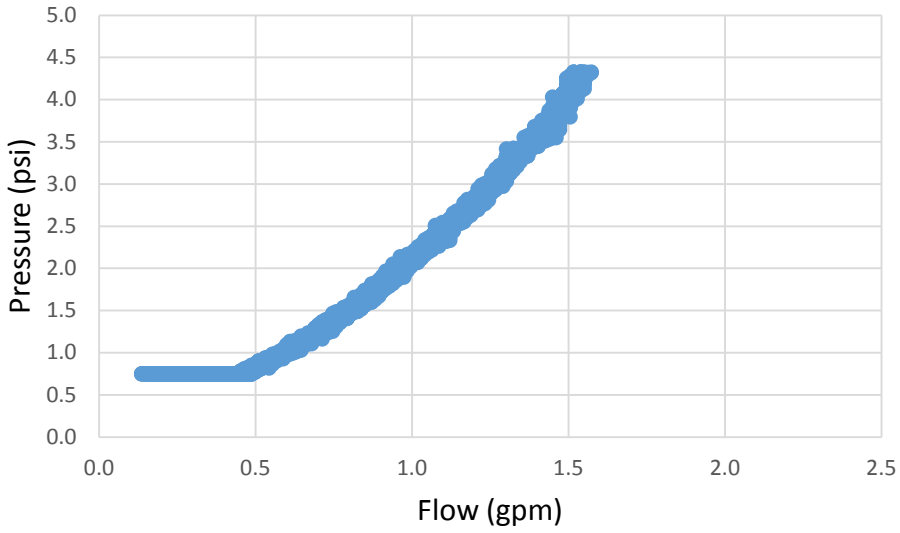

Figure B2.5. Batch 3 test 1 47.12 sec/qt pressure vs flow

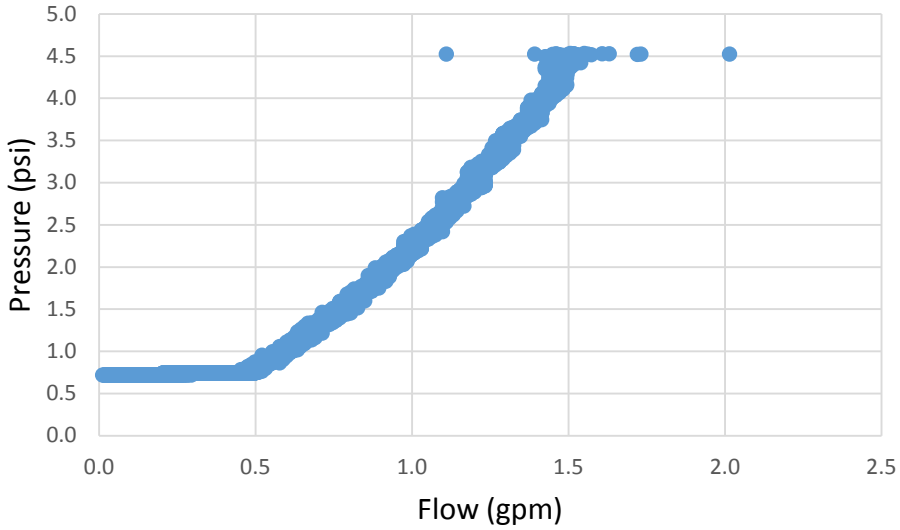

Figure B2.6. Batch 3 test 2 45.56 sec/qt pressure vs flow

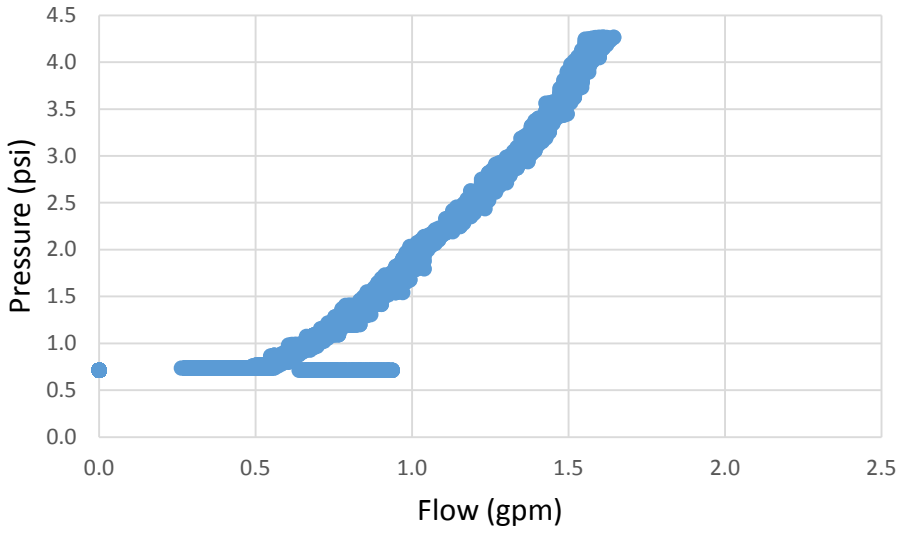

Figure B2.7. Batch 4 test 2 39.30 sec/qt pressure vs flow

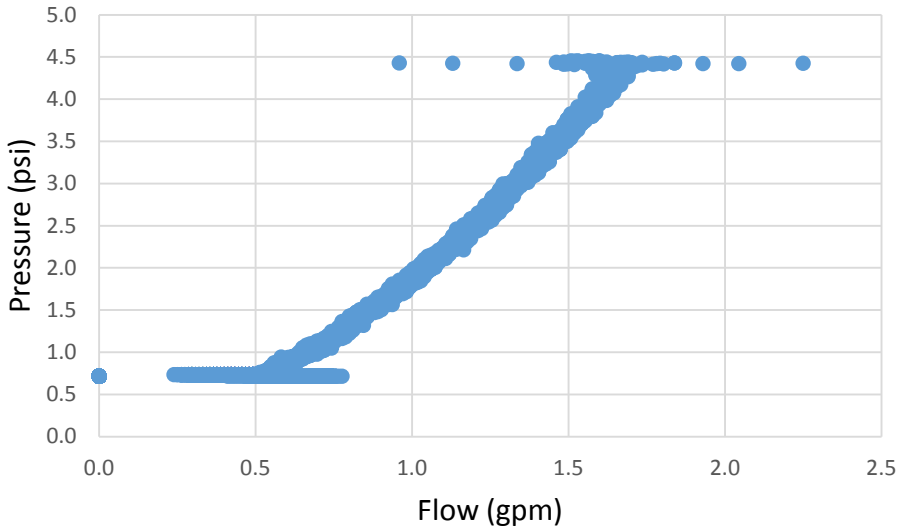

Figure B2.8. Batch 4 test 1 38.85 sec/qt pressure vs flow

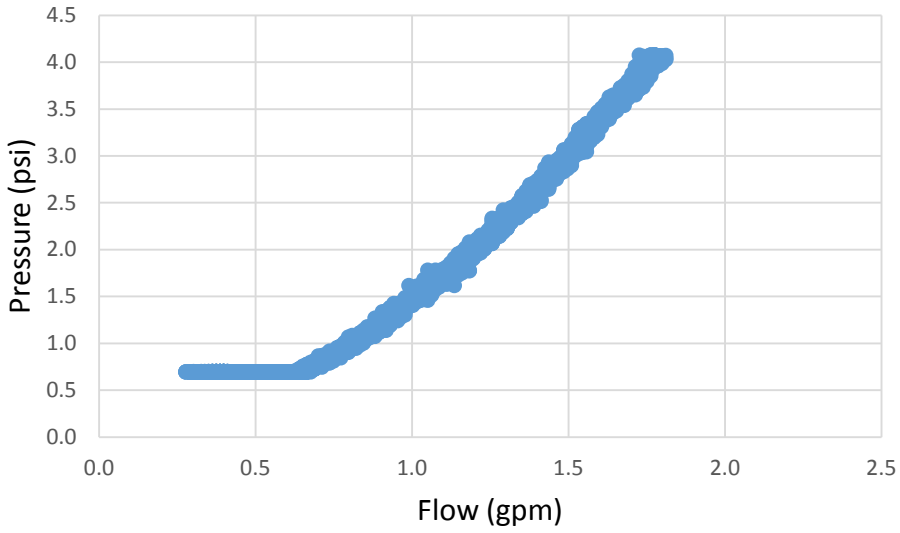

Figure B2.9. Batch 5 test 1 30.72 sec/qt pressure vs flow

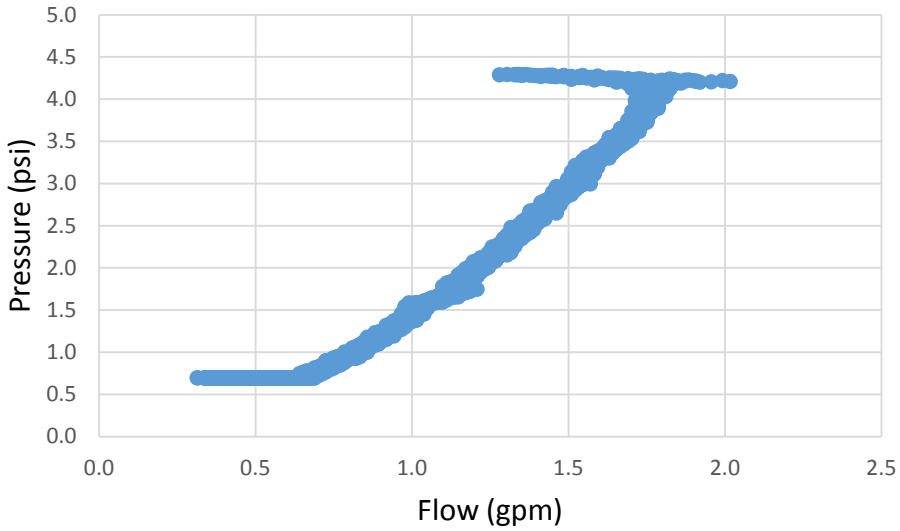

Figure B2.10. Batch 5 test 2 30.89 sec/qt pressure vs flow

APPENDIX C: 0.37 IN ID NOZZLE VISCOSITY DATA AND PRESSURE VS FLOW CURVES

Table C.1 Slurry viscosities

	Test #	Marsh (sec/qt)	Temp (°F)
Batch 1	001	127	77
	002	155.47	78
	003	146	78
	Average	143	77.7
5 gallons of slurry removed, 5 gallons of water added			
Batch 2	004	59.94	79
	005	58.78	79
	006	58.53	80
	Average	59	79.3
5 gallons of slurry removed, 5 gallons of water added			
Batch 3	007	46.72	80
	008	45.62	80
	009	45.65	80
	Average	46	80.0
5 gallons of slurry removed, 5 gallons of water added			
Batch 4	010	40.5	80
	011	39.72	80
	012	39.66	80
	Average	40	80.0
5 gallons of slurry removed, 5 gallons of water added			
Batch 4	010	40.5	80
	011	39.72	80
	012	39.66	80
	Average	40	80.0
15 gallons of slurry removed, 15 gallons of water added			
Batch 5	013	31.09	80
	014	31.12	79
	015	31.6	79
	Average	31	79.3

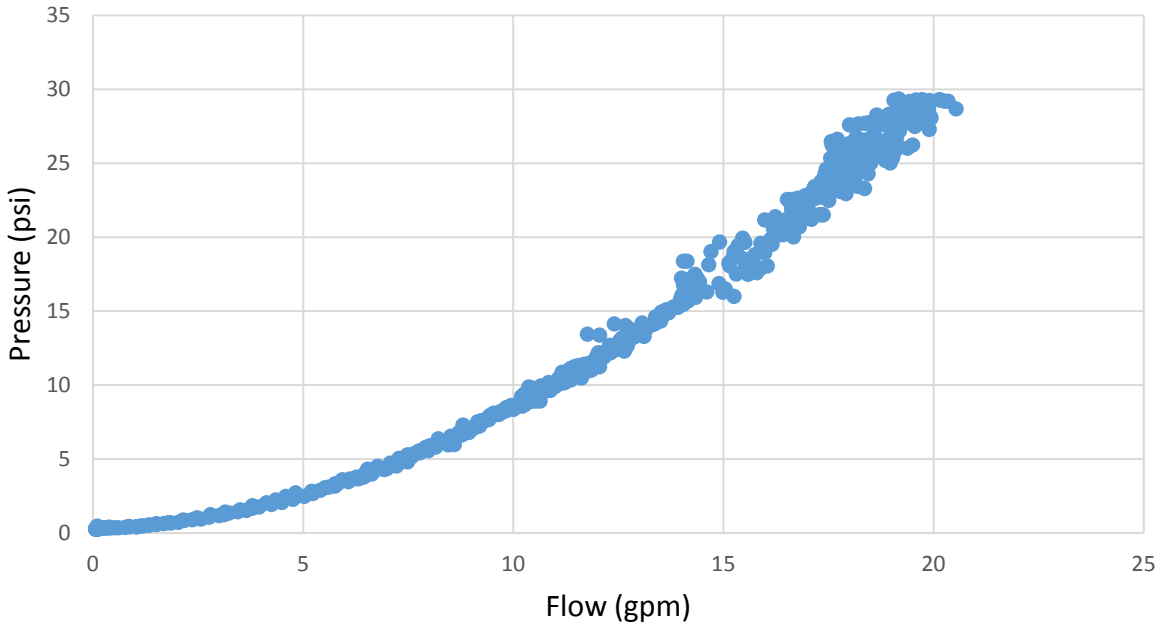

Figure C.1. Batch 1 test 1 127 sec/qt pressure vs flow

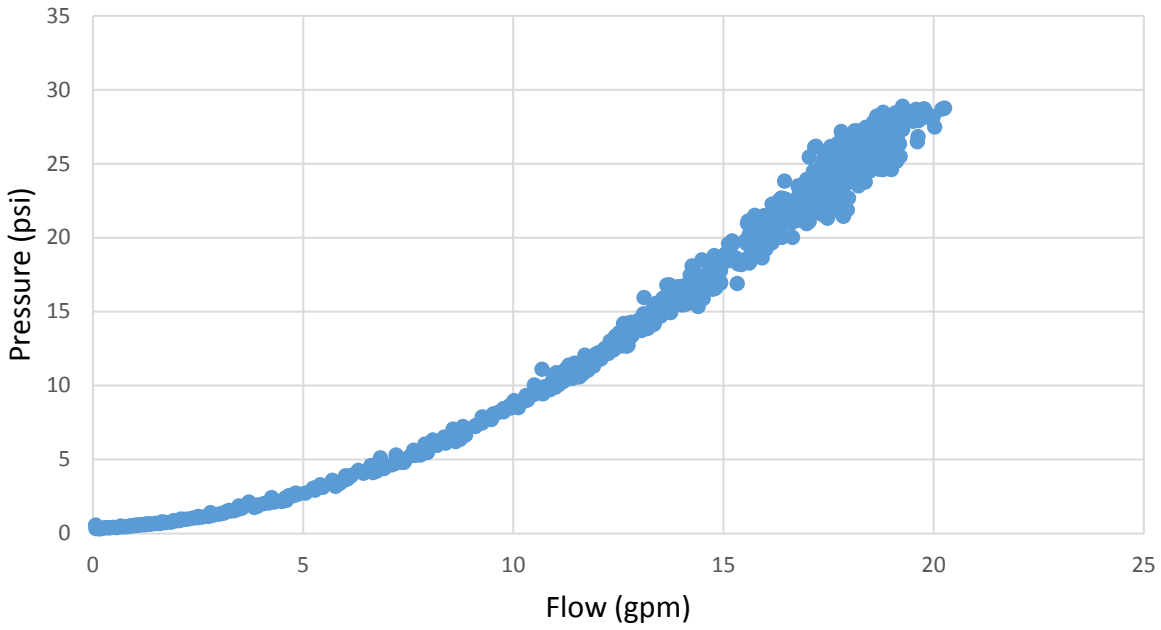

Figure C.2. Batch 1 test 2 155 sec/qt pressure vs flow

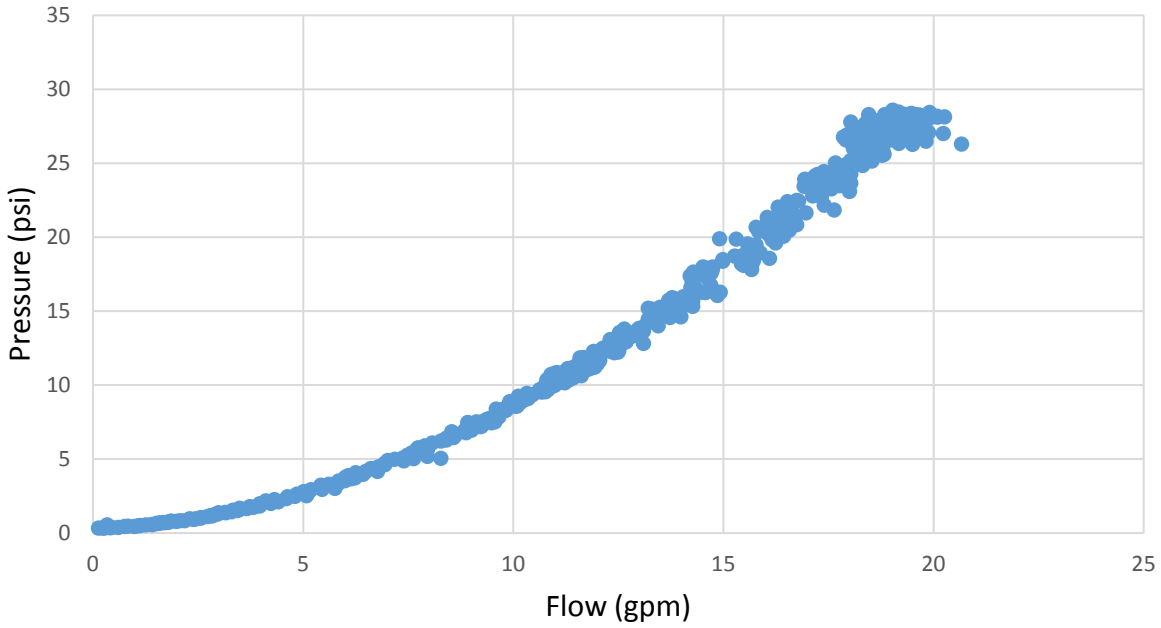

Figure C.3. Batch 1 test 3 146 sec/qt pressure vs flow

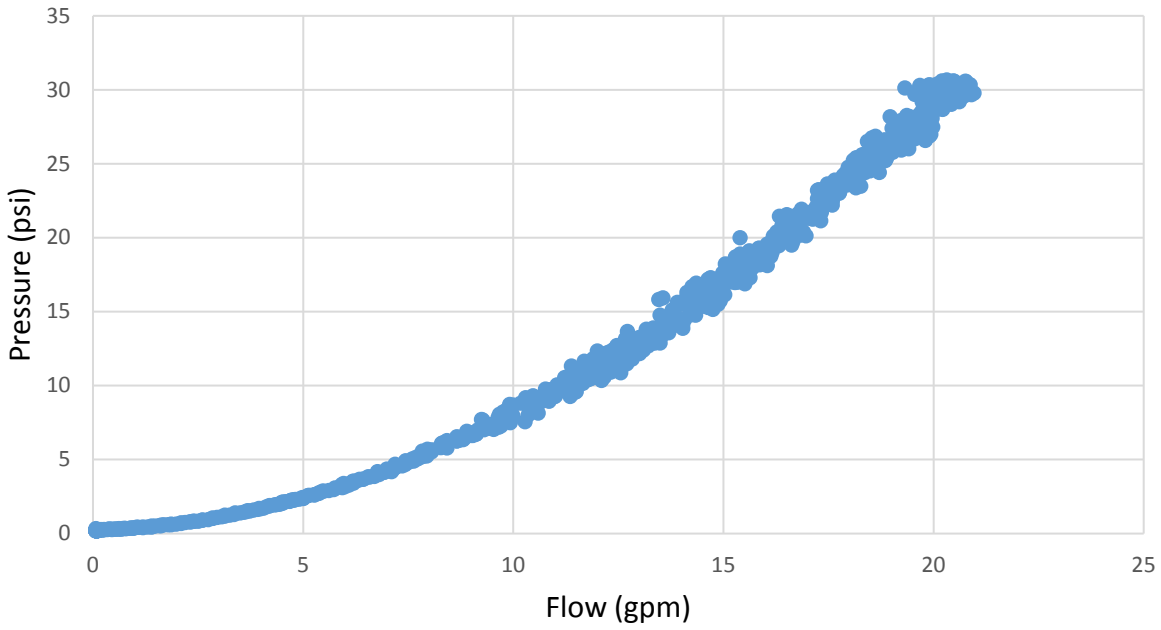

Figure C.4. Batch 2 test 1 60 sec/qt pressure vs flow

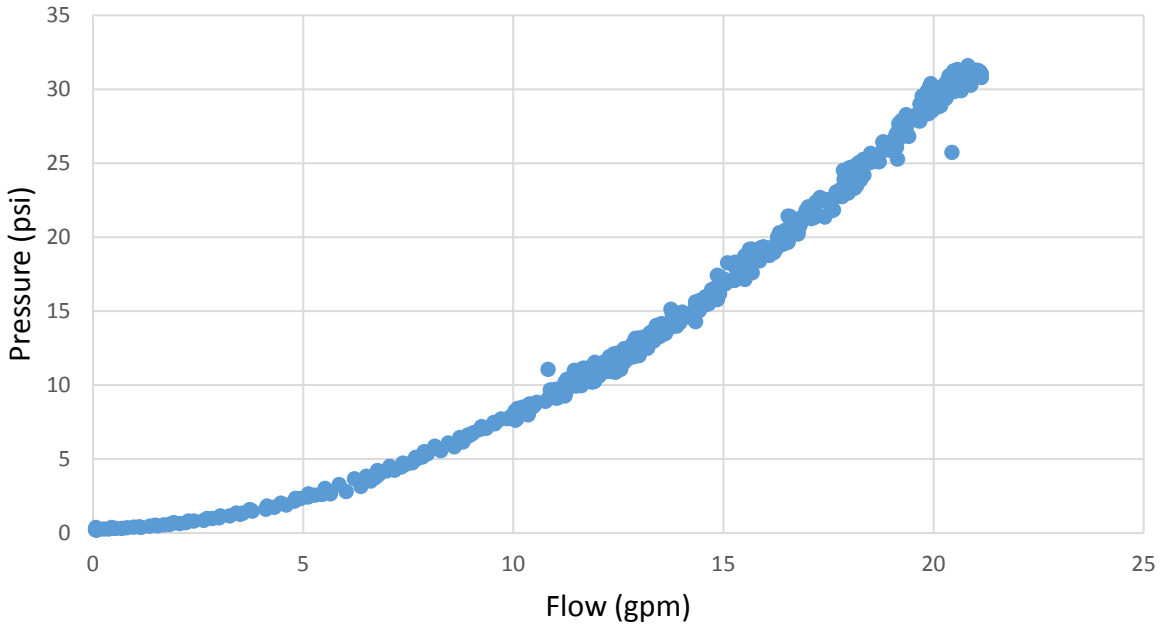

Figure C.5. Batch 2 test 2 59 sec/qt pressure vs flow

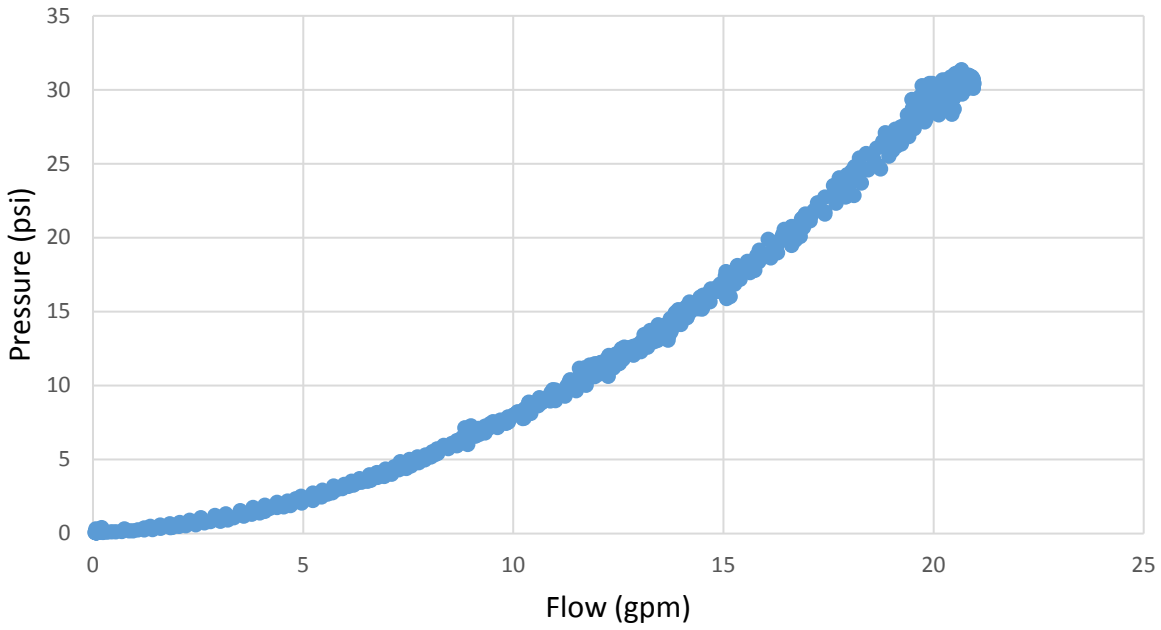

Figure C.6. Batch 2 test 3 59 sec/qt pressure vs flow

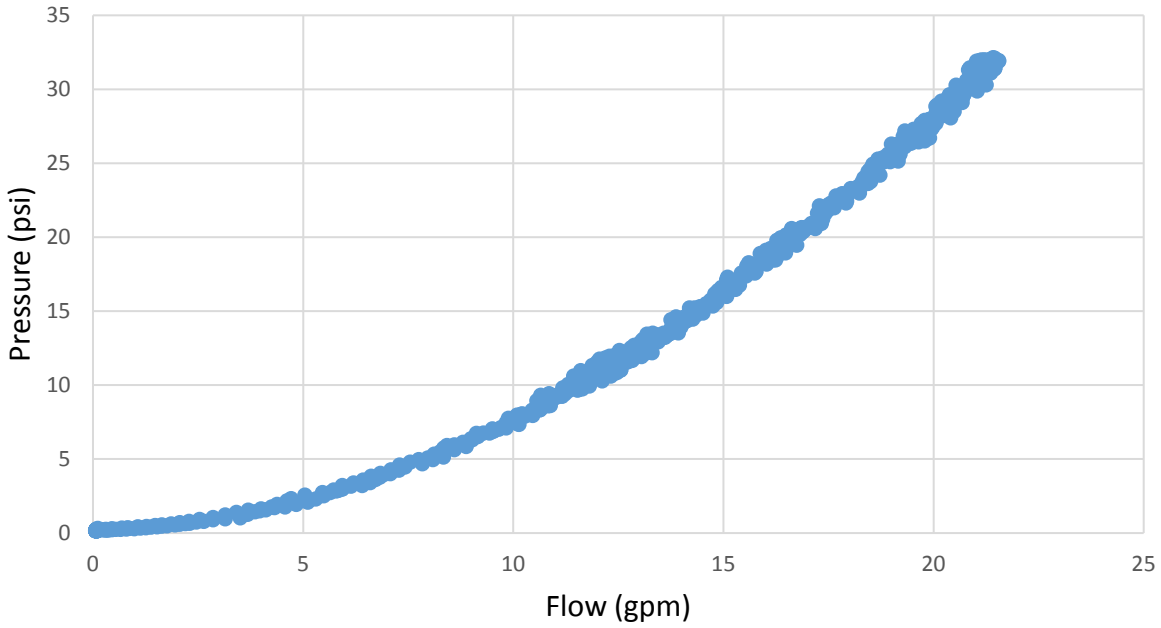

Figure C.7. Batch 3 test 1 47 sec/qt pressure vs flow

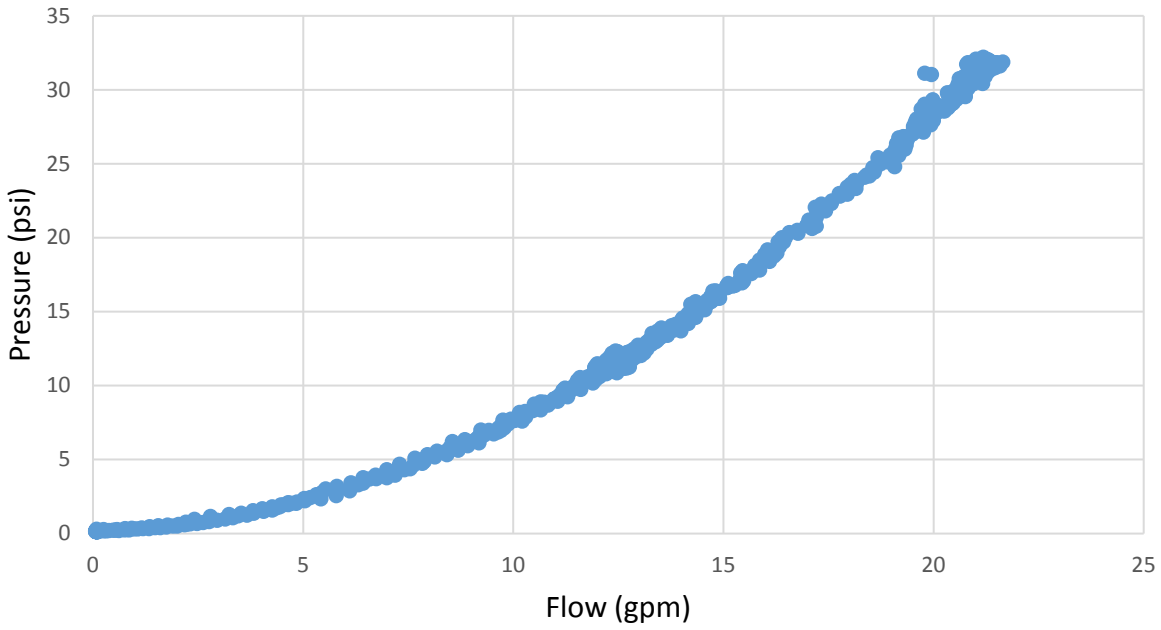

Figure C.8. Batch 3 test 2 46 sec/qt pressure vs flow

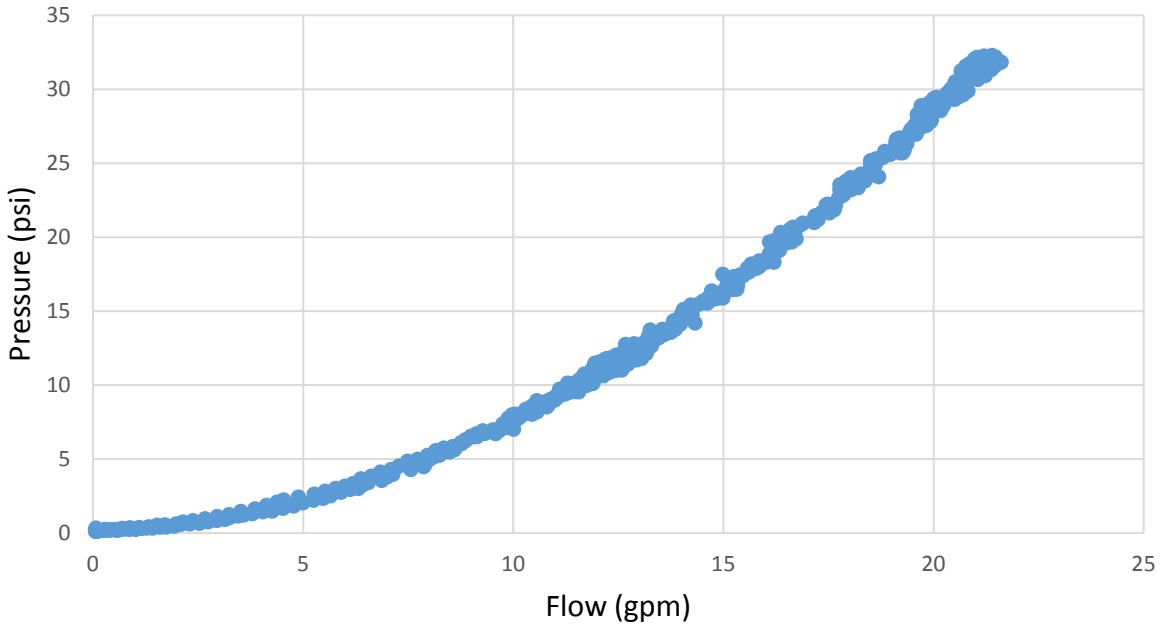

Figure C.9. Batch 3 test 3 46 sec/qt pressure vs flow

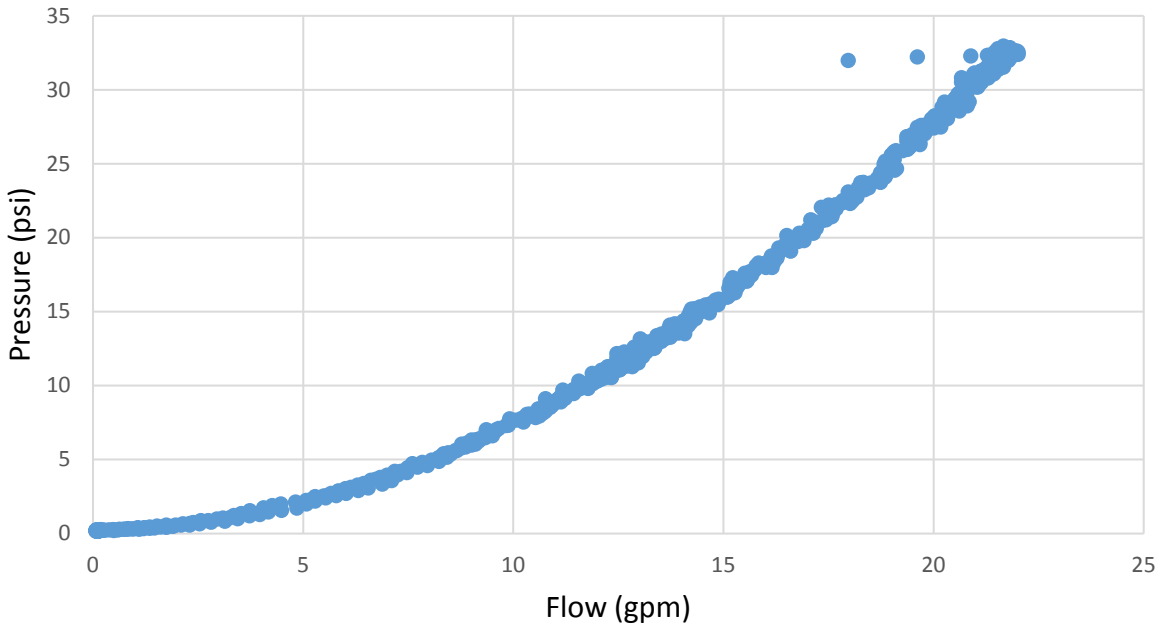

Figure C.10. Batch 4 test 1 41 sec/qt pressure vs flow

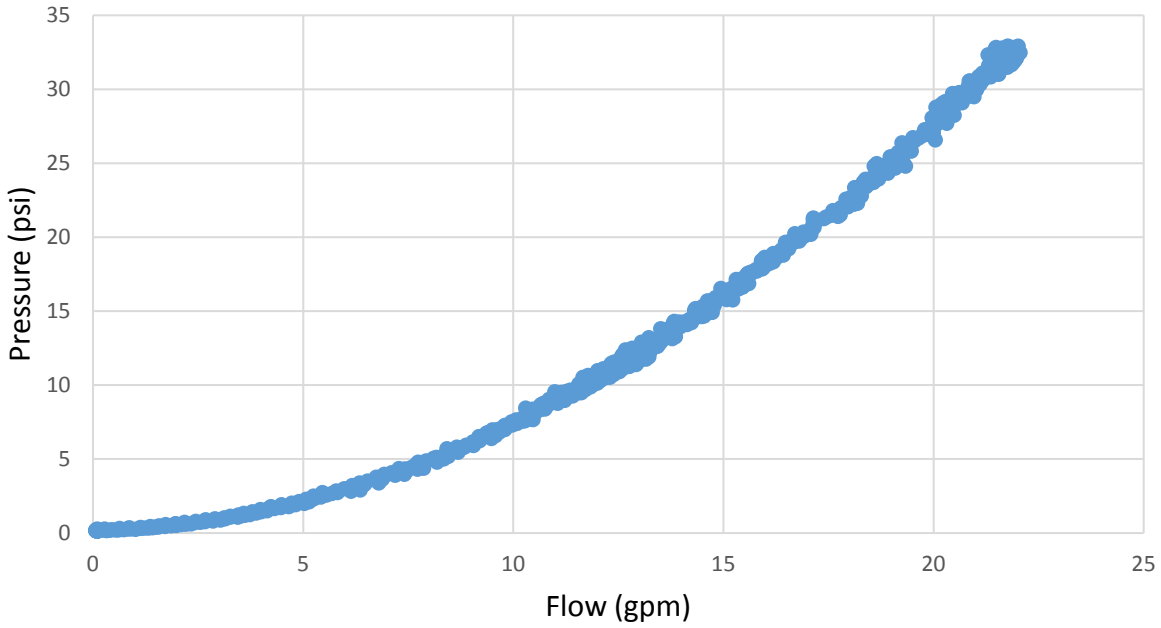

Figure C.11. Batch 4 test 2 40 sec/qt pressure vs flow

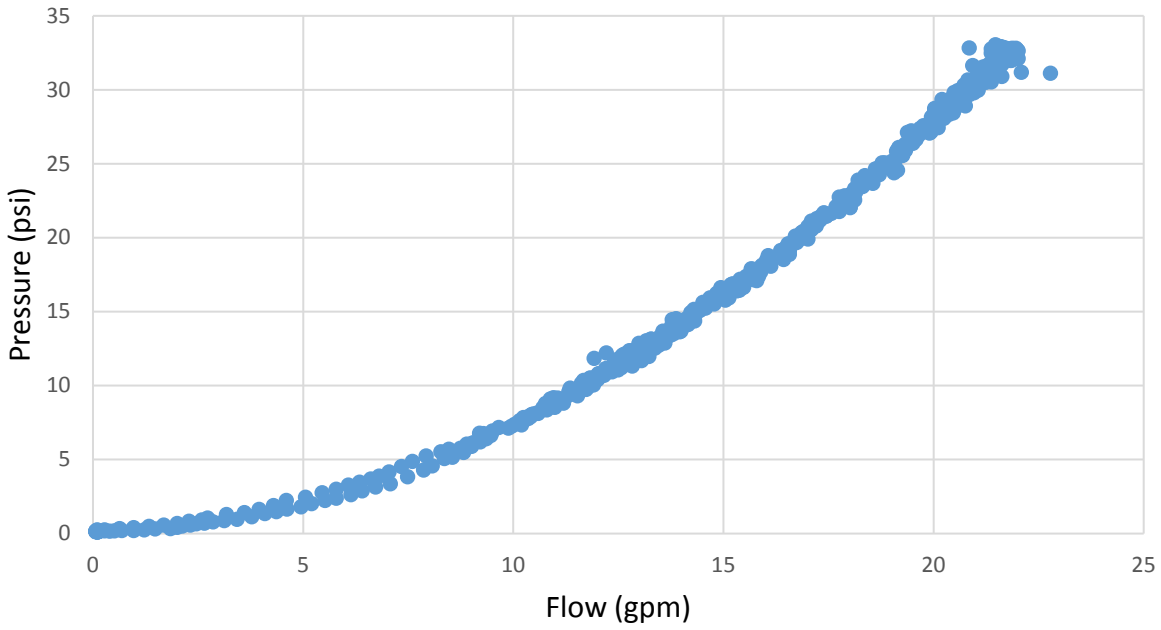

Figure C.12. Batch 4 test 3 40 sec/qt pressure vs flow

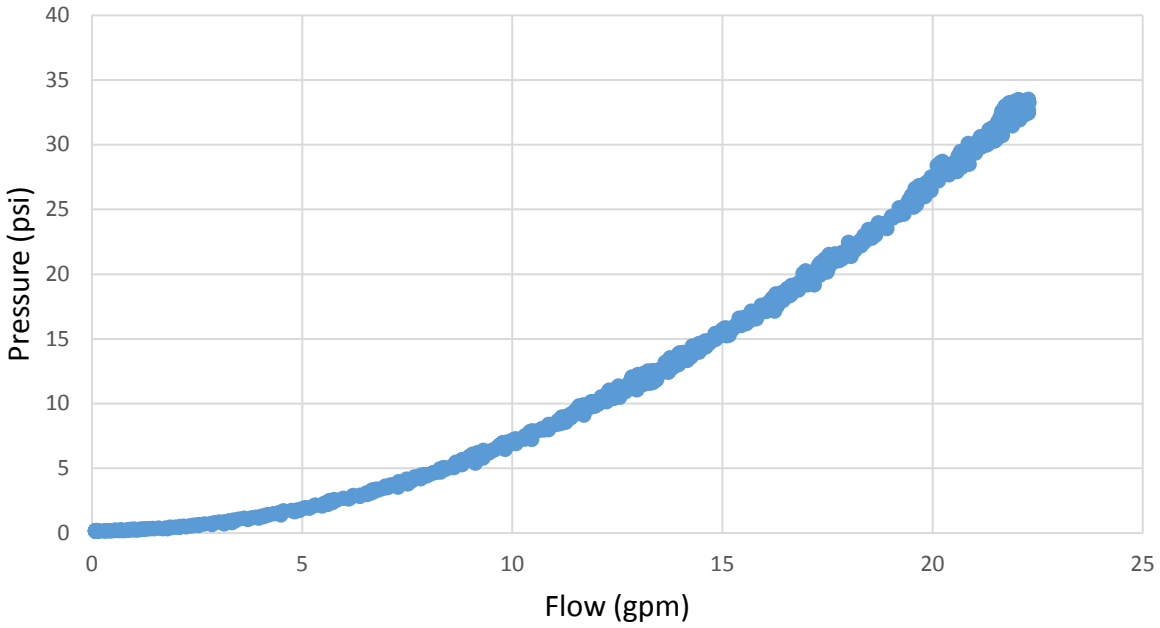

Figure C.13. Batch 5 test 1 31 sec/qt pressure vs flow

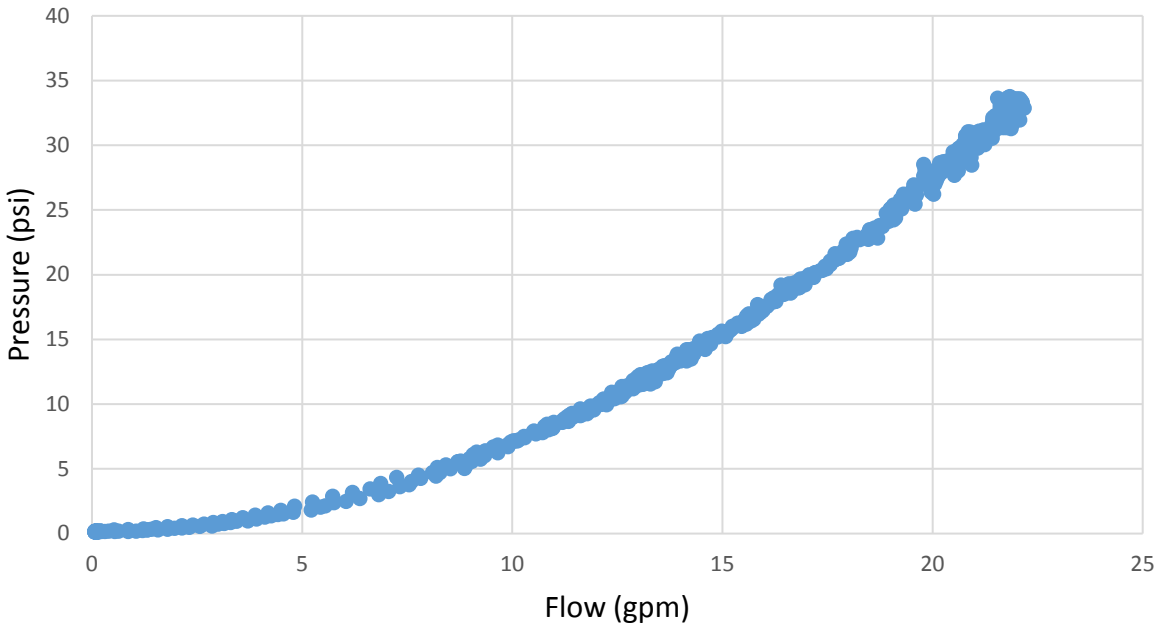

Figure C.14. Batch 5 test 2 31 sec/qt pressure vs flow

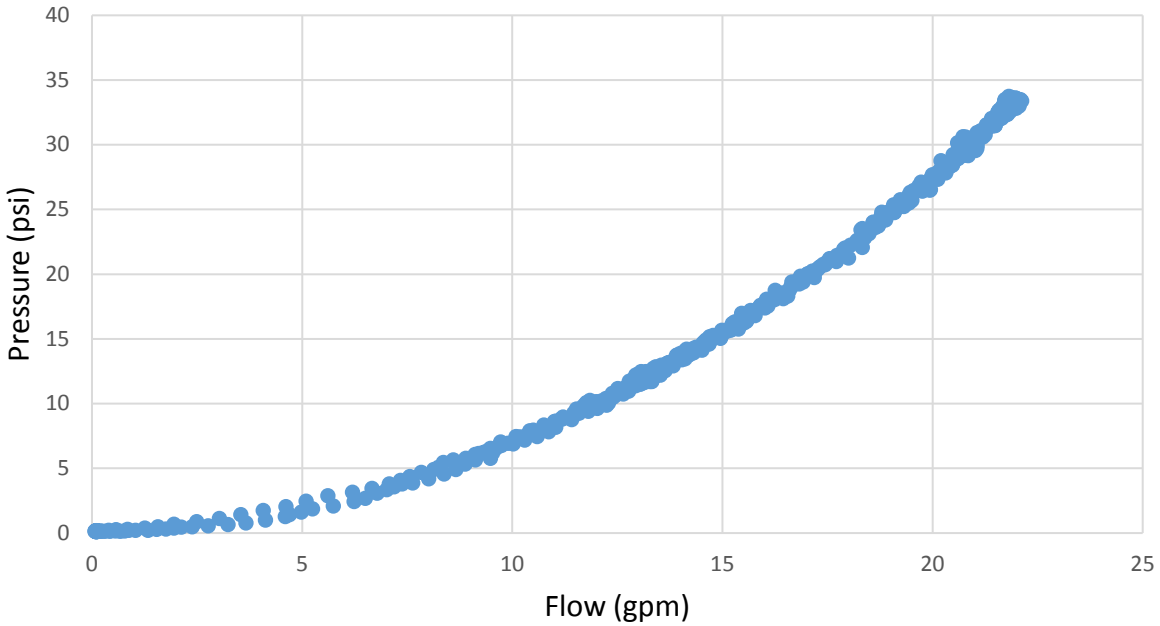

Figure C.15. Batch 5 test 3 32 sec/qt pressure vs flow

APPENDIX D1: ORIFICE TESTING PRESSURE VS FLOW CURVES

Table D1.1. Orifice diameter, length and test viscosities

	Test	Nominal Diameter (in)	Actual Diameter (in)	length (in)	Pre-Visc (sec/qt)	Post-Visc (sec/qt)
SLURRY	16	Nozzle	0.37		49	51.59
	17	0.5	0.63	12	51.59	49.55
	18	0.5	0.63	6	49.55	49.06
	19	0.375	0.495	6	49.06	49.18
	20	0.375	0.495	3	49.18	49.16
	21	0.25	0.368	6	49.16	48.37
	22	0.25	0.368	3	48.37	49.47
WATER	23	Nozzle	0.37		26.53	26.53
	24	0.5	0.63	6	26.53	26.53
	25	0.5	0.63	12	26.53	26.53
	26	0.375	0.495	3	26.53	26.53
	27	0.375	0.495	6	26.53	26.53
	28	0.25	0.368	3	26.53	26.53
	29	0.25	0.368	6	26.53	26.53

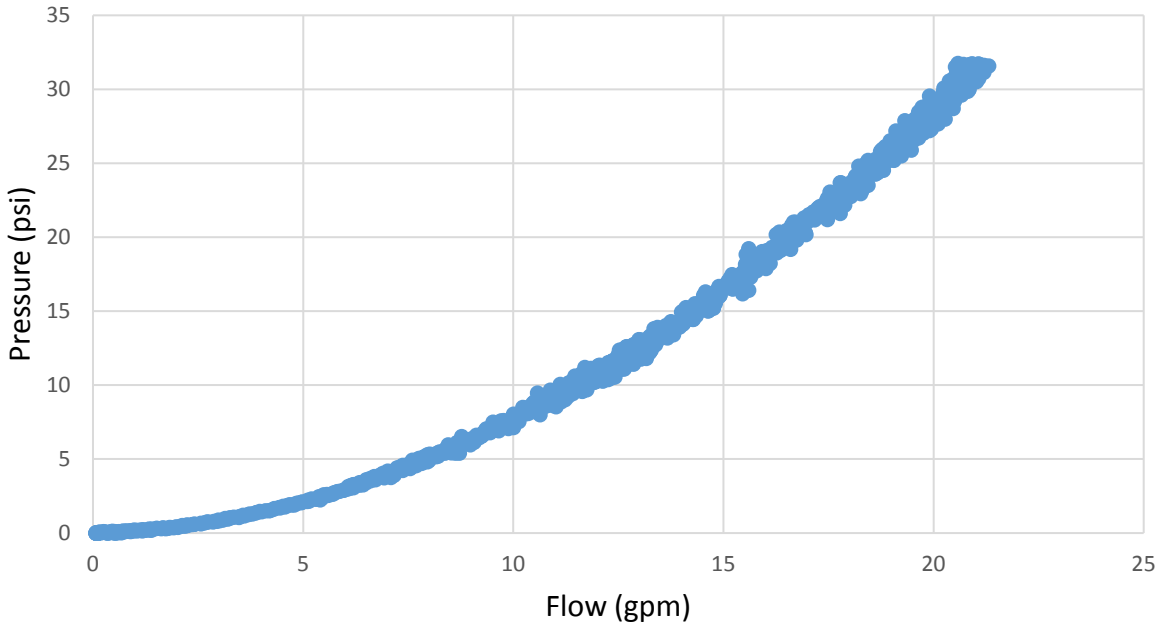

Figure D1.1. Nozzle (0.37 in ID)

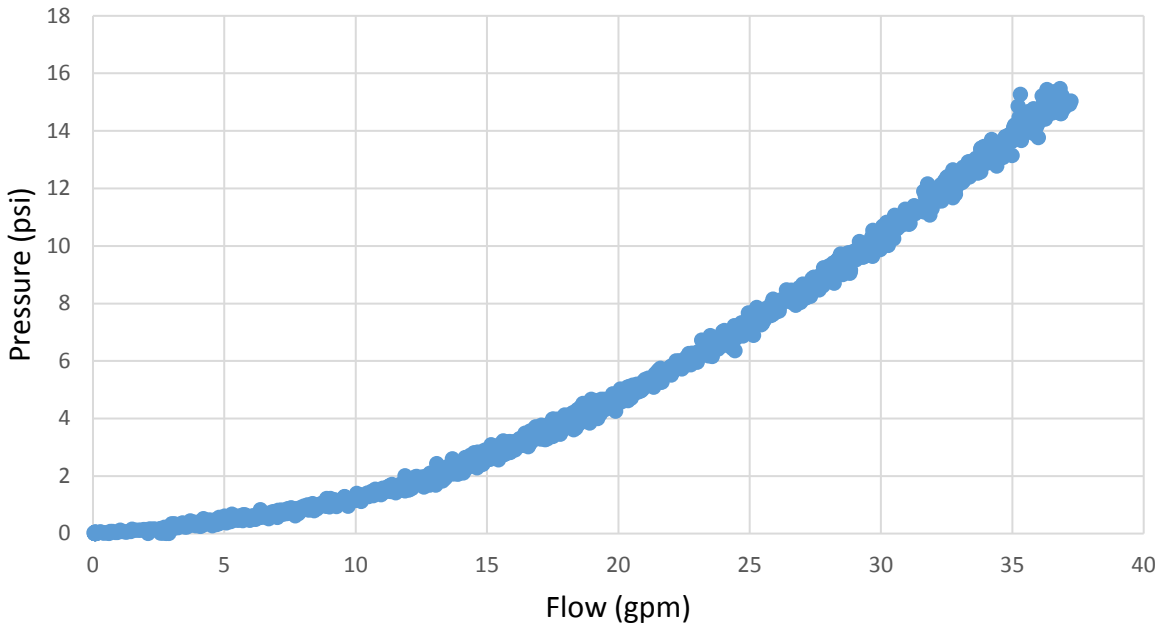

Figure D1.2. 0.63 in ID, 12 in length

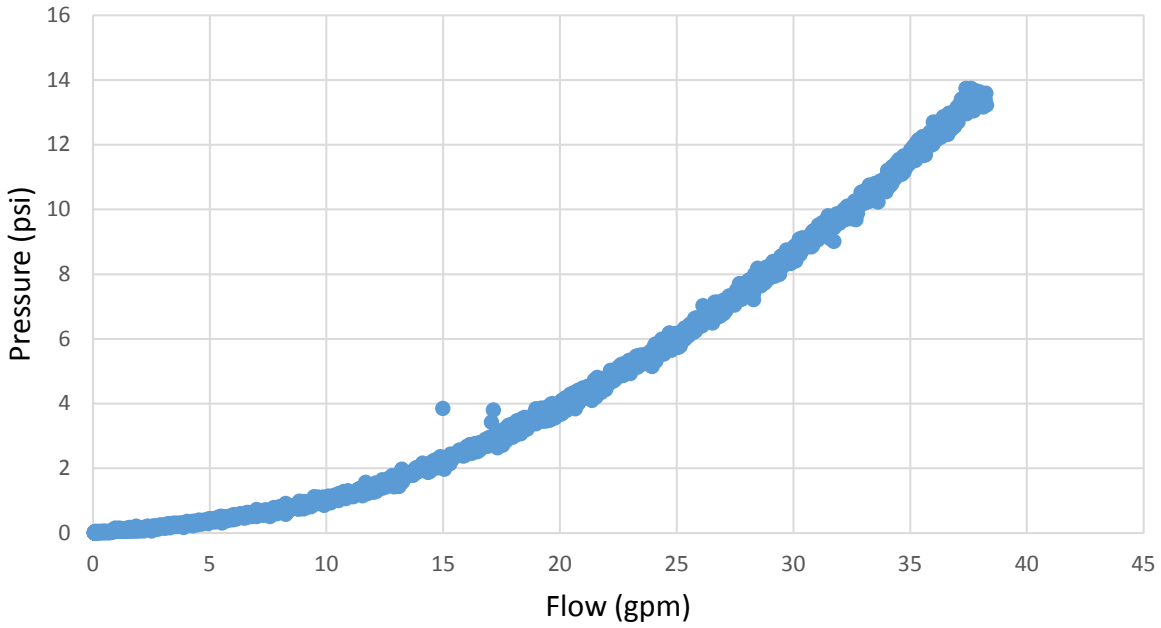

Figure D1.3. 0.63 in ID, 6 in length

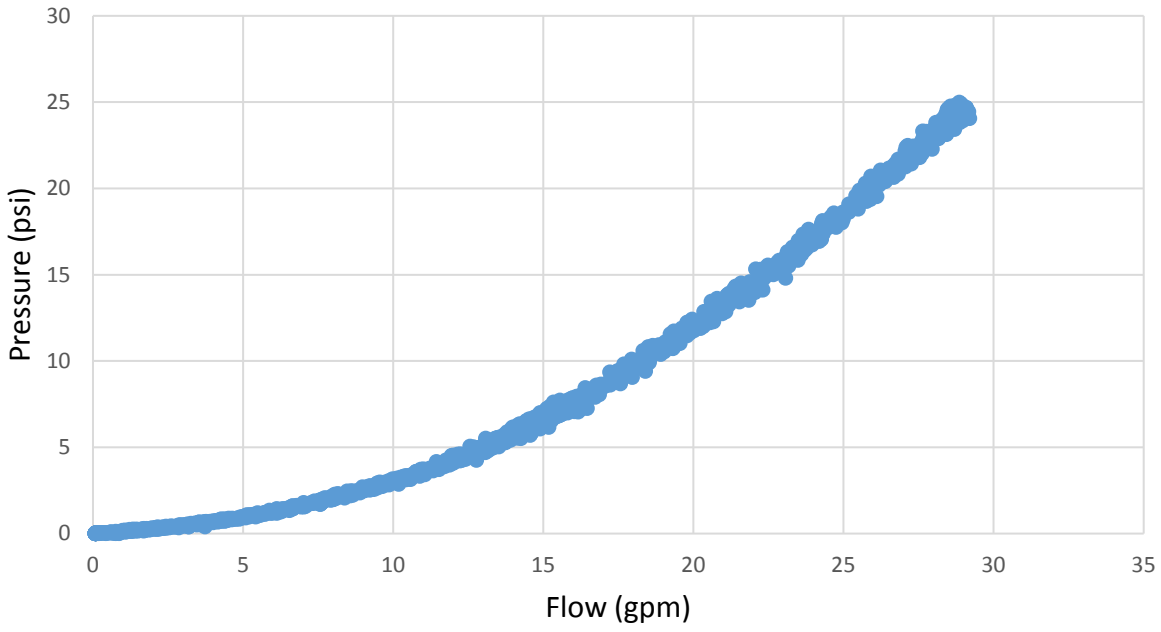

Figure D1.4. 0.495 in ID, 6 in length

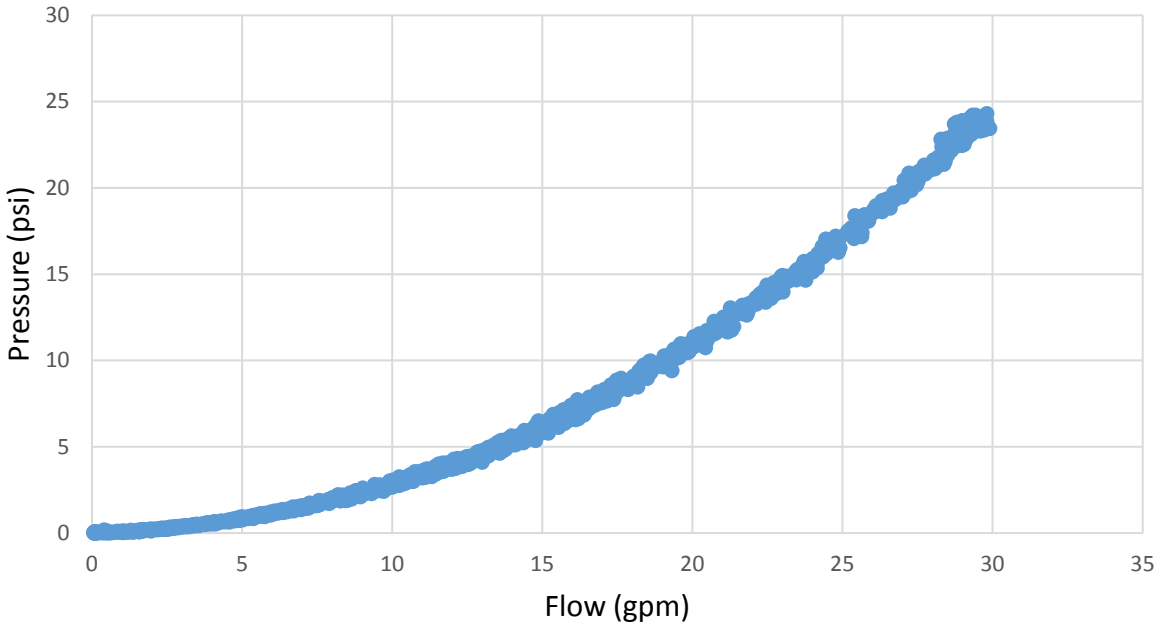

Figure D1.5. 0.495 in ID, 3 in length

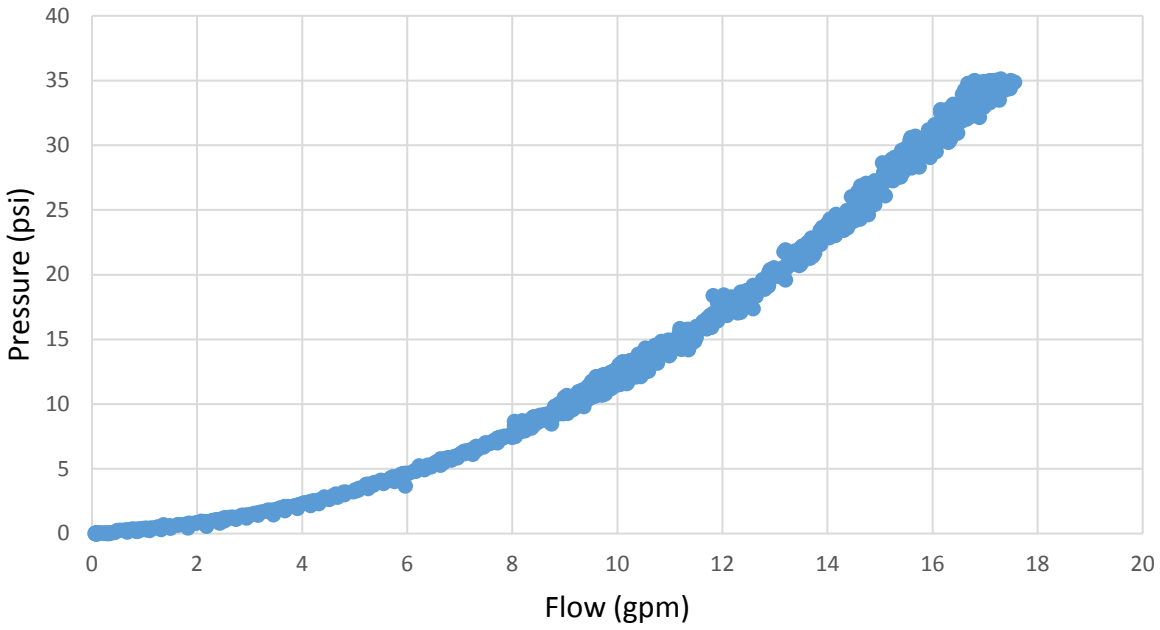

Figure D1.6. 0.368 in ID, 6 in length

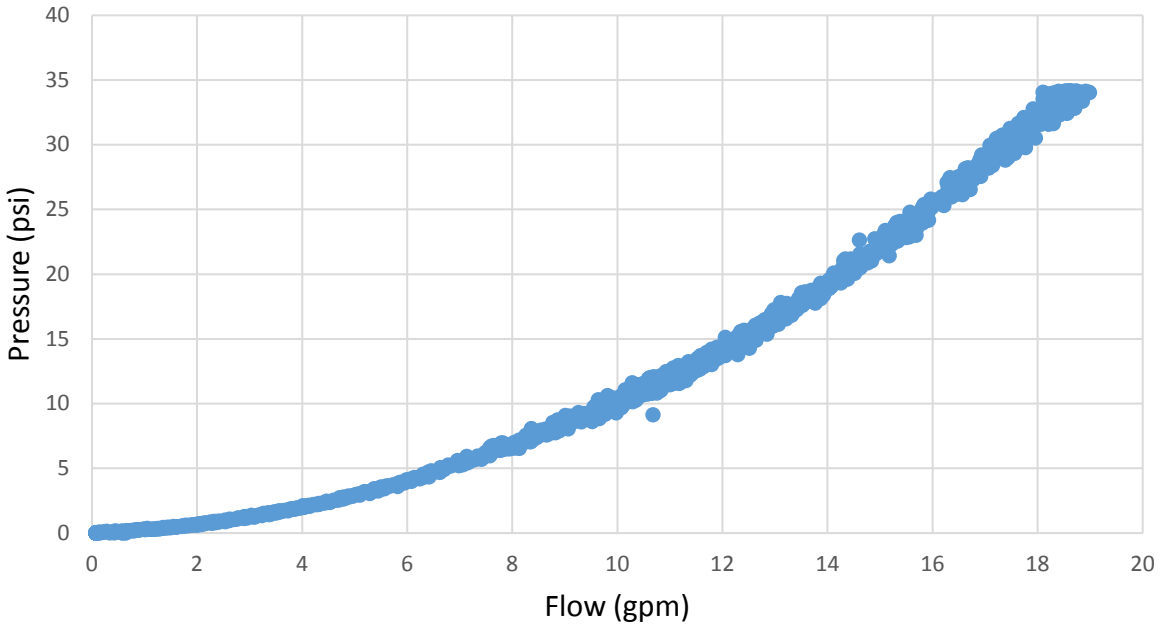

Figure D1.7. 0.368 in ID, 3 in length

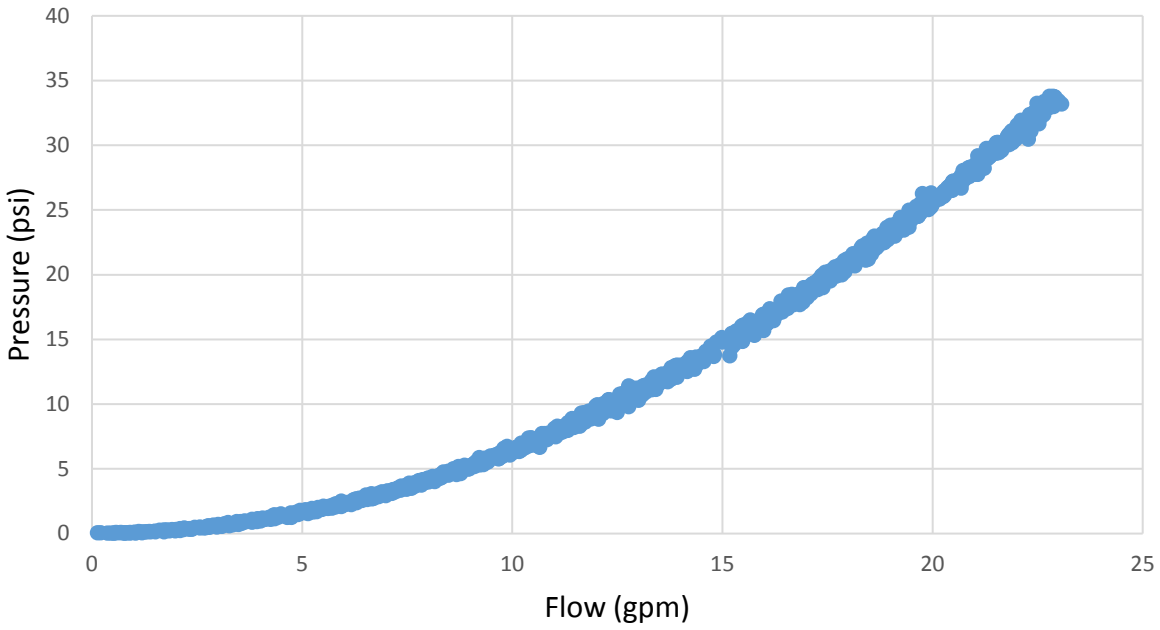

Figure D1.8. Nozzle (0.37 in ID)

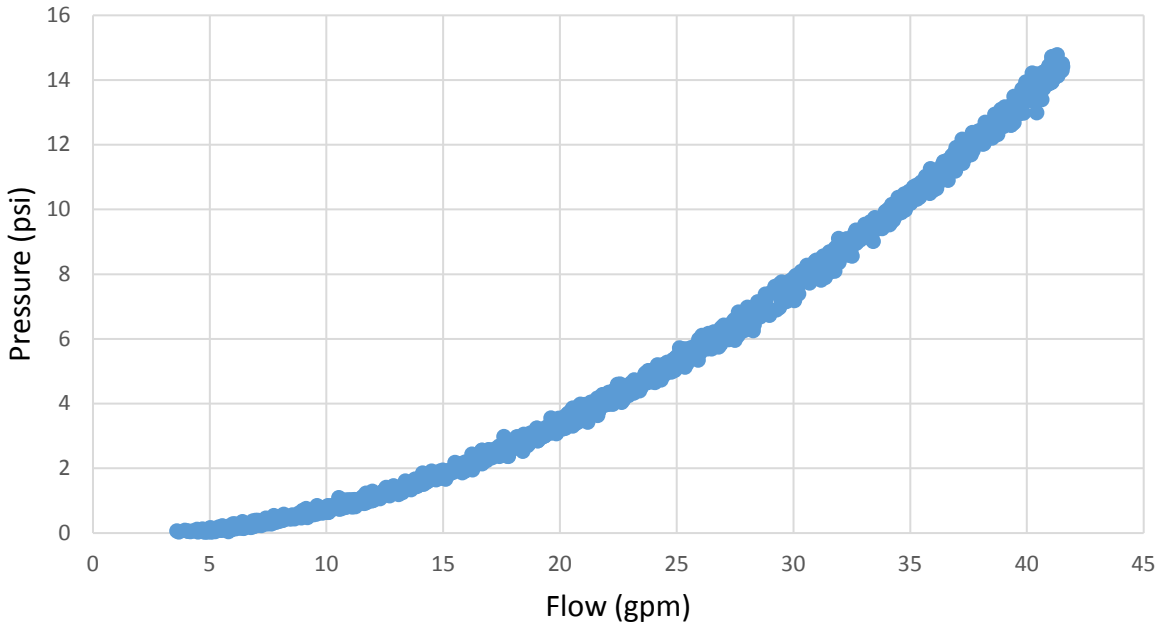

Figure D1.9. 0.63 in ID, 6 in length

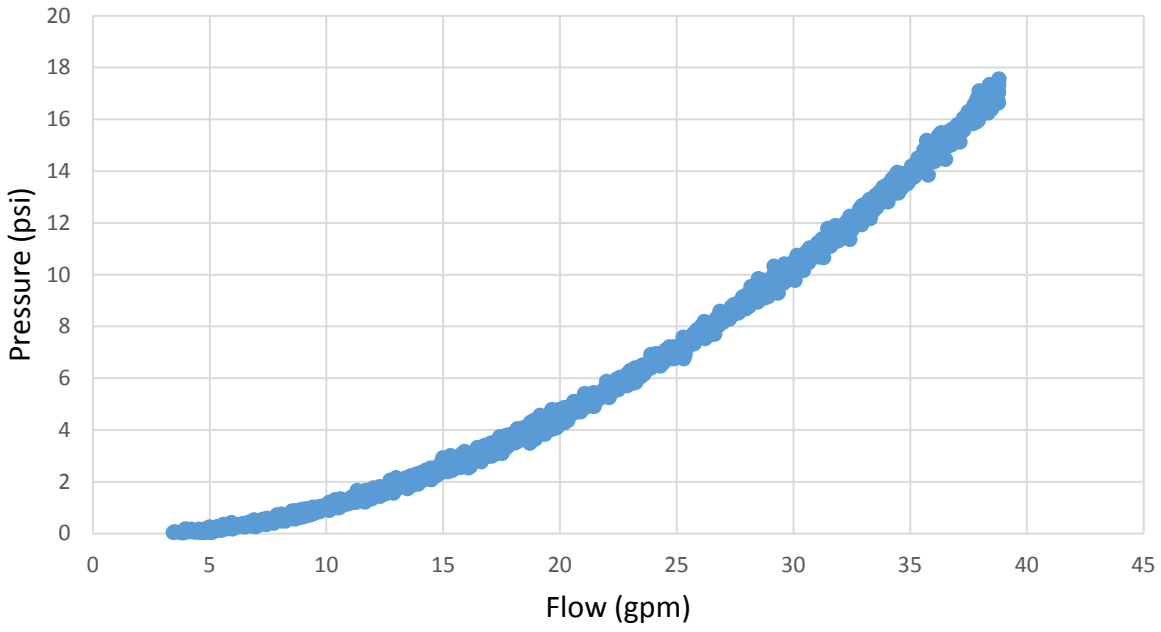

Figure D1.10. 0.63 in ID, 12 in length

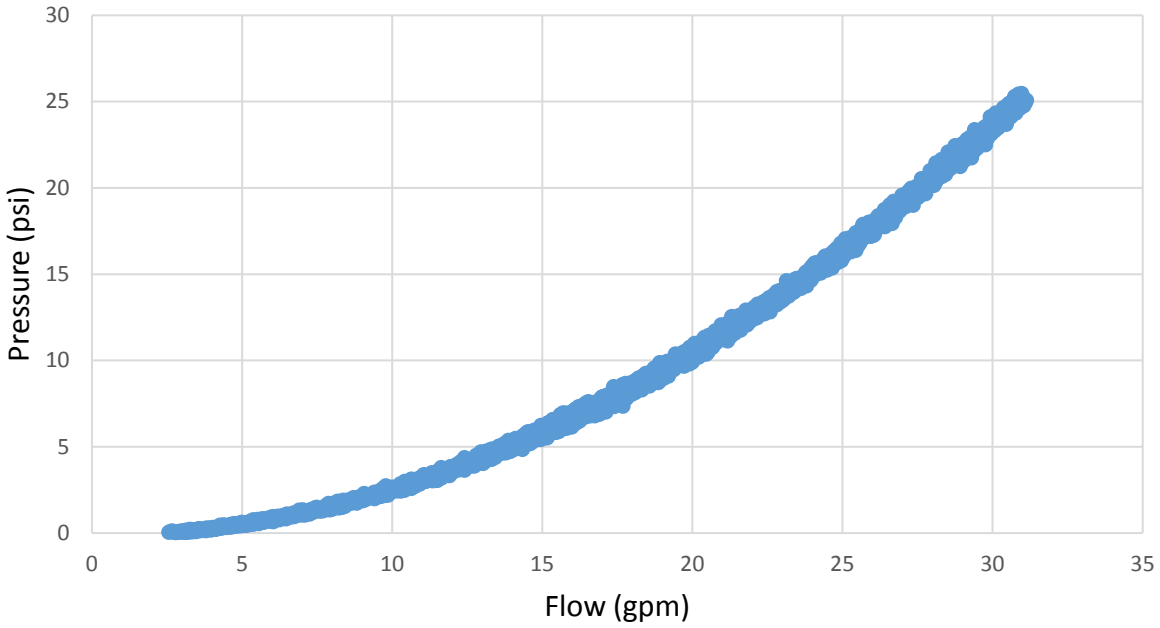

Figure D1.11. 0.495 in ID, 3 in length

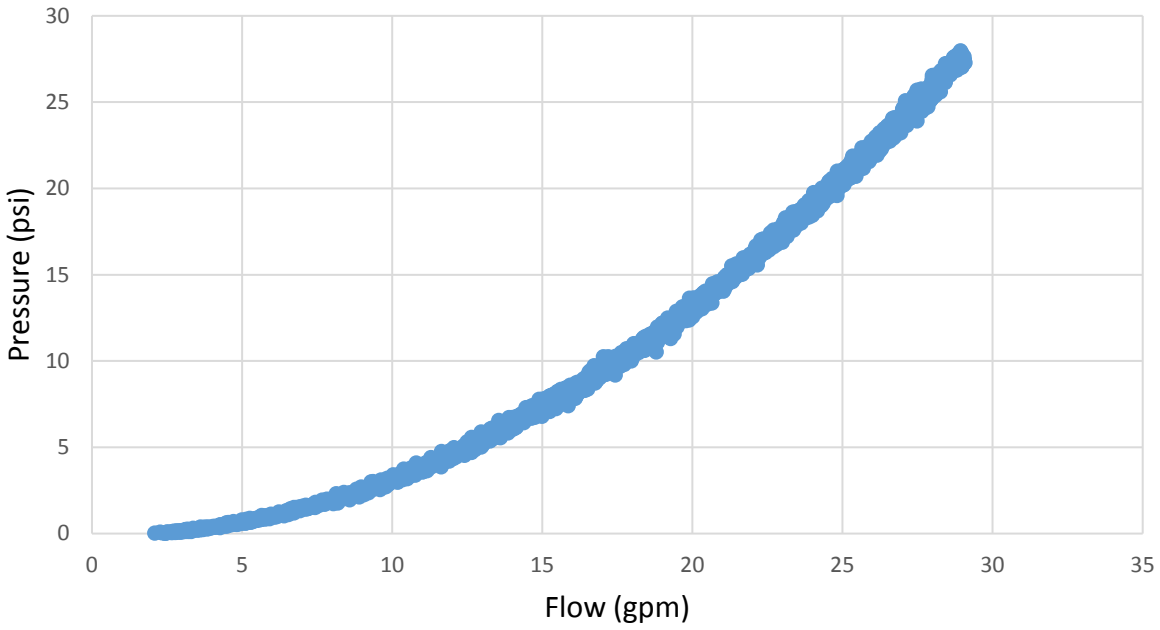

Figure D1.12. 0.495 in ID, 6 in length

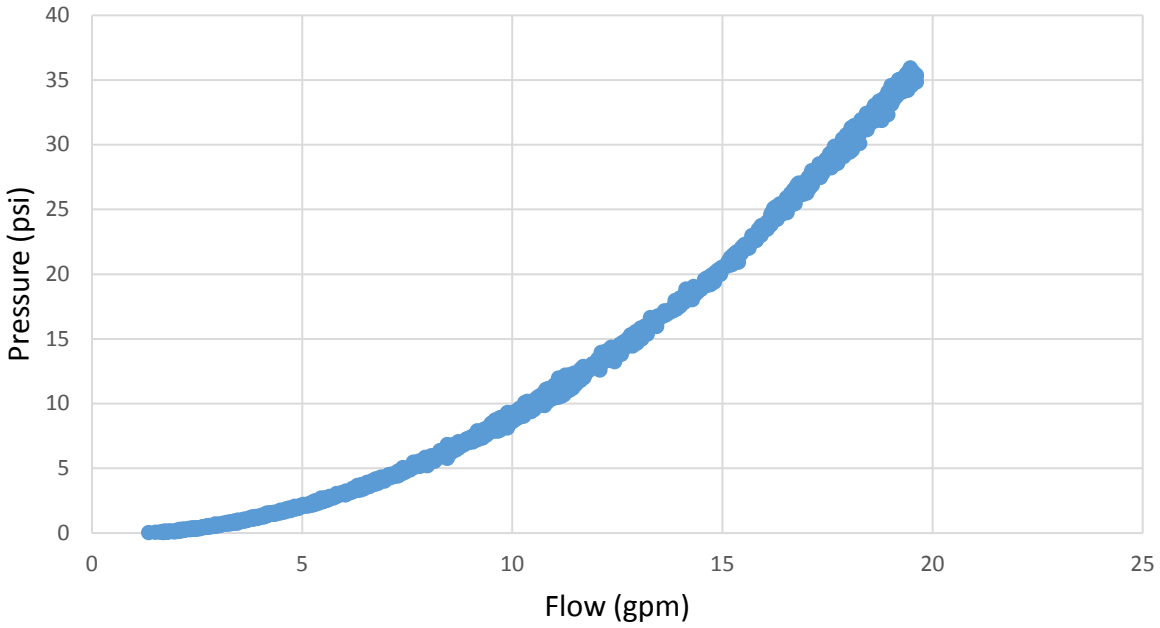

Figure D1.13. 0.368 in ID, 3 in length

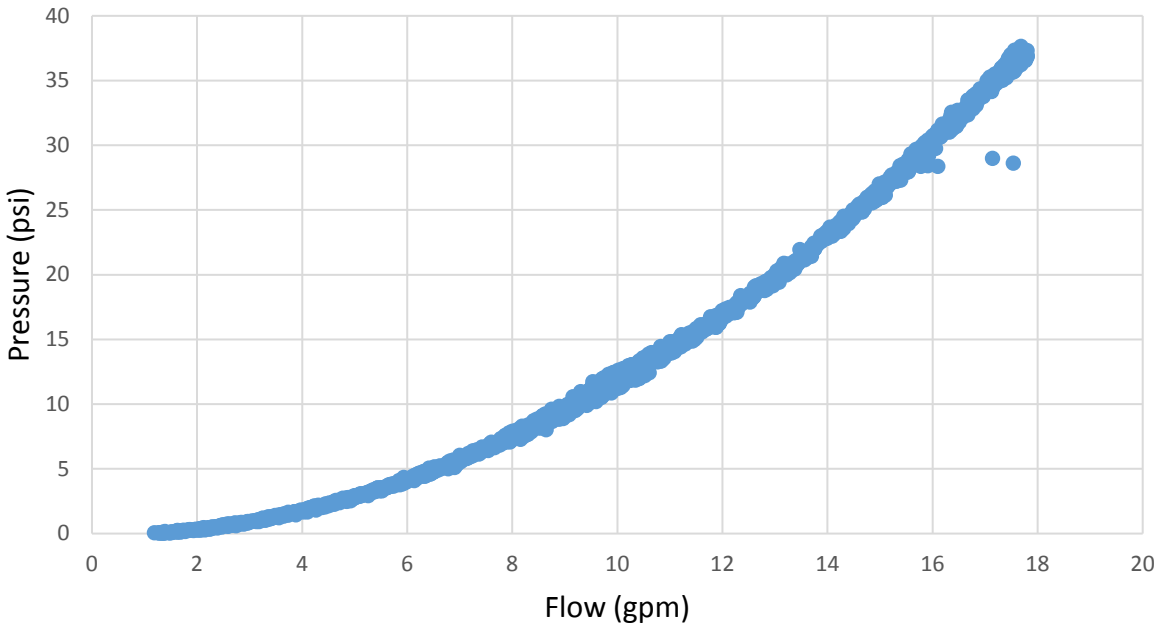

Figure D1.14. 0.368 in ID, 6 in length

APPENDIX D2: FINAL ORIFICE TESTING PRESSURE VS FLOW CURVES

Table D2.1. Final orifice optimization diameter and length

	Test #	Nominal Diameter (in)	Actual Inner Diameter (in)	Nominal Length (in)	Actual Length (in)	Avg Inner Diameter (in)
WATER	1	.375 OD	0.31	6	6.0625	0.30
	2	.375 OD	0.3	5	4.914	
	3	.375 OD	0.3	4	4.05	
	4	.375 OD	0.295	3	3.018	
	5	.375 OD	0.29	2	1.984	
	6	.375 OD	0.295	1	1.134	
	7	.25 OD	0.19	6	5.9375	0.18
	8	.25 OD	0.18	5	4.9375	
	9	.25 OD	0.177	4	3.985	
	10	.25 OD	0.183	3	3.04	
	11	.25 OD	0.19	2	2.045	
	12	.25 OD	0.18	1	1.074	
	13	0.125	0.28	4	3.966	0.28
	14	0.125	0.275	3	2.935	
	15	0.125	0.245	2	2.01	0.25
	16	0.125	0.247	1.5	1.498	
SLURRY	17	.375 OD	0.31	6	6.0625	0.30
	18	.375 OD	0.3	5	4.914	
	19	.375 OD	0.3	4	4.05	
	20	.375 OD	0.295	3	3.018	
	21	.375 OD	0.29	2	1.984	
	22	.375 OD	0.295	1	1.134	
	23	.25 OD	0.19	6	5.9375	0.18
	24	.25 OD	0.18	5	4.9375	
	25	.25 OD	0.177	4	3.985	
	26	.25 OD	0.183	3	3.04	
	27	.25 OD	0.19	2	2.045	
	28	.25 OD	0.18	1	1.074	
	29	0.125	0.28	4	3.966	0.28
	30	0.125	0.275	3	2.935	
	31	0.125	0.245	2	2.01	0.25
	32	0.125	0.247	1.5	1.498	

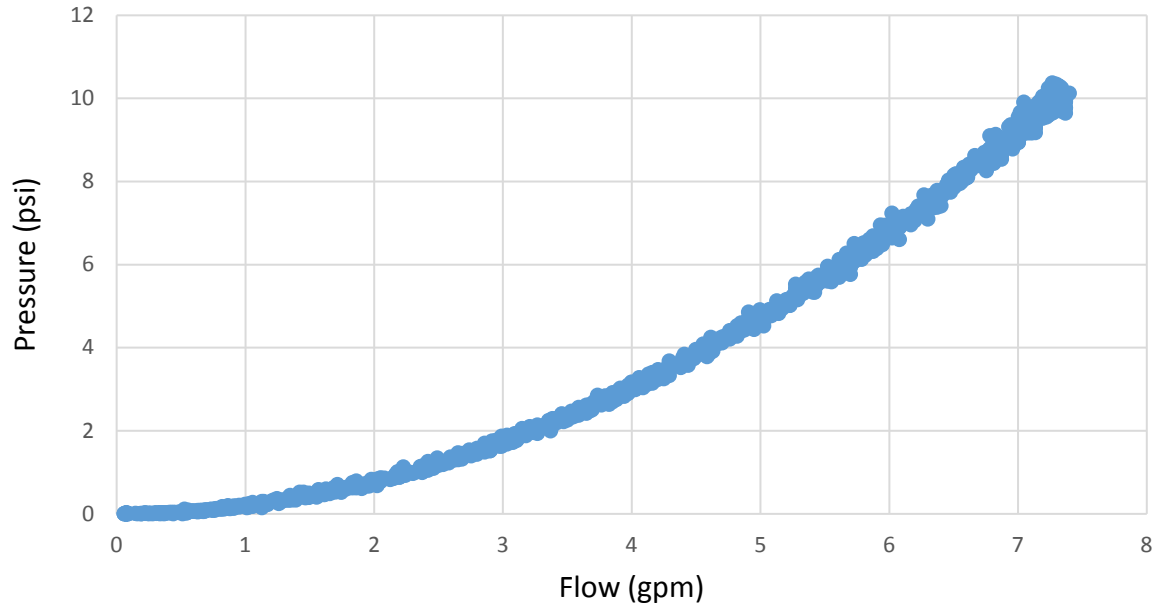

Figure D2.1. 0.31 in ID, 6 in length

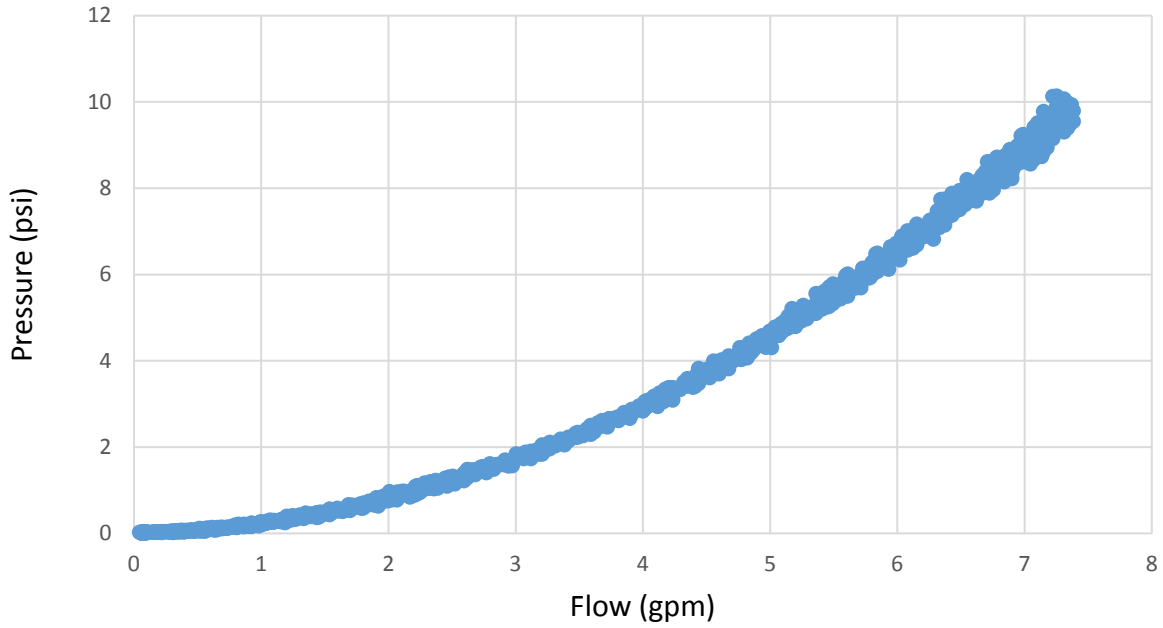

Figure D2.2. 0.3 in ID, 5 in length

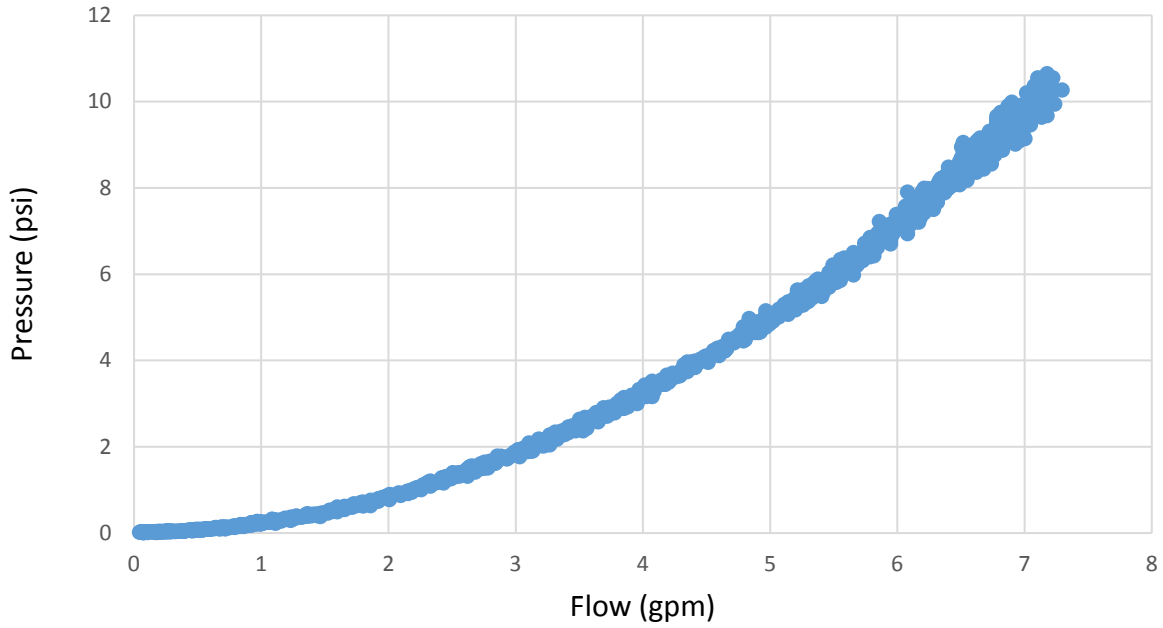

Figure D2.3. 0.3 in ID, 4 in length

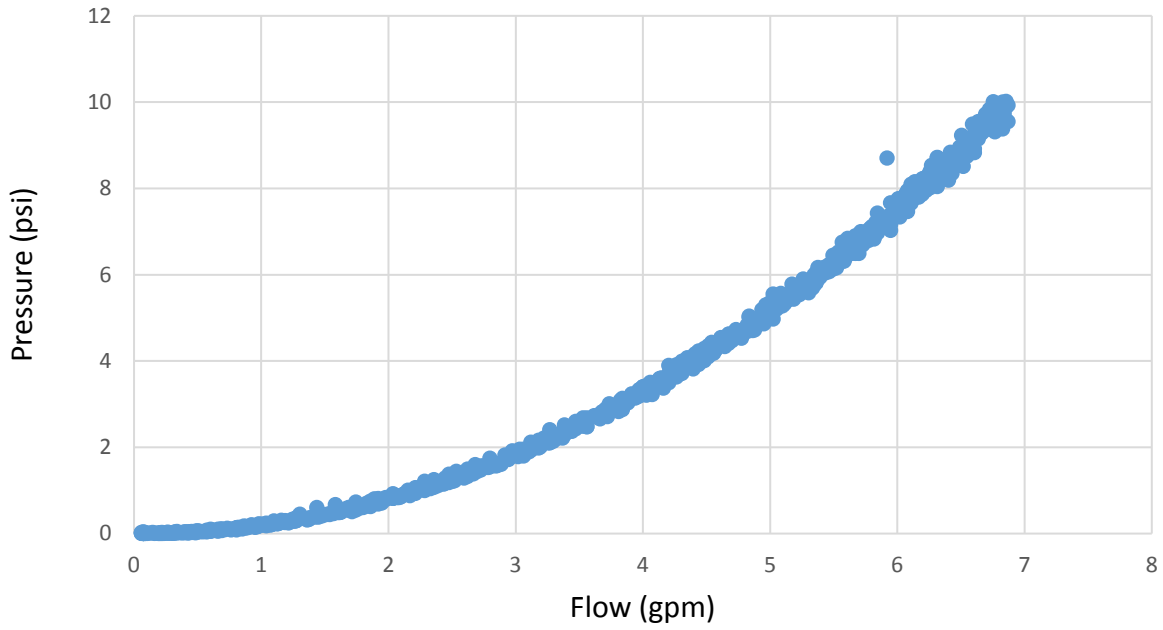

Figure D2.4. 0.295 in ID, 3 in length

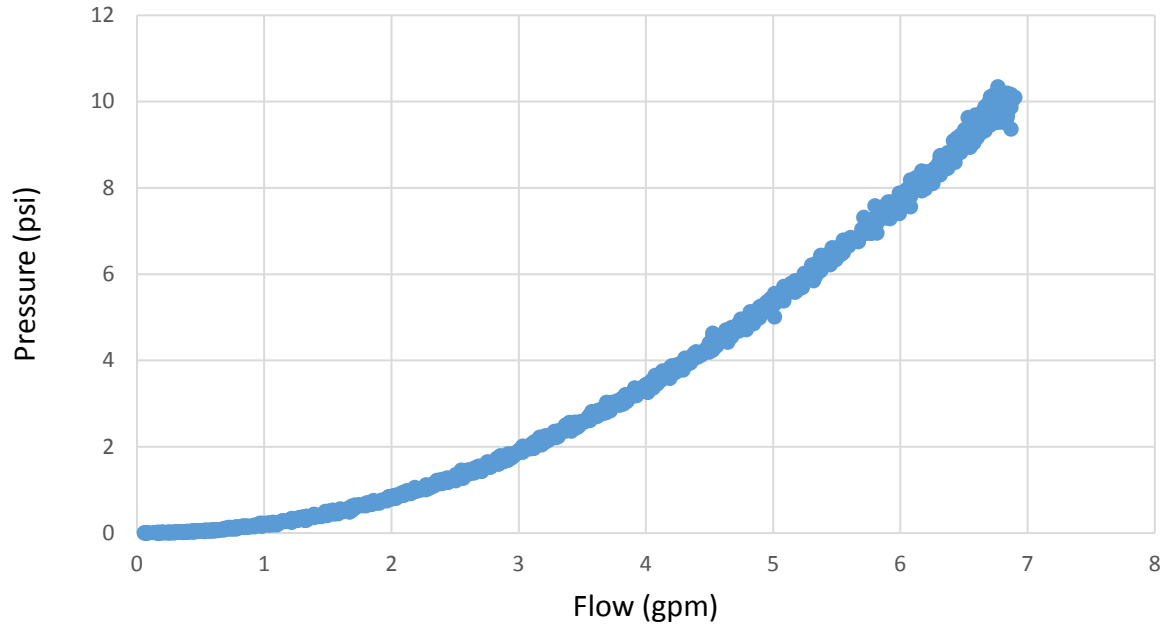

Figure D2.5. 0.29 in ID, 2 in length

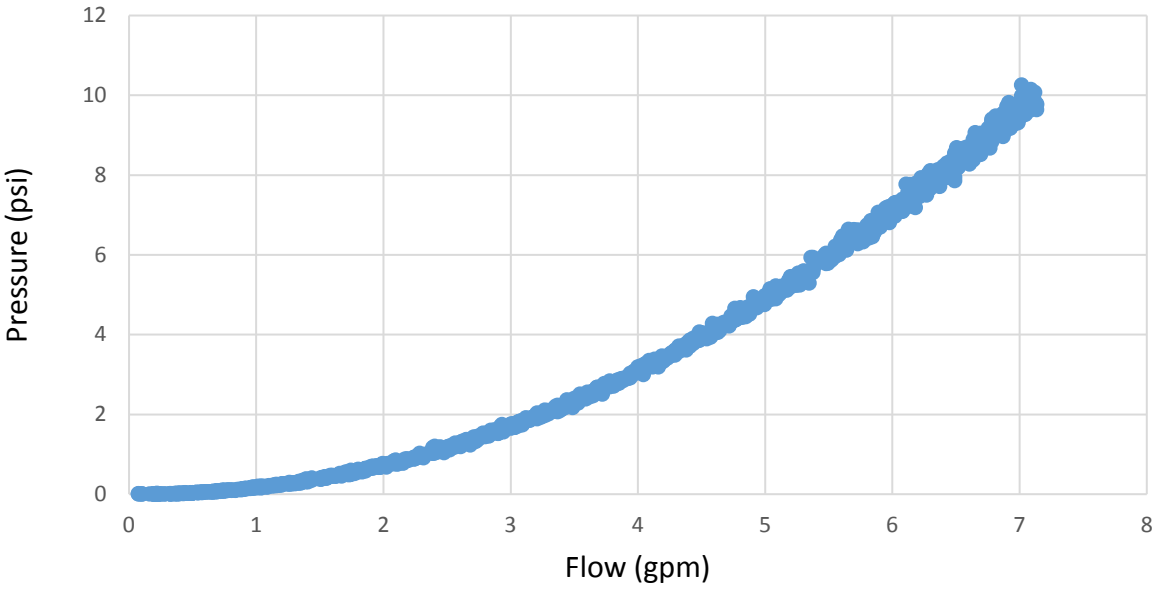

Figure D2.6. 0.295 in ID, 1 in length

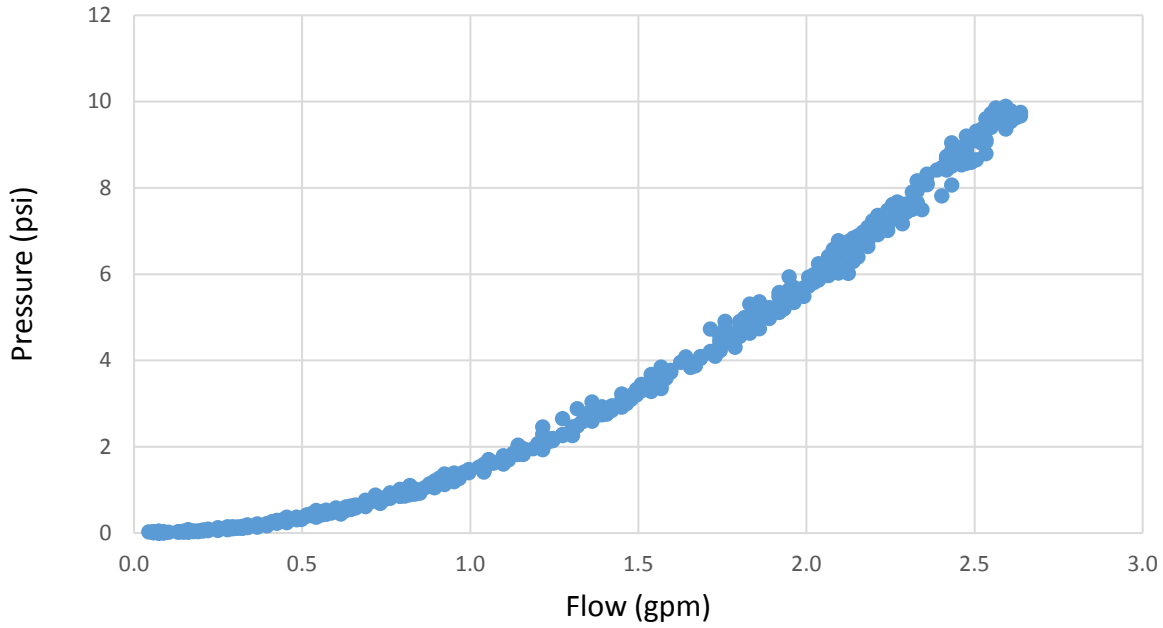

Figure D2.7. 0.19 in ID, 6 in length

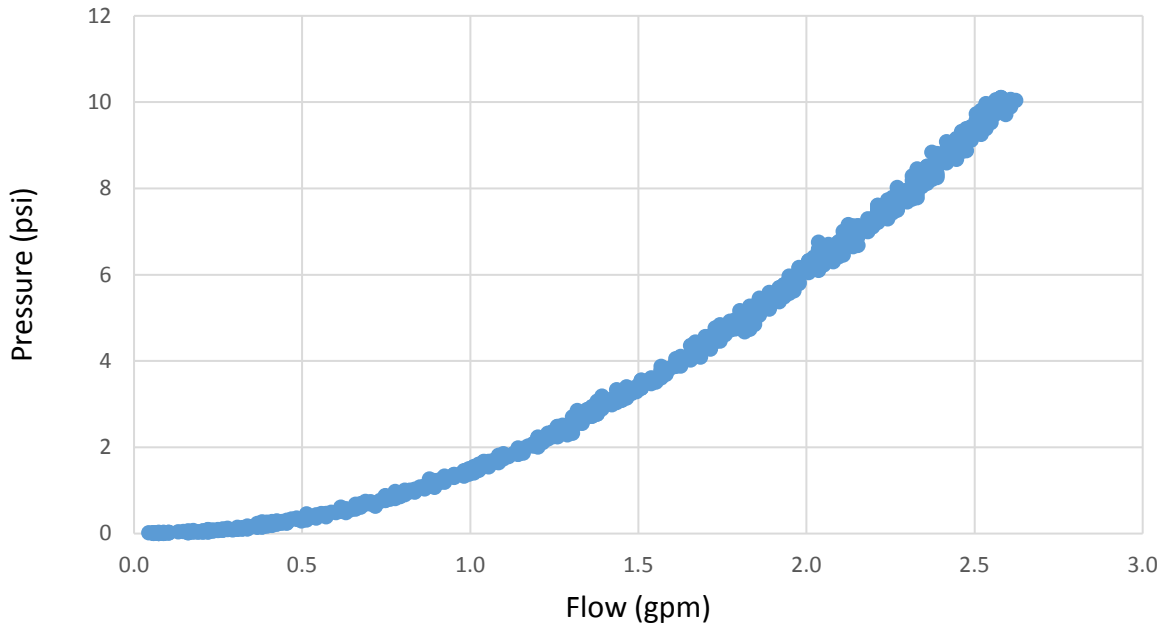

Figure D2.8. 0.18 in ID, 5 in length

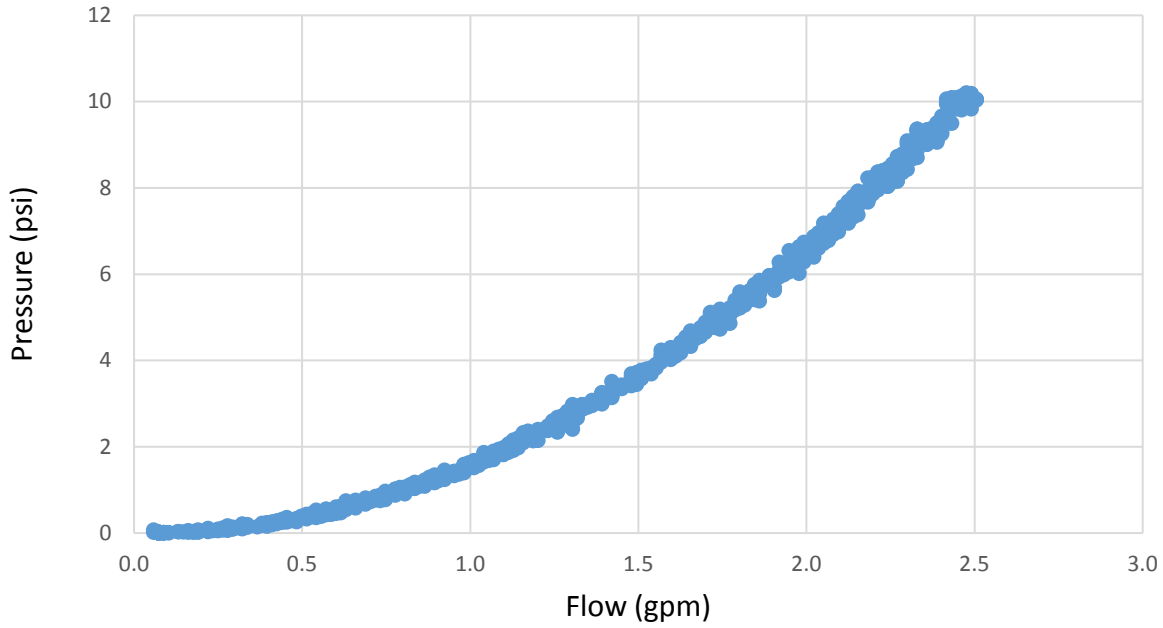

Figure D2.9. 0.177 in ID, 4 in length

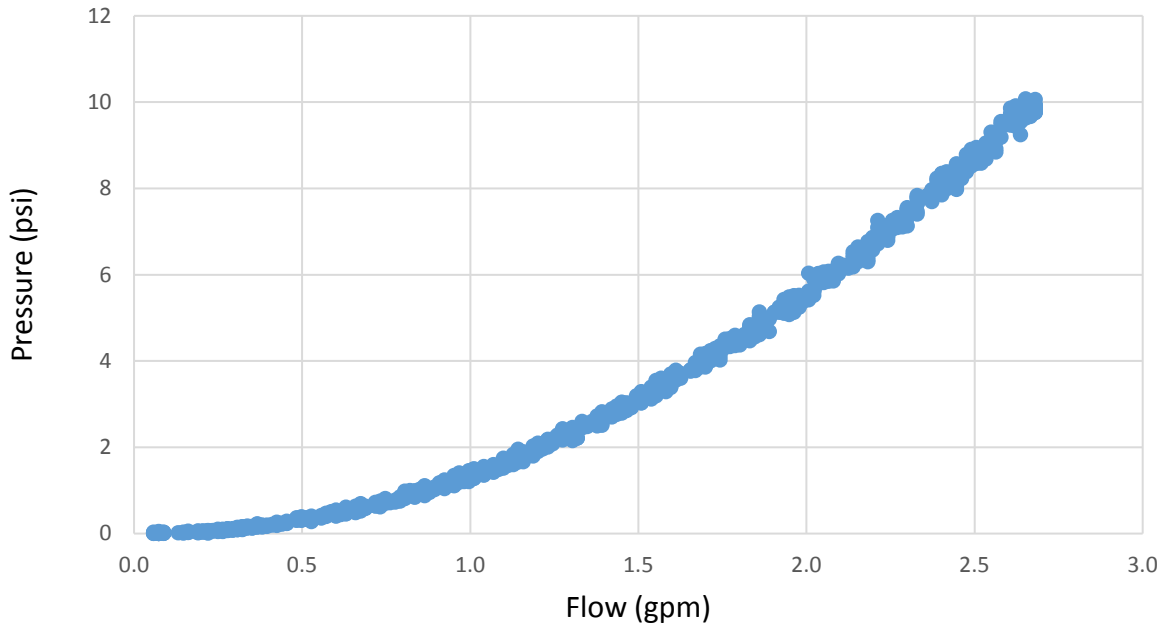

Figure D2.10. 0.183 in ID, 3 in length

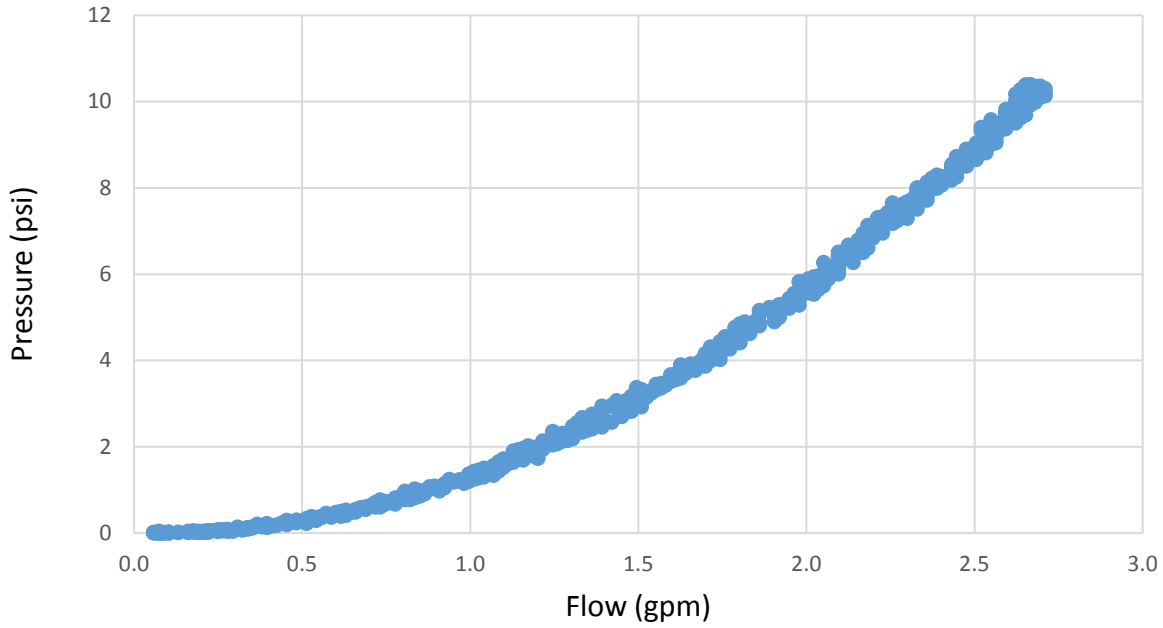

Figure D2.11. 0.19 in ID, 2 in length

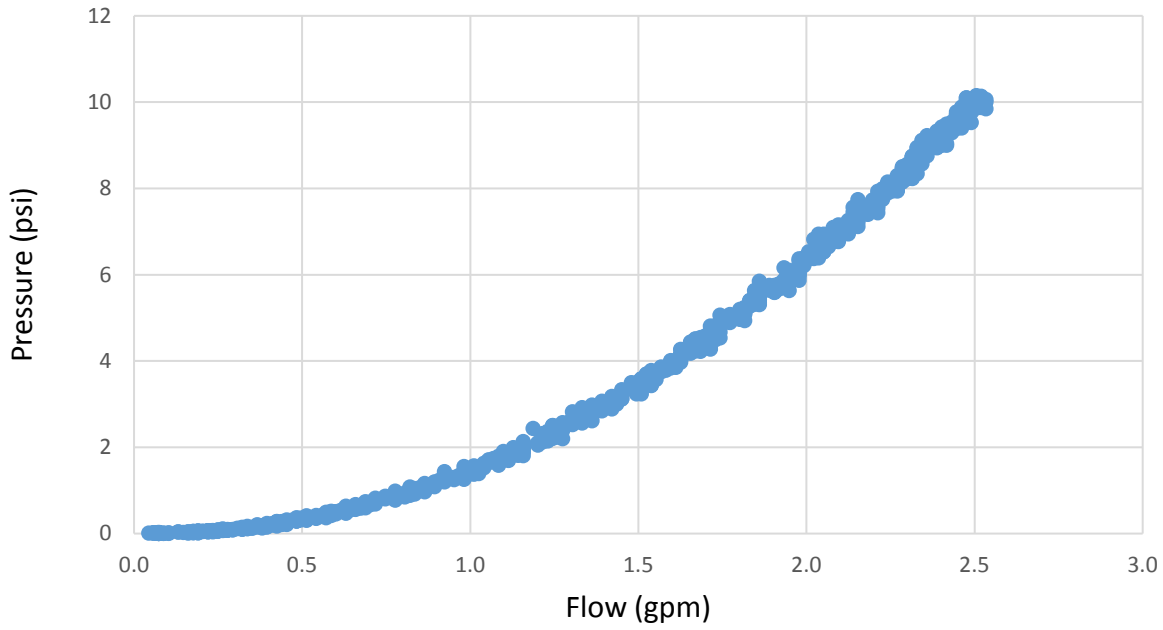

Figure D2.12. 0.18 in ID, 1 in length

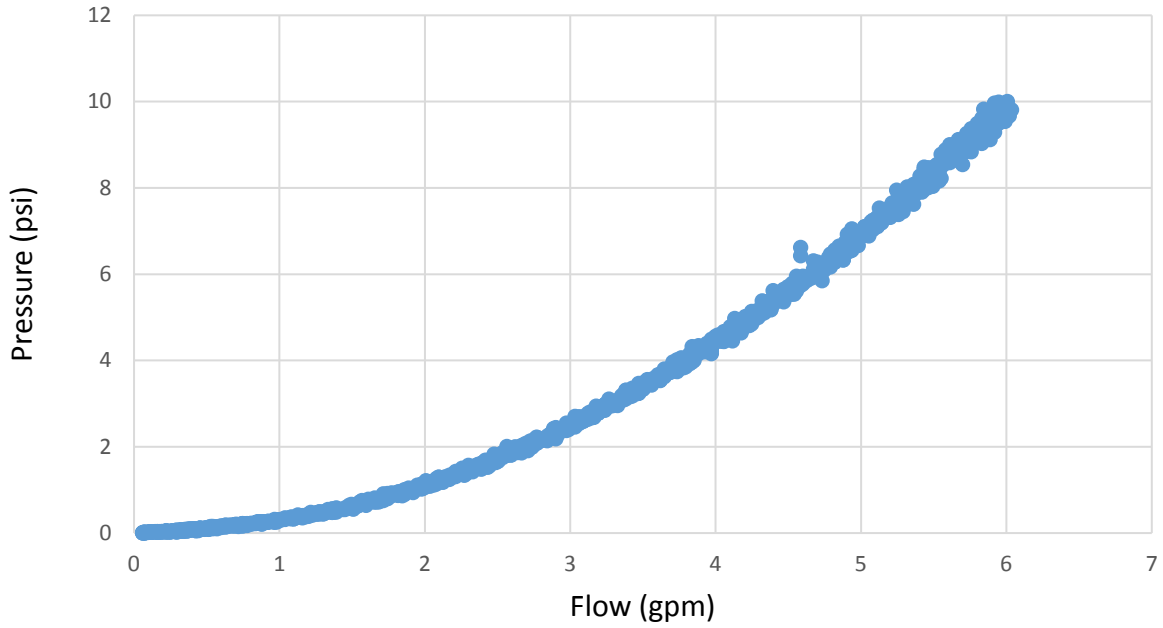

Figure D2.13. 0.28 in ID, 4 in length

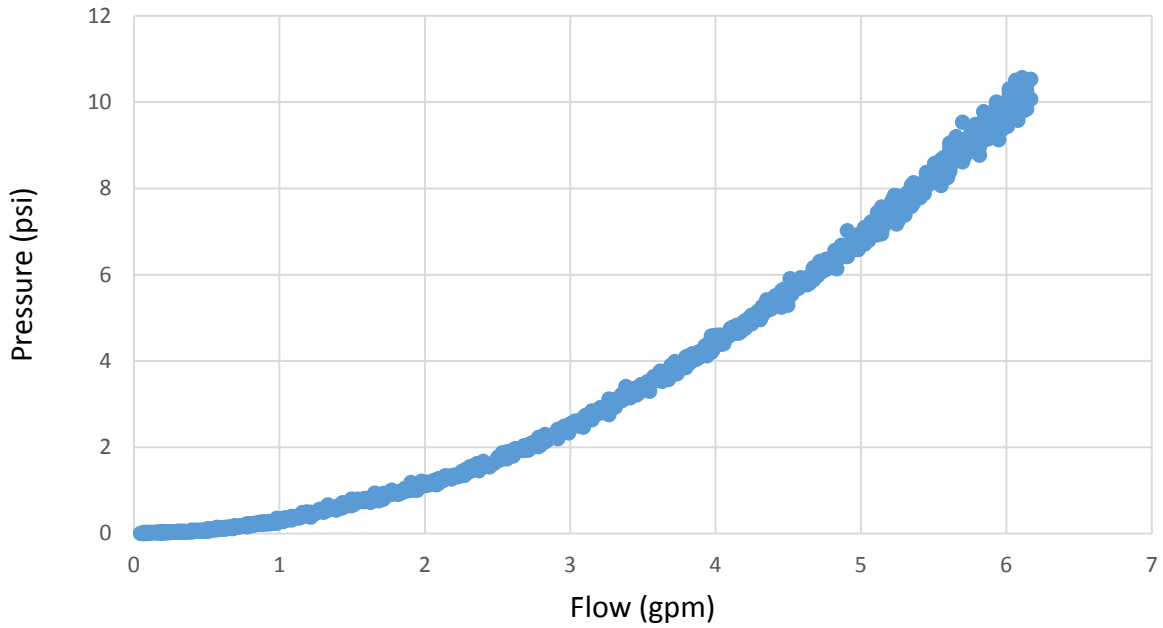

Figure D2.14. 0.275 in ID, 3 in length

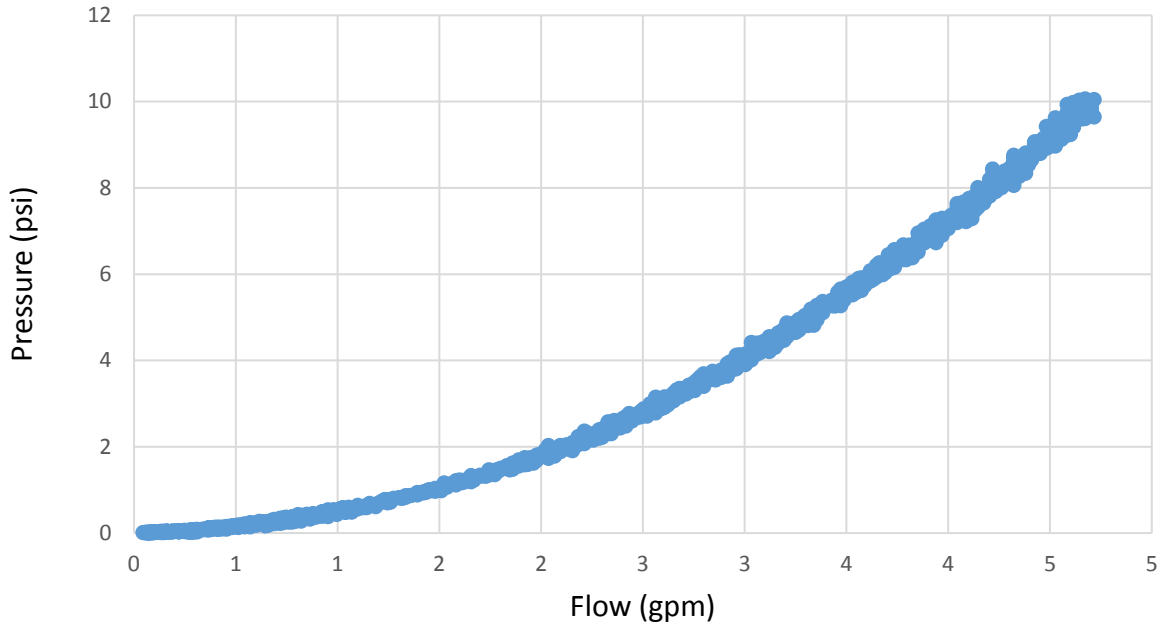

Figure D2.15. 0.245 in ID, 2 in length

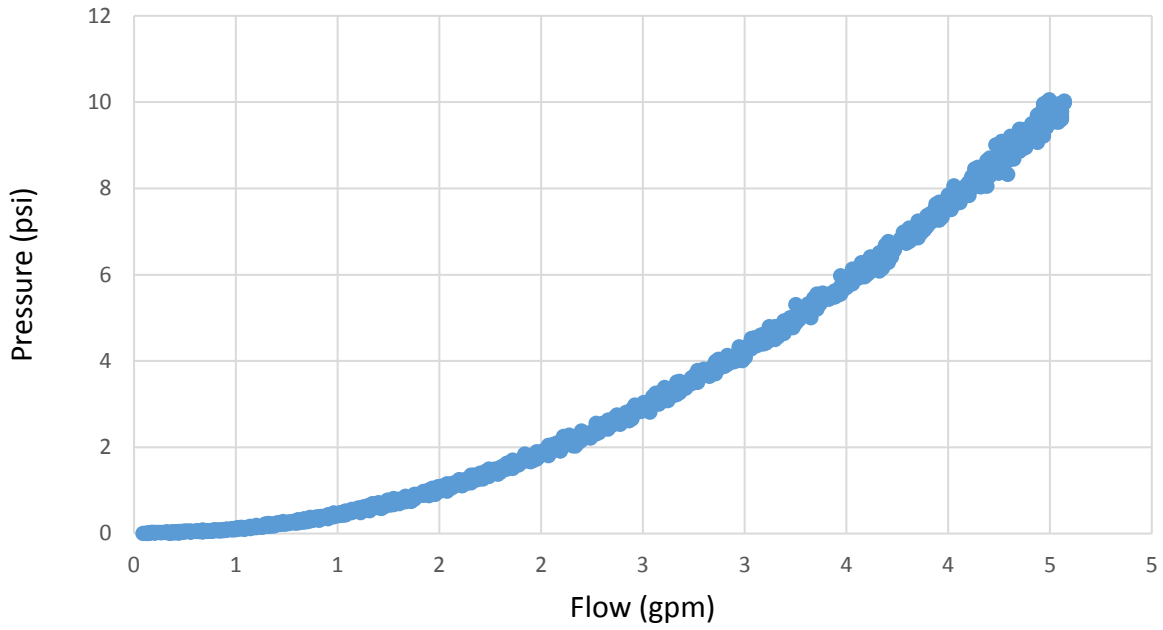

Figure D2.16. 0.247 in ID, 1.5 in length

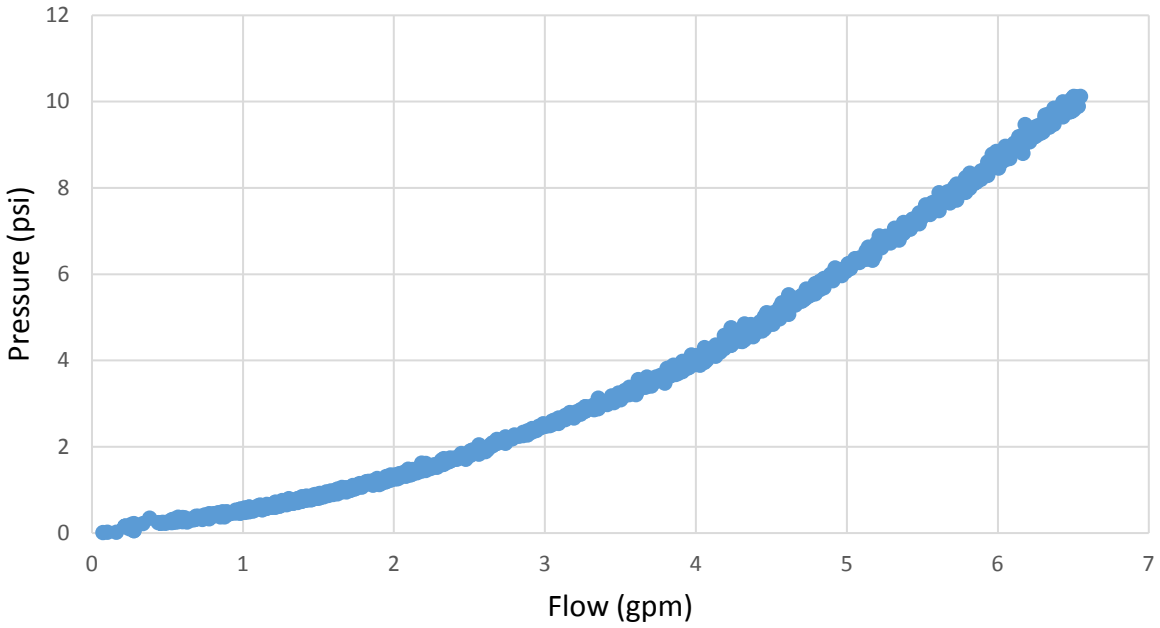

Figure D2.17. 0.31 in ID, 6 in length

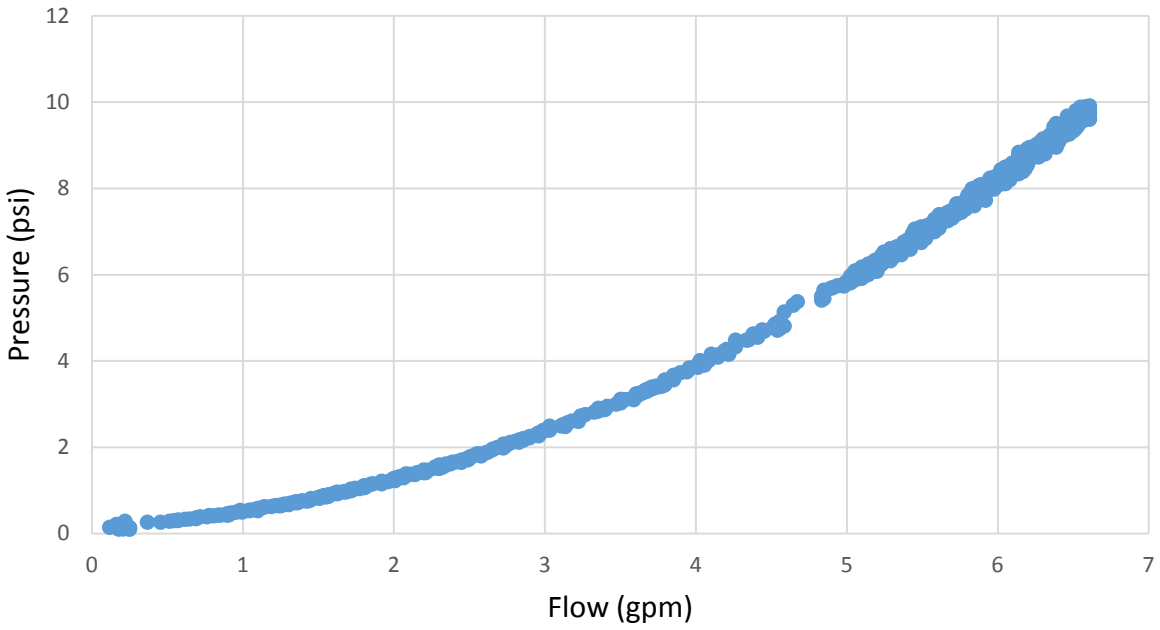

Figure D2.18. 0.3 in ID, 5 in length

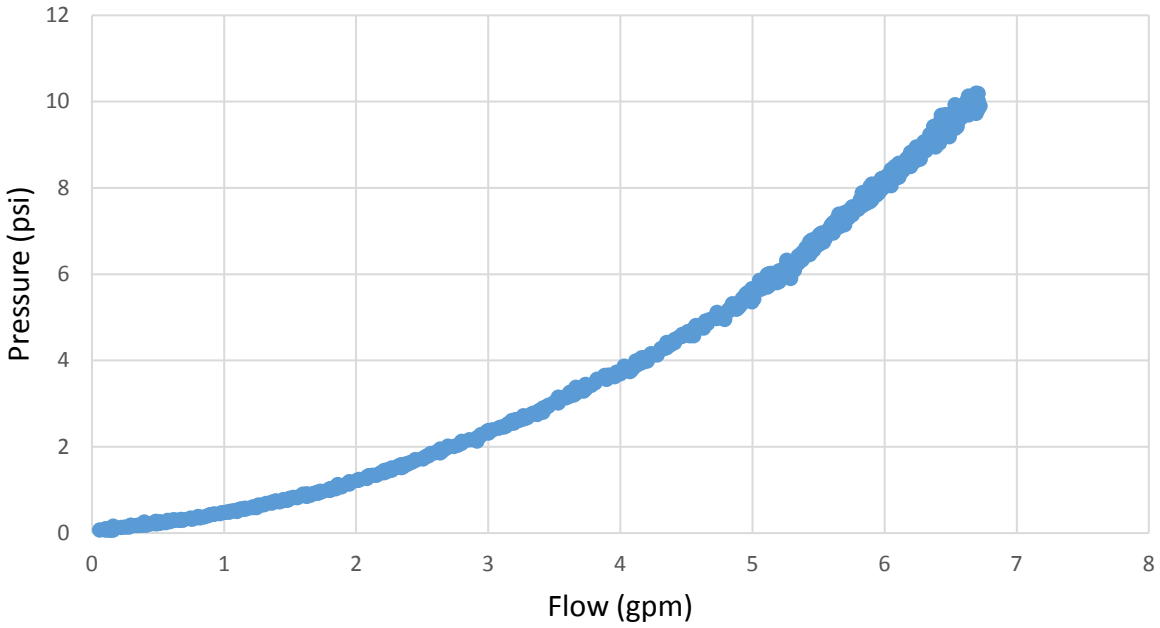

Figure D2.19. 0.3 in ID, 4 in length

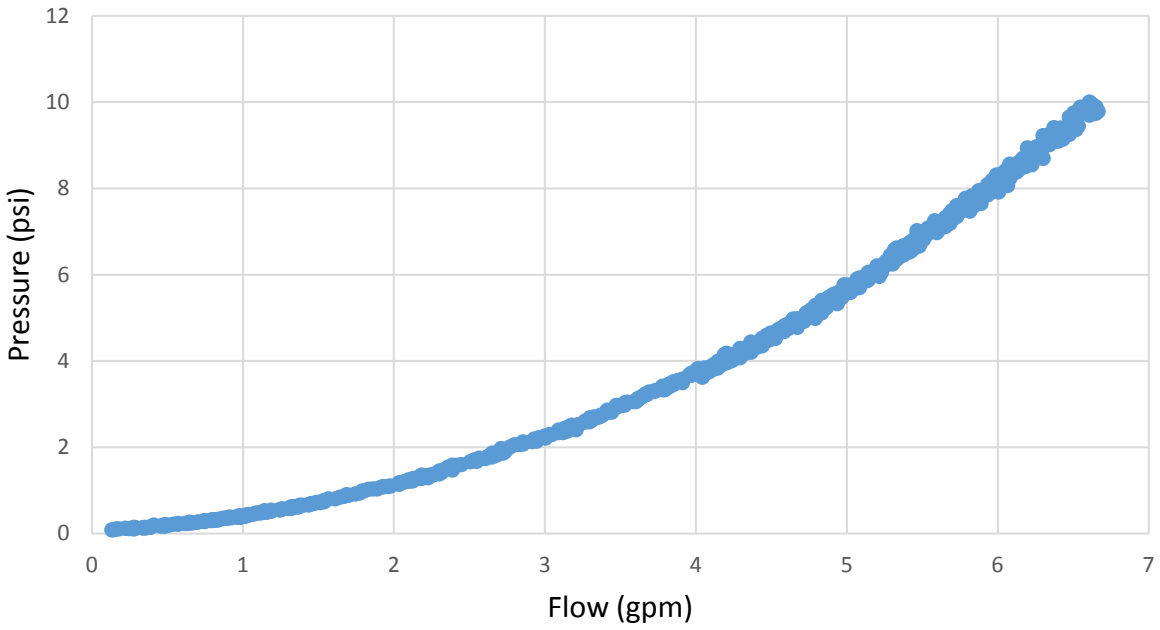

Figure D2.20. 0.295 in ID, 3 in length

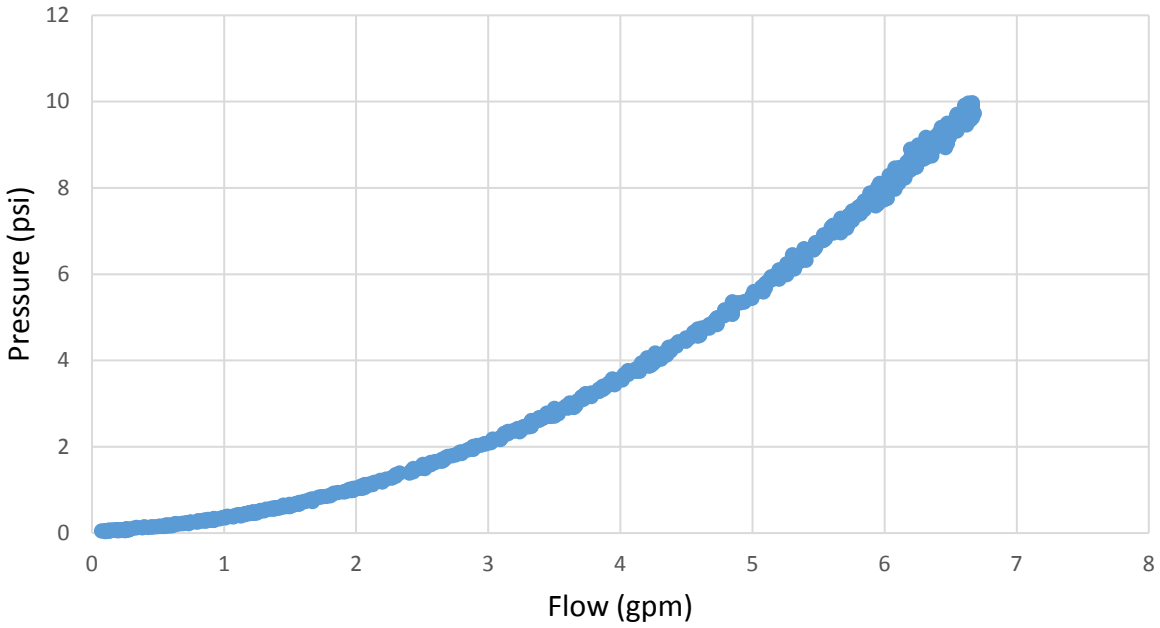

Figure D2.21. 0.29 in ID, 2 in length

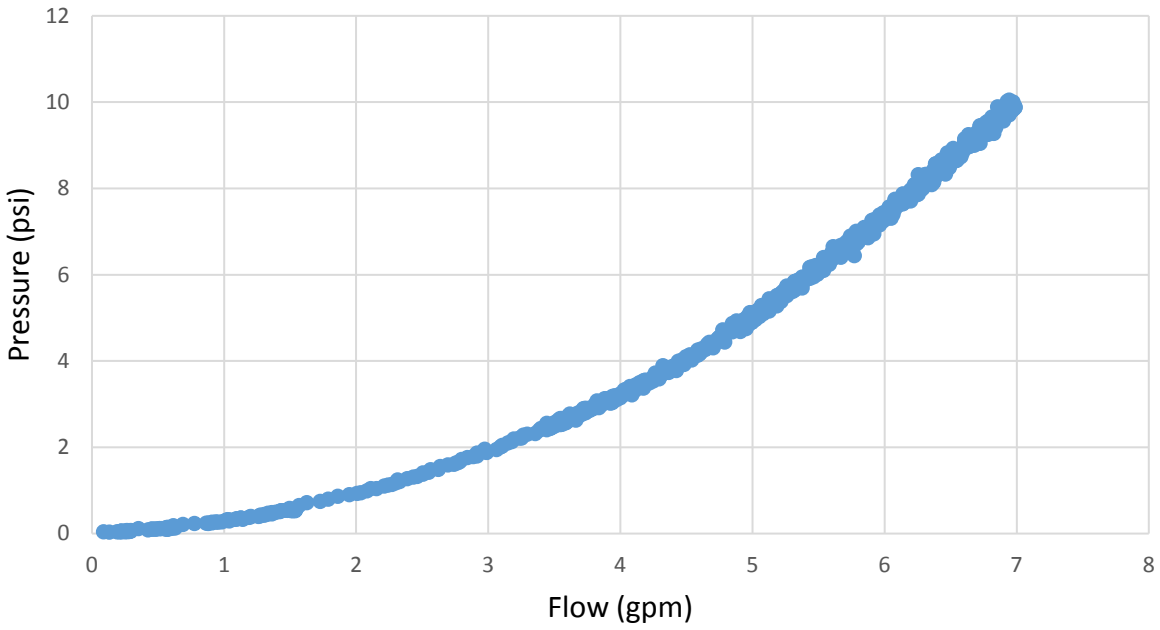

Figure D2.22. 0.295 in ID, 1 in length

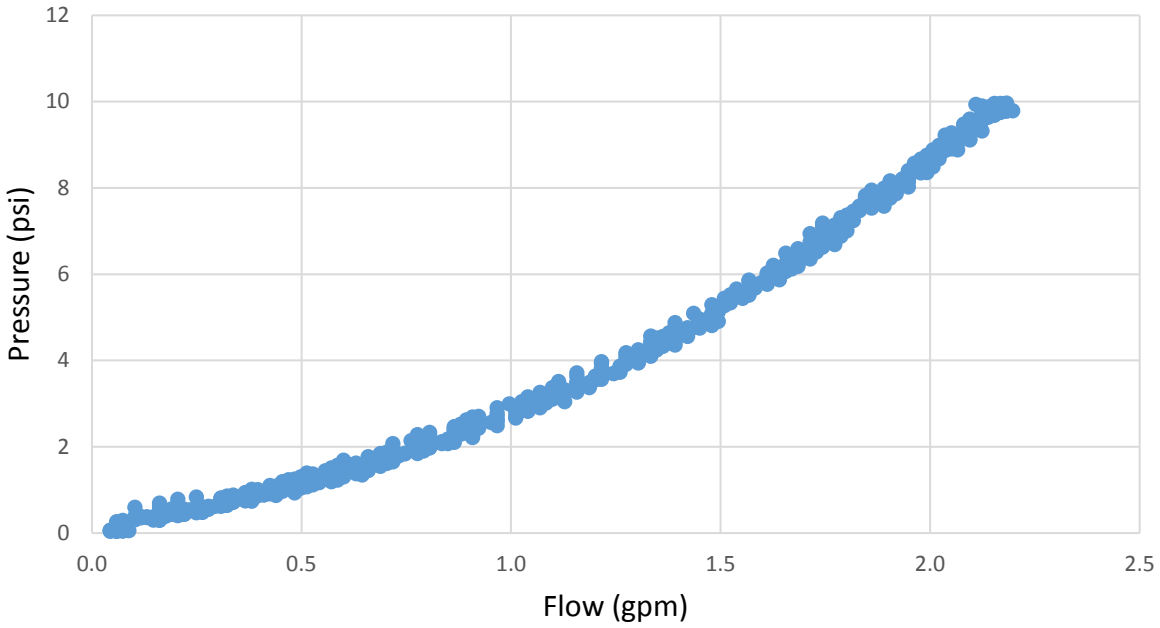

Figure D2.23. 0.19 in ID, 6 in length

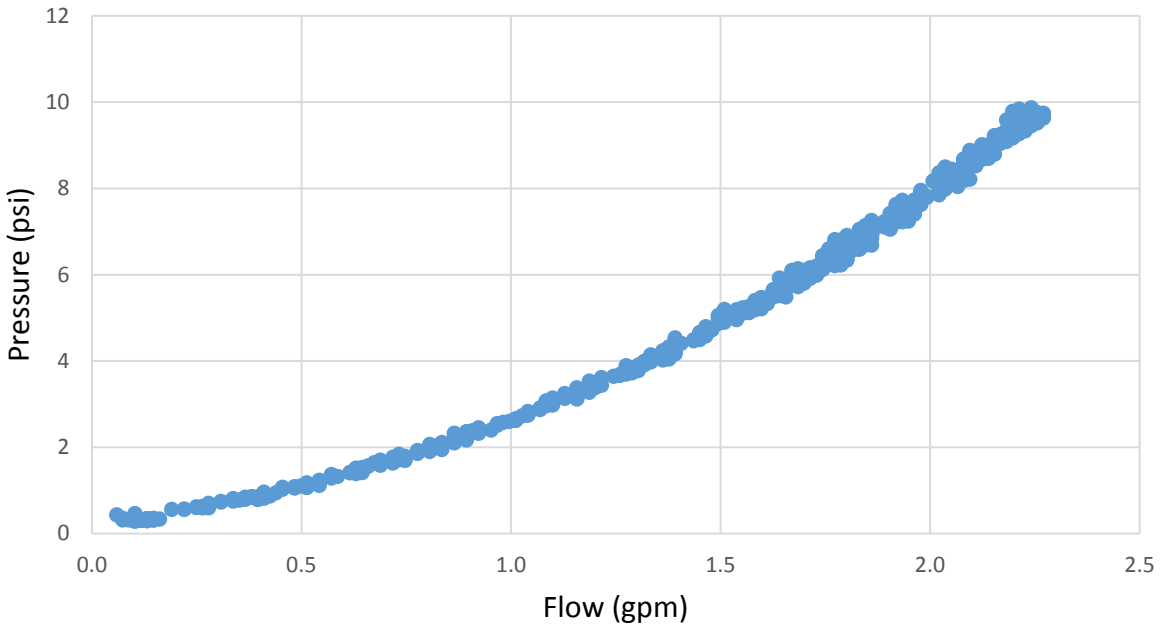

Figure D2.24. 0.18 in ID, 5 in length

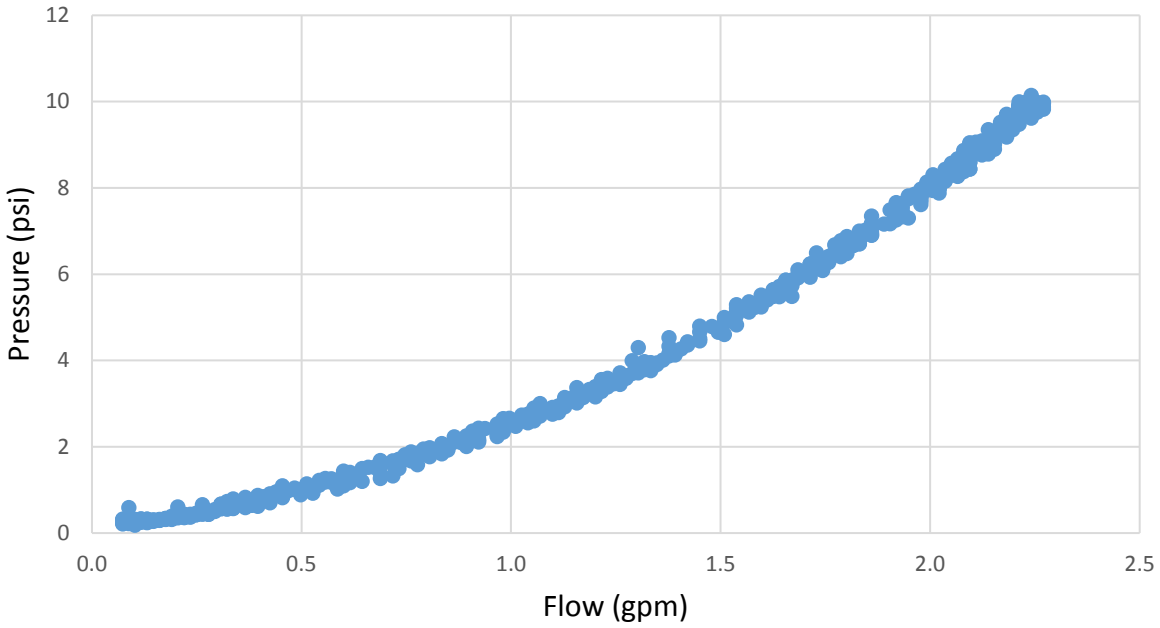

Figure D2.25. 0.177 in ID, 4 in length

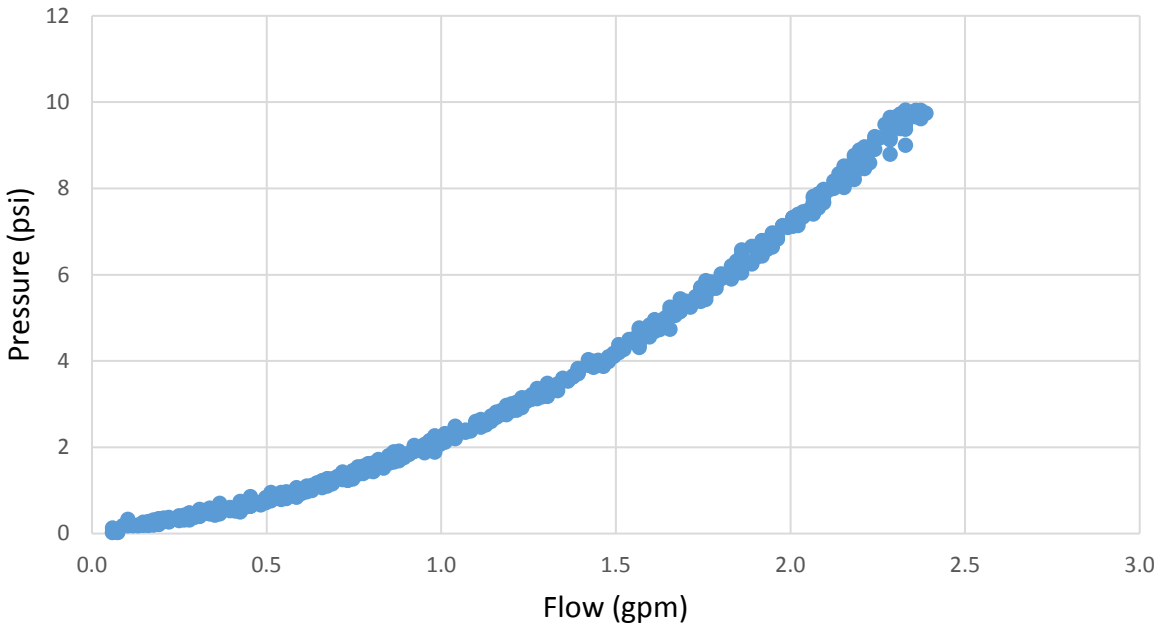

Figure D2.26. 0.183 in ID, 3 in length

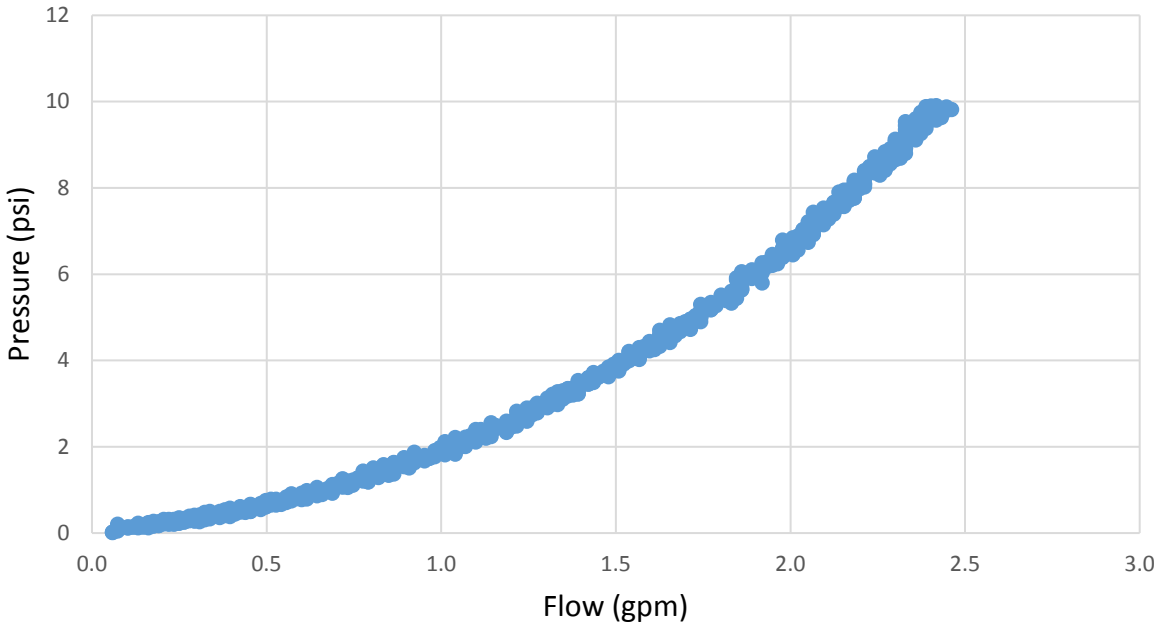

Figure D2.27. 0.19 in ID, 2 in length

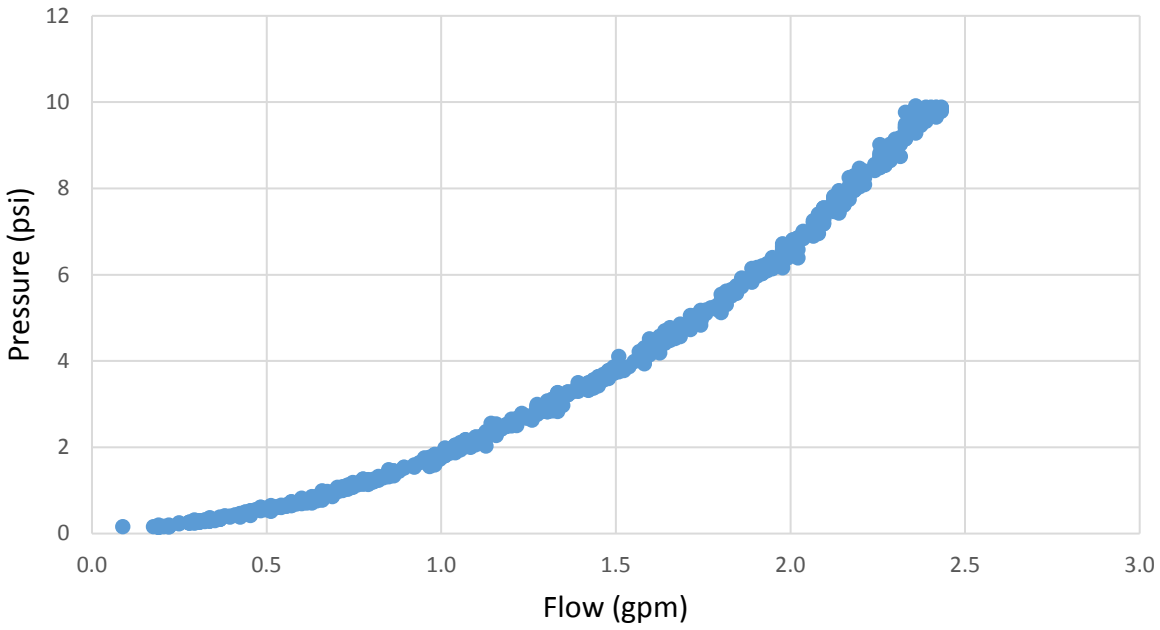

Figure D2.28. 0.18 in ID, 1 in length

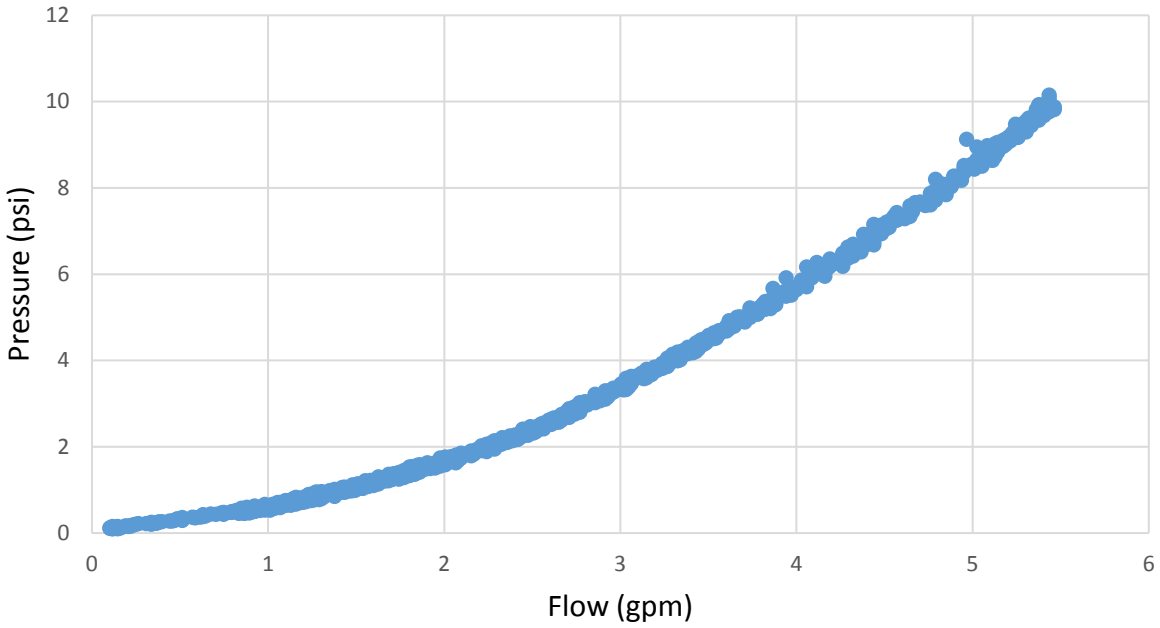

Figure D2.29. 0.28 in ID, 4 in length

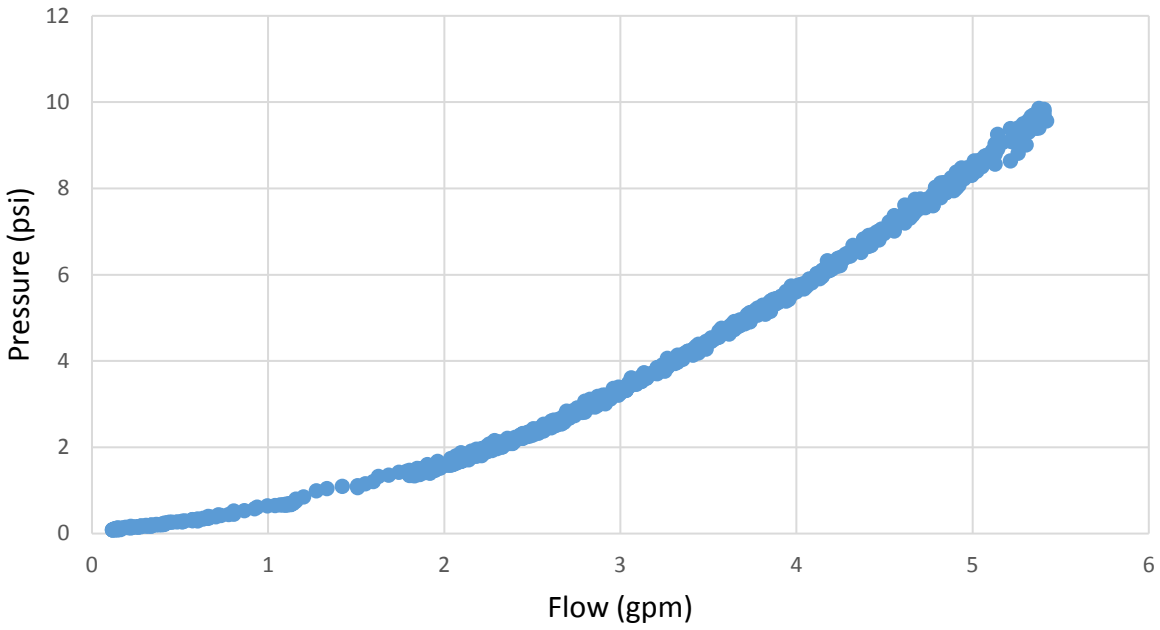

Figure D2.30. 0.275 in ID, 3 in length

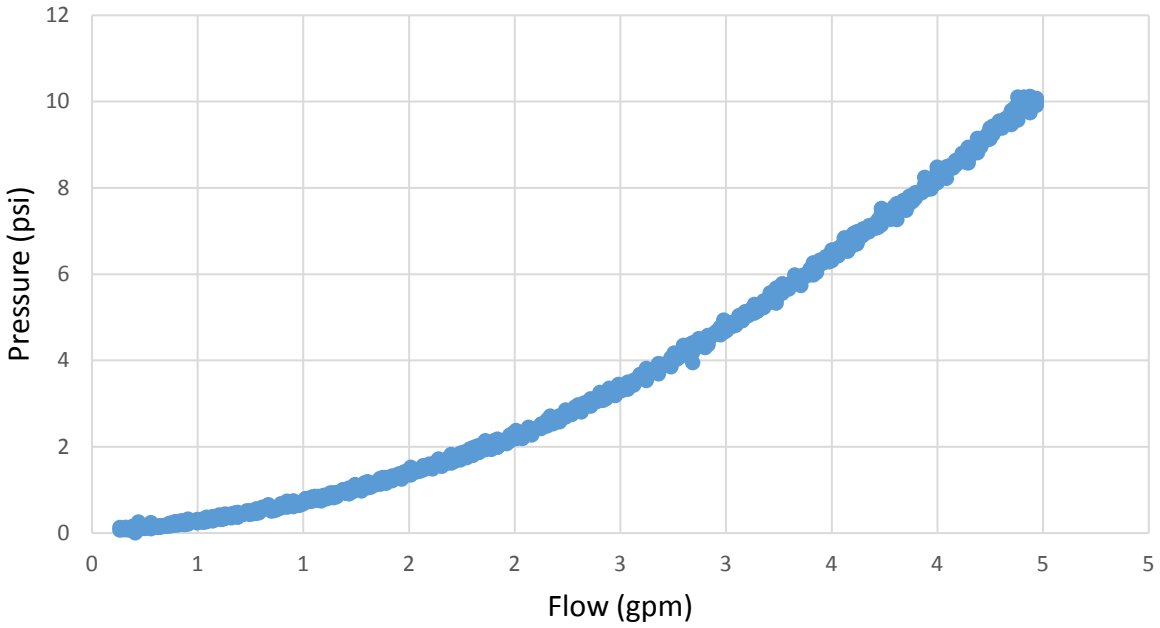

Figure D2.31. 0.245 in ID, 2 in length

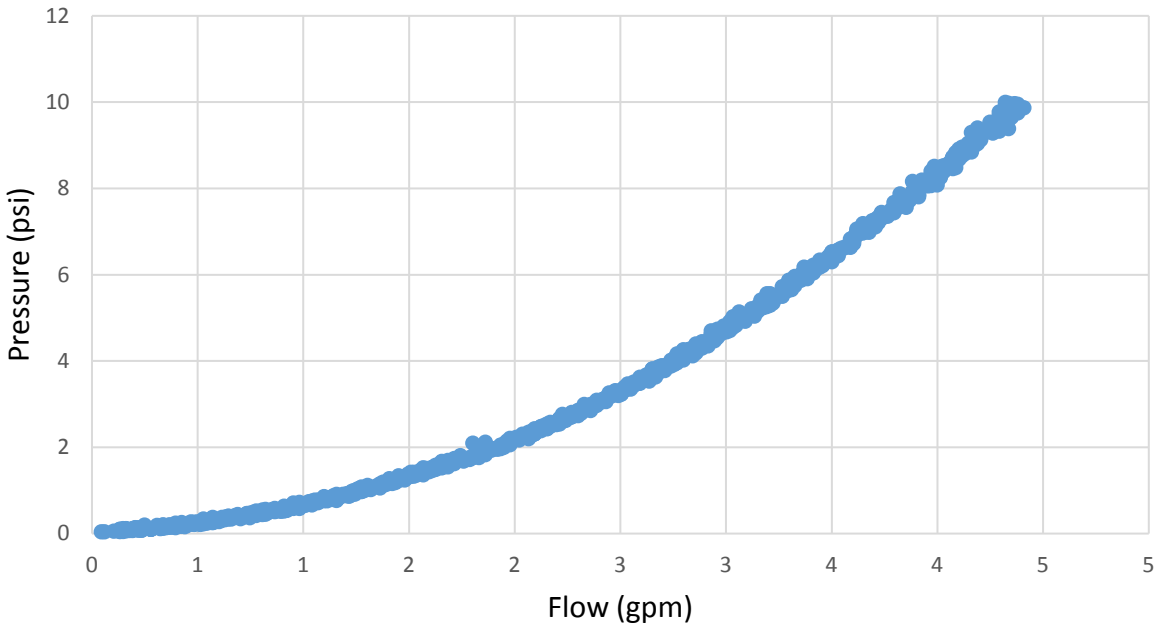

Figure D2.32. 0.247 in ID, 1.5 in length

APPENDIX E: FIELD TEST RAW DATA

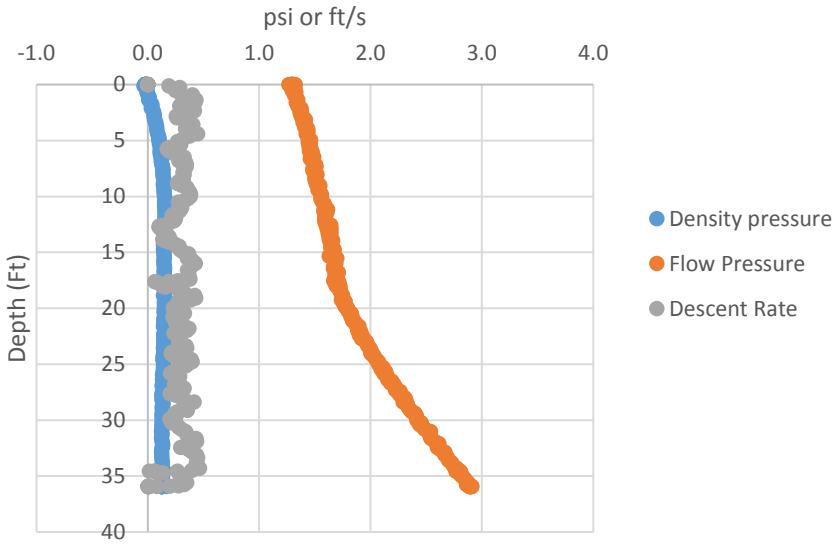

Figure E.1. Water calibration test 1 raw data vs depth

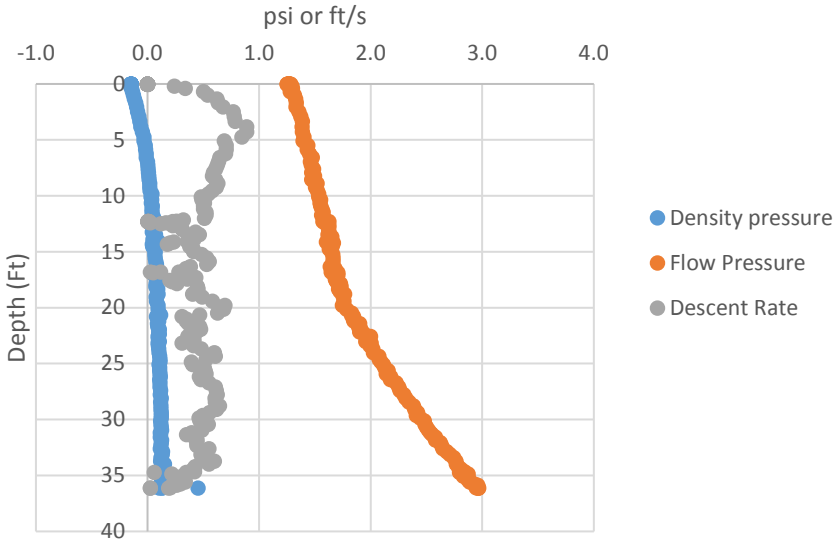

Figure E.2. Water calibration test 2 raw data vs depth

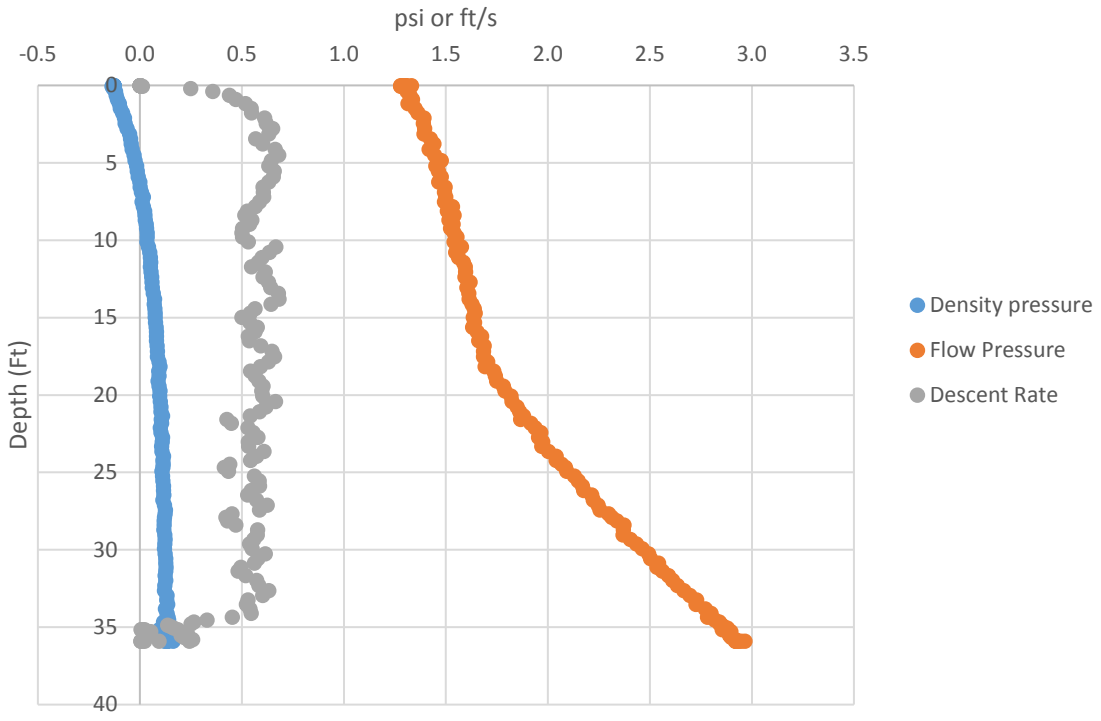

Figure E.3. Water calibration test 3 raw data vs depth

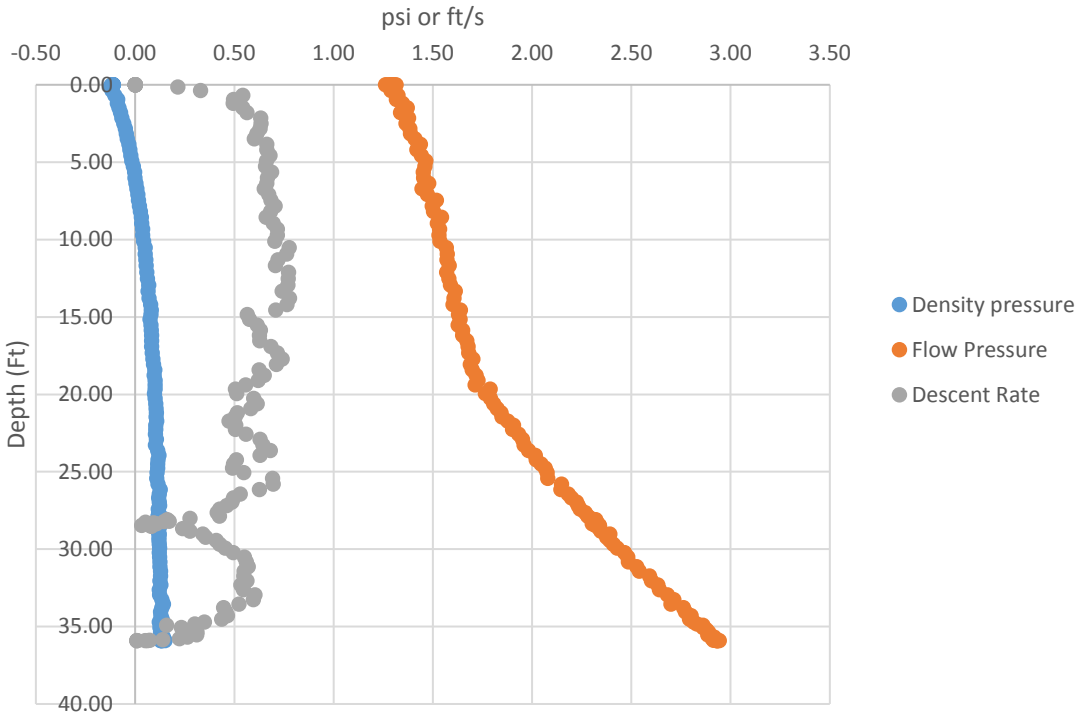

Figure E.4. Water calibration test 4 raw data vs depth

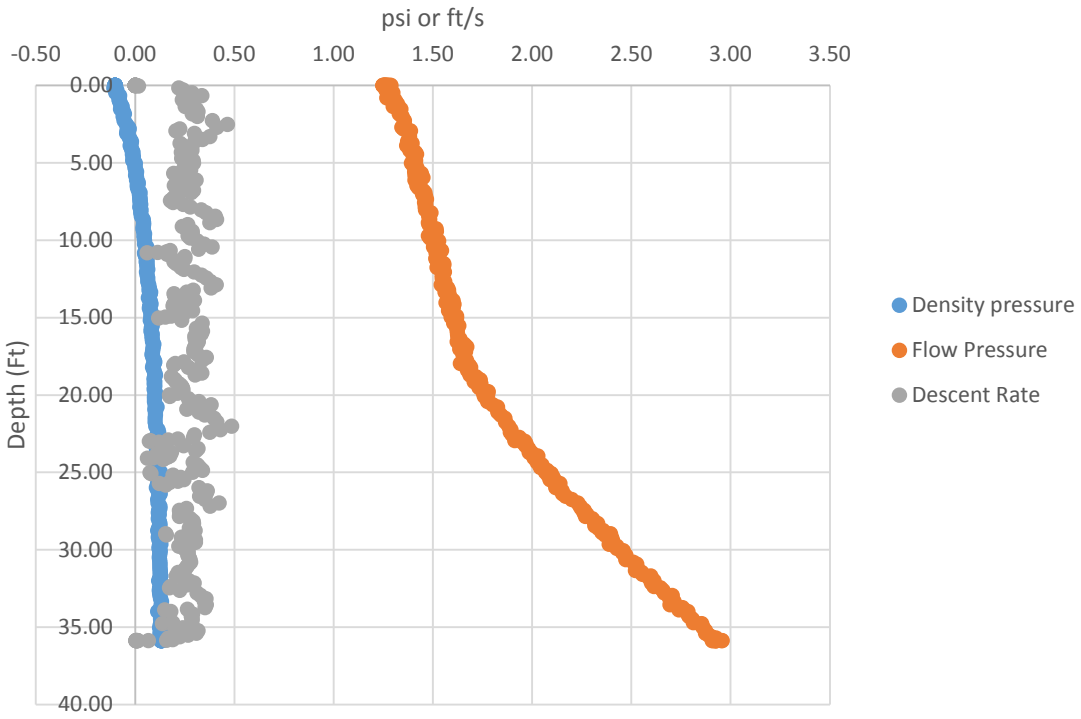

Figure E.5. Water calibration test 5 raw data vs depth

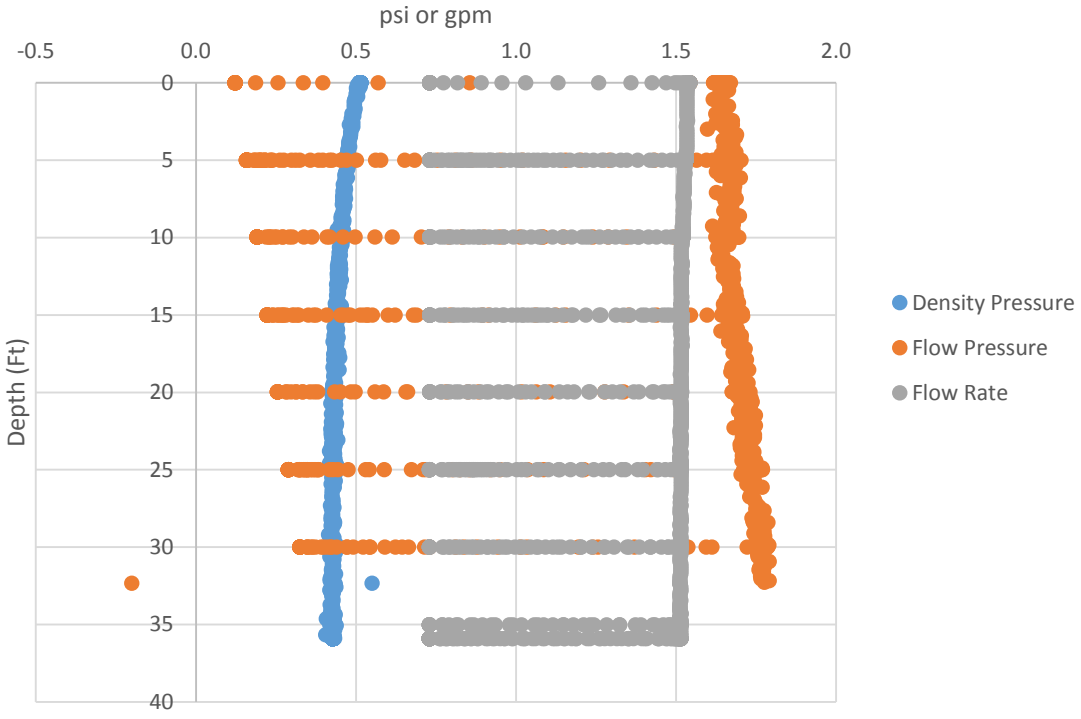

Figure E.6. Water calibration test 6 raw data vs depth

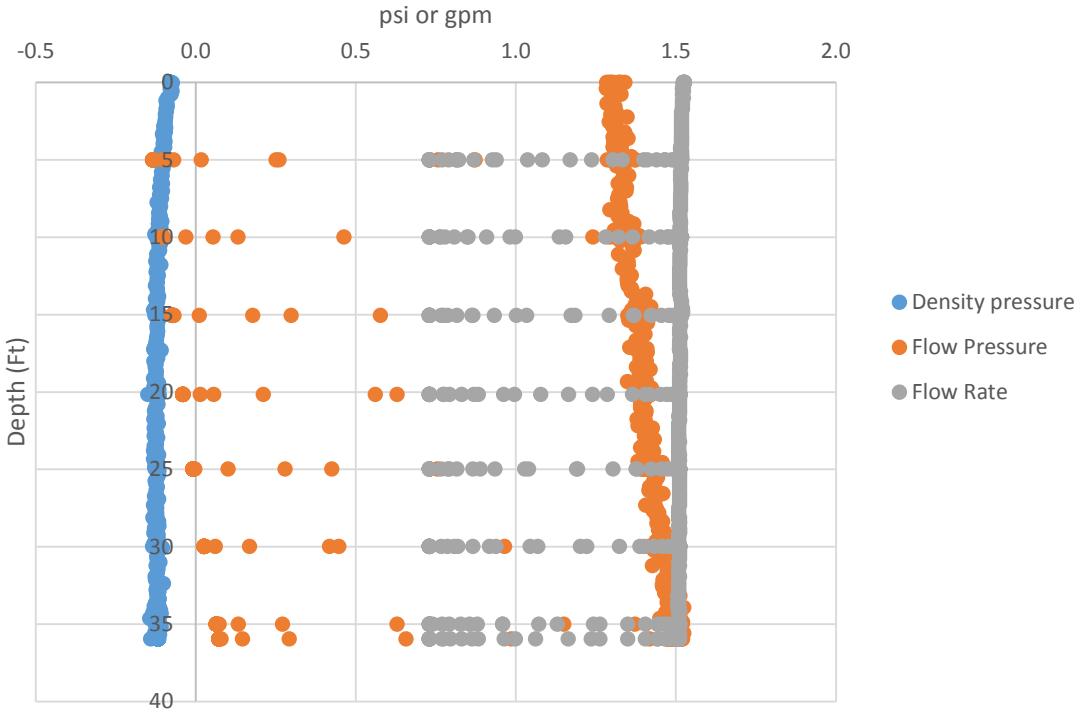

Figure E.7. Water calibration test 7 raw data vs depth

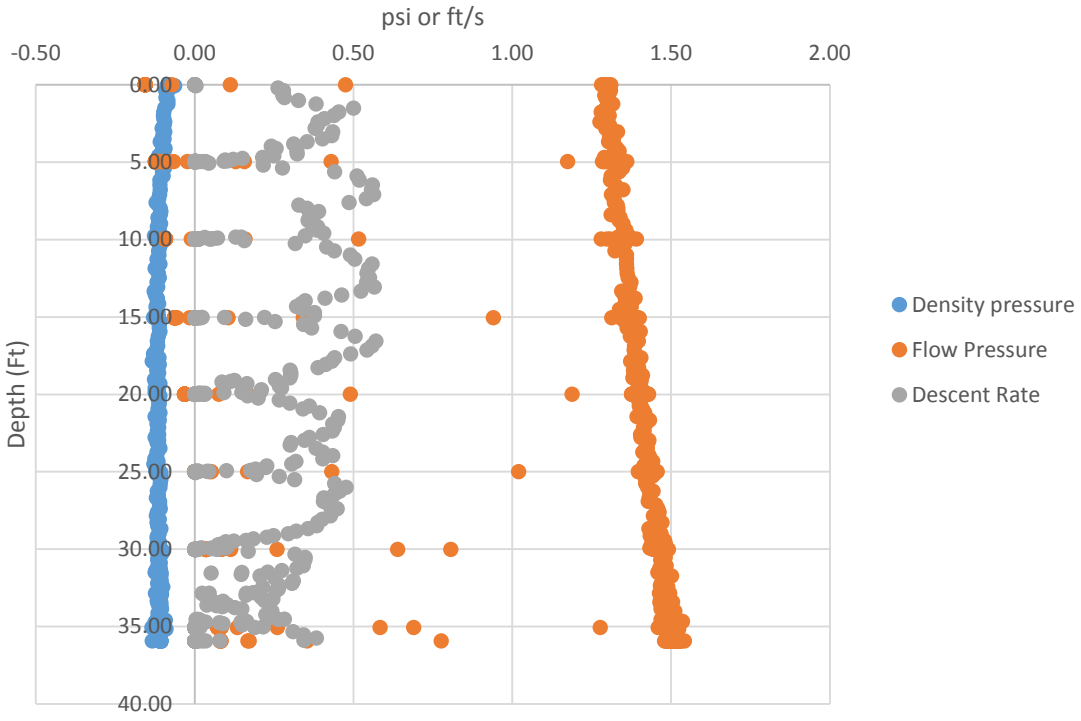

Figure E.8. Water calibration test 8 raw data vs depth

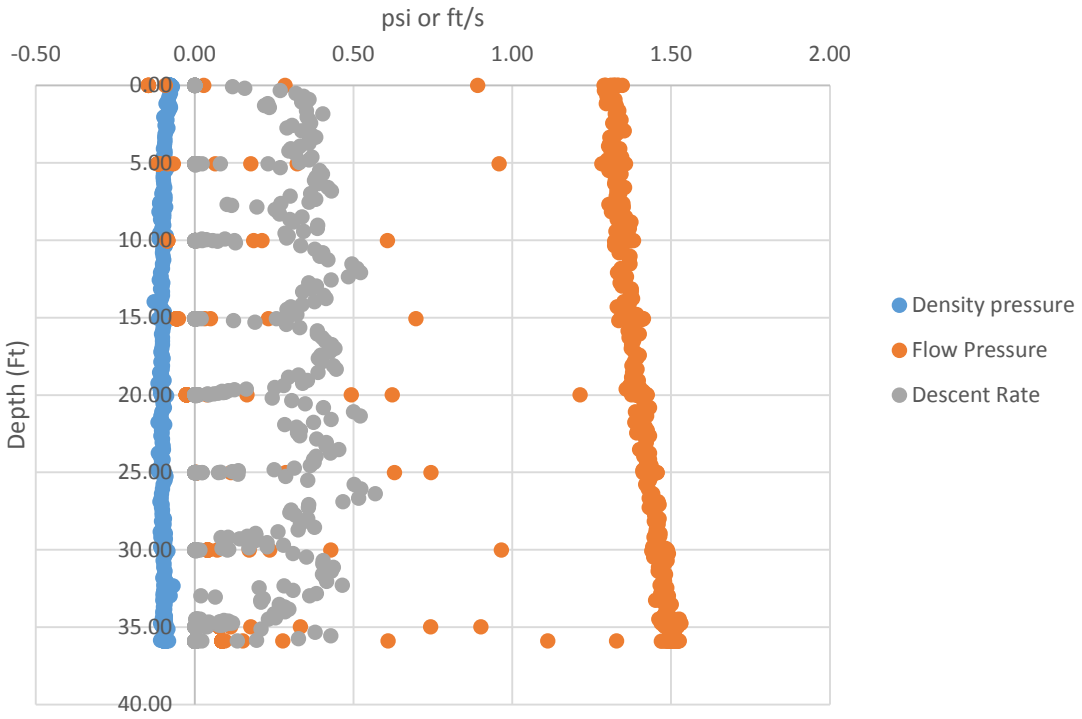

Figure E.9. Water calibration test 9 raw data vs depth

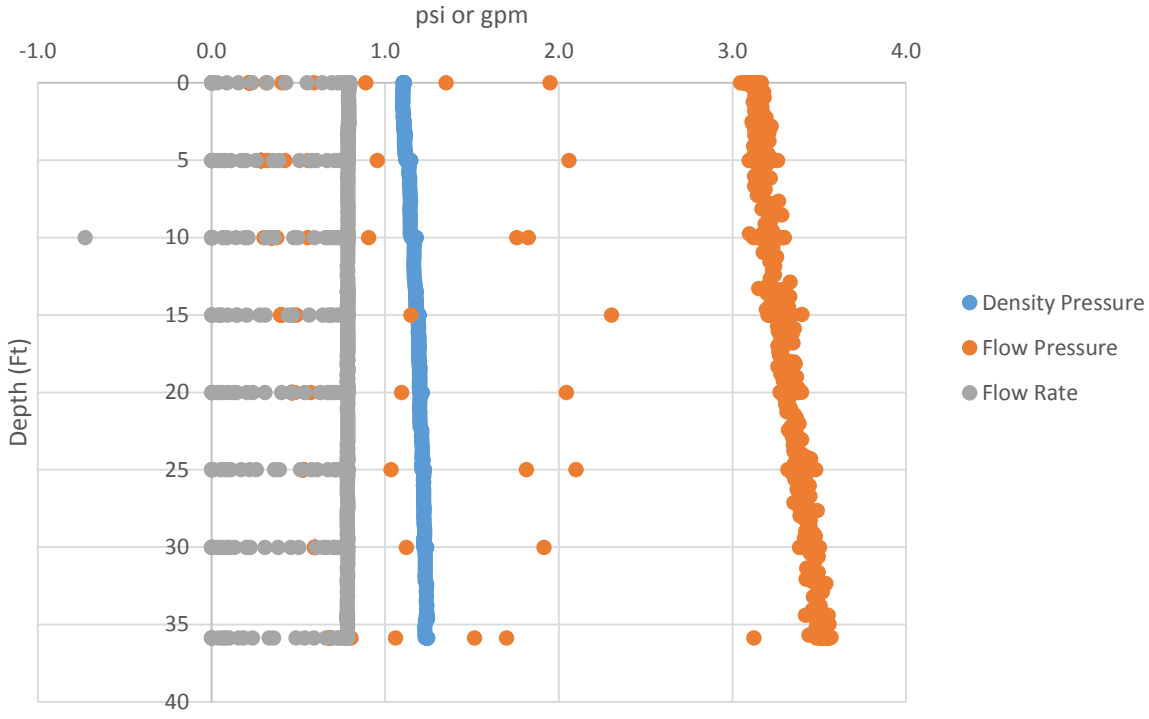

Figure E.10. Water calibration test 10 raw data vs depth

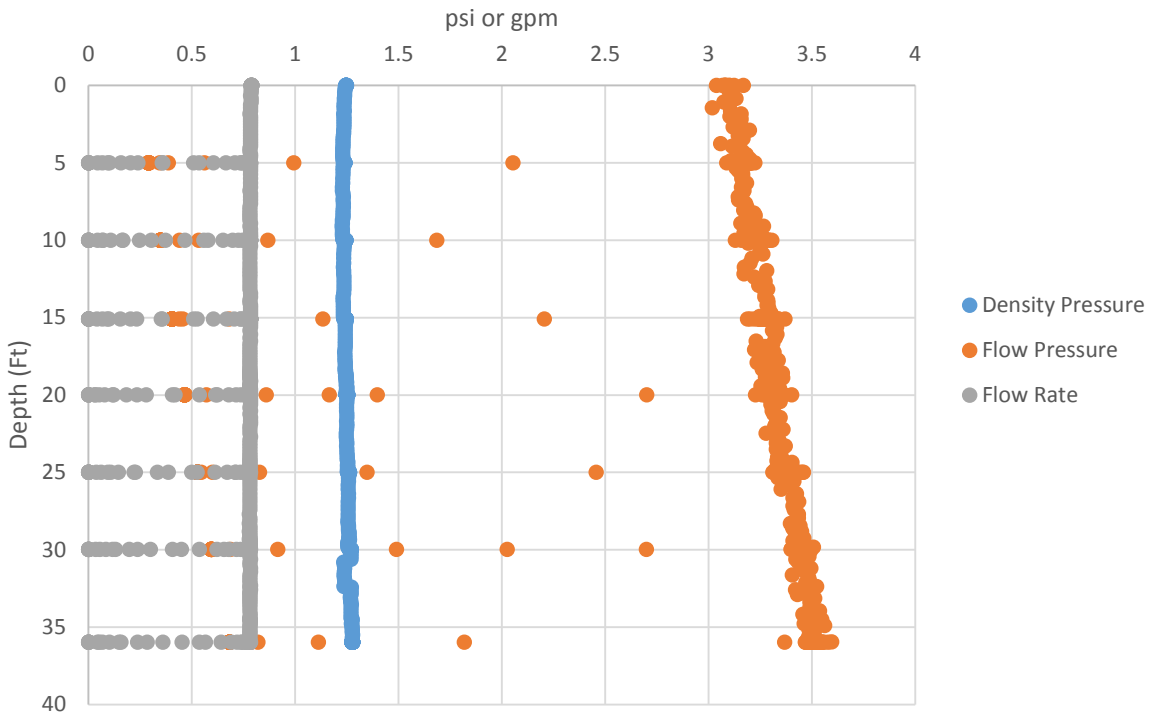

Figure E.11. Water calibration test 11 raw data vs depth

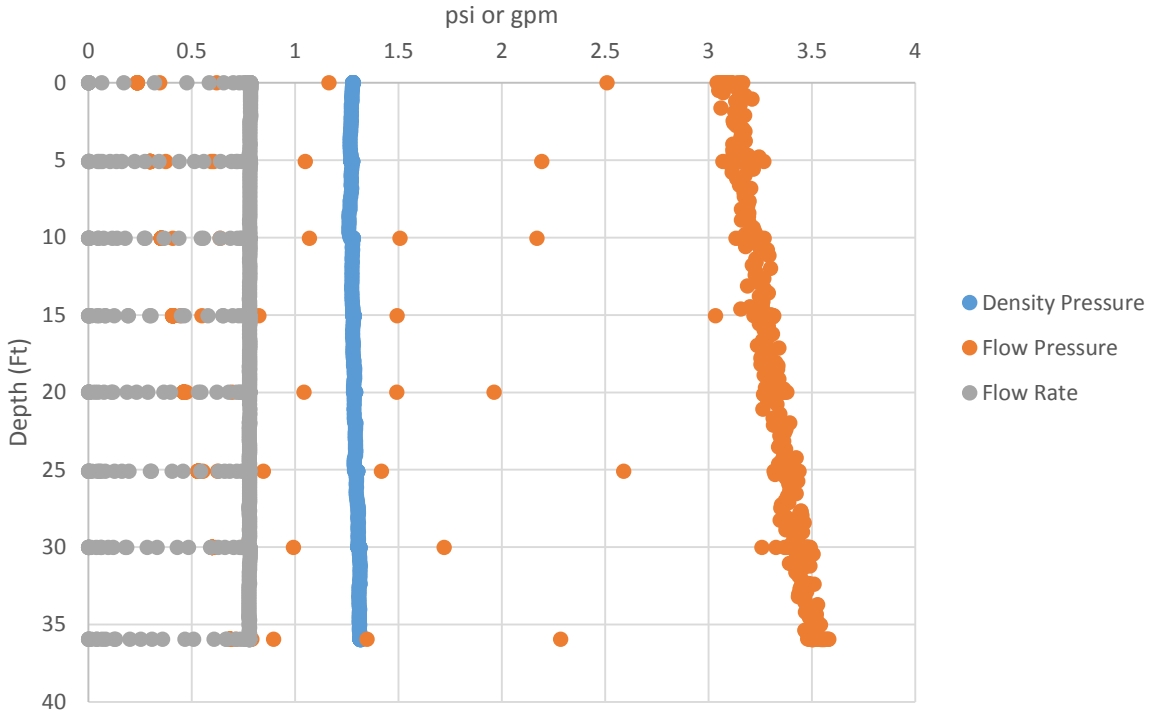

Figure E.12. Water calibration test 12 raw data vs depth

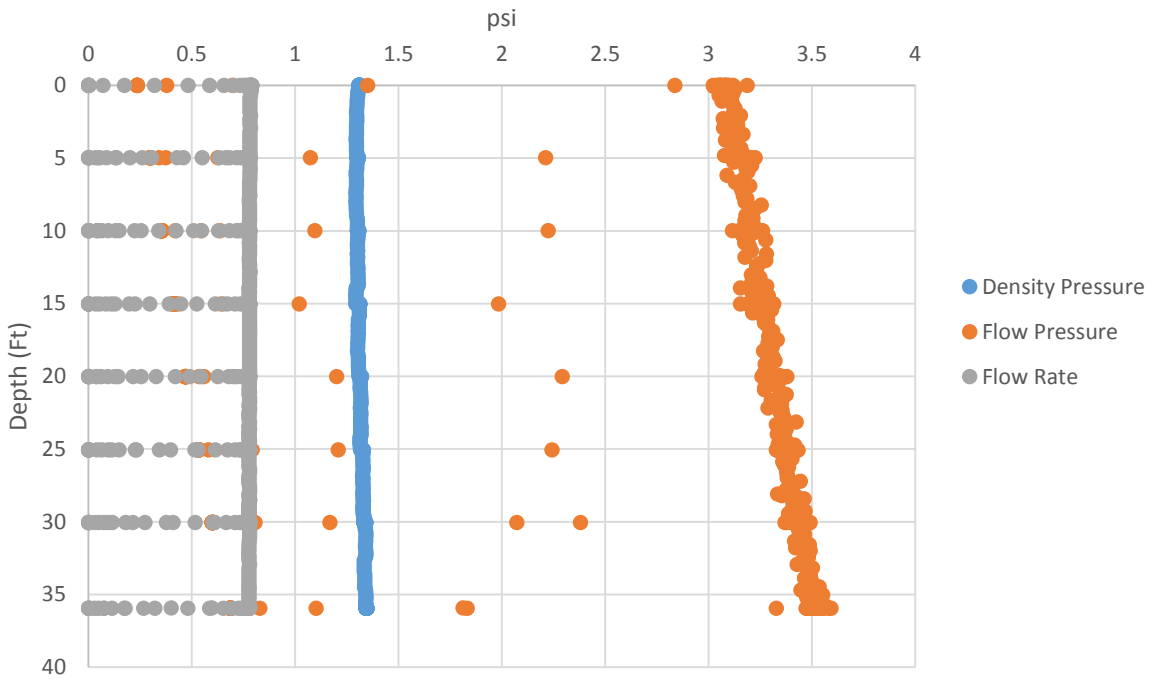

Figure E.13. Water calibration test 13 raw data vs depth

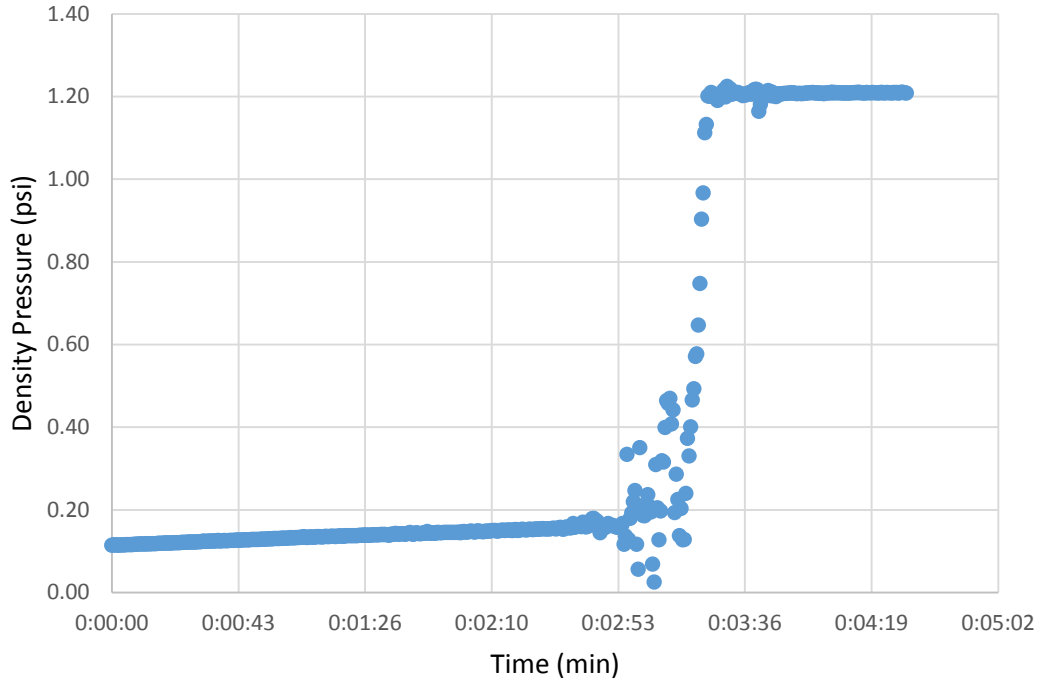

Figure E.14. Water calibration test 14 raw data vs depth (density pressure drift)

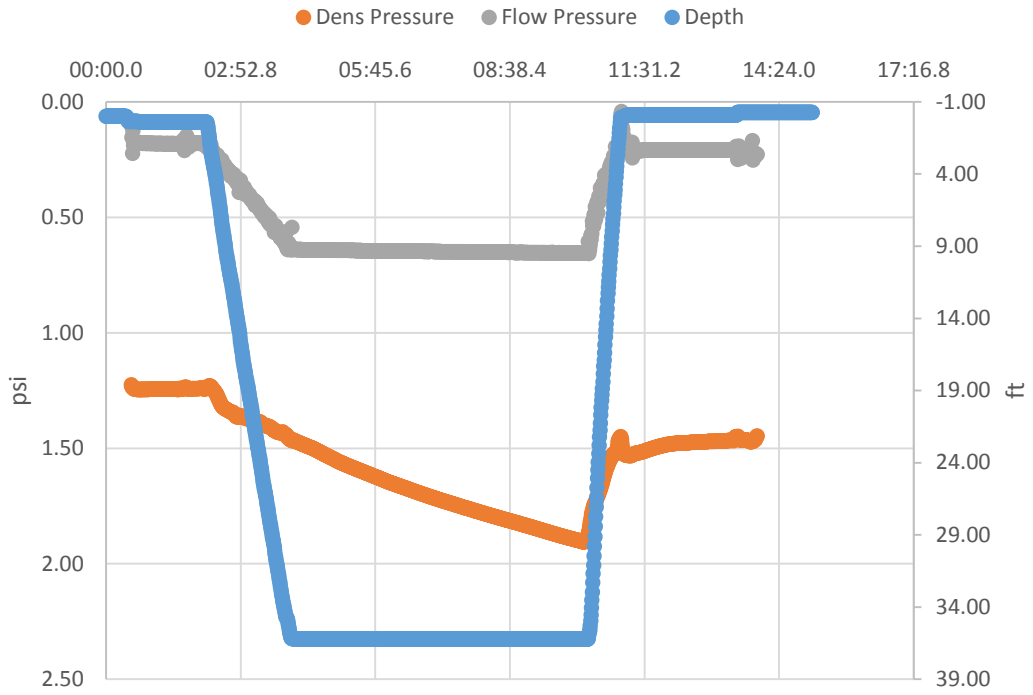

Figure E.15. Water calibration test 15 raw data vs depth (density low pressure port leak)

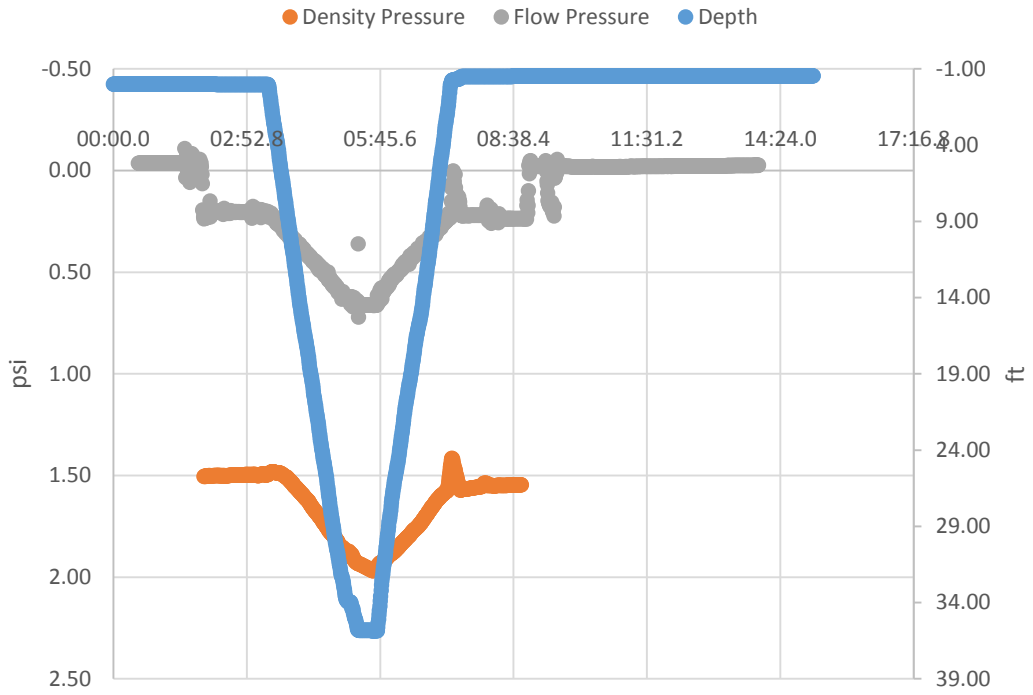

Figure E.16. Water calibration test 16 raw data vs depth (both low pressure ports have air in lines)

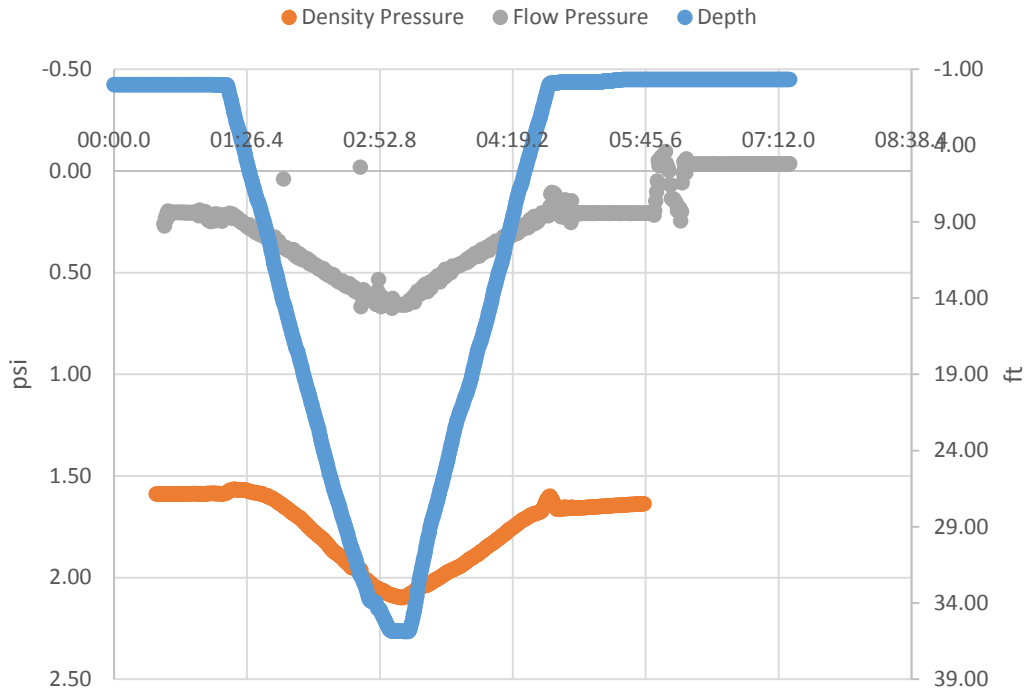

Figure E.17. Water calibration test 17 raw data vs depth

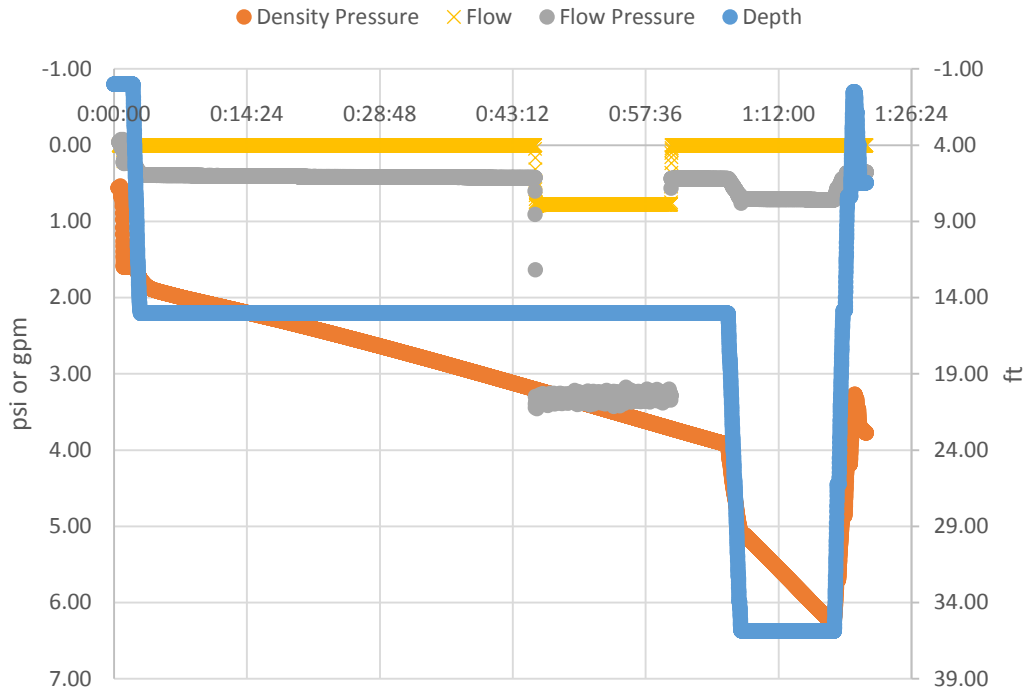

Figure E.18. Water calibration test 18 raw data vs depth (density low pressure port leak)

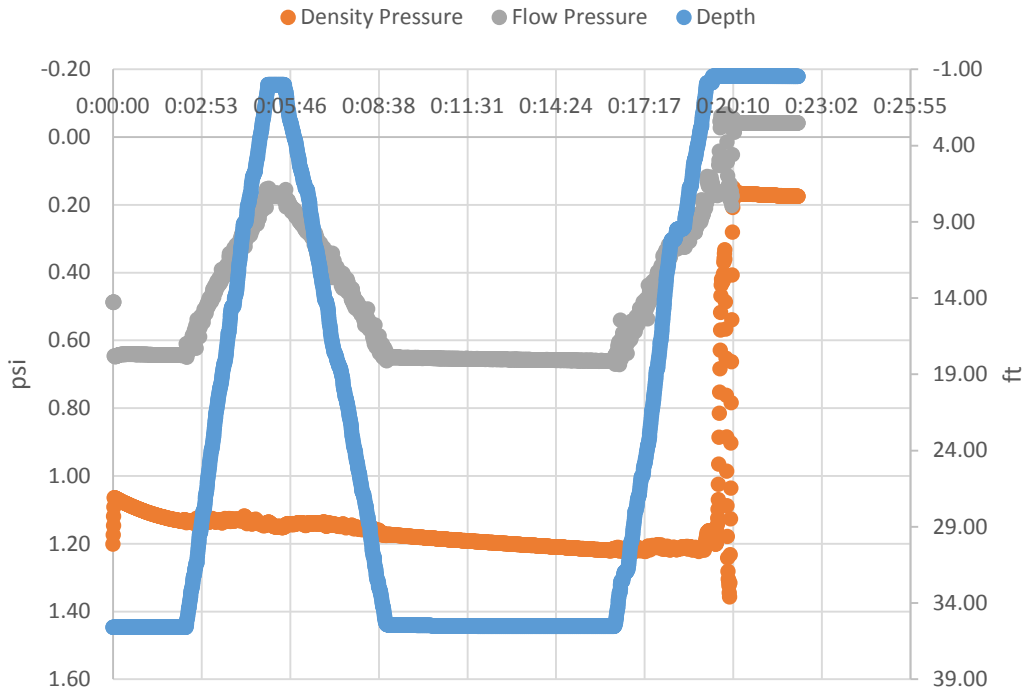

Figure E.19. Water calibration test 19 raw data vs depth

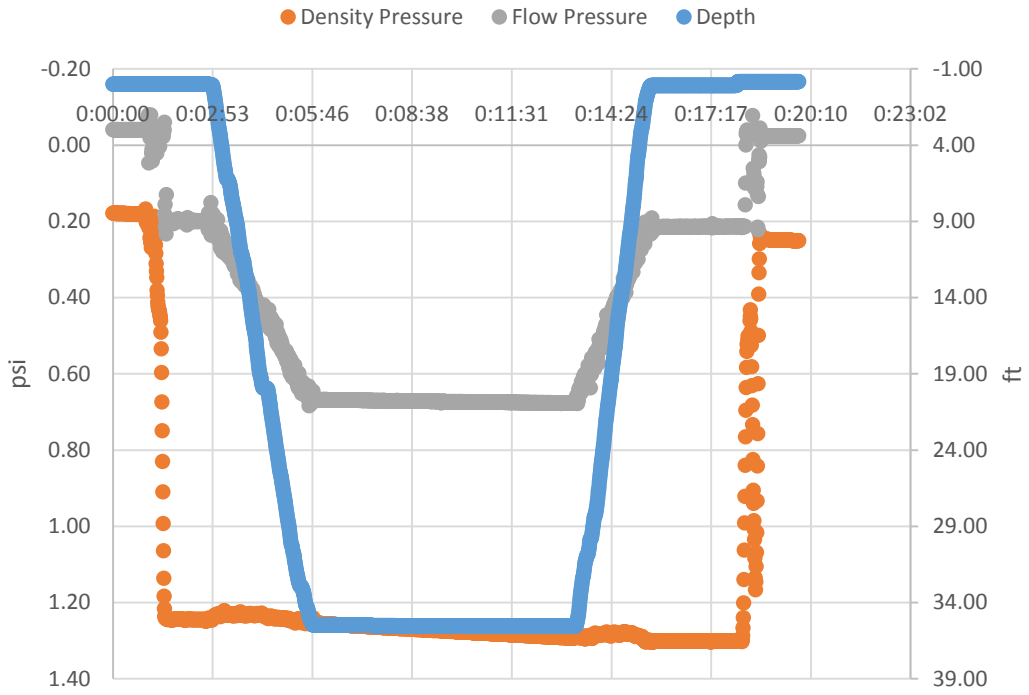

Figure E.20. Water calibration test 20 raw data vs depth

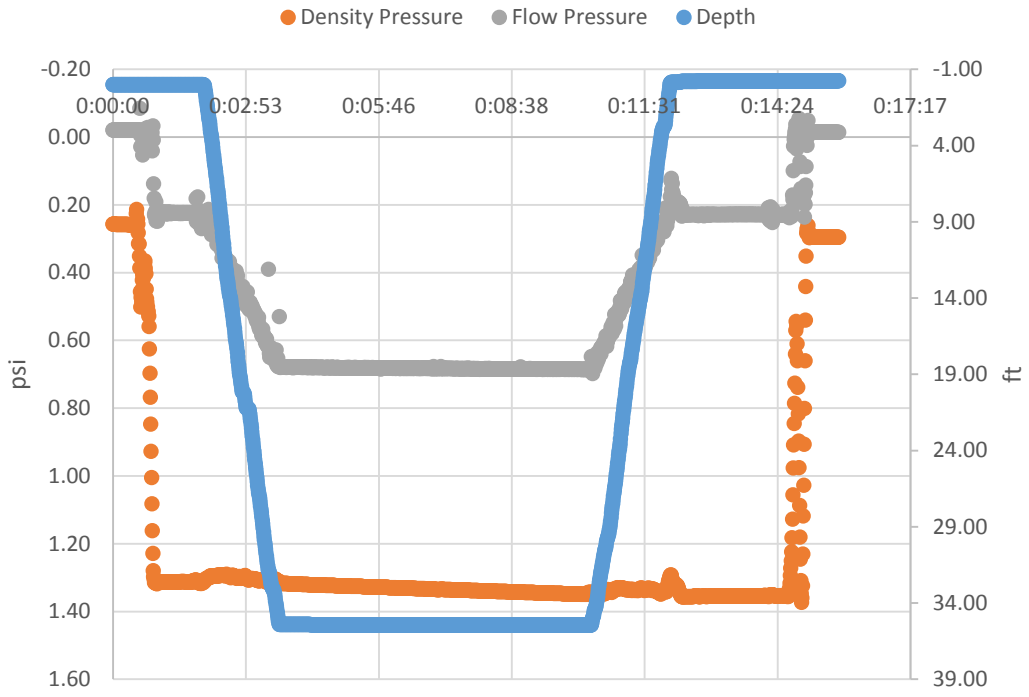

Figure E.21. Water calibration test 21 raw data vs depth

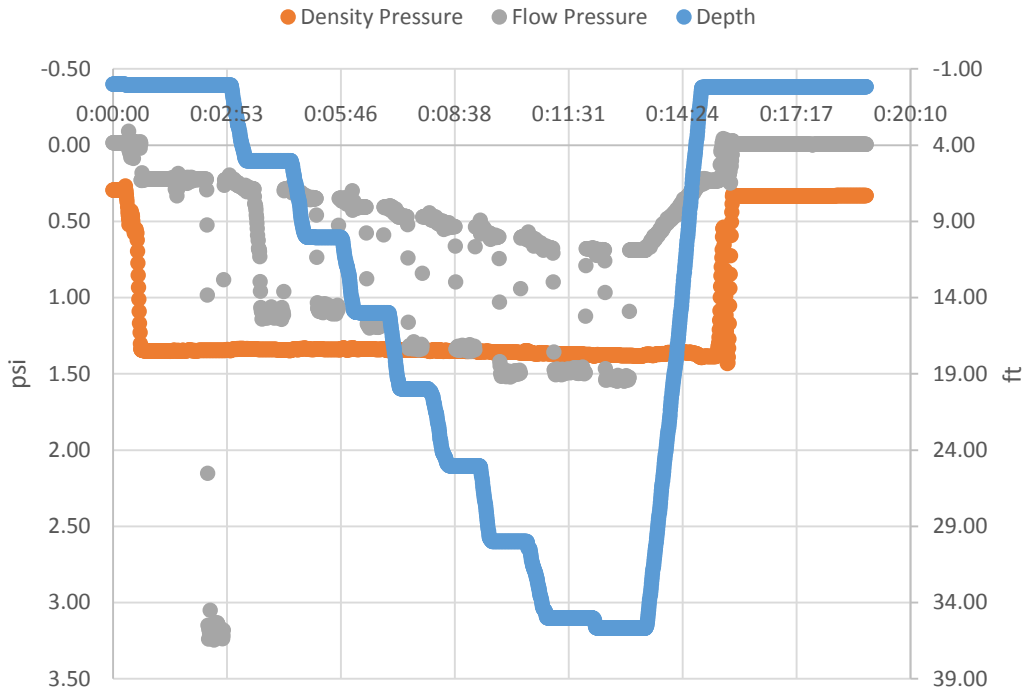

Figure E.22. Water calibration test 22 raw data vs depth

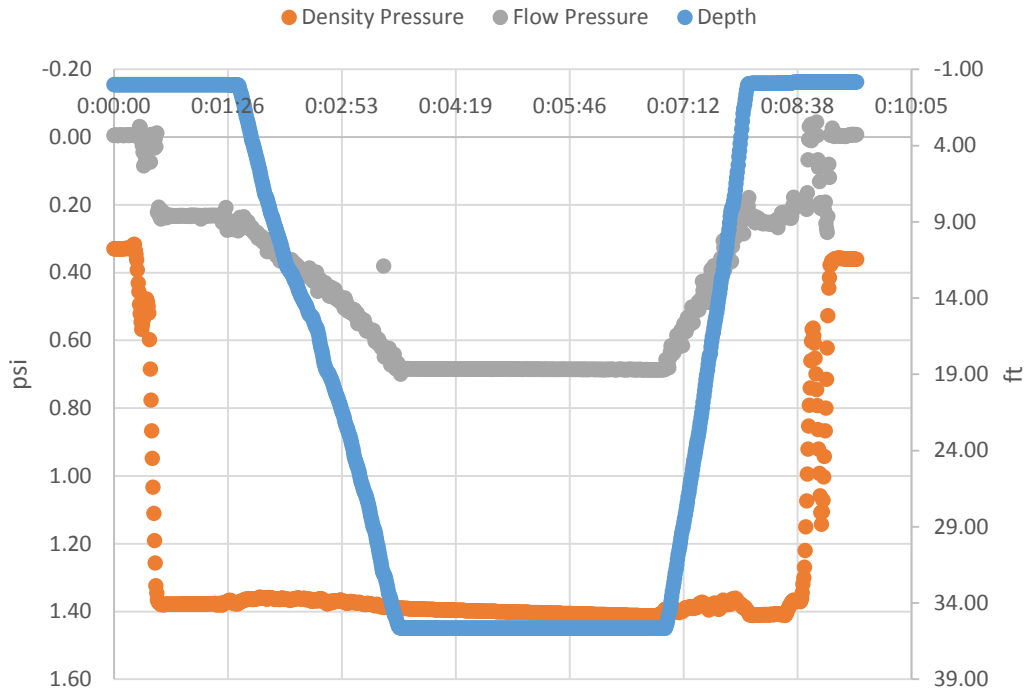

Figure E.23. Water calibration test 23 raw data vs depth

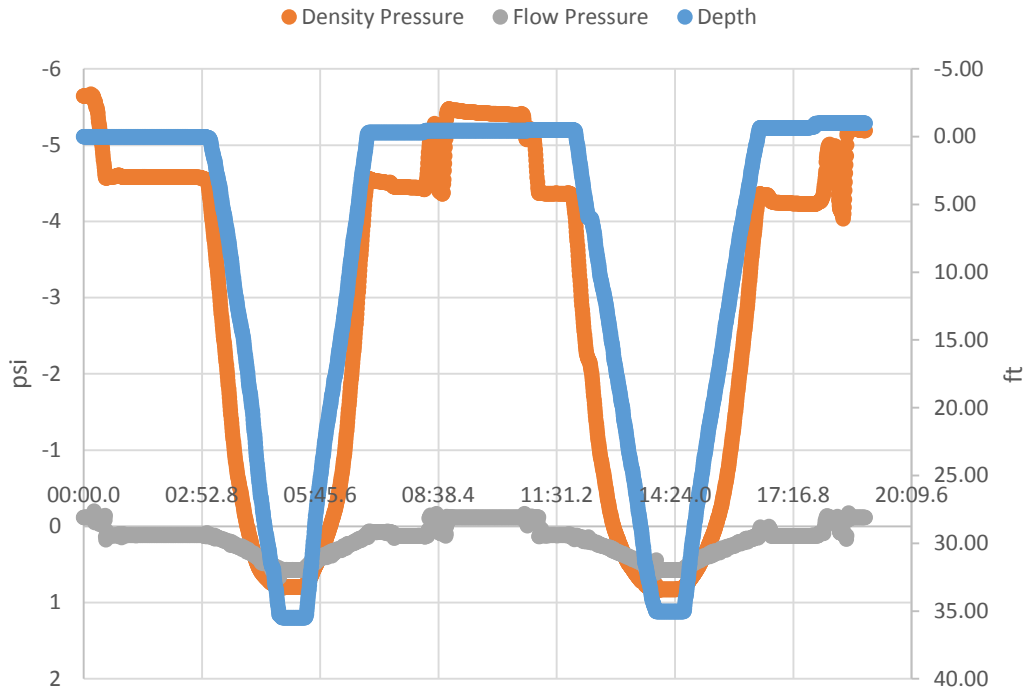

Figure E.24. Water calibration test 24 raw data vs depth (broken low pressure port)

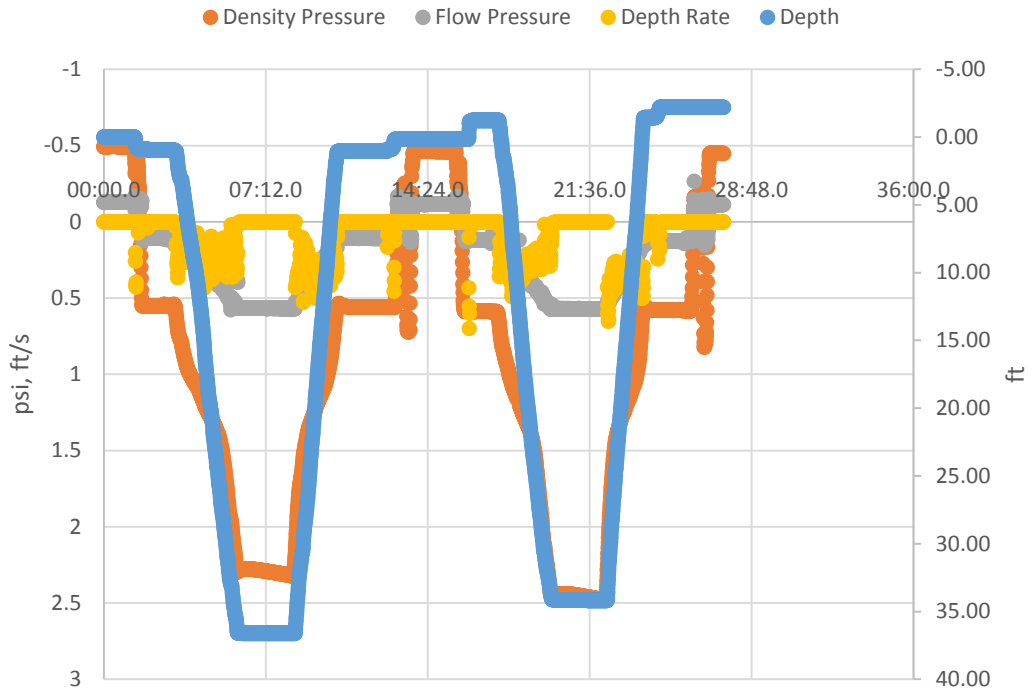

Figure E.25. Water calibration test 25 raw data vs depth (density port re-purged but still broken)

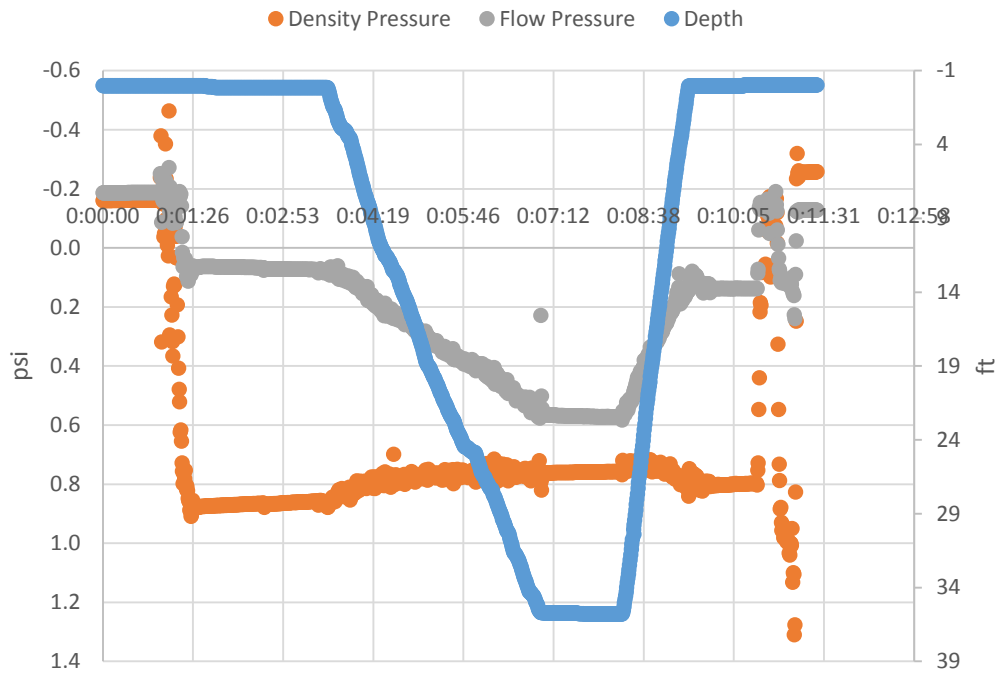

Figure E.26. Slurry column test 1 raw data in clear water

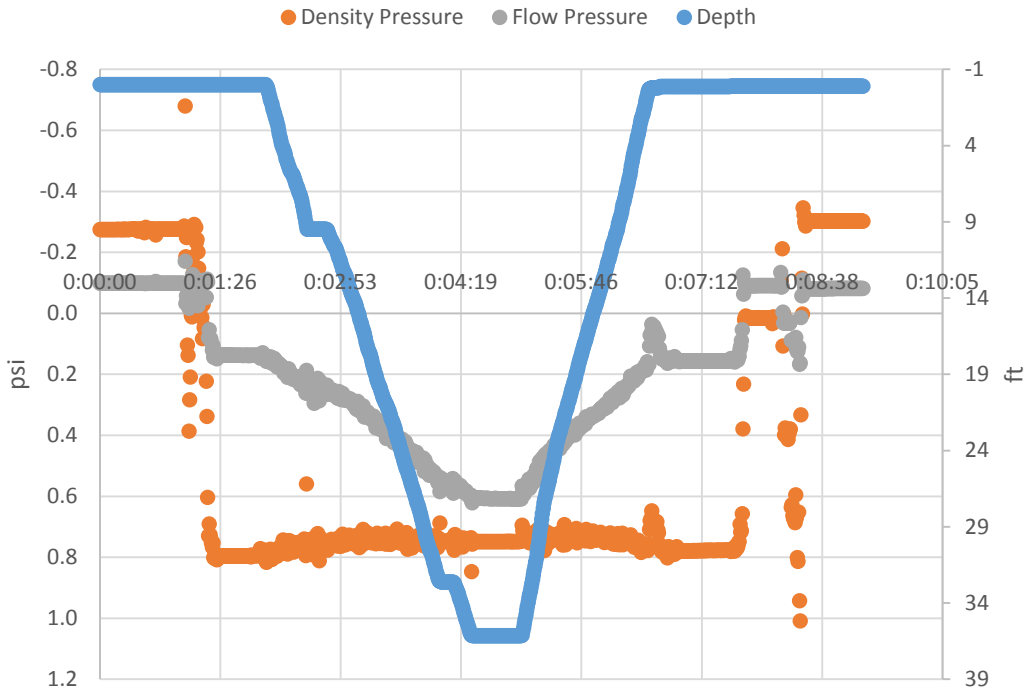

Figure E.27. Slurry column test 2 raw data in clear water

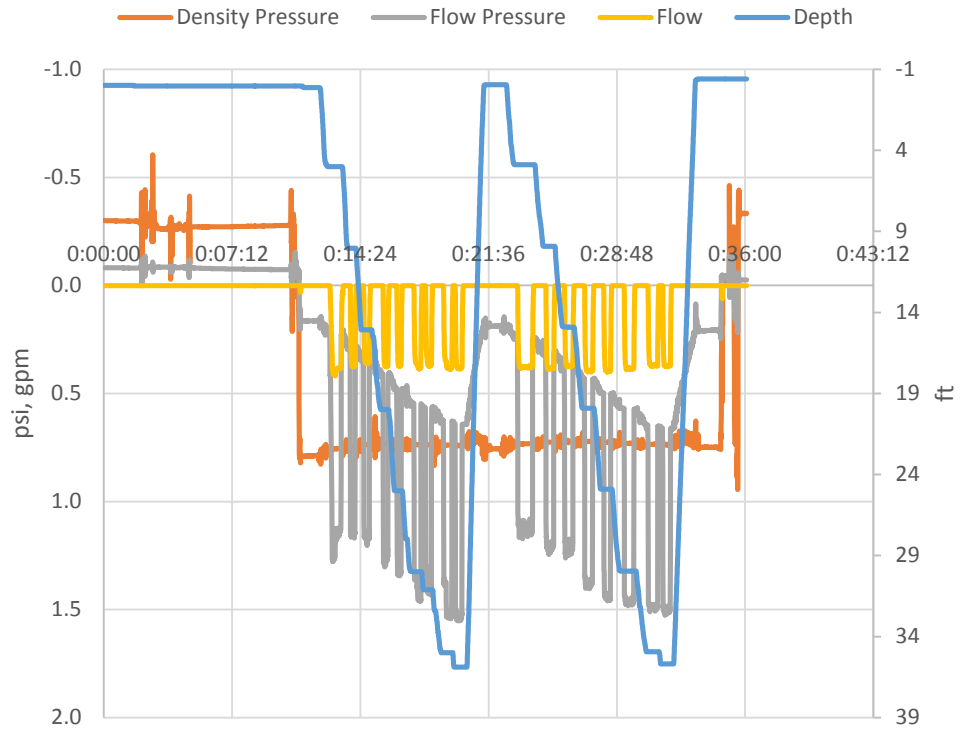

Figure E.28. Slurry column test 3 raw data in clear water

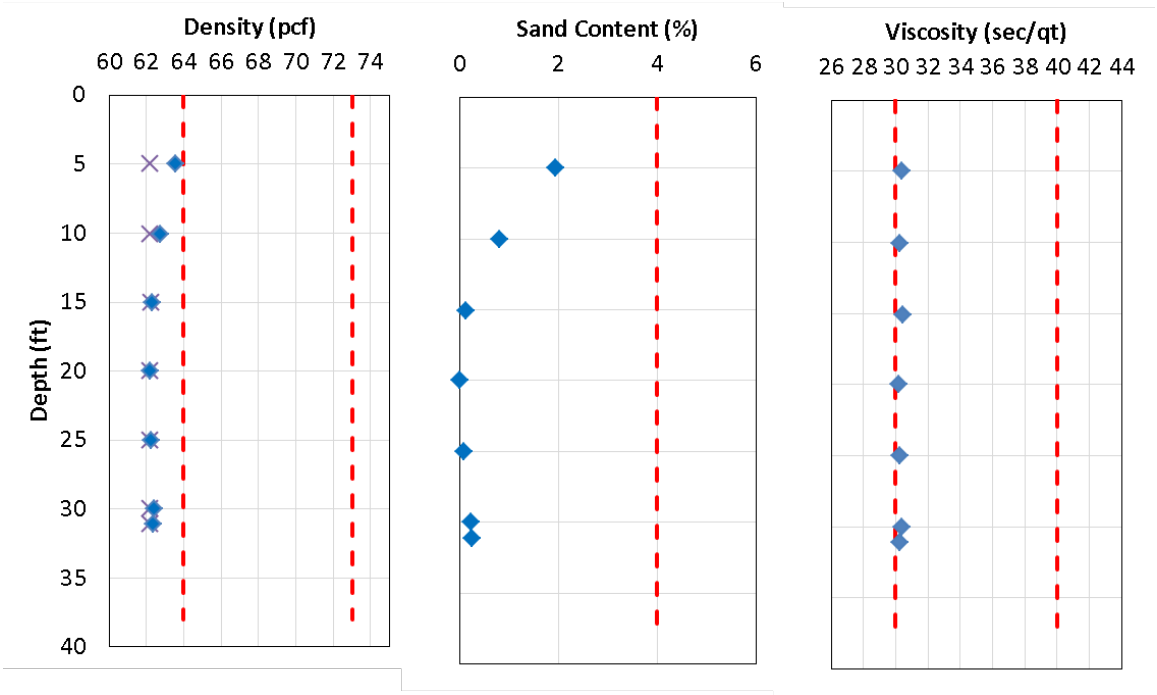

Figure E.29. Slurry column test 3 with no sand

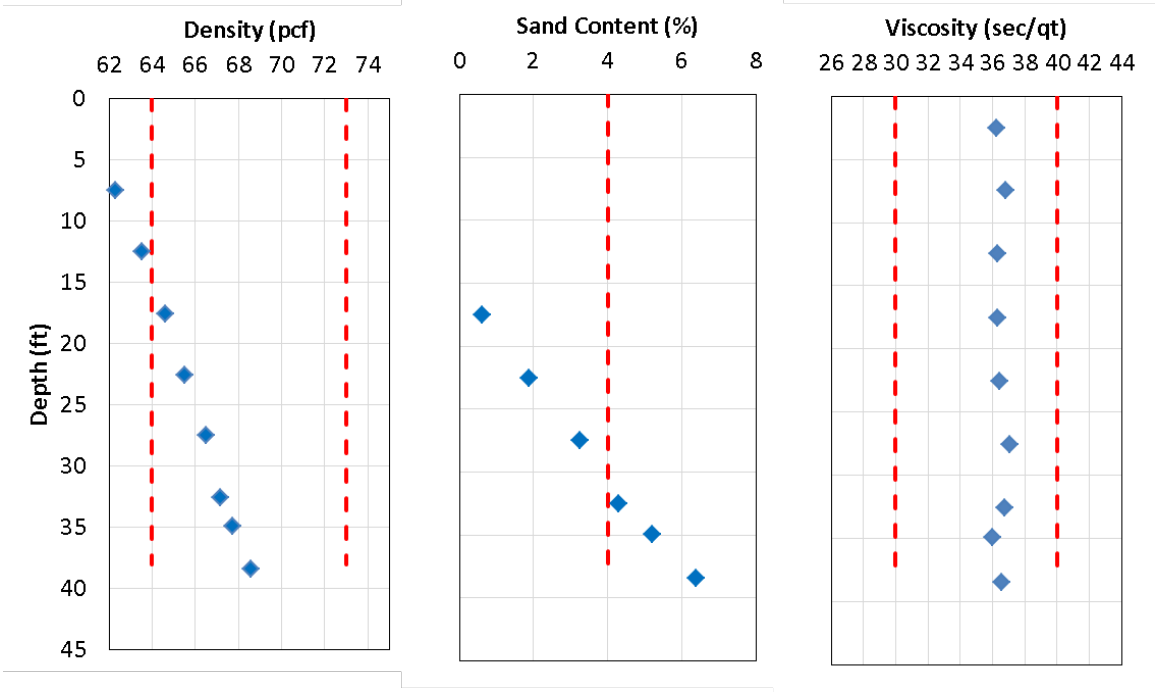

Figure E.30. Slurry column test 4 with no sand

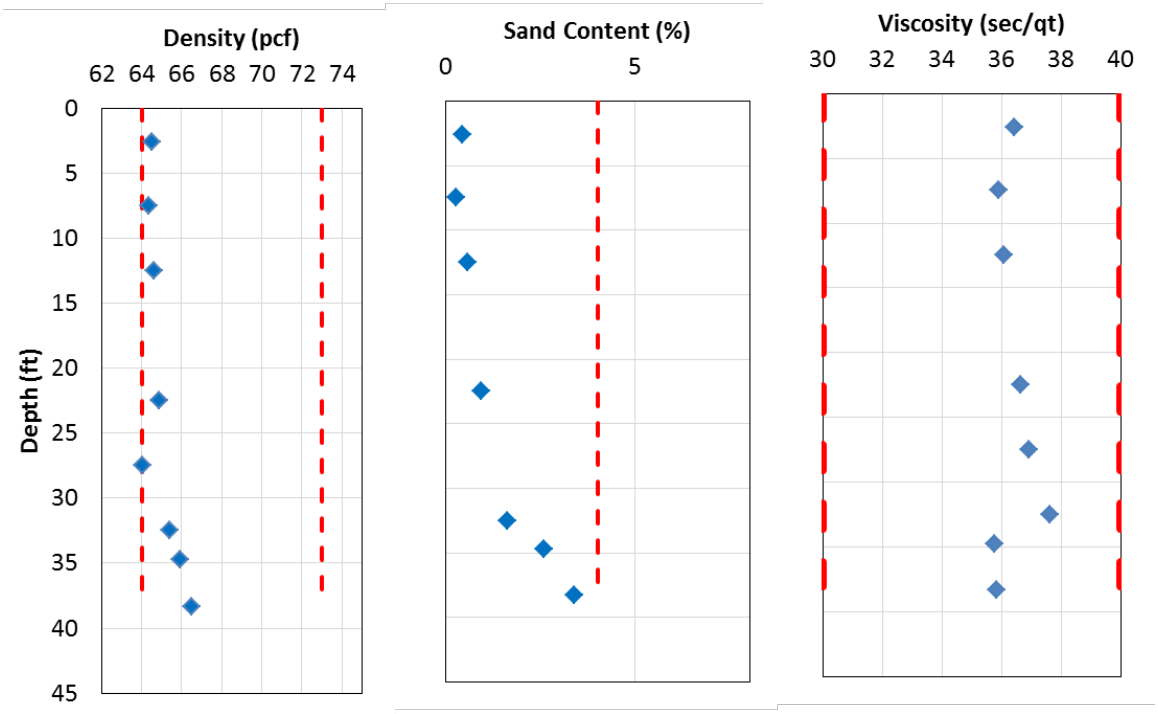

Figure E.31. Slurry column test 5 with no sand

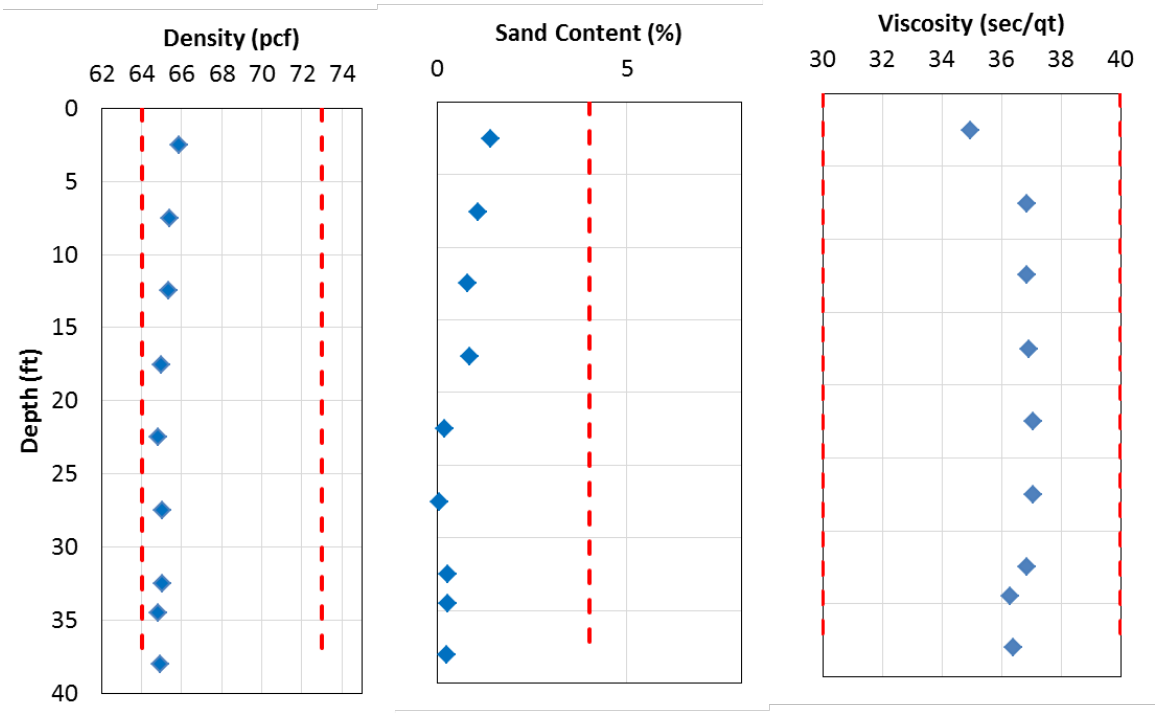

Figure E.32. Slurry column test 6 with no sand

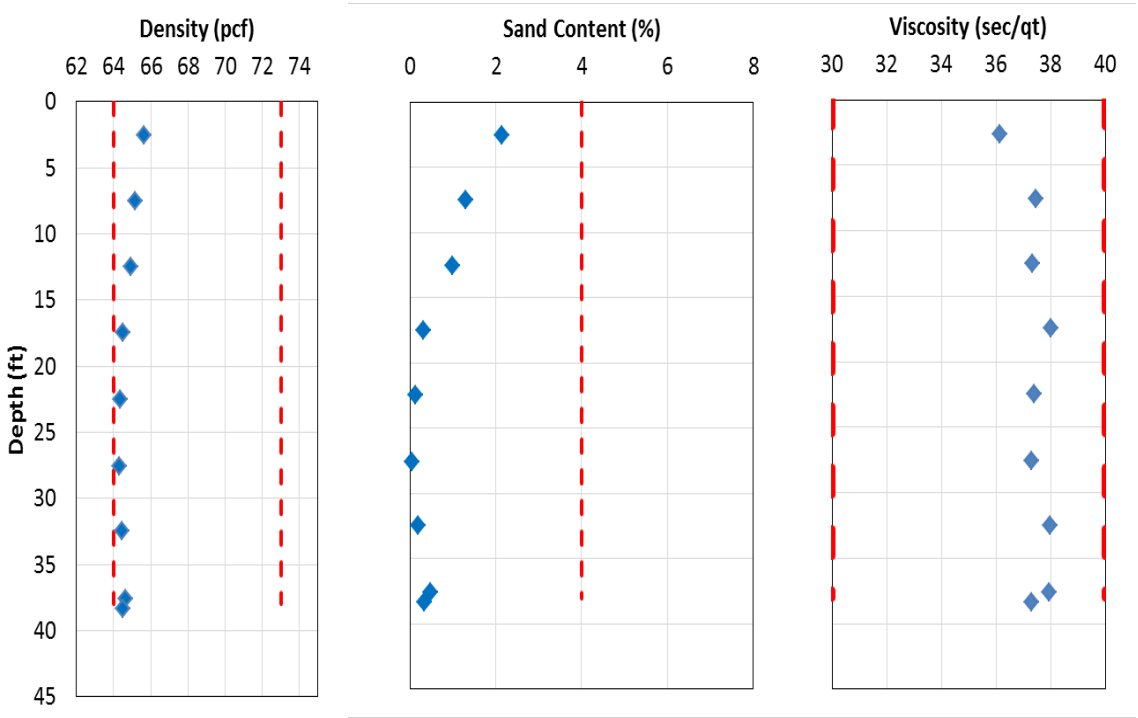

Figure E.33. Slurry column test 7 with no sand

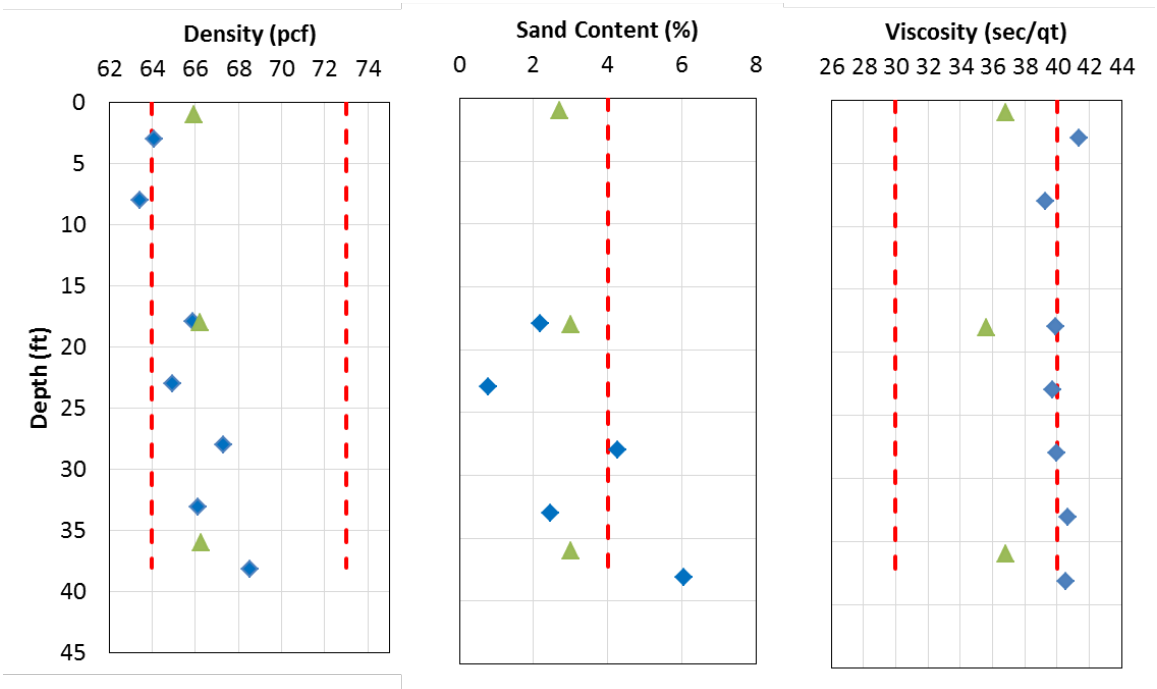

Figure E.34. Slurry column test 8 with approximately 4% sand added (discharge nozzle partially clogged making viscosity erroneously high)

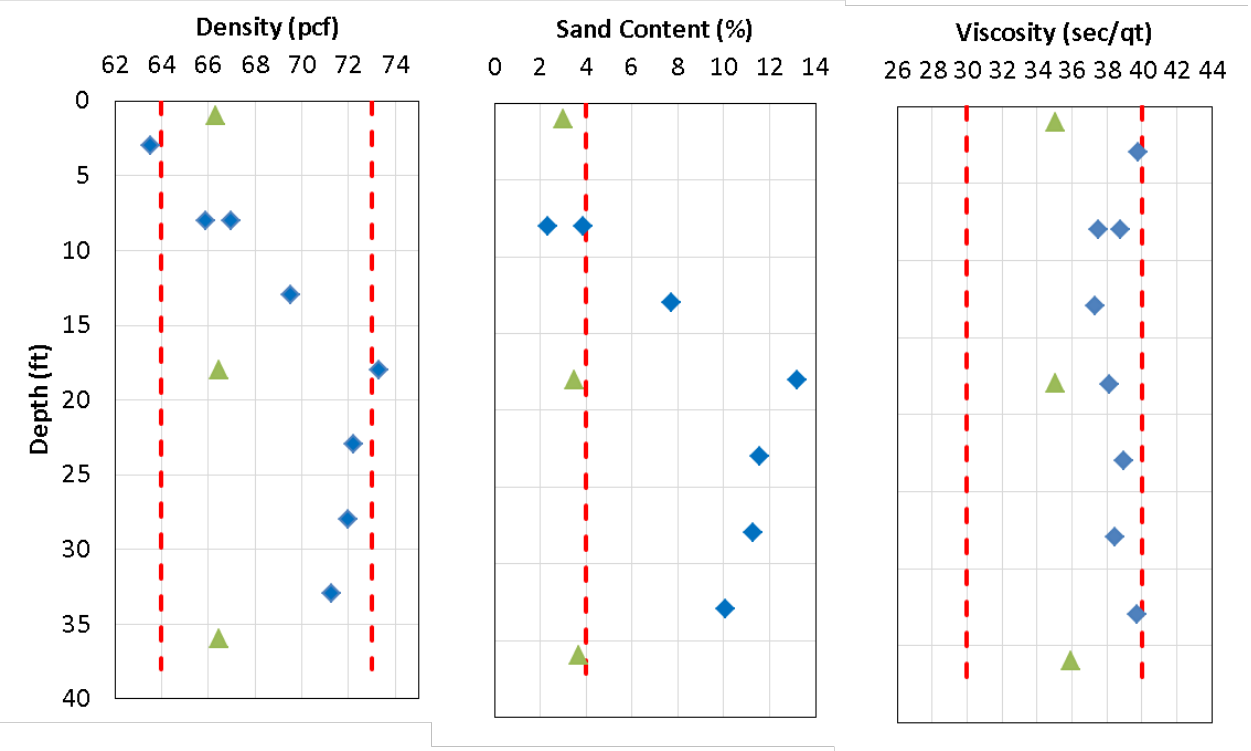

Figure E.35. Slurry column test 9 with approximately 4% sand added (entire system left out in sun between tests without flushing)

STATE OF

STATE OF FLORIDA DEPARTMENT OF TRANSPORTATION

DRILLED SHAFT LOG

700-010-84
CONSTRUCTION
3/16

						Page	1
Project Name	State Rd. 93 Charlotte					Pier No	N/A
FIN Project No	413043-2-52-01					Shaft I.D. or #	Pole P104
Contractor	Astaldi					Station	406+67
Inspected by	Chris McGrath	TIN #	M26311770-220-0	Date	4/27/2016	Offset (ft)	116' RT. Harbor Ramp "D"
Approved by				Date		Bridge/Structure #	High Mast Lighting
	(Project Admin or Permit Manager)						

Casing information

	Outside Casing (Casing 2 in Form 700-010-89)	Inside Casing (Casing 1 in Form 700-010-89)	Input sequence				
Type	Temp. Steel		Lowest section	second lowest section	third lowest section	fourth lowest section	Fifth Lowest Section
ID (in)	60.00						
OD (in)	61.00						
Length (ft)	8.00						
Top Elev.	7.63						
Bot. Elev.	-0.37						
Per Plan	N/A						

Date Information

Date (s) Cased:	Perm.	
	Temp.	4/22/2016
Date (s) Excavated:		4/27/2016
Date (s) Poured:		4/27/2016

Elevations:

Initial Reference Elev. (ft)		4.96
Reference Elev. location:		Stake
Ground surface / Mud line Elev. (ft)		4.96
Water table Elev. (ft)		2.00
Shaft Top Elev. (ft)	Per Plan:	6.96
	Actual (As Built):	6.96
Drilled Shaft Bottom elev. (ft)	Per Plan:	-23.04
	Actual (As Built):	-23.45

Dimensions:

Auger Diameter (in)		
	In Temp. Casing:	54.00
	In Perm. Casing:	N/A
Dia. Of Rock Socket (ft)		4.50
Rock socket length (ft)		22.50
Shaft Diameter (in)		54.00
Was shaft overreamed?		No
Constructed Shaft Lenght (ft)		30.41

Concrete Volume:

Theoretical (CY)	18.71
Actual (CY)	21.45
Ratio (A/T)	1.15

Comments:

Gray Mullins PH.D., P.E. Professor at USF onsite today from 12:28 PM. To 1:03 PM. Conducting testing and sampling of slurry inside the drill shaft.

Depth (ft)	Time In	Time Out	Elevation (ft)	Ref. elev. (ft)	Soil / Rock Description & Notes
3.50	7:40 AM	7:46 AM	4.13	7.63	3 flight auger. Brown sandy soil.
8.00	7:48 AM	7:53	-0.37	7.63	3 flight auger. Brown sandy soil.
8.50	7:55 AM	7:58 AM	-0.87	7.63	3 flight auger. Brown sandy soil.
10.00	7:59 AM	8:02 AM	-2.37	7.63	3 flight auger. Light brown and grey silty sand.
10.50	8:03 AM	8:07 AM	-2.87	7.63	3 flight auger. Light brown and grey silty sand.
11.50	8:08 AM	8:12 AM	-3.87	7.63	3 flight auger. Light brown and grey silty sand.
12.67	8:14 AM	8:19 AM	-5.04	7.63	3 flight auger. Light brown and grey silty sand.
15.00	8:24 AM	8:28 AM	-7.37	7.63	3 flight auger. Light grey sand.
17.00	8:29 AM	8:32 AM	-9.37	7.63	3 flight auger. Light grey and white sand.
17.50	8:33 AM	8:36 AM	-9.87	7.63	3 flight auger. Light grey and white sand.
19.00	8:40 AM	8:43 AM	-11.37	7.63	3 flight auger. Light grey and white sand.
19.41	8:44 AM	8:48 AM	-11.78	7.63	3 flight auger. Light grey and white sand.
20.25	8:49 AM	8:55 AM	-12.62	7.63	3 flight auger. Light grey and white sand.
22.00	8:56 AM	8:59 AM	-14.37	7.63	3 flight auger. Light grey and white sand.
23.00	9:00 AM	9:04 AM	-15.37	7.63	3 flight auger. Light grey and white sand.
24.50	9:05 AM	9:08 AM	-16.87	7.63	3 flight auger. Light grey and white sand.
25.50	9:10 AM	9:14 AM	-17.87	7.63	3 flight auger. Light grey fine sand with shell.
26.00	9:15 AM	9:23 AM	-18.37	7.63	3 flight auger. Light grey fine sand with shell.
26.00	9:26 AM	9:34 AM	-18.37	7.63	3 flight auger. Light grey fine sand with shell.
25.50	9:39 AM	9:46 AM	-17.87	7.63	3 flight auger. Light grey fine sand with shell.
26.25	9:47 AM	9:54 AM	-18.62	7.63	3 flight auger. Light grey fine sand with shell.
26.50	9:55 AM	10:03 AM	-18.87	7.63	3 flight auger. Light grey fine sand with shell.
27.92	10:04 AM	10:12 AM	-20.29	7.63	3 flight auger. Light grey fine sand with shell.
28.33	10:16 AM	10:20 AM	-20.70	7.63	3 flight auger. Light grey fine sand with shell.
28.75	10:22 AM	10:31 AM	-21.12	7.63	3 flight auger. Light grey fine sand with shell.
29.75	10:33 AM	10:39 AM	-22.12	7.63	3 flight auger. Light grey fine sand with shell.
29.50	10:40 AM	10:46 AM	-21.87	7.63	End 3 flight auger. Light grey fine sand with shell.
28.67	10:56 AM	11:04 AM	-21.04	7.63	Start clean-out bucket. Fine white and grey sand.
29.25	11:10 AM	11:19 AM	-21.62	7.63	Clean-out bucket. Fine white and grey sand,
29.50	11:25 AM	11:30 AM	-21.87	7.63	Clean-out bucket. Fine white and grey sand.
30.17	11:38 AM	11:45 AM	-22.54	7.63	Clean-out bucket. Fine white and grey sand.
30.50	11:50 AM	11:56 AM	-22.87	7.63	Clean-out bucket. Fine whitw anf grey sand.
30.83	12:02 PM	12:08 PM	-23.20	7.63	Clean-out bucket. Fine white and grey sand. See next page.

Equipment and methods used to install each casing used: Temporary casing installed by hand digging and then 3 flight auger down to desired depth.

Figure E.36. Drilled shaft construction logs

700-010-04
CONSTRUCTION
3/16

STATE OF FLORIDA DEPARTMENT OF TRANSPORTATION

DRILLED SHAFT LOG

Page 2

Depth (ft)	Time In	Time Out	Elevation (ft)	Ref. elev. (ft)	Soil / Rock Description & Notes
31.08	12:16 PM	12:21 PM	-23.45	7.63	End clean-out bucket. Light grey fine sand with shell.

Rebar Cage Check List:

	yes	no
Proper # Vert. Bars	X	
Proper # Horiz. Bars	X	
Side Spacers	X	
CSL Tubes	X	
Ties & Connections	X	

Clean Out:

Bottom Clean Out Method

Clean-Out Bucket: X Pump: Air Lift:

Time and Date of Final Clean Out

12:21 PM, 4-27-16

Shaft Bottom/Cleanliness Check:

Inspection type:
Visual
Sounding: X
SID

Reference Elevation used for shaft bottom depth and cleanliness check: 7.63 ft

Time Started: 2:05 PM.
Time finished: 2:10 PM.

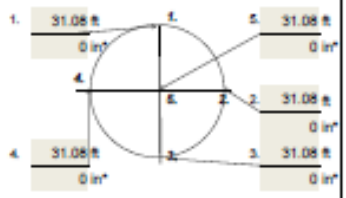

Note (in*) : Input the sediment thickness in inches in these fields

Avg. Shaft Bottom El. (ft)	-23.45
Avg. Shaft Bottom Depth (ft)	31.08

NOTE TO INSPECTOR: Attach additional forms to document bottom checks as needed

Comments:

Approved for pouring: X Yes No

Given to: Brian Ferndon By: Chris McGrath

X Verbal Written

Time: 2:01PM. Date: 4-27-16

Figure E.36. (continued)

APPENDIX F: COPYRIGHT PERMISSIONS

Below is permission for the use of Figure 2.15 in Chapter 2.

Miles Mullins <mpmullin@mail.usf.edu> Jun 10

to tomg

Hello,

I am interested obtaining copyright permission for the use of the following pictures obtained from http://www.smartmeasurement.com/LinkClick.aspx?fileticket=3U-pygiolJ0%3d&tabid=144 in my thesis for a Masters of Science in Civil Engineering degree from the University of South Florida. The thesis is about the determination of drilling mud properties and the photographs are being used to give an example of currently available differential pressure flow meters. If you have any questions or concerns about these permissions, please let me know.

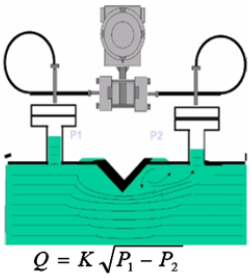

Regards,

...

--
Miles Mullins, E.I.
Graduate Research Assistant
University of South Florida
Civil and Environmental Engineering
4202 E. Fowler Ave.
Tampa, FL 33620

Tom Jun 10

to Riaz, me

Miles,

It was a pleasure speaking with you earlier. Please consider this e-mail to be my formal permission to use the two images contained in your message below for your Master's Tesis. Best of luck to you with this project and all of your future endeavors.

Regards,

Tom Genack
General Manager
SmartMeasurement, Inc.
(414) 299-3896
tomg@smartmeasurement.com

Below is permission for the use of the Figure 2.14 in Chapter 2.

Miles Mullins <mpmullin@mail.usf.edu> Jun 10

to dadams

Hello,

I am interested obtaining copyright permission for the use of the following picture obtained from alicat.com in my thesis for a Masters of Science in Civil Engineering degree from the University of South Florida. If you have any questions or concerns about these permissions, please let me know.

Regards,

--
Miles Mullins, E.I.
Graduate Research Assistant
University of South Florida
Civil and Environmental Engineering
4202 E. Fowler Ave.
Tampa, FL 33620

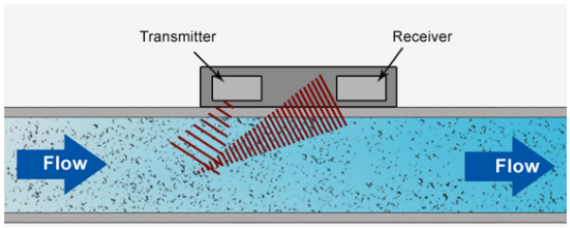

Danielle Adams danielle.adams@alicat.com via alicatscientific.onmicrosoft.com Jun 16 (10 days ago)

to me

Hi Miles,

Please forgive my delay in getting back to you on this. What is the topic of your thesis? As far as the image goes, we have had that image on our website for a long time, and we're not certain at this point how we obtained them. That said, we are happy to extend permission for you to use this image. Please let me know if there are any forms I need to fill out for this.

Best regards,

Danielle Adams
Director of Marketing
dadams@alicat.com

Alicat Scientific, Inc.
7641 N. Business Park Drive
Tucson, AZ 85743 USA
Phone (520) 290-6060
FAX (520) 290-0109
www.alicat.com

Join the Alicat community on:

Stay up to date on Alicat Products and Services – sign up for our newsletter!

Below is permission for Figures 2.8, 2.13, 2.16, and 2.19.

June 24, 2016

Proquest
Attn: Ms. Jackie Bueno
789 E. Eisenhower Parkway
Ann Arbor, MI 48108

Dear Ms. Bueno:

Omega Engineering, Inc. hereby grants to Proquest the limited right to reproduce the following images, as included in Miles Mullins' Master's thesis in Civil Engineering Degree at the University of South Florida strictly in accordance with the conditions set forth herein:

1. LCM101 and LCM111 Series – S Beam Load Cells
   http://www.omega.com/pptst/lcm101_lcm111.html

2. Pre-Wired strain gages – see p.2
   http://www.omega.com/prodinfo/straingages.html

3. PX01-MV - Pressure Transducer
   http://www.omega.com/pptst/PX01-MV.html

4. The Magmeter and Its Components – Fig. 4-1
   http://www.omega.com/literature/transactions/volume4/t9904-09-elec.html

   Credit Line shall read: "© 2000 Putman Media Inc. and Omega Engineering, Inc. Reproduced with permission of Omega Engineering, Inc. www.omega.com."

5. FMG90 Series – Electromagnetic Flowmeter with PVDF and 316L Construction
   http://www.omega.com/pptst/FMG90.html

6. FDT-40 Series – Clamp-On Ultrasonic Flow for Liquids
   http://www.omega.com/pptst/FDT-40.html

7. PHE-5580-20, PHE-5590-20 – Industrial Ground Loop Protection and Solution Ground pH Sensors
   http://www.omega.com/pptst/PHE558020_559020.html

OMEGA Engineering, Inc. • One Omega Drive • Box 4047 • Stamford, CT 06907-0047 • (203) 359-1660
Visit: omega.com or email: info@omega.com

1. Reproduction is limited to the above-mentioned materials as included in Miles Mullins Master's thesis for use by the thesis committee and scholars for research purposes. Proquest will publish the materials in English worldwide and will be available online.

2. Except for No. 4 above, the credit line shall read:

"© OMEGA ENGINEERING, INC. ALL RIGHTS RESERVED. REPRODUCED WITH THE PERMISSION OF OMEGA ENGINEERING, INC., STAMFORD, CT USA 06907, www.omega.com."

3. The reproduction of the above referenced material shall be completed prior to December 31, 2016.

4. Upon completion of the work, please forward a copy to my attention at Omega Engineering, Inc. showing the manner in which Omega's materials were used.

5. Any further requests to reproduce this material must be forwarded to Omega Engineering, Inc.

You are requested to acknowledge your acceptance of the terms of this Agreement by signing and entering the date in the space provided below, and returning an executed copy of this letter for our records.

Sincerely,

B. Christine Riggs
In-House Counsel

AGREED AND ACCEPTED:

SIGNATURE: _____

NAME: _____
(Please print or type)

TITLE: _____

DATE: _____

Below is permission for Figures 3.1, 2.10 and 4.20.

Miles Mullins <mpmullin@mail.usf.edu>
to Gray

Dr. Mullins,

I am interested in obtaining copyright permission for the use of the following graphs from your research in my thesis for USF.

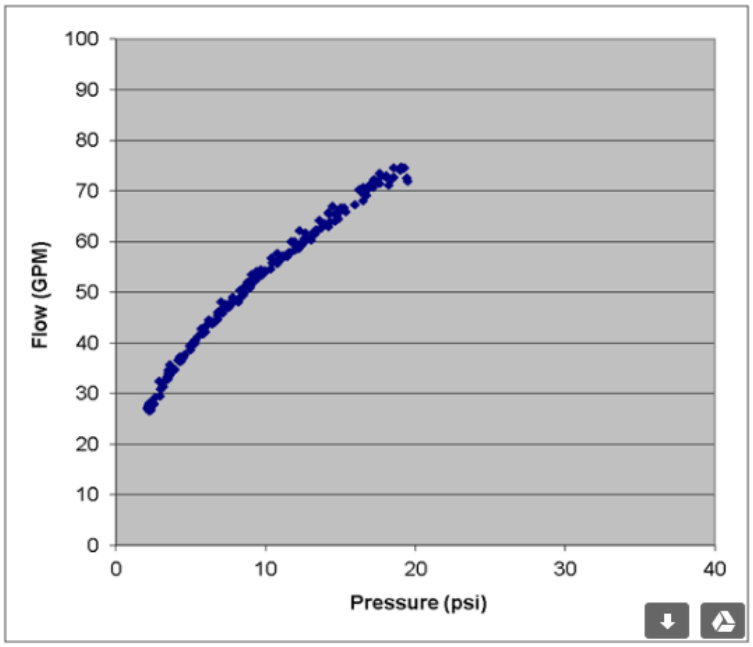

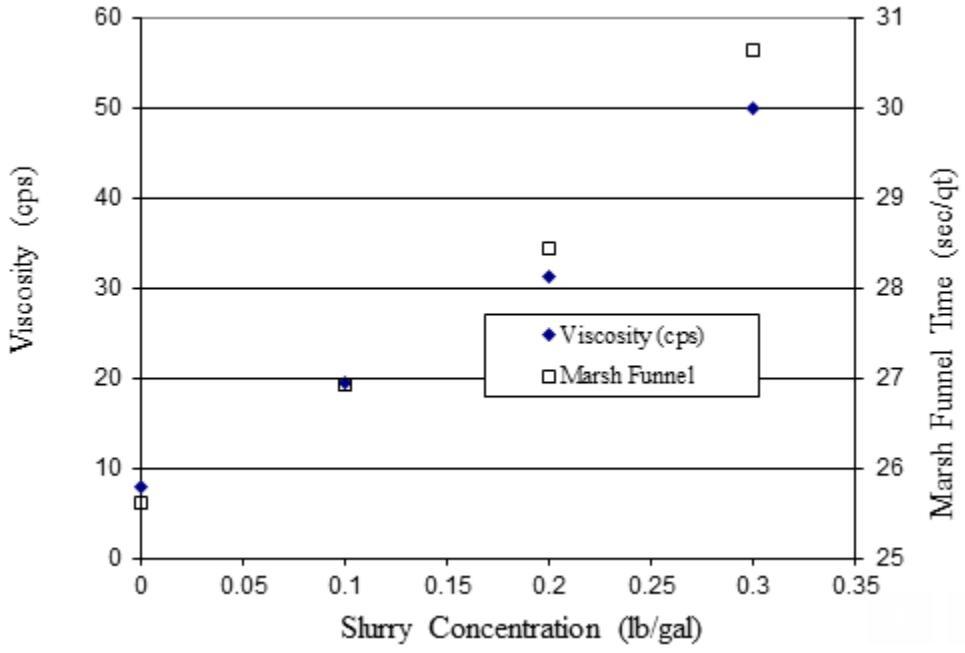

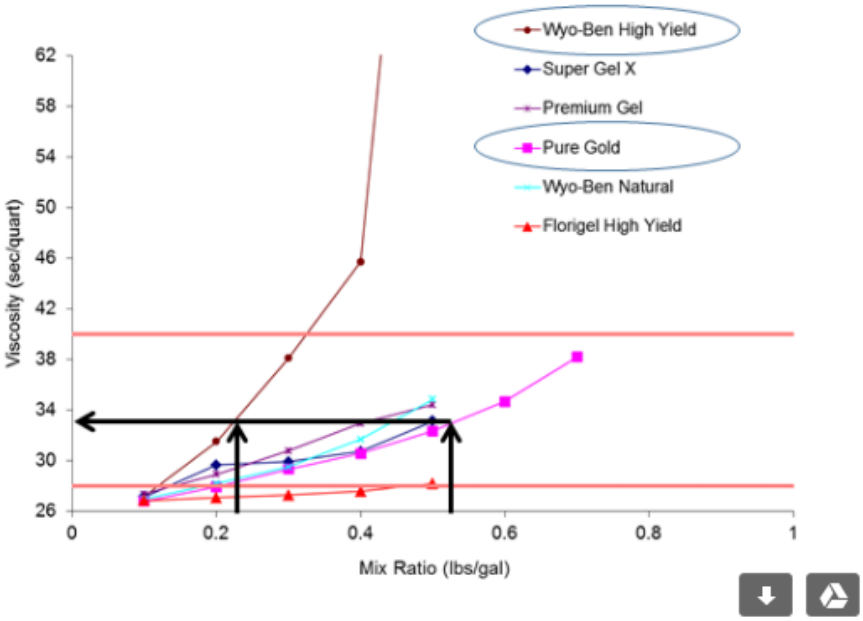

Thanks,

...

--
Miles Mullins, E.I.
Graduate Research Assistant
University of South Florida
Civil and Environmental Engineering
4202 E. Fowler Ave.
Tampa, FL 33620

Mullins, Gray
to me

Miles,
Yes, you can use the requested graphs. As I recall, you are using adapted versions of two of these curves which are not exact reproductions.

Gray Mullins, Ph.D., P.E.
Professor
Department of Civil and Environmental Engineering
University of South Florida
4202 E. Fowler Avenue, ENB 118
Tampa, FL 33620
813 974-5845 (office)
813 974-5829 (fax)
813 690-3736 (mobile)
gmullins@usf.edu
http://geotech.eng.usf.edu